

POLITECHNIKA WARSZAWSKA
DZIEDZINA NAUK ŚCISŁYCH I PRZYRODNICZYCH
NAUKI CHEMICZNE

Rozprawa doktorska

mgr inż. Mariola Stypik

Opracowanie i synteza innowacyjnych związków
małocząsteczkowych, inhibitorów kinazy PI3K, jako potencjalnych
leków w leczeniu toczenia rumieniowatego oraz innych chorób
zapalnych i autoimmunologicznych.

Promotor
dr hab. inż. Zbigniew Ochal, prof. PW

Opiekun pomocniczy
dr inż. Marcin Zagozda

WARSZAWA 2023

Podziękowania

Serdecznie dziękuję Panu Profesorowi Doktorowi inżynierowi Zbigniewowi Ochalowi, mojemu promotorowi, za fantastyczną opiekę naukową, poświęcony czas oraz cenne wskazówki podczas przygotowywania każdego wystąpienia i wykonywania całej rozprawy doktorskiej.

Szczególnie dziękuję Doktorowi inżynierowi Marcinie Zagozda, mojemu opiekunowi pomocniczemu, a jednocześnie liderowi projektu i zespołu w firmie Celon Pharma S.A., za wsparcie, przekazaną wiedzę, cierpliwość, możliwość rozwijania ambicji i zainteresowań, życzliwą pomoc oraz poświęcony czas podczas wykonywania wszelkich prac i analiz oraz przygotowywania niniejszej pracy.

Dziękuję wszystkim pracownikom Działu Chemii Medycznej firmy Celon Pharma S.A., w szczególności zespołowi L3, L4, L5, Zespołowi NMR, Bioinformatycznemu oraz Analitycznemu za wszelką pomoc, wskazówki oraz niezwykłą i niezapomnianą atmosferę pracy.

Dziękuję Dyrektorowi Działu Chemii Medycznej, Krzysztofowi Dubiel, oraz Prezesowi firmy farmaceutycznej Celon Pharma S.A., Maciejowi Wieczorek, za możliwość rozwoju i realizacji doktoratu wdrożeniowego.

Ogromnie dziękuję mojej Rodzinie, szczególnie Mężowi Bartoszowi, Synowi Adamowi, Rodzicom Wandzie i Andrzejowi oraz Bratu Radosławowi za ogromne wsparcie, cierpliwość, wyrozumiałość, dodawanie otuchy oraz możliwość rozwoju i realizowania pasji, a także wykonania wszelkich prac w ramach niniejszego doktoratu.

Dziękuję także moim najbliższym Przyjaciołom i Znajomym za wsparcie, podtrzymywanie na duchu, wszystkie słowa otuchy i chwile, które dodawały mi sił podczas realizacji niniejszej pracy.

Dziękuję!

Spis treści

1. Streszczenie w języku polskim	6
2. Streszczenie w języku angielskim (Abstract in English).....	8
3. Spis publikacji stanowiących podstawę rozprawy doktorskiej.....	10
4. Komentarz do rozprawy doktorskiej.....	12
4.1. Wstęp/Wprowadzenie	12
4.2. Cel pracy	18
4.3. Metodologia i zakres badań.....	19
4.3.1. Projektowanie inhibitorów kinazy PI3K.....	19
4.3.2. Wybranie struktury najbardziej aktywnej i określenie związku wiodącego	19
4.3.3. ADMET, badania <i>in vitro</i> i <i>in vivo</i>	20
5. Omówienie wyników stanowiących podstawę rozprawy doktorskiej.....	21
5.1. Publikacja 1	21
5.2. Publikacja 2.....	25
5.3. Publikacja 3.....	31
6. Wyniki wchodzące w skład publikacji w trakcie przygotowania.....	35
7. Doktorat wdrożeniowy – wdrożenie do przemysłu	37
8. Podsumowanie i wnioski.....	38
9. Literatura cytowana/Bibliografia	40
10. Wykaz publikacji nie wchodzących w skład rozprawy doktorskiej	47
11. Wykaz posterów i komunikatów ustnych.....	48
12. Publikacje stanowiące podstawę rozprawy doktorskiej	50
12.1. Publikacja 1 – P1	50
12.2. Publikacja 1 – P2	83
12.3. Publikacja 1 – P3	118
13. Oświadczenia współautorów publikacji	135

1. Streszczenie w języku polskim

Kinazy PI3K (ang.: *Phosphoinositide 3-kinase*) to rodzina kinaz lipidowych zdolnych do fosforylacji grupy hydroksylowej znajdującej się w pozycji 3 pierścienia fosfatydyloinozytolu. Enzymy te biorą udział w wielu kluczowych procesach komórkowych takich jak proliferacja, wzrost, migracja, produkcja cytokin czy apoptoza [1-4]. Ze względu na budowę strukturalną oraz powinowactwo względem substratów zostały one podzielone na trzy klasy (I, II, III). Najlepiej poznana jest klasa I, w której skład wchodzi cztery heterodimeryczne białka PI3K α , PI3K β , PI3K γ i PI3K δ . Wszystkie opisane funkcje sprawiają, że klasa I kinazy PI3K jest doskonałym celem terapeutycznym w ujęciu chorób nowotworowych, zapalnych i autoimmunologicznych, takich jak rak piersi, jelita grubego, toczeń rumieniowaty układowy (SLE; ang.: *Systemic Lupus Erythematosus*) lub stwardnienie rozsiane (MS; ang.: *Multiple Sclerosis*) [1-8]. Poszukiwanie i tworzenie nowych, odpowiednich, aktywnych i selektywnych związków względem kinazy PI3K (szczególnie I klasy) może pozwolić na przeprowadzenie skutecznych terapii w leczeniu pacjentów obciążonych poważnymi i coraz powszechniejszymi chorobami.

Prace badawcze będące podstawą dysertacji polegały na zaprojektowaniu, opracowaniu i syntezie nowych, innowacyjnych związków małowcząsteczkowych o wysokiej aktywności i selektywności względem wszystkich kinaz, a w szczególności w obrębie klasy I kinazy PI3K (przede wszystkim PI3K δ). Prowadzone były również prace nad syntezą analogów w oparciu o modyfikacje związku, potencjalnego rdzenia inhibitora PI3K δ (opracowanego i otrzymanego przez firmę Celon Pharma S.A., zabezpieczona poprzez zgłoszenie patentowe [9]). Modyfikacje dotyczyły podstawników znajdujących się przy pierścieniu pirazolo[1,5-*a*]pirymidyny stanowiącym rdzeń cząsteczki [10,11]. Wykonano szereg reakcji chemicznych prowadzących do otrzymania biblioteki ponad 100 związków chemicznych, potencjalnych inhibitorów kinazy PI3K. Wszystkie struktury poddano identyfikacji i charakterystyce przy wykorzystaniu różnorodnych technik (m.in. NMR; ang.: *Nuclear Magnetic Resonance*, HPLC; ang.: *High Performance Liquid Chromatography*, MS; ang.: *Mass Spectroscopy*). Zbadano ich wpływ na hamowanie aktywności enzymu, a także zwrócono uwagę na korelacje dotyczące oddziaływania zsyntezowanych struktur (w zależności od ich budowy i charakterystyki podstawników) z białkiem.

Metodologia i zakres badań obejmowały badania literaturowe i patentowe, badania modelowania molekularnego w oparciu o odpowiednie programy, zaprojektowanie inhibitorów

kinaz PI3K, zaprojektowanie ścieżki syntetycznej prowadzącej do otrzymania pożądaných struktur, syntezę biblioteki związków, wybór kandydata do rozwoju (ang.: *hit compound*) na podstawie analizy otrzymaných danych biologicznych i fizykochemicznych, optymalizację struktury z otrzymaniem jednego lub kilku związków wiodących (ang.: *lead compound*). Dla wybranego związku wiodącego przeprowadzono prace nad powiększeniem skali (do otrzymania szarż walidacyjnych w standardach GMP; ang.: *Good Manufacturing Practise*), a także badania ADMET, *in vitro* oraz *in vivo*. Na podstawie biblioteki otrzymaných struktur i analizy wszystkich wyników badań, wyselekcjonowano potencjalnego kandydata na nową substancję leczniczą. Zakres prac wykonanych w ramach doktoratu wdrożeniowego pozwolił na przygotowanie wybranego związku do rozpoczęcia I fazy badań klinicznych. CPL302415, jako aktywny i selektywny inhibitor o bardzo dobrych właściwościach i parametrach farmakokinetycznych został poddany badaniom toksykologicznym, a obecnie jest przygotowywany do rozpoczęcia I fazy badań klinicznych w leczeniu toczenia rumieniowatego.

Słowa kluczowe: kinaza PI3K, toczeń rumieniowaty (SLE), inhibitor, domena katalityczna białka, synteza chemiczna, badania kliniczne.

2. Streszczenie w języku angielskim (Abstract in English)

Phosphoinositide 3-kinases (PI3K) are the family of lipid kinases that are capable of catalyzing the phosphorylation reaction of the hydroxyl group at the third position of the phosphatidylinositol ring. These enzymes are involved in many key cellular processes such as proliferation, growth, migration, cytokine production, and apoptosis [1-4]. Due to their structure and substrate affinity, they are divided into three classes (I, II, III). The best known and described is the first class (I) which consists of four heterodimeric proteins PI3K α , PI3K β , PI3K γ , and PI3K δ . Due to all the functions described above, class I PI3K is an excellent therapeutic target in the treatment of cancer, inflammatory and autoimmune diseases, such as: breast cancer, colon cancer, systemic lupus erythematosus (SLE), multiple sclerosis (MS), rheumatoid arthritis (RA), chronic obstructive pulmonary disease (COPD), or inflammatory bowel disease (IBD) [1-8]. Designing and synthesis of new, active, and selective inhibitors of PI3K (especially the first class) may be very promising for patients with many troublesome diseases.

The studies described in this work is based on the design, synthesis, and development of new, innovative small molecules with high activity and selectivity I class PI3K inhibitors, in particular the PI3K γ and PI3K δ . The synthesis of compounds was multistep and created in two paths. The first one was synthesis „*de novo*” from simple substrates and the second one based on modifications of the pyrazolo[1,5-*a*]pyrimidine core [10,11] of described PI3K δ inhibitor which was synthesized in Celon Pharma S.A. [9]. Many chemical reactions were carried out to obtain a library of over 100 chemical compounds, potential PI3K kinase inhibitors. All structures have been identified and characterized using a variety of technics such as NMR – *Nuclear Magnetic Resonance*, HPLC – *High Performance Liquid Chromatography*, MS – *Mass Spectroscopy*. Their influence on the inhibition of enzyme activity was determined, and attention was paid to the correlations concerning the interaction of the synthesized structures (depending on their characteristics of the appropriate substituents) with the protein.

The research methodology included literature and patent research, molecular docking analysis based on appropriate programs, designing the structures of PI3K inhibitors, designing the synthetic path leading to the desired structures, synthesizing the appropriate library of compounds, selection the *hit* and *lead* (*hit to lead* path), selection the candidate for development. For the lead compound selected for further development, scale-up work has been

performed (to obtain validation batches in GMP - *Good Manufacturing Practice standards*), as well as ADMET and other in vitro and in vivo tests to select a clinical candidate.

Based on the library of obtained structures and the analysis of all results, one lead compound with the best parameters was selected. CPL302415, an active and selective inhibitor with very good properties and pharmacokinetic parameters, has been subjected to toxicological studies and is currently being prepared to start phase I clinical trials in the treatment of SLE.

Key words: PI3K kinase, SLE, inhibitor, catalytic domain of protein, chemical synthesis, clinical trials.

3. Spis publikacji stanowiących podstawę rozprawy doktorskiej

P1 - Publikacja 1:

Tytuł publikacji:

„Design, Synthesis, and Development of Pyrazolo[1,5-*a*]pyrimidine Derivatives as a Novel Series of Selective PI3K δ Inhibitors: Part I—Indole Derivatives.”

Spis autorów:

Stypik, M.; Zagozda, M.; Michałek, S.; Dymek, B.; Zdżalik-Bielecka, D.; Dziachan, M.; Orłowska, N.; Gunerka, P.; Turowski, P.; Hucz-Kalitowska, J.; Stańczak, A.; Stańczak, P.; Mulewski, K.; Smuga, D.; Stefaniak, F.; Gurba-Bryśkiewicz, L.; Leniak, A.; Ochal, Z.; Mach, M.; Dzwonek, K.; Lamparska-Przybysz, M.; Dubiel, K.; Wieczorek, M.

Czasopismo: *Pharmaceuticals* (*Pharmaceuticals* **2022**, *15*, 949)

Doi: <https://doi.org/10.3390/ph15080949>

Oznaczenie manuskryptu: pharmaceuticals-1805645

IF = 5.215; MNiSW = 100

P2 - Publikacja 2:

Tytuł publikacji:

„Design, Synthesis, and Development of Pyrazolo[1,5-*a*]pyrimidine Derivatives as a Novel Series of Selective PI3K δ Inhibitors: Part II—Benzimidazole Derivatives.”

Spis autorów:

Stypik, M.; Michałek, S.; Orłowska, N.; Zagozda, M.; Dziachan, M.; Banach, M.; Turowski, P.; Gunerka, P.; Zdżalik-Bielecka, D.; Stańczak, A.; Kędzierska, U.; Mulewski, K.; Smuga, D.; Maruszak, W.; Gurba-Bryśkiewicz, L.; Leniak, A.; Pietruś, W.; Ochal, Z.; Mach, M.; Zygmunt, B.; Pieczykolan, J.; Dubiel, K.; Wieczorek, M.

Czasopismo: *Pharmaceuticals* (*Pharmaceuticals* **2022**, *15*, 927)

Doi: <https://doi.org/10.3390/ph15080927>

Oznaczenie manuskryptu: pharmaceuticals-1805734

IF = 5.215; MNiSW = 100

P3 – Publikacja 3:

Tytuł publikacji:

„Tuning the biological activity of PI3K δ inhibitor by the introduction of a fluorine atom using the computational workflow.”

Spis autorów:

Pietruś W.; Stypik, M.; Banach M.; Zagozda M.; Gurba-Bryśkiewicz L.; Maruszak W.; Leniak A.; Kurczab R.; Ochal Z.; Dubiel K.; Wieczorek M.;

Czasopismo: *Molecules* (*Molecules* **2023**, 28(8), 3531)

Doi: <https://doi.org/10.3390/molecules28083531>

Oznaczenie manuskryptu: molecules-2260696

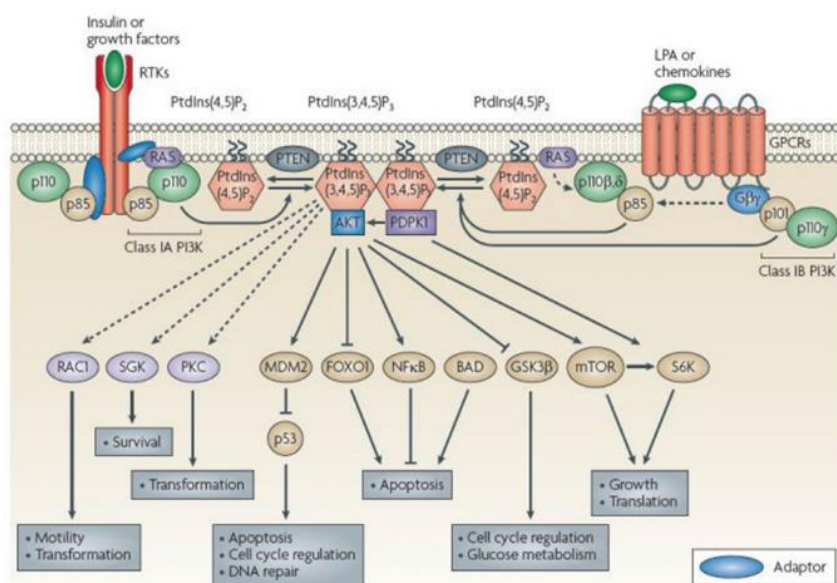
IF = 4.927; MNiSW = 100

IF_{średni} = 5.119; MNiSW_{sumaryczne} = 300

4. Komentarz do rozprawy doktorskiej

4.1. Wstęp/Wprowadzenie

Kinaza PI3K δ (kinaza 3-fosfatoinozytydyli) to kinaza lipidowa wchodząca w skład rodziny kinaz PI3K składającej się z trzech klas: I, II oraz III. W skład I klasy wchodzi cztery heterodimeryczne białka PI3K α , PI3K β , PI3K γ i PI3K δ . Klasa II złożona jest z trzech enzymów: PI3K $C2\alpha$, PI3K $C2\beta$, PI3K $C2\gamma$, natomiast klasa III ma jednego reprezentanta – PI3K $C3$ [1,4]. Wszystkie izoformy PI3K klasy I ulegają ekspresji w wielu tkankach organizmu. PI3K γ oraz PI3K δ charakteryzują się szczególnie wysokim poziomem ekspresji w leukocytach (neutrofile, makrofagi, limfocyty T i limfocyty B) [1-3, 5-8, 12], co ma wpływ na udzielanie odpowiedzi immunologicznej przez organizm. PI3K α i PI3K β natomiast biorą udział w regulacji metabolizmu, są niezbędne do prawidłowej embriogenezy i utrzymania homeostazy glukozy. Ze względu na zaangażowanie tych enzymów w fosforylację fosfatidyloinozytydylo-4,5-difosfonianu (PIP₂) do fosfatidyloinozytydylo-3,4,5-trifosfonianu (PIP₃), kinazy PI3K zapoczątkowują kaskadę aktywacji wielu ważnych procesów komórkowych, takich jak wzrost komórkowy, proliferacja, czy różnicowanie (Rysunek 1) [13-16].



Rysunek 1. Rodzaje białek zaangażowanych w ścieżkę PI3K/AKT oraz ich rola w komórce ludzkiej, *Nature Reviews Drug Discovery*, 2009

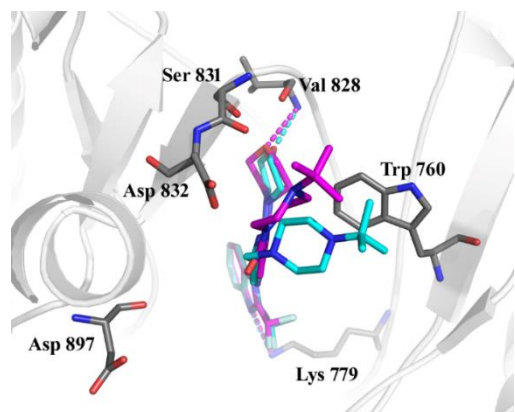
Wszystkie opisane funkcje sprawiają, że klasa I kinazy PI3K jest doskonałym celem terapeutycznym w ujęciu chorób nowotworowych, zapalnych i autoimmunologicznych, takich jak rak piersi, jelita grubego, toczeń rumieniowaty układowy (SLE; ang.: *Systemic Lupus Erythematosus*), stwardnienie rozsiane (MS; ang.: *Multiple Sclerosis*), reumatoidalne zapalenie stawów (RA; ang. *Rheumatoid Arthritis*), przewlekła obturacyjna choroba płuc (POChP; ang.

COPD; ang. *Chronic Obstructive Pulmonary Disease*) czy nieswoiste zapalenie jelit (IBD; ang.: *Inflammatory Bowel Disease*) [1-8]. Poszukiwanie i tworzenie nowych, odpowiednich, aktywnych i selektywnych związków względem kinazy PI3K (szczególnie I klasy) może pozwolić na przeprowadzenie skutecznych terapii w leczeniu pacjentów obciążonych poważnymi i coraz powszechniejszymi chorobami.

Pierwszym inhibitorem PI3K była Wortmanina, odkryta na początku lat 90., jako nieodwracalny inhibitor wiążący się kowalencyjnie w kieszeni ATP kinazy. Jest to związek pochodzenia naturalnego, wyizolowany z grzybów z gatunku *Penicillium funiculosum* [12]. Pierwszym syntetycznym związkiem hamującym ten enzym jest LY294002 [17]. Niestety oba inhibitory charakteryzują się bardzo ograniczoną specyficznością w obrębie kinaz PI3K, dużą toksycznością oraz niekorzystnym profilem farmakologicznym. Wszystko to sprawia, że poszukiwanie nowych, aktywnych i selektywnych związków małącząsteczkowych, inhibitorów kinazy PI3K, jest bardzo potrzebnym i wymagającym wyzwaniem.

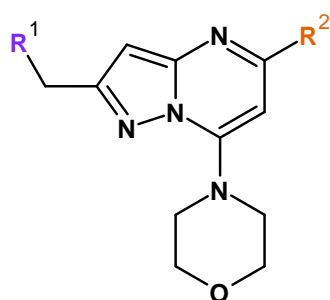
Wszystkie izoformy I klasy występują jako białka regulatorowe (p85) z odpowiednią podjednostką katalityczną (odpowiednio p110 α , p110 β i p110 δ) [18,19]. W przypadku kinazy PI3K δ wspomniana podjednostka p110 δ i jej miejsce wiązania z ATP zawiera kilka istotnych funkcjonalnie fragmentów, takich jak region zawiasowy, tzw. „*hinge region*”, kieszeń powinowactwa, czy region hydrofobowy położony poniżej miejsca aktywnego enzymu. Interakcja potencjalnego inhibitora z dużą, płaską powierzchnią hydrofobowego zakonserwowanego fragmentu tyrozyny (Tyr-876) została zaobserwowana podczas wielu prac badawczych i opisana w wielu publikacjach [3,7,16,17,19]. Ponadto wiele związków wykazywało obecność dodatkowych wiązań wodorowych z kieszenią powinowactwa enzymu, gdzie mogą wystąpić dodatkowe oddziaływania, np. wiązania wodorowe z lizyną (Lys-833) [20-22]. Większość selektywnych inhibitorów kinazy PI3K δ wykazuje kluczowe oddziaływania z dwoma aminokwasami, tryptofanem-760 (Trp-760) oraz metioniną-752 (Met-752) [23-25]. Oddziaływanie z tzw. „półką tryptofanową” (Trp-760) ma wpływ na selektywność względem omawianej kinazy. Wynika to z faktu, że pozostałe izoformy zawierają inne, dodatnio naładowane aminokwasy, co wpływa na sposób wiązania zasadowego fragmentu aminokwasu względem enzymu. Zawady steryczne w obrębie rejonu tryptofanowego mają wpływ na selektywność ze względu na niekorzystne wiązania z innymi izoformami kinazy PI3K. Charakterystycznym, istotnym wiązaniem niekowalencyjnym jest wiązanie wodorowe (HB; ang. *Hydrogen Bond*) z waliną Val-828 (szczególnie w przypadku inhibitorów PI3K δ) [23,25]. Oddziaływanie to najczęściej obserwowane jest pomiędzy atomem

tlenu z ugrupowania (fragmentu) morfolinowego w cząsteczce inhibitora a Val-828 w rejonie zawiąsowym enzymu (Rysunek 2).



Rysunek 2. Model wiązania, związku CPL302415 i jego odpowiednika z mostkiem karbonylowym w kieszeni katalitycznej kinazy PI3K δ (PDB ID:2WXL).

Struktura związku chemicznego, zarówno rdzenia, jak i pozostałych części, ma kluczowe znaczenie w projektowaniu aktywnych i selektywnych inhibitorów, w tym inhibitorów PI3K δ . Wybór odpowiednich podstawników decyduje o właściwościach cząsteczki. Każdy fragment ma swoją funkcję, może wpływać na właściwości fizykochemiczne i jest odpowiedzialny za tworzenie swoistych dla danego receptora oddziaływań. W przypadku wybranych struktur opartych na szkielecie pirazolo[1,5-*a*]pirymidynowym fragment benzimidazolowy odpowiada za aktywność i selektywność związku, natomiast część aminowa w pozycji drugiej rdzenia odpowiada za jego selektywność (Rysunek 3). W najbardziej aktywnym związku - CPL302415 są to odpowiednio difluorometylobenzimidazol (R^2) oraz *N*-*tert*-butylo-piperazyna (R^1).



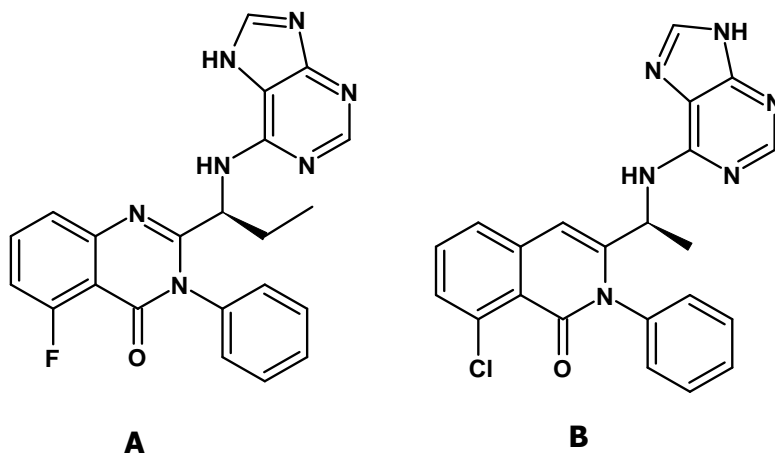
Rysunek 3. Struktura ogólna pochodnych pirazolo[1,5-*a*]pirymidynowych z zaznaczonymi fragmentami: rdzeniem (zaznaczony na czarno), fragmentem odpowiadającym za selektywność (zaznaczony na fioletowo), fragmentem odpowiadającym za aktywność i selektywność (zaznaczony na pomarańczowo).

Nadaktywność oraz rozregulowanie systemu immunologicznego są najczęstszą przyczyną powstawania chorób zapalnych i autoimmunologicznych, do których zaliczają się toczeń rumieniowaty (SLE), reumatoidalne zapalenie stawów (RA), czy astma [22]. Choroby te postępują kaskadowo, prowadzą do uszkodzenia poszczególnych narządów, a w konsekwencji także dysfunkcji wielonarządowej, ponadto są zwykle progresywne i uciążliwe dla pacjentów (Schemat 1).



Schemat 1. Kaskada uszkodzenia wielonarządowego w SLE.

Zostało udowodnione i udokumentowane, że PI3K δ zaangażowana jest w rozwój procesów alergicznych prowadzących do astmy (poprzez np. aktywację ekspresji cytokin przez komórki Th2, aktywację produkcji przeciwciał (m.in. IgE) przez limfocyty B, lub aktywację bazofili [1, 2, 26-30]. Selektywnymi znanymi inhibitorami są Idealisib (selektywny względem PI3K δ) [31] oraz Duvelisib (selektywny względem PI3K δ i PI3K γ) [32] (Rysunek 4), jednak ich toksyczność oraz efekty uboczne wykluczyły je jako potencjalnych kandydatów w leczeniu astmy.



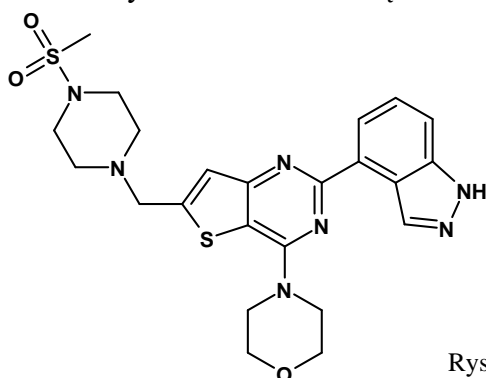
Rysunek 4. Wzory strukturalne inhibitorów: Idealisib (A) oraz Duvelisib (B).

Z kolei w SLE kluczowa okazała się niekontrolowana nadprodukcja przeciwciał w której główną rolę odgrywały limfocyty T oraz B. Wzmoczona aktywność szczególnie dwóch izoform gamma i delta kinazy PI3K (PI3K γ i PI3K δ) wskazuje na rozwój tego schorzenia. Aktywacja PI3K δ w limfocytach T została zaobserwowana u 70% pacjentów z toczniem [2]. Ze względu na zaangażowanie podjednostki p110 δ kinazy PI3K δ w produkcji interleukiny 17 (IL-17) przez komórki Th17 [2,33,34], enzym ten jest obiecującym celem terapeutycznym w leczeniu np. SLE. Jest to choroba wielonarządowa o złożonym mechanizmie. 90% pacjentów (zachorowalność jest szacowana na ok. 50 przypadków na 100 000) [35] to kobiety w różnym

wieku(15-60 lat). W terapii na SLE obecnie nie ma skutecznego leku [36,37]. Leczenie polega jedynie na łagodzeniu objawów oraz obniżeniu degradacji narządów. Ponadto, dobrze poznany mechanizm działania tej kinazy na poziomie molekularnym stwarza doskonałe warunki do racjonalnego projektowania, syntezy i wdrażania nowych leków przeciwzapalnych i autoimmunologicznych. Opracowanie nowych, aktywnych związków pozwoli na rozwój terapii i dobór odpowiedniego leczenia dla pacjentów zmagających się z tego typu schorzeniami. Jest to szczególnie ważne z punktu widzenia chorych, którzy wiążą nadzieję z powstawaniem nowych leków, dzięki którym możliwe jest zatrzymanie choroby bądź jej całkowity regres. Ma to znaczenie również w ujęciu rozwoju nauki.

Selektywne inhibitory PI3K δ mogą zostać otrzymane na drodze odpowiednich modyfikacji, np. zamiany heterocykla okupującego kieszeń katalityczną (wiążąca, ang. *binding pocket*) enzymu.

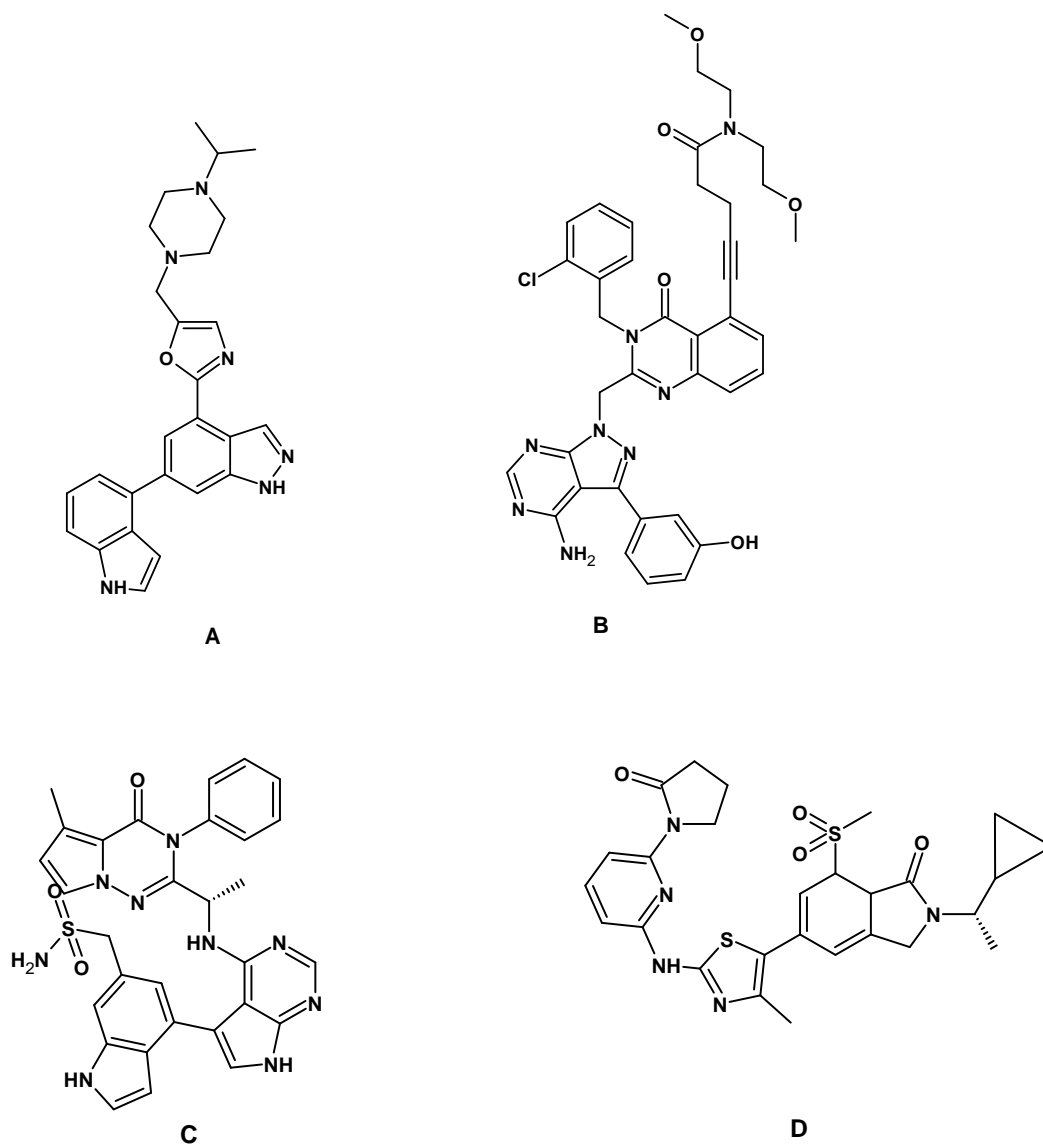
Przykładowo dla znanego inhibitora GDC-0941(Rysunek 5) [38] zamiana grupy indazolowej na 2-metylobenzimidazolową skutkowałą poprawieniem selektywności cząsteczki [24,39].



Rysunek 5. Wzór strukturalny inhibitora GDC-0941.

Na selektywność oraz właściwości farmakodynamiczne mają również wpływ także oddziaływania z półką tryptofanową (Trp-760) i innymi aminokwasami [22,24,39]. Optymalizacja podstawników w wybranych związkach może prowadzić do poprawy aktywności i selektywności względem interesującego nas enzymu, a także poprawy właściwości farmakokinetycznych.

Związki o strukturach opartych na rdzeniach bicyklicznych zostały opisane jako efektywne i aktywne inhibitory PI3K. Większość z nich, wliczając tienopirymidyny czy pirydynopirymidyny znane są jako inhibitory pan-PI3K (nieselektywne) [23-25, 38]. Ze względu na pojawiające się problemy z zależną od czasu inhibicją CYP, selektywnością, biodostępnością i rozpuszczalnością, zaprojektowano, zsyntezowano i opisano nowe struktury oparte na rdzeniach, takich jak izoksazolopirymidyny, imidazopirymidyny czy pirazolopirymidyny (Rysunek 6) [23,39,40-42].



Rysunek 6. Wzory strukturalne inhibitorów PI3K δ lub PI3K γ/δ , kandydatów w leczeniu astmy i POChP: A – Nemiralisib (GSK2269557), B – RV-1729, C – LAS195319, D – AZD8154.

Wiele inhibitorów PI3K wykazało potencjał w oddziaływaniu ugrupowania morfolinowego z rejonem zawiasowym enzymu, tzw. „hinge-binding motif”. Cząsteczki zawierające wspomniane ugrupowanie charakteryzowały się zazwyczaj lepszą aktywnością niż struktury, które go nie zawierały. Rola morfoliny polegała na tym, że jest akceptorem wiązania wodorowego w tej pozycji. Ważnym oddziaływaniem jest, co zostało udowodnione i opisane w wielu badaniach, interakcja morfoliny z aminokwasem waliną w pozycji 828 (Val-828) [23,25,26]. Od roku 2012 zostało otrzymanych i opublikowanych wiele inhibitorów zawierających grupę morfolinową, w tym również związków opartych na pochodnych 2-difluorometylo-1*H*-benzimidazolu [23,43-45]. Opisane struktury opierały się na 1,3,5-triazynowym rdzeniu oraz pierścieniu morfoliny oddziałującym z rejonem zawiasowym enzymu. Rozbudowa monocyklicznych rdzeni do bi- i multi-cyklicznych z różnymi,

odpowiednio dobranymi podstawnikami umożliwiła stworzenie biblioteki związków i wybór związku wiodącego, a co za tym idzie, pozwoliła na rozwój i znalezienie najlepiej dobranego, aktywnego i selektywnego inhibitora PI3K δ [23,26,46].

4.2. Cel pracy

Głównymi celami pracy były:

- badania *in silico* – modelowanie molekularne, m.in. dokowanie z indukowanym dopasowaniem, dynamika molekularna uwzględniająca wykrystalizowane struktury kinaz PI3K;
- projektowanie struktur nowych związków chemicznych: spełniających reguły Lipińskiego, potencjalnie aktywnych i selektywnych względem poszczególnych izoform PI3K, mało toksycznych i o odpowiednich właściwościach fizykochemicznych;
- synteza biblioteki inhibitorów PI3K – nowych struktur opartych na szkielecie pirazolo[1,5-*a*]pirymidyny, wyselekcjonowanych na podstawie wcześniejszych badań i modelowania;
- przeprowadzenie analizy SAR (ang.: *Structure-Active Relationship*), a następnie na jej podstawie zaprojektowanie i otrzymanie grupy związków oraz wybór związku wiodącego (*lead compound*) o odpowiednich właściwościach fizykochemicznych i farmakologicznych;
- projektowanie ścieżki syntetycznej i optymalizacja procesu dla wybranego związku wiodącego, w tym zmniejszenia liczby etapów syntezy oraz zredukowanie kosztów otrzymania produktu końcowego przy wykorzystaniu wybranych techniki technologii takich jak TLC-MS, HPLC, HPLC-MS, UPLC, NMR, a także wydajnych sprzętów, takich jak reaktor do reakcji w przepływie (*flow chemistry*), reaktor do reakcji mikrofalowych;
- otrzymanie związku będącego kandydatem na substancję czynną do stosowania w leczeniu SLE i wdrożenie do produkcji opracowanej technologii syntezy – otrzymanie do badań toksykologicznych oraz wdrożenie do I fazy badań klinicznych.

4.3. Metodologia i zakres badań

4.3.1. Projektowanie inhibitorów kinazy PI3K

Struktury chemiczne związków o potencjalnym charakterze inhibitorów kinazy PI3K zostały zaproponowane na podstawie analizy piśmiennictwa dotyczącego PI3K, zarówno inhibitorów typu pan (nieselektywnych względem izoform) oraz inhibitorów selektywnych względem podjednostki δ [1-8,10,19,21-25,29]. Następnie, w oparciu o badania czystości patentowej i potwierdzeniu dostępnej przestrzeni patentowej (bazy Espacenet, Patentscope) zaprojektowano możliwe do zsyntezowania struktury. Białka do dokowania zostały wybrane w oparciu o opisane uprzednio badania i dokowania dostępnych, opracowanych i wykrytych z kinazą inhibitorów. Procedura dokowania molekularnego została opracowana w oparciu o strukturę PI3K δ zdeponowaną w krystalograficznej bazie PDB, ang.: *Protein Data Bank* (PDB ID: 2WXP, 2WXL) za pomocą programu AutoDock Vina [47-49]. Trójwymiarowa struktura związków została przygotowana na podstawie obliczonych wartości odpowiednich parametrów, m.in. pK_a z zastosowaniem programu JChem 21.13.0 [50] (ustalenie odpowiednich stanów protonacyjnych struktur). Po przeanalizowaniu wyników dokowania zaproponowane zostały modyfikacje wybranych struktur w celu poprawy ich właściwości. Wybór i dostosowanie poszczególnych grup funkcyjnych (wzbogacających rdzeń cząsteczki) oparty był na wynikach wyżej wspomnianego dokowania molekularnego, a także wynikał z obliczonych i przybliżonych za pomocą odpowiednich programów (np. MarvinSketch) wartości parametrów fizykochemicznych. Badania zależności pomiędzy strukturą a aktywnością biologiczną związków (SAR, ang.: *Structure – Activity Relationship*) pozwoliły na zbudowanie bazy danych i selekcję najlepszych pretendentów do syntezy i stworzenia odpowiedniej biblioteki związków. Dodatkowo, w celu znalezienia idealnego kandydata na lek, opatentowany związek firmy Celon Pharma S.A. [12] został poddany modyfikacjom – synteza szkieletu pirazolo[1,5-*a*]pirymidyny z różnymi, nowymi podstawnikami. Dzięki takim zmianom otrzymano wysoce aktywny i selektywny inhibitor PI3K δ – potencjalną substancję czynną do zastosowania w leczeniu chorób autoimmunologicznych i zapalnych.

4.3.2. Wybór kandydatów do rozwoju i określenie związku wiodącego

Dysponując zsyntezowaną biblioteką związków (synteza chemiczna wyselekcjonowanych molekuł o najlepszych parametrach po wstępnych badaniach *in silico*, a

mianowicie wspomnianym wyżej dokowaniu oraz porównaniu właściwości fizykochemicznych obliczonych w oparciu o konkretne programy, opisanych w punkcie 4.3.1.) wybrane struktury poddane zostały dalszej optymalizacji w celu poprawy ich właściwości fizykochemicznych (rozpuszczalność, lipofilowość, stabilność chemiczna) oraz parametrów farmakokinetycznych. Modyfikacji uległy różne grupy funkcyjne odpowiedzialne za wiązanie z białkiem, a także fragmenty wpływające na rozpuszczalność (tzw. fragment dorozpuszczalnikowy inhibitora). Po dokonaniu syntezy i przeprowadzeniu wstępnych badań wybrana została niewielka grupa kandydatów do dalszego rozwoju (związki o największym powinowactwie do kinazy i najbardziej optymalnych właściwościach fizykochemicznych). W celu przeprowadzenia dalszych badań fizykochemicznych oraz biologicznych badań przedklinicznych wykonano syntezę wybranych kandydatów w większej skali (do 10 g). Dla związków wykonano kolejne badania fizykochemiczne, stabilnościowe, testy na komórkach i zwierzętach w celu wyłonienia związku wiodącego (proces „*hit to lead*”). Kolejnym etapem dla związku wiodącego są badania toksykologiczne, a następnie kliniczne (wejście do I fazy badań klinicznych).

4.3.3. ADMET, badania *in vitro* oraz *in vivo*

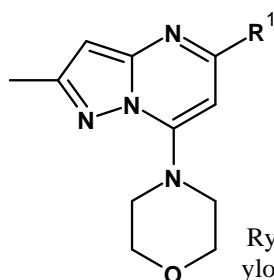
Badania ADMET (ang.: (A) *Absorption* - wchłanianie (D) *Distribution* - dystrybucja (M) *Metabolism* - metabolizm (E) *Excretion* - wydalanie and (T) *Toxicity* - toksyczność) wykonano w Laboratorium Analiz Fizykochemicznych oraz Dziale Badań Przedklinicznych firmy Celon Pharma S.A. Współpraca z wyżej wymienionymi działami pozwoliła także na wykonanie niezbędnych badań *in vitro* oraz *in vivo*. Określone zostały eksperymentalne wartości parametrów fizykochemicznych takich jak lipofilowość czy rozpuszczalność, jak również zbadana została stabilność chemiczna i metaboliczna wybranych związków. Wykonane testy biochemiczne i komórkowe pozwoliły na wyznaczenie parametru IC_{50} świadczącego o aktywności i selektywności badanych cząsteczek (mierzone przez zdolność związków do hamowania konwersji ATP do ADP podczas reakcji enzymatycznej). Wykorzystano zestaw do oznaczania kinazy ADP-Glo firmy Promega, kinazy $PI3K\alpha$, $PI3K\beta$, $PI3K\gamma$ i $PI3K\delta$ firmy Merck Millipore). Określono także parametry farmakokinetyczne takie jak klirens (Cl), maksymalne stężenie substancji (c_{max} , ang.: *maximum concentration*), czas półtrwania ($t_{1/2}$), czas od podania do osiągnięcia maksymalnego stężenia substancji (t_{max}) czy objętość dystrybucji (V_d). Zbadana została stabilność w mikrosomach mysich oraz ludzkich, gdzie jako związki referencyjne zastosowano verapamil jako kontrolę pozytywną oraz

donepezil jako kontrolę negatywną. Analiza otrzymanych danych pozwoliła na dokonanie wyboru właściwego związku wiodącego do dalszych badań toksykologicznych oraz badań klinicznych.

5. Omówienie wyników stanowiących podstawę rozprawy doktorskiej

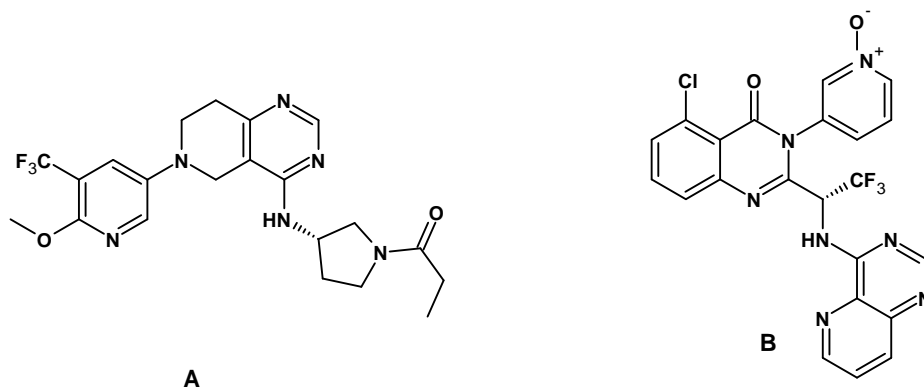
5.1. Publikacja 1 – P1

Na podstawie opisanego w literaturze znaczenia w strukturach inhibitorów PI3K układów typu „morfolina-pirymidyna”, a także wybranego w oparciu o badania czystości patentowej bicyklicznego rdzenia pirazolo[1,5-*a*]pirymidynowego, opracowana, otrzymana i opisana została w przytoczonej publikacji biblioteka nowych związków, które docelowo miały zostać potencjalnymi kandydatami w leczeniu POChP (Przewlekłe Obstrukcyjna Choroba Płuc) [48]. Uwaga została skupiona na morfolinie podstawionej w pozycji C(7) pirazolo[1,5-*a*]pirymidynie (motyw 7-(morfolin-4-ylo)pirazolo[1,5-*a*]pirymidyny) jako najbardziej kluczowym do zachowania aktywności fragmencie (Rysunek 7).



Rysunek 7. Wzór strukturalny motywu „morfolina-pirymidyna” – 2-metylo-7-(morfolin-4-ylo)pirazolo[1,5-*a*]pirymidyna.

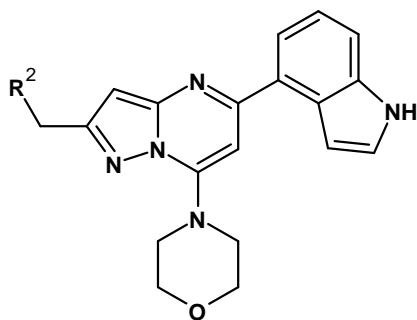
Na podstawie dostępnej literatury zauważyć można, że związki oparte na szkielecie bicyklicznym skondensowanych pierścieni pięcio- i sześcioczłonowych są bardziej aktywne i potencjalnie bardziej obiecujące jako kandydaci kliniczni w leczeniu astmy lub POChP, niż związki oparte na szkielecie bicyklicznym skondensowanych pierścieni sześcio- i sześcioczłonowych, np. związek CDZ 173 (**A**) [51-53] lub UCB-5857 (**B**) (Rysunek 8) [54-57].



Rysunek 8. Wzory strukturalne inhibitorów PI3K: A - CDZ 173 (Leniolisib), B – UCB-5857 (Seletalisib).

Z tego powodu główna część pracy poświęcona została otrzymaniu pochodnych zbudowanych na szkielecie pierścienia bicyklicznego pirazolo[1,5-*a*]pirymidyny (podobnie jak w przypadku m.in. pan-inhibitora GDC-0941) [58-60], co z odpowiednimi modyfikacjami może prowadzić do otrzymania aktywnych i selektywnych związków o aktywności inhibitorów PI3K δ .

Do weryfikacji i wybrania najbardziej odpowiedniego podstawnika w pozycji C(5), przy zachowanym, wcześniej wspomnianym układzie z morfoliną w pozycji C(7), otrzymana została grupa pochodnych 2-metylopirazolo[1,5-*a*]pirymidyny. Na podstawie analizy wartości IC₅₀ względem PI3K δ i PI3K α oraz wyliczonej selektywności PI3K α/δ jako najbardziej obiecujący rdzeń została wybrana 5-indol-4-ilo-pirazolo[1,5-*a*]pirymidyna (Rysunek 9).



Rysunek 9. Wzór ogólny wybranego szkieletu - 5-indol-4-ilo-pirazolo[1,5-*a*]pirymidyny.

Następnym etapem była optymalizacja podstawnika R². Fragment ten jest odpowiedzialny za poprawę rozpuszczalności związku (tzw. część „dorozpuszczalnikowa”), a dodatkowo obecność w samym R² heteroatomów (N, O, S) lub odpowiednich grup (NH, OH, CO, SO) pozwoliło na wytworzenie dodatkowego wiązania wodorowego pomiędzy ligandem i białkiem, co powinno mieć wpływ na poprawę aktywności cząsteczki. Optymalizacja polegała na funkcjonalizacji aminy heterocyklicznej, np. piperidyny, z wprowadzeniem podstawników rozbudowanych sterycznie. Wyniki badań wskazały, że cykliczne aminy pięciocłonowe lub sześciocłonowe, np. morfolina, pochodne mocznikowe, jak również ugrupowanie metylowe

czy estrowe w tej pozycji nie są preferowane i charakteryzują się niższą aktywnością względem PI3K δ . Ze względu na fakt, że podstawnik mesylopiiperazynowy obecny w GDC0941 wpłynął na poprawę inhibicji kinazy, został on także włączony w strukturę pirazolo[1,5-*a*]pirymidyny jako R², co jednak nie przyczyniło się do poprawy aktywności. Najbardziej aktywnymi cząsteczkami okazały się analogi *N,N*-dimetylo-4-aminopiperydyny oraz 4-(*N*-metylopiiperazyn-1-yl)opiperydyny (IC₅₀ względem PI3K δ równe odpowiednio 37 nM oraz 52 nM). Analiza wyników optymalizacji fragmentu R² pozwoliła na sformułowanie wniosku iż, obecność pierścieni piperazynowych lub piperydynowych z odpowiednimi, dużymi podstawnikami alifatycznymi pozwala na otrzymanie aktywnych i selektywnych inhibitorów kinazy PI3K. W celu weryfikacji selektywności otrzymanych struktur względem pozostałych izoform, dla dwóch wybranych amin (*N-tert*-butylopiiperazyny oraz 2-(piperydyn-4-yl)opropan-2-olu) w pozycji R²) zsyntezowano analogi z różnymi ugrupowaniami w pozycji piątej rdzenia. Otrzymana została grupa pochodnych z szeregiem podstawników R¹ (azaindol, fluorindol) (Tabela 1, Tabela 2). Najbardziej selektywne okazały się pochodne indolowe lub azaindolowe.

Tabela 1. Poziom inhibicji PI3K δ wyznaczony dla pochodnych pirazolo[1,5-*a*]pirymidyny.

Numer związku	R ¹	IC ₅₀ PI3K δ [nM]	IC ₅₀ PI3K α [nM]	IC ₅₀ PI3K β [nM]	IC ₅₀ PI3K γ [nM]	Selektywność		
						α/δ	β/δ	γ/δ
36		13	15 820	4 310	15 900	1 217	332	1 223
49		40	34 400	11 300	47 800	860	283	1 195
50		28	3 650	5 260		130	188	
51		23	9 750	26 800		424	1 165	

Wartości IC₅₀ zostały wyliczone jako średnia arytmetyczna z dwóch niezależnych eksperymentów.

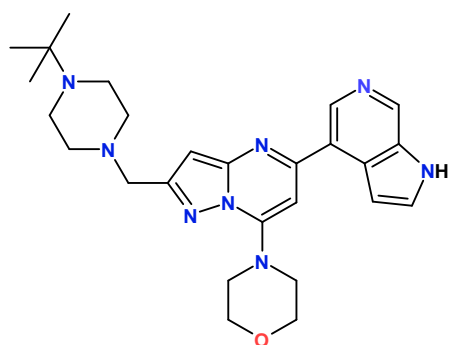
Tabela 2. Poziom inhibicji PI3K δ wyznaczony dla pochodnych pirazolo[1,5-*a*]pirymidyny.

Numer związku	R ¹	IC ₅₀ PI3K δ [nM]	IC ₅₀ PI3K α [nM]	IC ₅₀ PI3K β [nM]	IC ₅₀ PI3K γ [nM]	Selektywność			IC ₅₀ CD19 [nM]
						α/δ	β/δ	γ/δ	
37		6,6	12 470	5 470	>60 000	1 889	829	>9 091	20
53		11	19 300	19 450	>60 000	1 754	1 768	>5 455	
54		2,8	2 670	21 600	34 400	954	7 714	12 286	19
55		45	2 960	32 000		66	711		

Wartości IC₅₀ zostały wyliczone jako średnia arytmetyczna z dwóch niezależnych eksperymentów.

Związkami najbardziej obiecującymi spośród całej otrzymanej biblioteki okazały się cząsteczki zawierające indol lub azaindol jako podstawnik R¹ oraz *N-tert*-butylopiperyzynę jako grupa R²

Dokowanie molekularne pokazało silne oddziaływanie związku z tzw. „półką tryptofanową” – Trp-760, w które zaangażowana jest hydrofobowa/lipofilowa grupa *N-tert*-butylowa we fragmencie aminowym (*N-tert*-butylopiperyzyna). Ponadto wybrany związek, CPL302253 (Rysunek 10) wykazywał wysoką stabilność metaboliczną oraz dobrą rozpuszczalność kinetyczną (Tabela 3).



Rysunek 10. Wzór strukturalny CPL302453 (54).

Tabela 3. Porównanie wybranych parametrów dla związków **37** i **54**; MLM (ang.: *Mouse Liver Microsomes*) – badanie na mikrosomach mysich, HLM (ang.: *Human Liver Microsomes*) – badania na mikrosomach ludzkich.

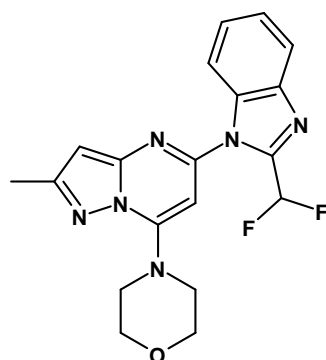
Numer związku	Rozpuszczalność [μM]	MLM $t_{1/2}$ [min]	MLM CI [ml × min ⁻¹ × mg ⁻¹]	HLM $t_{1/2}$ [min]	HLM CI [ml × min ⁻¹ × mg ⁻¹]
37	444	126	13.7	76	22.8
54	>500	198	7.0	370	3.7

CPL302253 został wyselekcjonowany jako obiecujący kandydat kliniczny w leczeniu astmy.

Wyniki powyższych badań zostały szczegółowo opisane w publikacji **P1**, stanowiącej część rozprawy doktorskiej.

5.2. Publikacja 2 – P2

W pracy uwaga została skupiona na rdzeniu pirazolo[1,5-*a*]pirymidyny, który stanowi najkorzystniejszą bazę do dalszej funkcjonalizacji oraz projektowania potencjalnych leków do zastosowania w terapii chorób nowotworowych, jak również schorzeń autoimmunologicznych i wirusowych [61-67]. W pracy opisane zostały biblioteki związków z różnymi podstawnikami (aminami) w pozycji C(2) rdzenia oraz odmiennymi ugrupowaniami benzimidazolowymi w pozycji C(5). W poprzedniej pracy wykazano, że pochodne 5-indol-4-ilo-pirazolo[1,5-*a*]pirymidyny, jako inhibitory PI3K δ wykazywały najwyższą selektywność względem pozostałych izoform α, β i γ [48]. Z drugiej strony określono, iż pochodna 2-difluorometylobenzimidazolu (Rysunek 11) wykazuje największą aktywność względem PI3K δ .

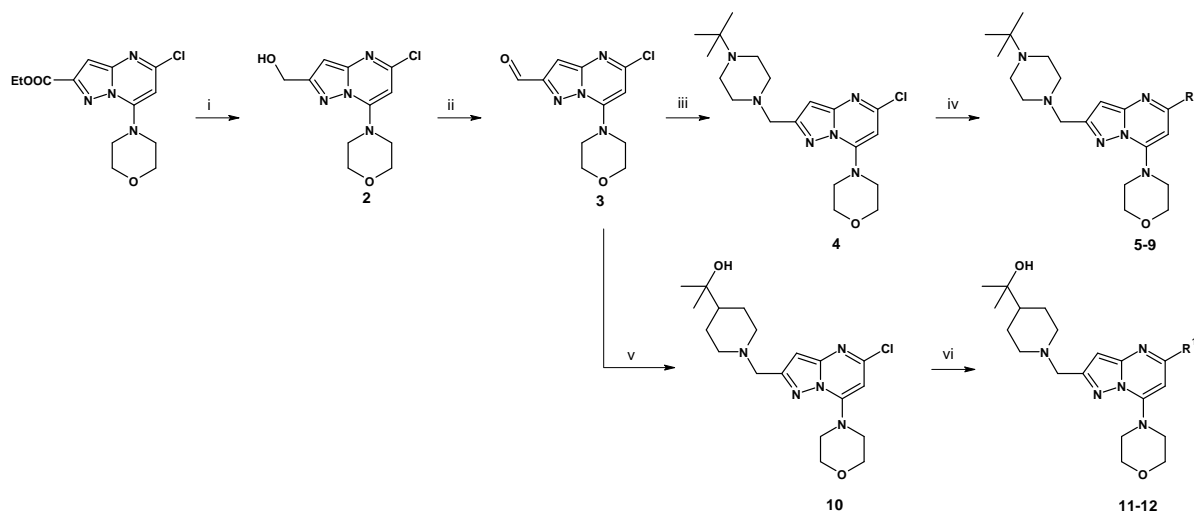


Rysunek 11. Wzór strukturalny wyjściowej pochodnej do budowania biblioteki – 2-metylo-5-(2-difluorometylo)pirazolo[1,5-*a*]pirymidyna; IC₅₀ PI3K δ =475 nM, IC₅₀ PI3K α =1060 nM.

Na podstawie otrzymanych danych, zaprojektowano odpowiednie modyfikacje rdzenia 5-bezimidazol-1-ilo-pirazolo[1,5-*a*]pirymidyny, które przyczyniły się do poprawy zarówno aktywności, jak i selektywności otrzymywanych struktur. Z tego powodu, w oparciu o badania

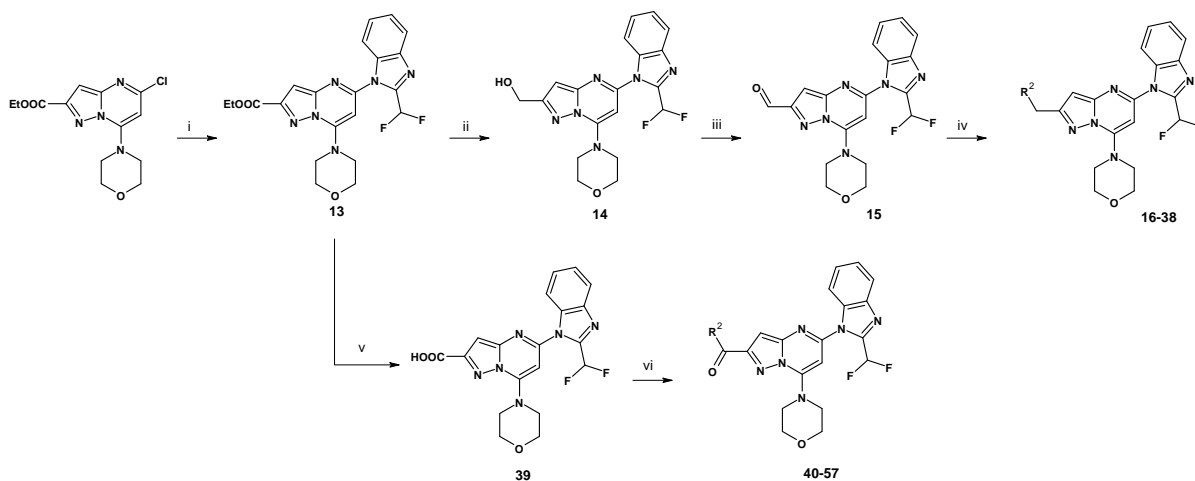
SAR (ang. *Structure-Activity Relationship*) w pracy zostały opisane i otrzymane nowe, bardzo aktywne i obiecujące inhibitory PI3K δ [49].

Na drodze wieloetapowej syntezy zostały otrzymane związki z modyfikacjami w pozycjach C(2) – podstawnik R² (Schemat 2), oraz C(5) – podstawnik R¹ (Schemat 1). W przypadku R¹ były to różnego rodzaju benzimidazole (dla dwóch wybranych amin: piperazyny i piperidyń).



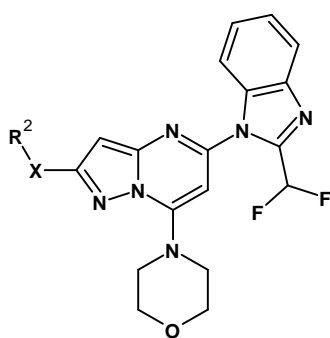
Schemat 1. Synteza pochodnych benzimidazolowych. Reagenty i warunki prowadzenia reakcji: (i) CaCl₂, NaBH₄, EtOH, t.wrz., 3 h, 99%; (ii) odczynnik Dess–Martina, DMF, t.pok., 2 h, 46%; (iii) 1-*tert*-butylpiperazyna, triacetoksyborowoderek sodu, DCM, t.pok., 18 h, 84%; (iv) benzimidazol, tris(dibenzylidenoaceton)dipalladu(0), 9,9-dimetylo-4,5-bis(difenylofosfino)xanten, Cs₂CO₃, toluen, 150 °C, 6 h, 200 W, MW, 4–93%; (v) 2-(4-piperidyl)-2-propanol, triacetoksyborowoderek sodu, DCM, t.pok., 63%; (vi) benzimidazol, tris(dibenzylidenoaceton)dipalladu(0), 9,9-dimetylo-4,5-bis(difenylofosfino)xanten, Cs₂CO₃, toluen, 150 °C, 6 h, 200 W, MW, 52–66%.

W zależności od rodzaju i wielkości podstawnika, aktywność związków wykazywała wartości IC₅₀ PI3K δ od 0,1 μ M do ponad 1 μ M. Jako najlepszy został wybrany 2-(difluorometylo)-1*H*-benzimidazol. Po wyselekcjonowaniu najlepszego podstawnika w pozycji R¹, optymalizacji został poddany R² (Schemat 2).



Schemat 2. Synteza pochodnych 5-(2-difluorometylobenzimidazo-1-ylo)pirazolo[1,5-*a*]pirymidyny. Reagenty i warunki prowadzenia reakcji: **(i)** 2-(difluorometylo)-1*H*-benzimidazol, TEACl, K₂CO₃, DMA, 160 °C, 3 h, 89%; **(ii)** LiAlH₄, THF, 0 °C, 3 h, 89%, **(iii)** odczynnik Dess–Martina, DMF, t.pok., 1 h, 78% or MnO₂, toluen:octan butylu, t.wrz. 1.5 h, 68%; **(iv)** amina, triacetoksyborowoderek sodu, DCM, t.pok., 18 h, 38–93%; **(v)** LiOH, MeOH, H₂O, t. pok., 98%; **(vi)** amina, HATU, TEA, t.pok., 2 h, 33–81%.

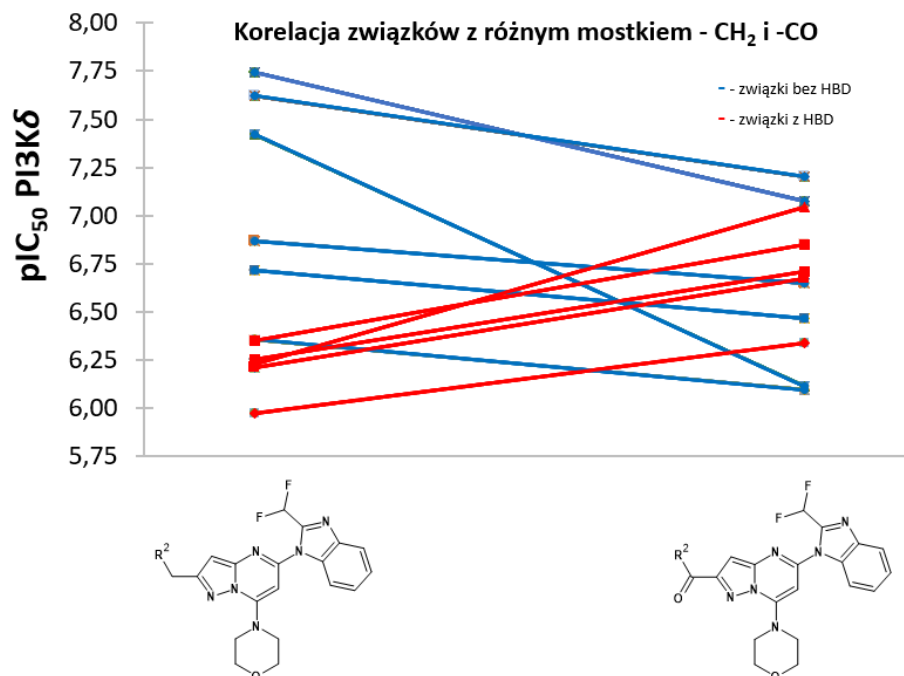
W tym wypadku, w oparciu o analizę wyników dokowania molekularnego, wybrano różnego rodzaju heterocykliczne aminy, takie jak np. pochodne piperazyny, piperydyny, aminy heterocykliczne pięcioczłonowe oraz inne aminy z rozbudowanymi sterycznie grupami. Ponadto, analiza modelu wiązania w kieszeni katalitycznej wykazała, że możliwe jest powstanie dodatkowych wiązań wodorowych, w zależności od heterocyklu, stabilizujących ułożenie i konformację ligandu w białku. Może to być uzyskane dzięki zastąpieniu mostka metylenowego (X, Rysunek 12), mostkiem karbonylowym (powstanie układu amidowego). Synteza takich związków nie była skomplikowana, składała się z mniejszej liczby etapów, a dodatkowo nie wymagała drogich reagentów.



Rysunek 12. Wzór ogólny analogów inhibitorów PI3K δ .

Zmiana wspomnianego mostka X pozwoliła na sformułowanie wniosku dotyczącego wpływu obecności lub braku grupy HBD (ang. *Hydrogen Bond Donor*) w strukturze podstawnika R². Dla związków z mostkiem metylenowym bardziej aktywne są analogi bez

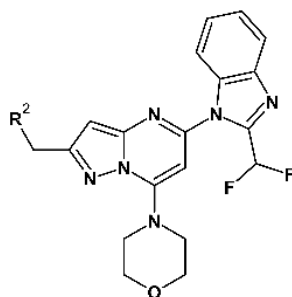
wyżej wspomnianej grupy. Z kolei dla związków z mostkiem karbonylowym obecność HBD jest bardziej preferowana (Schemat 3).



Schemat 3. Schemat przedstawiający korelację związków z różnym mostkiem w pozycji „X” dla wybranych związków posiadających HBD i bez HBD.

Z całej biblioteki otrzymanych struktur, na podstawie ich właściwości, zostało wybranych pięć związków najbardziej obiecujących, tzw. „hitów” (jedenaście związków wykazywało aktywność inhibitorów względem PI3K δ z wartością poniżej 100 nM, wspomniane pięć osiągało wartość IC₅₀ na poziomie równym 52 nM lub poniżej tej wartości; Tabela 3).

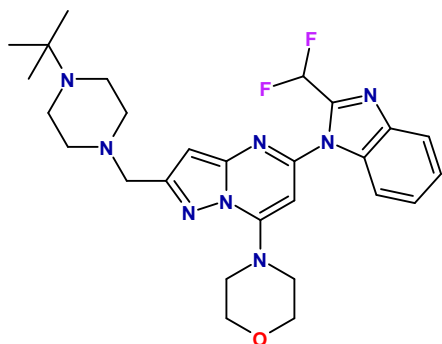
Tabela 3. Wartości aktywności i selektywności dla wybranych, najbardziej obiecujących związków.



Numer związku	R ²	IC ₅₀ PI3K δ [nM]	IC ₅₀ PI3K α [nM]	IC ₅₀ PI3K β [nM]	IC ₅₀ PI3K γ [nM]	α/δ	β/δ	γ/δ	IC ₅₀ CD19 [nM]
6		18	1 428	25 475	16 904	79	1 415	939	41
11		52	1 729		6 347	33		122	
16		43	44	13 577	111	1,0	316	2,6	114
17		31	624	44 753	2 197	20	1 444	71	52
18		24	73	47 360	156	3,0	1 973	6,5	58

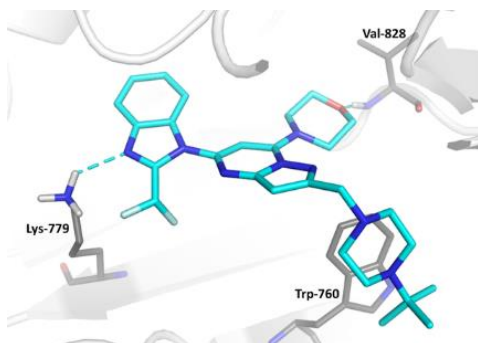
Wartości IC₅₀ zostały wyliczone jako wartość średnia z dwóch niezależnych eksperymentów.

Spośród aktywnych związków, biorąc pod uwagę aktywność enzymatyczną i komórkową, stabilność metaboliczną, jak również stopień wiązania z białkami oraz szereg innych ważnych z punktu widzenia chemii medycznej parametrów (parametry farmakokinetyczne, farmakodynamiczne oraz ADMET), wyselekcjonowany został jeden jako najbardziej obiecujący inhibitor PI3K δ - (1-{2-[(4-*tert*-butylopiperazyn-1-ylo)metylo]-7-(morfolin-4-ylo)pirazolo[1,5-*a*]pirymidyn-5-ylo}-2-(difluorometylo)-1*H*-benzimidazol (CPL302415) (Rysunek 13).



Rysunek 13. Wzór strukturalny CPL302415.

Związek charakteryzuje się wysoką aktywnością ($IC_{50} = 18 \text{ nM}$) oraz selektywnością ($PI3K\alpha/PI3K\delta = 79$; $PI3K\beta/\delta = 1415$; $PI3K\gamma/PI3K\delta = 939$). Analiza modelu wiązania związku CPL302415 wykazała, że związek ten tworzy wiązania wodorowe z Val-828 oraz Lys-779, jak również widoczne jest oddziaływanie z „półką tryptofanową” – Trp-760, co ma odzwierciedlenie w bardzo dobrej aktywności i selektywności struktury (Rysunek 14).



Rysunek 14. Model dokowania 3D kluczowych wiązań z aminokwasami na przykładzie związku CPL302415 (PDB ID:2WXL).

Pozostałe parametry, takie jak rozpuszczalność, stabilność mikrosomalna, przepuszczalność przez błony czy zdolność do wiązania innych białek (ang. PPB: *Protein Protein Binding*) także są optymalne i gwarantujące wysoki potencjał terapeutyczny (Tabela 4).

Tabela 4. Wybrane parametry związku CPL302415 (6).

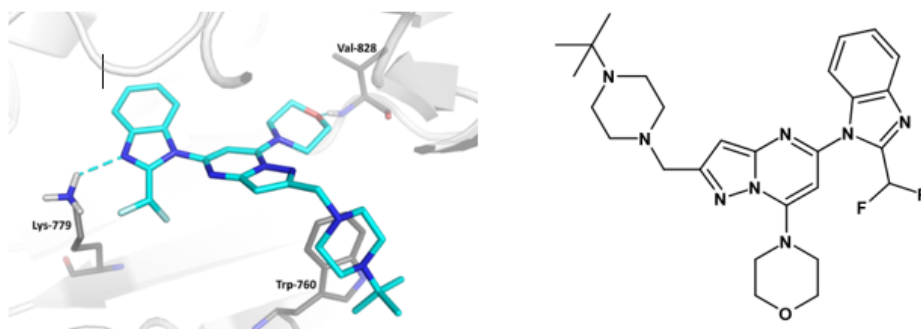
Rozpuszczalność kinetyczna pH 7.4 [mM]	Stabilność metaboliczna				PAMPA [$10^{-6} \text{ cm} \times \text{s}^{-1}$]	Procent wiązania z białkiem PPB [%]				
	MLM $t_{1/2}$ [min]	MLM CL [$\text{mL} \times \text{mn}^{-1} \times \text{mg}^{-1}$]	HLM $t_{1/2}$ [min]	HLM CL [$\text{mL} \times \text{min}^{-1} \times \text{mg}^{-1}$]		Człowiek	Małpa	Mysz	Szczur	
6	>500	378	3,7	145	9,6	13,3	79	81	83	82

Przeprowadzono także analizę kosztów, a następnie syntezę w większej skali (etap powiększania skali) celem otrzymania cząsteczki w skali jednego kilograma do badań toksykologicznych. Związek CPL302415 został wyselekcjonowany jako związek wiodący, tzw. „lead” do badań toksykologicznych oraz jako doskonały kandydat do pierwszej fazy badań klinicznych w leczeniu toczenia rumieniowatego.

Wyniki powyższych badań zostały opisane szczegółowo w publikacji **P2**, stanowiącej część rozprawy doktorskiej.

5.3. Publikacja 3 – P3

W celu racjonalnego projektowania nowych biologicznie aktywnych związków chemicznych, m.in. inhibitorów enzymów, potencjalnych kandydatów na leki, wykorzystywane są metody modelowania molekularnego. Zalicza się do nich między innymi dokowanie molekularne, dokowanie z indukowanym dopasowaniem (IFD; ang.: *Induced-Fit Docking*), *quantum-polarized ligand docking*, QPLD – ligand traktowany na poziomie kwantowym, otoczenie – aminokwasy na poziomie pola sił OPLS3e, (ang.: *Quantum Polarized Ligand Docking*), dynamika molekularna (MD; ang.: *Molecular Dynamic*), czy zaburzenia energii swobodnej. Wykorzystywane są one do oceny możliwości tworzenia kompleksów ligand-receptor i umożliwiają szybką ocenę dopasowania struktur do kieszeni katalitycznej z obszernej biblioteki związków. Najczęściej wykorzystywana jest metoda dokowania molekularnego, jednak ma ona główne dwa ograniczenia, a mianowicie sztywna konformacja kieszeni wiążącej enzymu (ograniczenia systemowe), a także przypisane ładunki atomowe (brak złożonych efektów indukcyjnych lub rezonansowych), co ma znaczenie w przypadku np. pochodnych fluorowych. Z tych powodów w pracy opisano nowy, zaawansowany model obliczeniowy do projektowania i określania aktywności biologicznej związków, inhibitorów kinazy PI3K δ . Skupiono się na fluorowanych pochodnych, analogach CPL302415 (Rysunek 15) oraz przedstawiono wpływ atomu fluoru na właściwości wybranych struktur. W celu weryfikacji metody, dane otrzymane z modelu obliczeniowego zestawiono i skorelowano z wynikami aktywności związków otrzymanymi w badaniach *in vitro* (wartości IC₅₀).



Rysunek 15. Model wiązania CPL302145 w centrum katalitycznym kinazy PI3K δ otrzymany poprzez dokowanie molekularne (po lewej); struktura CPL302415 (po prawej).

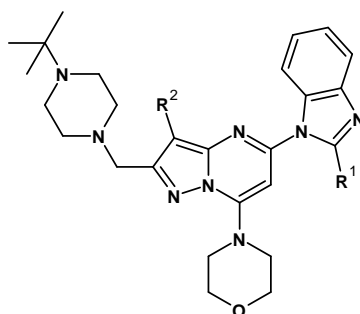
Atom fluoru odgrywa bardzo ważną rolę w chemii medycznej i projektowaniu leków. Wpływa na zmianę parametrów, takich jak lipofilowość, zasadowość bądź kwasowość sąsiadujących grup funkcyjnych oraz aktywność biologiczną, w tym biodostępność i metabolizm. Potwierdzają to wyraźnie statystyki – ponad 50% najbardziej dochodowych leków na świecie (ang.: *blockbusters drugs*) stanowią fluorowane farmaceutyki, a w przeciągu ostatniego dziesięciolecia FDA zatwierdziło prawie 30% leków zawierających w swojej strukturze atom fluoru lub grupy fluoroalkilowe [68, 69].

Dokowanie molekularne struktury CPL302415 [48,49] za pomocą oprogramowania Maestro Schrödinger potwierdziły sposób wiązania z kinazą PI3K δ , który wcześniej został określony za pomocą oprogramowania AutoDock Vina. Wszystkie obecne kluczowe oddziaływania inhibitora z aminokwasami Lys-779, Val-828 oraz Trp-760 pokrywały się w obu modelach. Warto podkreślić, że standardowe podejście dokowania nie zakłada dynamicznego charakteru struktur biologicznych, jedynie statyczne, dlatego potrzebne są bardziej zaawansowane metody (IFD, QPLD) [70]. Zbadane i zaprojektowane zostały związki zawierające atom fluoru, zarówno w strukturze rdzenia pirazolo[1,5-*a*]pirymidynowego, jak i odpowiednio sfunkcjonalizowanej aminy stanowiącej podstawnik w pozycji C(2) rdzenia. Porównanie położenia (tzw. *póz*) każdego związku w białku oraz zbadanie zmian molekularnych pozwoliły określić różnice sposobu wiązania fluorowanych struktur (oddziaływania ligand-receptor), co wpływa na aktywność biologiczną inhibitorów. Wyniki porównano z otrzymanymi eksperymentalnie wartościami IC₅₀ dla PI3K δ .

Ze względu na dużą elektroujemność atomu fluoru (największa spośród pierwiastków układu okresowego), wpływa on na zmianę efektów w rozkładzie gęstości elektronowej poprzez efekty rezonansowe i indukcyjne. W tym celu wykorzystano QPLD, aby uwzględnić wspomniane efekt, a ponadto zminimalizować niepewność pozycji i jednocześnie przy pomocy modelu GBSA (ang.: *Generalized Born Surface Area*) oszacowano entalpię swobodną oddziaływań ligand-receptor. Dodatkowo, atom fluoru może być użyty jako bioizoster atomu wodoru (ze względu na zbliżony promień atomowy), dlatego też fluor nie powinien powodować dużych zmian konformacyjnych [71-74]. Zastosowany model obliczeniowy opierał się na wykorzystaniu dokowania z dopasowaniem indukowanym, symulacji dynamiki molekularnej oraz kwantowego dokowania spolaryzowanego ligandu połączonego z obliczeniami energetycznymi (metoda MM-GBSA, ang.: *Molecular Mechanics Generalized Born Surface Area*) [75-77].

Analiza trajektorii dynamiki molekularnej dla CPL302415 wykazała i potwierdziła, że oddziaływania z kinazą są stabilne, a atom fluoru nie tworzy dodatkowych oddziaływań z białkiem. W celach porównawczych zsyntezowano i przeanalizowano również pochodne z podstawionym chlorem i bromem (Tabela 5). Niestety ze względów syntetycznych nie udało się otrzymać analogicznej pochodnej fluorowej. Wyraźnie zaobserwowano, że CPL302415 jest najbardziej aktywną i obiecującą cząsteczką, co potwierdzają obliczenia (Tabela 5).

Tabela 5. Wpływ atomu/atomów fluoru na PI3K δ oraz wyznaczone wartości parametrów dokowania dla każdego związku.

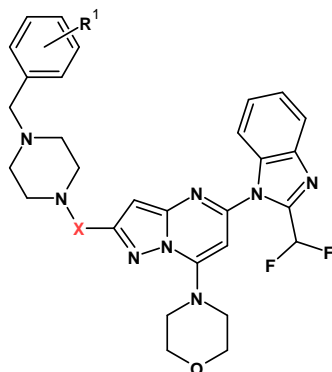


Związek	R ¹	R ²	IC ₅₀ PI3K δ [nM] ^a	$\overline{\Delta G}$	$\Delta\Delta G$
1	CH ₃	H	236	-75.0	-
2	CHF ₂	H	18	-82.6	-7.6
3	CF ₃	H	907	-69.6	-5.4
4	CHF ₂	Cl	44	-81.3	1.3 ^b
5	CHF ₂	Br	50	-81.2	1.4 ^b

^a Wartości IC₅₀ zostały wyliczone jako wartość średnia z dwóch niezależnych eksperymentów; ^b Wartości $\Delta\Delta G$ obliczono jako różnicę pomiędzy daną pochodną a jej nichalogenowanym analogiem 2-(difluorometylo)-1H-benzimidazolu.

Dla pochodnych z obecnym atomem fluoru w części aminowej inhibitora, aktywność zmienia się wraz z pozycją podstawienia fluoru, co potwierdzają wartości zarówno obliczeniowe, jak i eksperymentalne (Tabela 6).

Tabela 6. Wpływ atomu/atomów fluoru na PI3K δ oraz wyznaczone wartości parametrów dokowania dla każdego związku.



Związek	X	R ¹	IC ₅₀ PI3K δ [nM] ^a	$\overline{\Delta G}$	$\Delta\Delta G$
6	CH	-	118	-86.7	-
7	CH	<i>o</i> -F	640	-83.4	3.3
8	CH	<i>m</i> -F	751	-81.8	4.9
9	CH	<i>p</i> -F	489	-84.1	2.6
10	CO	-	275	-78.9	-
11	CO	<i>o</i> -F	212	-83.8	-4.9
12	CO	<i>m</i> -F	92	-86.6	-7.7
12	CO	<i>p</i> -F	181	-83.8	-4.9

^a Wartości IC₅₀ zostały wyliczone jako wartość średnia z dwóch niezależnych eksperymentów; ^b Wartości $\Delta\Delta G$ obliczono jako różnicę pomiędzy daną pochodną a jej niehalogenowanym analogiem (difluorometylo)-1*H*-benzimidazolu.

W pracy wykazano, że wykorzystanie wyżej wymienionego protokołu obliczeniowego może być wykorzystane do projektowania oraz oceny nowych związków biologicznie aktywnych. Dodatkowo, pozwala ocenić wpływ atomu fluoru na cząsteczkę z uwzględnieniem efektów rezonansowych i indukcyjnych. Wyniki dalszych badań potwierdziły, że proponowany model jest właściwym narzędziem obliczeniowym do projektowania nowych związków, o potencjalnych właściwościach leczniczych.

Wyniki powyższych badań zostały szczegółowo opisane w publikacji **P3**, stanowiącej część rozprawy doktorskiej.

6. Wyniki wchodzące w skład publikacji w trakcie przygotowania

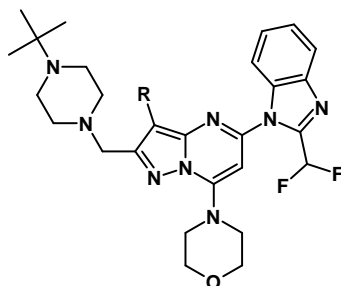
Interesującym zagadnieniem jest wpływ podstawnika w pozycji trzeciej układu pirazolo[1,5-*a*]pirymidynowego. Wprowadzenie modyfikacji w tym miejscu poprzez zamianę atomu wodoru na halogen lub łańcuch alifatyczny pozwoli określić wpływ na aktywność i selektywność. Uzyskanie danych z hamowania aktywności enzymatycznej białka PI3K δ dla tych związków pozwoli określić możliwości oddziaływania z odpowiednimi aminokwasami. Optymalizacji poddano związek wiodący, wybrany jako kandydat do I fazy badań klinicznych, CPL302415.

CPL302415 tworzy charakterystyczne wiązania wodorowe z miejscem wiążącym enzymu. Należą do nich: oddziaływanie między waliną Val-828 a ugrupowaniem morfolinowym, oddziaływanie pomiędzy atomem azotu pochodzącym z benzimidazolu a Lys-779, oraz pomiędzy *N-tert*-butylopiiperazyną a Trp-760 (zwaną "półką tryptofanową"). Oddziaływania zostały szczegółowo opisane w **P1** oraz **P2**. Wraz ze zmianą podstawnika w pozycji trzeciej rdzenia cząsteczki, oddziaływania mogą ulegać modyfikacji i rearanzacji.

Bardziej rozbudowane, obszerne sterycznie podstawniki mogą powodować zwiększenie dystansu od poszczególnych aminokwasów oraz zmianę a nawet zanik charakterystycznych oddziaływań. Otrzymano szereg analogów CPL302415 opierających się na szkielecie pirazolo[1,5-*a*]pirymidyny. Związki posiadały różne grupy w pozycji trzeciej rdzenia (podstawnik R; Tabela 7). Zsyntezowano struktury zawierające jako R grupę metylową, etylową, izopropylową, a także halogenopochodne (pochodna chlorowana, bromowana, fluorowana). Synteza chemiczna opierała się na ścieżce jedno- lub dwuetapowej z wykorzystaniem reakcji substytucji oraz sprzęgania – reakcja Suzuki z odpowiednimi kwasami lub estrami boranowymi. Z powodu problemów syntetycznych z otrzymaniem części analogów, synteza kilku pochodnych nadal podlega optymalizacji, a ścieżka syntetyczna jest zmieniana i optymalizowana. Prace nad otrzymaniem pochodnej izopropylowej oraz fluorowanej trwają do chwili obecnej. Otrzymane związki poddane zostały enzymatycznym testom kinazowym w celu wyznaczenia wartości IC₅₀ (Tabela 7). Określona zostanie aktywność i selektywność otrzymanych związków, a także znaczenie podstawnika/ugrupowania w pozycji trzeciej rdzenia. Zweryfikowana zostanie hipoteza postawiona w wyniku przeprowadzonego dokowania molekularnego cząsteczek (podstawionych różnymi grupami w pozycji trzeciej

rdzenia) w kieszeni wiążącej enzymu, a szczegółowa analiza otrzymanych danych oraz wyniki zostaną opublikowane w odrębnej pracy. Obecnie manuskrypt jest w przygotowaniu.

Tabela 7. Poziom inhibicji PI3K δ wyznaczony dla pochodnych pirazolo[1,5-*a*]pirymidyny (modyfikacje pozycji trzeciej rdzenia).



Numer związku	R	IC ₅₀ PI3K δ [nM]	IC ₅₀ PI3K α [nM]	IC ₅₀ PI3K β [nM]	IC ₅₀ PI3K γ [nM]	α/δ	β/δ	γ/δ
1	H	18	1 428	25 475	16 904	80	1 415	939
2	CH ₃	8	1 565	37 704	9 567	196	4713	1 196
3	CH ₃ CH ₂	34	ND	ND	12 730	ND	ND	374
4	<i>i</i> -Pr	ND	ND	ND	ND	ND	ND	ND
5	F	ND	ND	ND	ND	ND	ND	ND
6	Cl	47	ND	ND	17 350	ND	ND	369
7	Br	48	1 729	ND	14 191	ND	ND	296

ND – dane niedostępne, w opracowaniu, wartości w trakcie wyznaczania/ związek w trakcie syntezy lub optymalizacji.

*Wartości IC₅₀ zostały wyliczone jako wartość średnia z dwóch niezależnych eksperymentów

7. Doktorat wdrożeniowy – wdrożenie do przemysłu

Powyższa rozprawa doktorska weszła w poczet doktoratu wdrożeniowego, została wykonana w ramach współpracy pomiędzy Politechniką Warszawską a firmą farmaceutyczną Celon Pharma S.A. Praca dotyczyła zaprojektowania, zsyntezowania aktywnego inhibitora kinazy PI3K δ , (cel terapeutyczny w leczeniu toczenia rumieniowatego lub innych chorób zapalnych i autoimmunologicznych) wykonania wszystkich niezbędnych analiz fizykochemicznych i biologicznych, a następnie powiększenia skali z otrzymaniem związku w ilości niezbędnej do wykonania badań toksykologicznych celem możliwości wejścia w pierwszą fazę badań klinicznych. Efektem doktoratu jest wdrożenie technologii syntezy substancji czynnej CPL302415. Zakończone sukcesem wdrożenie technologii syntezy umożliwi realizację kolejnych etapów prac rozwojowych. Dalsze badania wymagane do wprowadzenia nowego produktu leczniczego do praktyki klinicznej przekraczają ramy niniejszego doktoratu i obejmują:

- badania toksykologiczne,
- opracowanie formy leku i wdrożenie jej technologii,
- wytworzenie badanego produktu leczniczego do badań klinicznych,
- ocena bezpieczeństwa i farmakokinetyki badanego produktu leczniczego w badaniu klinicznym I fazy,
- ocenę zależności dawka-odpowiedź terapeutyczna oraz wstępną ocenę skuteczności w leczeniu toczenia rumieniowatego (SLE) oraz potencjalnie innych chorób zapalnych i autoimmunologicznych w badaniach II fazy,
- ocenę skuteczności i bezpieczeństwa w badaniach III fazy,
- złożenie dokumentacji rejestracyjnej.

Wykonane w ramach doktoratu wdrożenie technologii syntezy jest spełnieniem warunku koniecznego do wprowadzenia do praktyki klinicznej nowego produktu leczniczego zawierającego związek CPL302415 jako substancję czynną. Pomyślna realizacja kolejnych etapów prac rozwojowych pozwoli na poprawę jakości życia pacjentów z SLE, co było głównym przesłaniem podjęcia pracy doktorskiej i wdrożenia jej wyników.

8. Podsumowanie i wnioski

Celem niniejszej pracy było otrzymanie aktywnego i selektywnego inhibitora kinazy PI3K δ , potencjalnego kandydata klinicznego, a w przyszłości leku w leczeniu toczenia rumieniowatego i innych chorób zapalnych i autoimmunologicznych. Wykorzystując narzędzia modelowania molekularnego z pełną analizą struktury krystalograficznej białka zaprojektowany został cały szereg związków, potencjalnych inhibitorów PI3K δ . Modelowanie molekularne pozwoliło określić, gdzie występuje największe prawdopodobieństwo wiązania liganda z białkiem, oraz które oddziaływania są kluczowe do osiągnięcia pożądanej aktywności związków. Dzięki tym informacjom, a także odpowiednim predykcjom właściwości cząsteczek, zaprojektowano odpowiednie podstawniki wybranego rdzenia pirazolo[1,5-*a*]pirymidyny. Następnym etapem była synteza biblioteki wybranych, zaprojektowanych związków. Wieloetapowa synteza chemiczna prowadziła do otrzymania biblioteki ponad 100 związków – pochodnych indolowych (część z nich opisanych w pierwszej publikacji: 33 związki, **P1**) oraz pochodnych benzimidazolowych (część z nich opisanych w drugiej publikacji: 48 związków, **P2**). Z szeregu otrzymanych związków zostały wyselekcjonowane najkorzystniejsze, zarówno pod względem aktywności, selektywności, parametrów fizykochemicznych, jak farmakokinetycznych i toksykologicznych. Z pochodnych indolowych wybrano związek CPL302253 – kandydat w leczeniu astmy i POChP (**P1**). CPL302415 został wyselekcjonowany jako związek wiodący w leczeniu toczenia rumieniowatego - najbardziej aktywna i selektywna struktura oparta na strukturze 2-metylodifluorobenzimidazolu (**P2**). Cząsteczka została zsyntezowana w większej skali (jednego kilograma) i poddana badaniom toksykologicznym. Jako obiecująca struktura jest kandydatem klinicznym do przeprowadzenia badań klinicznych, a w przypadku pomyślnych wyników w przyszłości może być wytwarzana jako substancja czynna produktu leczniczego stosowanego w terapii toczenia rumieniowatego. Pomyślny przebieg dalszych prac rozwojowych pozwoli na pełną realizację założeń doktoratu wdrożeniowego – poprawę zdrowia i jakości życia pacjentów z SLE.

Opisany w pracy model predykcji aktywności związków w oparciu o dokowanie molekularne połączone z odpowiednim modelem matematycznym (**P3**) może być narzędziem wykorzystywanym w kolejnych projektach badawczych. Przewidywane aktywności wynikające z obliczeń modelowych zostały potwierdzone eksperymentalnie z określeniem wartości parametru IC₅₀. Pozwala to na obiecujące projektowanie nowych leków, szczególnie dla cząsteczek halogenopochodnych.

Uwagę skupiono także na badaniu wpływu podstawnika w pozycji trzeciej rdzenia pirazolo[1,5-*a*]pirymidyny. Porównano wyniki badań dokowania molekularnego, przeanalizowano struktury krystalograficzne, wyznaczono aktywność i selektywność dla pochodnych alifatycznych (pochodna metylowa, etylowa) i halogenowych (chloropochodna, bromopochodna) we wspomnianej pozycji. Zsyntezowano odpowiednie struktury w oparciu o modyfikacje aktywnego inhibitora CPL302415. Sprawdzono wpływ podstawnika w pozycji trzeciej rdzenia cząsteczki na oddziaływania z aminokwasami w kieszeni wiążącej białka. Przeanalizowano zależność rodzaju i wielkości podstawnika na zmiany sposobu wiązania z kinazą, a w konsekwencji na aktywność i selektywność związku jako inhibitora kinazy PI3K. Wyniki opisano w kolejnym manuskrypcie, który obecnie jest w trakcie recenzji.

9. Literatura cytowana/ Bibliografia

- [1] Foster, J.G.; Blunt, M.D.; Carter, E.; Ward, S.G.; “Inhibition of PI3K Signaling Spurs New Therapeutic Opportunities in Inflammatory/Autoimmune Diseases and Hematological Malignancies”; *Pharmacol. Rev.* **2012**, 64, 1027–1054;
- [2] Banham-Hall, E.; “The Therapeutic Potential for PI3K Inhibitors in Autoimmune Rheumatic Diseases”; *Open Rheumatol. J.* **2012**, 6, 245–258;
- [3] Stark A.K., Sriskantharajah S., Hessel E. M., Okkenhaug K.; “PI3K inhibitors in inflammation, autoimmunity and cancer”; *Curr Opin Pharmacol.* **2015**, 23, 82–91;
- [4] Peter K. Vogt, Jonathan R. Hart, Marco Gymnopoulos, Hao Jiang, Sohye Kang, Andreas G. Bader, Li Zhao, Adam Denley; “Phosphatidylinositol 3-kinase (PI3K): The Oncoprotein”; *Curr Top Microbiol Immunol.* **2010**, 347,79–104;
- [5] Puri K.D., Gold M.R.; “Selective inhibitors of phosphoinositide 3-kinase delta: modulators of B-cell function with potential for treating autoimmune inflammatory diseases and B-cell malignancies”; *Front Immunol.* **2012**, 23,3–256;
- [6] Suarez-Fueyo A., Rojas J.M., Cariaga A.E., Garcia E., Steiner B.H., Barber D.F., Puri K.D., Carrera A.C.; “Inhibition of PI3K Reduces Kidney Infiltration by Macrophages and Ameliorates Systemic Lupus in the Mouse”; *J. Immunol.* **2014**, 193(2), 544–54;
- [7] Haselmayer P., Camps M., Muzerelle M., Bawab S., Waltzinger C., Bruns L., Abla N., Polokoff M.A., Jond-Necand, Gaudet M., Benoit A., Bertschy Meier D., Martin C., Gratener D., Lombardi M.S., Grenningloh R., Ladel C., Petersen J.S., Gaillard P., Ji H.; “Charakterization of novel PI3K δ inhibitors as potential therapeutics for SLE and lupus nephritis in pre-clinical studies”; *Front Immunol.* **2014**, 22, 5,233;
- [8] Suarez-Fueyo A., Barber D.F., Martinez-Ara J., Zea-Mendoza A.C., Carrera A.C.; “Enhanced Phosphoinositide 3-Kinase δ Activity Is a Frequent Event in Systemic Lupus Erythematosus that Confers Resistance to Activation-Induced T Cell Death”; *J. Immunol.* **2011**, 1, 187(5), 2376–85;
- [9] – Zgłoszenie patentowe MX 2017011423 (A); “7-(Morpholin-4-yl)pyrazole[1,5-

- a]pyrimidine derivatives which are useful for the treatment of immune or inflammatory diseases or cancer” ;
- [10] Zgłoszenie patentowe WO 2013/28263; “Pyrazolopyrimidine derivatives as PI3 Kinase inhibitors”;
- [11] Zgłoszenie patentowe WO 2003/101993; “Pyrazolo[1,5-*a*]pyrimidine Compounds as Antiviral Agents”;
- [12] Liu Y., Shreder K.R., Gai W., Corral S., Ferris D.K., Rosenblum I.; “Wortmannin, a widely used phosphoinositide- 3-kinase inhibitor, also potently inhibits mammalian polo-like kinase”; *Chem. Biol.* **2005**; 12: 99-107;
- [13] Okkenhaug, K.; Vanhaesebroeck, B.; „PI3K-Signalling in B- and T-Cells: Insights from Gene-Targeted Mice”; *Biochem. Soc. Trans.*; **2003**, 31, 270–274;
- [14] Okkenhaug, K.; Vanhaesebroeck, B.; „PI3K in Lymphocyte Development, Differentiation, and Activation”; *Nat. Rev. Immunol.* **2003**, 3, 317–330;
- [15] Rommel, C.; Camps, M.; Ji, H.; „PI3K δ and PI3K γ : Partners in Crime in Inflammation in Rheumatoid Arthritis and Beyond?”; *Nat. Rev. Immunol.*; **2007**, 7, 191–201;
- [16] Thomas, M.; Owen, C.; „Inhibition of PI-3 Kinase for Treating Respiratory Disease: Good Idea or Bad Idea?”; *Curr. Opin. Pharmacol.*; **2008**, 8, 267–274.
- [17] Chris J. Vlahos, et al. (1994); “A Specific Inhibitor of Phosphatidylinositol 3-Kinase, 2 (4- Morpholinyl)-8-phenyl-4H-I-benzopyran-4-one (LY 294002); *J. Biol. Chem.*; **1994**; 269(7): 5241-5248; 9;
- [18] Cantley, L.C.; “The Phosphoinositide 3-Kinase Pathway”; *Science* **2002**, 296, 1655 1657;
- [19] Liu, P.; Cheng, H.; Roberts, T.M.; Zhao, J.J.; “Targeting the Phosphoinositide 3-Kinase Pathway in Cancer”; *Nat. Rev. Drug Discov.*; **2009**, 8, 627–644;
- [20] Knight, Z.A.; Gonzalez, B.; Feldman, M.E.; Zunder, E.R.; Goldenberg, D.D.; Williams, O.; Loewith, R.; Stokoe, D.; Balla, A.; Toth, B.; et al.; „A Pharmacological Map of the PI3-K Family Defines a Role for P110 α in Insulin Signaling”; *Cell* **2006**, 125, 733–747;
- [21] Berndt, A.; Miller, S.; Williams, O.; Le, D.D.; Houseman, B.T.; Pacold, J.I.; Gorrec, F.; Hon, W.-C.; Ren, P.; Liu, Y.; et al.; „Erratum: Corrigendum: The P110 δ Structure:

- Mechanisms for Selectivity and Potency of New PI(3)K Inhibitors”; *Nat. Chem. Biol.* **2010**, 6, 244–244;
- [22] Cushing, T.D.; Metz, D.P.; Whittington, D.A.; McGee, L.R.; “PI3K δ and PI3K γ as Targets for Autoimmune and Inflammatory Diseases”; *J. Med. Chem.* **2012**, 55, 8559–8581;
- [23] Perry, M.W.D.; Abdulai, R.; Mogemark, M.; Petersen, J.; Thomas, M.J.; Valastro, B.; Westin Eriksson, A.; „Evolution of PI3K γ and δ Inhibitors for Inflammatory and Autoimmune Diseases.” *J. Med. Chem.* **2019**, 62, 4783–4814;
- [24] Murray, J.M.; Sweeney, Z.K.; Chan, B.K.; Balazs, M.; Bradley, E.; Castanedo, G.; Chabot, C.; Chantry, D.; Flagella, M.; Goldstein, D.M.; et al.; „Potent and Highly Selective Benzimidazole Inhibitors of PI3-Kinase Delta”; *J. Med. Chem.* **2012**, 55, 7686–7695;
- [25] Sutherlin, D.P.; Baker, S.; Bisconte, A.; Blaney, P.M.; Brown, A.; Chan, B.K.; Chantry, D.; Castanedo, G.; DePledge, P.; Goldsmith, P.; et al.; „Potent and Selective Inhibitors of PI3K δ : Obtaining Isoform Selectivity from the Affinity Pocket and Tryptophan Shelf”; *Bioorg. Med. Chem. Lett.* **2012**, 22, 4296–4302;
- [26] Stark A.K., Sriskantharajah S., Hessel E.M., Okkenhaug K. ;P”I3K inhibitors in inflammation, autoimmunity and cancer”; *Curr Opin Pharmacol*; **2015**, 23: 82-91;
- [27] Puri, K.D.; Gold, M.R.; “Selective Inhibitors of Phosphoinositide 3-Kinase Delta: Modulators of B-Cell Function with Potential for Treating Autoimmune Inflammatory Diseases and B-Cell Malignancies”; *Front. Immunol.* **2012**, 3, 256;
- [28] Suárez-Fueyo, A.; Rojas, J.M.; Cariaga, A.E.; García, E.; Steiner, B.H.; Barber, D.F.; Puri, K.D.; Carrera, A.C.; “Inhibition of PI3K δ Reduces Kidney Infiltration by Macrophages and Ameliorates Systemic Lupus in the Mouse.”; *J. Immunol.* **2014**, 193, 544–554;
- [29] Haselmayer, P.; Camps, M.; Muzerelle, M.; el Bawab, S.; Waltzinger, C.; Bruns, L.; Abla, N.; Polokoff, M.A.; Jond-Necand, C.; Gaudet, M.; et al.; “Characterization of Novel PI3K δ Inhibitors as Potential Therapeutics for SLE and Lupus Nephritis in Pre Clinical Studies”; *Front. Immunol.* **2014**, 5, 1-15;
- [30] Park, S.J.; Lee, K.S.; Kim, S.R.; Min, K.H.; Moon, H.; Lee, M.H.; Chung, C.R.; Han, H.J.; Puri, K.D.; Lee, Y.C.; “ Phosphoinositide 3-Kinase Inhibitor Suppresses Interleukin-17 Expression in a Murine Asthma Model.”; *Eur. Respir. J.* **2010**, 36, 1448–1459;
- [31] Zhang J.Q., Luo Y. J., Xiong Y. S., Yu Y., Tu Z. C., Long Z. J., Lai X. J., Chen H. X.,

- Luo Y., Weng J., Lu G. *J. Med. Chem.* **2016**, 59, 15, 7268–7274;
- [32] Ren, P.; Liu, Y.; Wilson, T.E.; Chan, K.; Rommel, C.; Li, L. Certain Chemical Entities, Compositions and Methods. WO2009088986, **2009**;
- [33] Haylock-Jacobs, S.; Comerford, I.; Bunting, M.; Kara, E.; Townley, S.; Klingler Hoffmann, M.; Vanhaesebroeck, B.; Puri, K.D.; McColl, S.R.; “PI3K δ Drives the Pathogenesis of Experimental Autoimmune Encephalomyelitis by Inhibiting Effector T Cell Apoptosis and Promoting Th17 Differentiation”; *J. Autoimmun.* **2011**, 36, 278–287;
- [34] Ambrosi, A.; Espinosa, A.; Wahren-Herlenius, M.; “IL-17: A New Actor in IFN-Driven Systemic Autoimmune Diseases”; *Eur. J. Immunol.* **2012**, 42, 2274–2284;
- [35] <https://emedicine.medscape.com/article/332244-overview>;
- [36] Smotij D.; „Leczenie tocznia rumieniowatego układowego – wyzwania i perspektywy na przyszłość”; *Varia Medica* 2018; tom 2, nr 5; 430-438;
- [37] Simard JF, Costenbader KH.; „What can epidemiology tell us about systemic lupus erythematosus? *Int J Clin Pract.*”; **2007**; 61(7): 1170–1180;
- [38] Folkes, A.J.; Ahmadi, K.; Alderton, W.K.; Alix, S.; Baker, S.J.; Box, G.; Chuckowree, I.S.; Clarke, P.A.; Depledge, P.; Eccles, S.A.; et al.; „The Identification of 2-(1*H* Indazol-4-*Yl*)-6-(4-Methanesulfonyl-Piperazin-1-*Ylmethyl*)-4-Morpholin-4-*Yl* Thieno[3,2-*d*]Pyrimidine (GDC-0941) as a Potent, Selective, Orally Bioavailable Inhibitor of Class I PI3 Kinase for the Treatment of Cancer”. *J. Med. Chem.* **2008**, 51, 5522–5532;
- [39] Safina, B.S.; Baker, S.; Baumgardner, M.; Blaney, P.M.; Chan, B.K.; Chen, Y.-H.; Cartwright, M.W.; Castanedo, G.; Chabot, C.; Cheguillaume, A.J.; et al.; “Discovery of Novel PI3-Kinase δ Specific Inhibitors for the Treatment of Rheumatoid Arthritis: Taming CYP3A4 Time-Dependent Inhibition”; *J. Med. Chem.* **2012**, 55, 5887–5900;
- [40] Guo, J.; Pei, Y.; Lang, H.; “Pyrimidine Derivative, Cytotoxic Agent, Pharmaceutical Composition and Use Thereof”; WO Patent 2016127455, **2016**;
- [41] Samby, K.; Surase, Y.; Amale, S.; Gorla, S.; Patel, P.; Verma, A.; “6-Morpholinyl-2] Pyrazolyl-9h-Purine Derivatives and Their Use as Pi3k Inhibitors.”; WO Patent 2016157074, **2016**;
- [42] Dymek, B.; Zagozda, M.; Wieczorek, M.; Dubiel, K.; Stańczak, A.; Zdzalik, D.; Gunerka, P.; Sekular, M.; Dziachan, M.; “7-(Morpholin-4-*Yl*)Pyrazole [1,5-*a*]Pyrimidine Derivatives Which are Useful for the Treatment of Immune or Inflammatory Diseases or Cancer”; WO Patent 2016157091;

- [43] Brown, D.; Matthews, D.; “(Alpha-Substituted Cycloalkylamino and Heterocyclamino) Pyrimidinyl and 1,3,5-Triazinyl Benzimidazoles, Pharmaceutical Compositions Thereof, and Their Use in Treating Proliferative Diseases”; WO Patent 2012135175, **2012**;
- [44] Brown, D.; Matthews, D.; “(Fused Ring Arylamino and Heterocyclamino) Pyrimidinyl and 1,3,5-Triazinyl Benzimidazoles, Pharmaceutical Compositions Thereof, and Their Use in Treating Proliferative Diseases”; WO Patent 2012135166, **2012**;
- [45] Brown, D.; Matthews, D.; “(Alpha- Substituted Aralkylamino and Heteroarylalkylamino) Pyrimidinyl and 1,3,5 -Triazinyl Benzimidazoles, Pharmaceutical Compositions Containing Them, and These Compounds for Use in Treating Proliferative Diseases”; WO Patent 2012135160, **2012**;
- [46] Chiang, P.-C.; Sutherlin, D.; Pang, J.; Salphati, L.; “Investigation of Dose-Dependent Factors Limiting Oral Bioavailability: Case Study with the PI3K- δ Inhibitor”; *J. Pharm. Sci.* **2016**, 105, 1802–1809;
- [47] Trott, O.; Olson, A.J.; „AutoDock Vina: Improving the Speed and Accuracy of Docking with a New Scoring Function, Efficient Optimization, and Multithreading.”; *J. Comput. Chem.* **2009**, 31, 455–461;
- [48] Stypik, M.; Zagozda, M.; Michałek, S.; Dymek, B.; Zdżalik-Bielecka, D.; Dziachan, M.; Orłowska, N.; Gunerka, P.; Turowski, P.; Hucz-Kalitowska, J.; Stańczak, A.; Stańczak, P.; Mulewski, K.; Smuga, D.; Stefaniak, F.; Gurba-Bryśkiewicz, L.; Leniak, A.; Ochal, Z.; Mach, M.; Dzwonek, K.; Lamparska-Przybysz, M.; Dubiel, K.; Wieczorek, M.; „Design, Synthesis, and Development of pyrazolo[1,5-*a*]pyrimidine Derivatives as a Novel Series of Selective PI3K δ Inhibitors: Part I—Indole Derivatives.”; *Pharmaceuticals* **2022**, 15, 949;
- [49] Stypik, M.; Michałek, S.; Orłowska, N.; Zagozda, M.; Dziachan, M.; Banach, M.; Turowski, P.; Gunerka, P.; Zdżalik-Bielecka, D.; Stańczak, A.; Kędzierska, U.; Mulewski, K.; Smuga, D.; Maruszak, W.; Gurba-Bryśkiewicz, L.; Leniak, A.; Pietruś, W.; Ochal, Z.; Mach, M.; Zygmunt, B.; Pieczykolan, J.; Dubiel, K.; Wieczorek, M.; „Design, Synthesis, and Development of Pyrazolo[1,5-*a*]pyrimidine Derivatives as a Novel Series of Selective PI3K δ Inhibitors: Part II—Benzimidazole Derivatives.”; *Pharmaceuticals* **2022**, 15, 927;
- [50] Instant JChem, Available online: <https://chemaxon.com/products/instant-jchem> (accessed on 31 May 2022);

- [51] Hoegenauer K, Soldermann N, Zécéri F, Strang RS, Graveleau N, Wolf RM, Cooke NG, Smith AB, Hollingworth GJ, Blanz J, Gutmann S, Rummel G, Littlewood-Evans A, Burkhart C.; „Discovery of CDZ173 (Leniolisib), Representing a Structurally Novel Class of PI3K Delta-Selective Inhibitors.”; *ACS Med Chem Lett.*; **2017** 25; 8(9):975-980.;
- [52] Rao VK, Webster S, Dalm VASH, Šedivá A, van Hagen PM, Holland S, Rosenzweig SD, Christ AD, Sloth B, Cabanski M, Joshi AD, de Buck S, Doucet J, Guerini D, Kalis C, Pylvaenaainen I, Soldermann N, Kashyap A, Uzel G, Lenardo MJ, Patel DD, Lucas CL, Burkhart C.; „Effective "activated PI3K δ syndrome"-targeted therapy with the PI3K δ inhibitor leniolisib.”; *Blood.* **2017**;130(21):2307-2316;
- [53] De Buck S, Kucher K, Hara H, Gray C, Woessner R.; „CYP3A but not P-gp plays a relevant role in the in vivo intestinal and hepatic clearance of the delta-specific phosphoinositide-3 kinase inhibitor leniolisib.”; *Biopharm Drug Dispos.* **2018** 39(8):394-402;
- [54] Allen RA, Brookings DC, Powell MJ, Delgado J, Shuttleworth LK, Merriman M, Fahy JJ, Tewari R, Silva JP, Healy LJ, Davies GCG, Twomey B, Cutler RM, Kotian A, Crosby A, McCluskey G, Watt GF, Payne A.; „Seletalisib: Characterization of a Novel, Potent, and Selective Inhibitor of PI3K δ .”; *J Pharmacol Exp Ther.* **2017**; 361(3):429-440;
- [55] Diaz N, Juarez M, Cancrini C, Heeg M, Soler-Palacín P, Payne A, Johnston GI, Helmer E, Cain D, Mann J, Yuill D, Conti F, Di Cesare S, Ehl S, Garcia-Prat M, Maccari ME, Martín-Nalda A, Martínez-Gallo M, Moshous D, Santilli V, Semeraro M, Simonetti A, Suarez F, Cavazzana M, Kracker S.; „Seletalisib for Activated PI3K δ Syndromes: Open-Label Phase 1b and Extension Studies.” *J Immunol.* **2020**; 205(11):2979-2987;
- [56] Yager N, Haddadeen C, Powell M, Payne A, Allen R, Healy E.; „Expression of PI3K Signaling Associated with T Cells in Psoriasis Is Inhibited by Seletalisib, a PI3K δ Inhibitor, and Is Required for Functional Activity.” *J Invest Dermatol.* **2018**; 138(6):1435-1439;
- [57] Scopelliti F, Mercurio L, Cattani C, Dimartino V, Albanesi C, Costanzo G, Mirisola C, Madonna S, Cavani A.; „The phosphoinositide-3-kinase (PI3K)-delta inhibitor seletalisib impairs monocyte-derived dendritic cells maturation, APC function, and promotes their migration to CCR7 and CXCR4 ligands.”; *J Leukoc Biol.* **2022**; 112(3):383-393;

- [58] Zheng J, Zou X, Yao J.; „The antitumor effect of GDC-0941 alone and in combination with rapamycin in breast cancer cells.”; *Chemotherapy*. **2012**; 58(4):273-81.;
- [59] Bhatia DR, Thiagarajan P.; „Combination effects of sorafenib with PI3K inhibitors under hypoxia in colorectal cancer.”; *Hypoxia (Auckl)*. **2016**:163-174;
- [60] Wang B, Jiang L, Guo H, Sun Q, Wang Y, Xie E, Xia Q.; „Screening of PI3K-Akt targeting Drugs for Silkworm against *Bombyx mori* Nucleopolyhedrovirus”.; *Molecules*. **2019** Apr 1;24(7):1260. doi: 10.3390/molecules24071260;
- [61] Arias-Gómez A, Godoy A, Portilla J.; „Functional Pyrazolo[1,5-*a*]pyrimidines: Current Approaches in Synthetic Transformations and Uses As an Antitumor Scaffold.”; *Molecules*. **2021**; 26(9):2708;
- [62] Castillo J.C., Portilla J.; „Recent advances in the synthesis of new pyrazole derivatives.”; *Targets Heterocycl. Syst.* **2018**;22:194–223;
- [63] Abu Elmaati T.M., El-Taweel F.M.; „New Trends in the Chemistry of 5 Aminopyrazoles.”; *J. Heterocycl. Chem.* **2004**; 41:109–134;
- [64] Asano T., Yamazaki H., Kasahara C., Kubota H., Kontani T., Harayama Y., Ohno K., Mizuhara H., Yokomoto M., Misumi K., et al.; „Identification, Synthesis, and Biological Evaluation of 6-[(6R)-2-(4-Fluorophenyl)-6-(hydroxymethyl)-4,5,6,7 tetrahydropyrazolo[1,5-*a*]pyrimidin-3-yl]-2-(2-methylphenyl)pyridazin-3(2H)-one (AS1940477), a Potent p38 MAP Kinase Inhibitor.”; *J. Med. Chem.* **2012**; 55:7772-7785;
- [65] Zhao M., Ren H., Chang J., Zhang D., Yang Y., He Y., Qi C., Zhang H.; „Design and synthesis of novel pyrazolo[1,5-*a*]pyrimidine derivatives bearing nitrogen mustard moiety and evaluation of their antitumor activity in vitro and in vivo.”; *Eur. J. Med. Chem.* **2016**; 119:183–196;
- [66] Babaoglu K., Boojamra C.G., Eisenberg E.J., Hui H.C., Mackman R.L., Parrish J.P., Sangi M., Saunders O.L., Siegel D., Sperandio D., et al.; „Pyrazolo[1,5-*a*]pyrimidines as antiviral agents.”; WO2011163518A1. *Patent*. **2011**;
- [67] Naidu B.N., Patel M., D’andrea S., Zheng Z.B., Connolly T.P., Langley D.R., Peese K., Wang Z., Walker M.A., Kadow J.F.; „Inhibitors of Human Immunodeficiency Virus Replication.”; WO2014028384A1. *Patent*. **2014**;
- [68] Berman, H.M. The Protein Data Bank. *Nucleic Acids Res.* **2000**, 28, 235–242;
- [69] Burley, S.K.; Bhikadiya, C.; Bi, C.; Bittrich, S.; Chen, L.; Crichlow, G. V.; Christie, C.H.; Dalenberg, K.; Di Costanzo, L.; Duarte, J.M.; et al. RCSB Protein Data Bank: powerful

- new tools for exploring 3D structures of biological macromolecules for basic and applied research and education in fundamental biology, biomedicine, biotechnology, bioengineering and energy sciences. *Nucleic Acids Res.* **2021**, 49, D437–D451;
- [70] Madhavi Sastry, G.; Adzhigirey, M.; Day, T.; Annabhimoju, R.; Sherman, W. Protein and ligand preparation: Parameters, protocols, and influence on virtual screening enrichments. *J. Comput. Aided. Mol. Des.* **2013**, 27, 221–234;
- [71] Berry, M.; Fielding, B.; Gamielien, J. Practical Considerations in Virtual Screening and Molecular Docking. In *Emerging Trends in Computational Biology, Bioinformatics, and Systems Biology*; Elsevier, **2015**; 2; 487–502;
- [72] Trott, O.; Olson, A.J. AutoDock Vina: Improving the speed and accuracy of docking with a new scoring function, efficient optimization, and multithreading. *J. Comput. Chem.* **2010**, 31(2), 455–61;
- [73] Pietruś, W.; Kurczab, R.; Stumpfe, D.; Bojarski, A.J.; Bajorath, J. Data-driven analysis of fluorination of ligands of aminergic G protein coupled receptors. *Biomolecules* **2021**, 11(11), 1647;
- [74] Pietruś, W.; Kafel, R.; Bojarski, A.J.; Kurczab, R. Hydrogen Bonds with Fluorine in Ligand–Protein Complexes—the PDB Analysis and Energy Calculations. *Molecules* **2022**, 27(3), 1005;
- [75] Cho, A.E.; Guallar, V.; Berne, B.J.; Friesner, R. Importance of accurate charges in molecular docking: Quantum Mechanical/Molecular Mechanical (QM/MM) approach. *J. Comput. Chem.* **2005**, 26, 915–931;
- [76] Dunning, T.H. Gaussian basis sets for use in correlated molecular calculations. I. The atoms boron through neon and hydrogen. *J. Chem. Phys.* **1989**, 90, 1007–1023;
- [77] Kurczab, R. The evaluation of QM/MM-driven molecular docking combined with MM/GBSA calculations as a halogen-bond scoring strategy. *Acta Crystallogr. Sect. B Struct. Sci. Cryst. Eng. Mater.* **2017**, 73, 188–194.

10. Wykaz publikacji nie wchodzących w skład rozprawy doktorskiej

Kotecki, M.; Ochal, Z.; Socha, P.; Szejko, V.; Dobrzycki, Ł.; **Stypik, M.**; Ziemkowska, W. Hydrogenation of β -Keto Sulfones to β -Hydroxy Sulfones with Alkyl Aluminum Compounds: Structure of Intermediate Hydroalumination Products. *Molecules* **2022**, 27, 2357. <https://doi.org/10.3390/molecules2707235>.

Zygmunt B. M., Kędzierska U.; Banach M.; Gala K.; Piwowarczyk C.; **Stypik M.**; Michalek S.; Orłowska N.; Wieczorek M.; Pieczykolan J. S.; *A novel PI3K δ inhibitor, CPL302415, demonstrates potent efficacy in the mouse model of systemic lupus erythematosus*; *International Immunopharmacology* 2022; Manuscript Number: INTIMP-D-22-04420

Gunerka P., Hucz-Kalitowska J., Turowski P., Zagozda M., Dziachan M., **Sekular M.**, Bujak A., Wieczorek M.; *Pharmacokinetics of selective PI3K δ inhibitors after intratracheal instillation in mice*; *European Respiratory Journal* 2015, 46(suppl 59) PA2123, doi: 10.1183/13993003.congress-2015.PA2123

Ruśkowski P., Gadomska A., Synoradzki L., Wojtkiewicz E., Rybak E., **Sekular M.**; *Optimization of polylactide production for biomedical purposes*; Warsaw University of Technology, Faculty of Chemistry, Laboratory of Technological Processes; 2009

11. Wykaz posterów i komunikatów ustnych

poster *Benzimidazole-derivatives as novel, active PI3K δ inhibitors -promising and highly potent drug candidates for SLE and other inflammatory and autoimmune diseases.*; **Stypik M.**, Michalek S., Zagozda M., Orłowska N., Banach M., Kędzierska U., Zygmunt B. M., Gala K., Dziachan M., Dymek B., Zdzalik-Bielecka D., Gunerka P., Turowski P., Ochal Z., Dubiel K., Pieczykolan J., Wieczorek M.; *EFMC- ISMC 2022*

poster *CPL302415 - pyrazolo[1,5-a]pyrimidine derivative as a novel, very active and selective PI3K δ inhibitor, highly potent drug candidate for SLE and other inflammatory and autoimmune diseases*; **Stypik M.**, Michalek S., Zagozda M., Orłowska N., Banach M., Kędzierska U., Zygmunt B. M., Gala K., Dziachan M., Dymek B., Zdzalik-Bielecka D., Gunerka P., Turowski P., Ochal Z., Dubiel K., Pieczykolan J., Wieczorek M.; *ACCORD 2022*

poster *Indol-4-yl pyrazolo[1,5-a]pyrimidine derivatives: highly active and selective inhibitors of PI3K δ – potential candidates for treatment of chronic obstructive pulmonary disease and Asthma*; Michalek S., **Stypik M.**, Zagozda M., Orłowska N., Banach M., Kędzierska U., Zygmunt B. M., Gala K., Dziachan M., Dymek B., Zdzalik-Bielecka D., Gunerka P., Turowski P., Ochal Z., Dubiel K., Pieczykolan J., Wieczorek M.; *ACCORD 2022*

poster *Novel benzimidazole-derived PI3K δ inhibitors as highly potent drug candidates for SLE and other inflammatory and autoimmune diseases*; **Stypik M.**, Zagozda M., Michalek S., Orłowska N., Banach M., Kędzierska U., Zygmunt B. M., Gala K., Dziachan M., Dymek B., Zdzalik-Bielecka D., Gunerka P., Turowski P., Ochal Z., Dubiel K., Pieczykolan J., Wieczorek M.; *EFMC-ISMC 2021*

poster *Potent and selective indol-4-yl pyrazolo[1,5-a]pyrimidine-derived PI3K δ inhibitors as potential candidates for treatment of COPD and Asthma*; Michalek S.; **Stypik M.**, Zagozda M., Orłowska N., Banach M., Kędzierska U., Zygmunt B. M., Gala K., Dziachan M., Dymek B.,

Zdzalik-Bielecka D., Gunerka P., Turowski P.; Ochal Z., Dubiel K., Pieczykolan J., Wieczorek M.; *EFMC-ISMIC 2021*

poster *In vitro* studies of a novel potent and selective PI3K δ inhibitor: CPL-302-266; Turowski P., Gunerka P., **Sekular M.**, Dziachan M., Zagozda M., Bujak A., Wieczorek M.; Innovative Drugs R&D Department, Celon Pharma S.A., Kielpin/Łomianki, Polska

poster “Design and development of a novel, highly potent and selective PI3K- δ inhibitor, CPL-302-215, as a potential treatment of hematologic malignancies”; Stańczak A., Gunerka P., Turowski P., Zagozda M., Dziachan M., **Sekular M.**, Hucz J., Dubiel K., Juszczynski P., Biaopiotrowicz E., Szydłowski M., Dymek B., Wieczorek M.; Innovative Drugs R&D Department, Celon Pharma S.A., Kielpin/Łomianki, Polska

komunikat ustny *CPL302145 – active and selective PI3K δ inhibitor - highly potent drug candidate in SLE and other inflammatory and autoimmune diseases.*; Precision in Drug Discovery and Preclinical Summit, PDDP Amsterdam, 2023

komunikat ustny *Pochodne pirazolo[1,5-a] pirymidyny - nowe, aktywne i selektywne inhibitory PI3K δ , jako potencjalne leki w leczeniu toczenia rumieniowatego i innych chorób przeciwzapalnych i autoimmunologicznych..*; I Forum Młodych 2023, konferencja on-line, Polska

komunikat ustny *Pyrazolo[1,5-a]pyrimidine derivatives as novel PI3K δ inhibitors, highly potent drugs candidates for SLE and other inflammatory and autoimmune diseases.*; IX Sympozjum Doktorantów Chemii 2022, Łódź, Polska

12. Publikacje stanowiące podstawę rozprawy doktorskiej

12.1. Publikacja 1 – P1

Article

Citation: Stypik, M.; Zagozda, M.; Michałek, S.; Dymek, B.; Zdzalik-Bielecka, D.; Dziachan, M.; Orłowska, N.; Gunerka, P.; Turowski, P.; Hucz-Kalitowska, J.; et al. Design, Synthesis, and Development of pyrazolo [1,5-*a*]pyrimidine Derivatives as a Novel Series of Selective PI3K δ Inhibitors. Part I—Indole Derivatives. *Pharmaceuticals* 2022, 12, x. <https://doi.org/10.3390/xxxxx>

Academic Editor: Thierry Besson

Received: 22 June 2022

Accepted: 28 July 2022

Published: date

Publisher's Note: MDPI stays neutral with regard to jurisdictional claims in published maps and institutional affiliations.



Copyright: © 2022 by the authors. Submitted for possible open access publication under the terms and conditions of the Creative Commons Attribution (CC BY) license

(<https://creativecommons.org/licenses/by/4.0/>).

Design, Synthesis, and Development of pyrazolo[1,5-*a*]pyrimidine Derivatives as a Novel Series of Selective PI3K δ Inhibitors: Part I—Indole Derivatives

Mariola Stypik ^{1,2,*}, Marcin Zagozda ¹, Stanisław Michałek ^{1,2}, Barbara Dymek ¹, Daria Zdzalik-Bielecka ¹, Maciej Dziachan ¹, Nina Orłowska ^{1,2}, Paweł Gunerka ¹, Paweł Turowski ¹, Joanna Hucz-Kalitowska ¹, Aleksandra Stańczak ¹, Paulina Stańczak ¹, Krzysztof Mulewski ¹, Damian Smuga ¹, Filip Stefaniak ¹, Lidia Gurba-Bryśkiewicz ¹, Arkadiusz Leniak ¹, Zbigniew Ochal ², Mateusz Mach ¹, Karolina Dzwonek ¹, Monika Lamparska-Przybysz ¹, Krzysztof Dubiel ¹ and Maciej Wiczorek ¹

¹ Celon Pharma S.A., ul. Marymoncka 15, 05-152 Kazuń Nowy, Poland; marcin.zagozda@celonpharma.com (M.Z.); stanislaw.michalek@celonpharma.com (S.M.); bdymek@op.pl (B.D.); dzdzalik@iimcb.gov.pl (D.Z.-B.); maciejdziachan@gmail.com (M.D.); orlowska.nina@gmail.com (N.O.); pgunerka@gmail.com (P.G.); tupaw@wp.pl (P.T.); joanna.hucz@celonpharma.com (J.H.-K.); apstanczak@gmail.com (A.S.); paulinaseweryna.stanczak@gmail.com (P.S.); kmulewski91@gmail.com (K.M.); damian.smuga@celonpharma.com (D.S.); stefaniak@gmail.com (F.S.); lidia.gurba@celonpharma.com (L.G.-B.); arkadiusz.leniak@celonpharma.com (A.L.); mateusz.mach@celonpharma.com (M.M.); karolina.dzwonek@gmail.com (K.D.); lamparska@poczta.onet.pl (M.L.-P.); krzysztof.dubiel@celonpharma.com (K.D.); maciej.wiczorek@celonpharma.com (M.W.)

² Faculty of Chemistry, Warsaw University of Technology, ul. Noakowskiego 3, 00-664 Warsaw, Poland; ochal@pw.edu.pl

* Correspondence: author: mariola.stypik@celonpharma.com

Abstract: Phosphoinositide 3-kinase δ (PI3K δ), a member of the class I PI3K family, is an essential signaling biomolecule that regulates the differentiation, proliferation, migration, and survival of immune cells. The overactivity of this protein causes cellular dysfunctions in many human disorders, for example, inflammatory and autoimmune diseases, including asthma or chronic obstructive pulmonary disease (COPD). In this work, we designed and synthesized a new library of small-molecule inhibitors based on indol-4-yl-pyrazolo[1,5-*a*]pyrimidine with IC₅₀ values in the low nanomolar range and high selectivity against the PI3K δ isoform. CPL302253 (**54**), the most potent compound of all the structures obtained, with IC₅₀ = 2.8 nM, is a potential future candidate for clinical development as an inhaled drug to prevent asthma.

Keywords: PI3K δ inhibitors; Asthma; COPD; 5-indole-pyrazolo[1,5-*a*]pyrimidine; CPL302253

1. Introduction

PI3Ks (phosphoinositide 3-kinases) are a family of lipid kinases that can perform the phosphorylation reaction of the hydroxyl group at the 3-position of the phosphatidylinositol ring. More specifically, they are capable of catalyzing the phosphorylation reaction of 4,5-phosphatidylinositol diphosphate (PIP₂) to 3,4,5-phosphatidylinositol triphosphate (PIP₃) [1–3]. This family of kinases consists of three classes (I, II, and III) in terms of the structure and affinity for the substrate. Most class I PI3Ks have been described in the literature. PI3K I consists of heterodimeric proteins: PI3K α , PI3K β , PI3K γ , and PI3K δ [1–4]. Each of them is involved in different functions and cellular processes, such as proliferation, migration, cytokine production, or apoptosis [1–4]. Cells involved in the body's immune response, such as macrophages, neutrophils, T, and B cells, highly expressed PI3K γ and PI3K δ [1–5]. The role of PI3K δ as the co-stimulator between T to B cell interactions was also reported [6,7]. In addition, two other subunits, PI3K α and PI3K β , are involved in normal embryogenesis or metabolism regulation. Therefore, PI3K δ has been identified as an attractive and promising therapeutic target for the treatment of cancer, autoimmune and inflammatory diseases [8–14].

One of the manifestations of inflammatory diseases is asthma, a chronic illness with a spectrum of respiratory symptoms burdensome for patients [15–17]. It was reported that PI3K δ is involved in the regulation of allergic asthma development processes, such as activation of cytokines expression by Th2 cells, activation of antibodies production (e.g., IgE) by B cells, activation of basophils, and accumulation following the migration of eosinophil in the lungs [2,15,18]. Thus far, several selective PI3K δ inhibitors have been developed, to name only: Idelalisib (PI3K δ selective) or Duvelisib (PI3K δ and γ selective; Figure 1) [15,19–21]. Unfortunately, the toxicity and side effects caused by these candidates' low selectivity in systemic action exclude them from the group of potential future therapeutics for asthma management [15,22,23]. Therefore, new approaches focused on developing safe, selective PI3K δ inhibitors designed to be conveniently delivered by inhalation remain an unfulfilled challenge [15,23]. Rich expression of PI3K δ by lung epithelial cells provides the rationale for the new drug design against asthma as the alternative for patients poorly responding to current treatments.

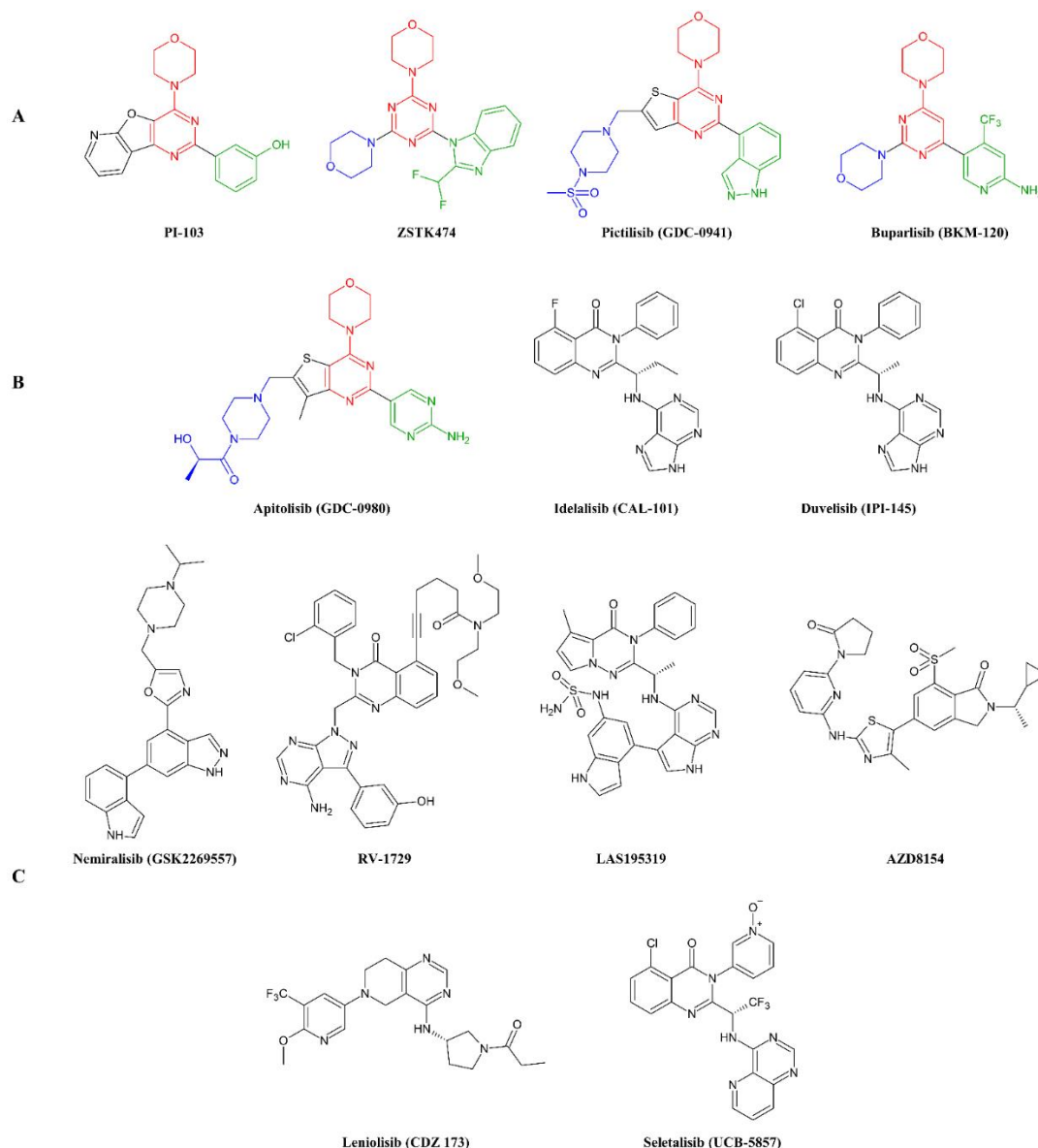


Figure 1. Chemical structures of selected PI3 kinase inhibitors. (A)—Pan-PI3K inhibitors, (B)—Isoform-specific inhibitors, and (C)—PI3K δ or PI3K γ/δ inhibitors as the candidates for the treatment of COPD or Asthma.

The therapeutic application of PI3K δ inhibition at the molecular level utilizes particular interactions of the respective inhibitors within the p110 δ subunit of the ATP binding site [24,25]. Several binding protein key sites are involved in this mechanism: the affinity pocket, the hinge pocket, and a hydrophobic region located below the non-conserved part of the enzyme's active site [25–27]. Numerous active PI3K δ inhibitors are characterized by the interactions with a conserved tyrosine residue (Tyr-876) and hydrogen bonds with Lys-833 located at the binding pocket [27,28]. Most selective PI3K δ inhibitors, however, form a specific hydrogen bond between two critical amino acids: Trp-760 and Met-752 [24,28,29]. In addition, opening the pocket between the Trp-812 and Met-804 has been identified as a selectivity improvement operation [25]. Moreover, PI3K δ selectivity strongly depends on the interaction with Trp-760, for which a 'tryptophan shelf' term was coined [6,24,25]. Binding to Asp-787 was also observed.

Many inhibitors of PI3K have been designed and developed to date. Of the small molecules [12,30,31] and non-specific inhibitors (pan-PI3K) PI-103 [32], ZSTK474 [33], Pictilisib (GDC-0941) [34], Copanlisib (BAY80-6946) [35] and Buparlisib (BKM-120) can be mentioned [36]. More selective inhibitors for particular enzyme isoforms were later developed, such as, e.g., Apitolisib (GDC-0980) [37], Idelalisib (CAL-101) [38], and Duvelisib (IPI-145) were developed [39]. Most of them are applied

in cancer therapies [31]. Only a few PI3K δ or PI3K γ/δ inhibitors have been considered potential drugs in the treatment of respiratory diseases such as chronic obstructive pulmonary disease (COPD) and asthma, namely Nemiralisib (GSK2269557) [40], RV-1729 [41], LAS195319 [42] and AZD8154 [43,44]. Among them, Nemiralisib (Figure 1, terminated in phase II clinical trials) [45] and GSK-2292767 (which did not cross phase I) were delivered by inhalation route [6,46]. In autoimmune and immunodeficiency diseases therapeutic area, two oral PI3K δ inhibitors have advanced to clinical phase three development: Leniosilib and Seletalisib [5,47–49].

Most of the pan-PI3K inhibitors hold in their molecular structure bicyclic cores such as thienopyrimidines (GDC-0941), purines, pyridopyrimidines, or furopyrimidines (Figure 1) [6,27]. The enormous activity and selectivity potential have been associated with the presence of the morpholine ring in the “morpholine-pyrimidine” system (marked in red in Figure 1) [6]. In the hinge-binding mechanism motif, the morpholine ring plays a role as an *H*-bond acceptor. The heteroaromatic or aromatic ring (marked in green in Figure 1), placed in a “meta”-like position to the morpholine ring, takes up space within the affinity pocket of the enzyme (binding to Val-828) [6,25,27]. This mutual interaction enhances the activity and selectivity of designed inhibitors. Moreover, the heterocyclic system (marked in blue in Figure 1) occupying the pocket responsible for the kinase’s specificity drives the selectivity of the designed compounds [6,25,27].

In our work, utilizing known “morpholine-pyrimidine” structure-PI3K δ -activity relationship and bicyclic pyrazolo[1,5-*a*]pyrimidine core, we developed a novel library of compounds focused on future COPD treatment. More specifically, we were fixed on the substitution of morpholine at the C(7) position leading to the 7-(morpholin-4-yl) pyrazolo[1,5-*a*]pyrimidine structural motif. According to mentioned in the above paragraphs’ correlations, we focused on the pyrazolo[1,5-*a*]pyrimidine core as probably the most promising structure (including the nitrogen atom in the five-membered ring), especially with the morpholine moiety in the appropriate position (to create the “morpholine-pyrimidine” system). We noticed that based on the structure of inhibitors as the candidates for the treatment of COPD or Asthma, cores based on bicyclic rings five-six-membered are more potent than six-six-membered, such as in CDZ 173 or UCB-5857. Moreover, we hoped that a five-six-membered ring, similar to pan-inhibitor GDC-0941 with appropriate modifications, could improve and increase the selectivity for isoform δ and thus becomes a selective PI3K δ inhibitor. As a result, we obtained a selection of indole derivatives with improved potency and selectivity towards PI3K δ inhibition. Moreover, we observed that 5-indole-pyrazolo[1,5-*a*]pyrimidine turned out to be the most promising core for future SAR studies.

2. Results and Discussion

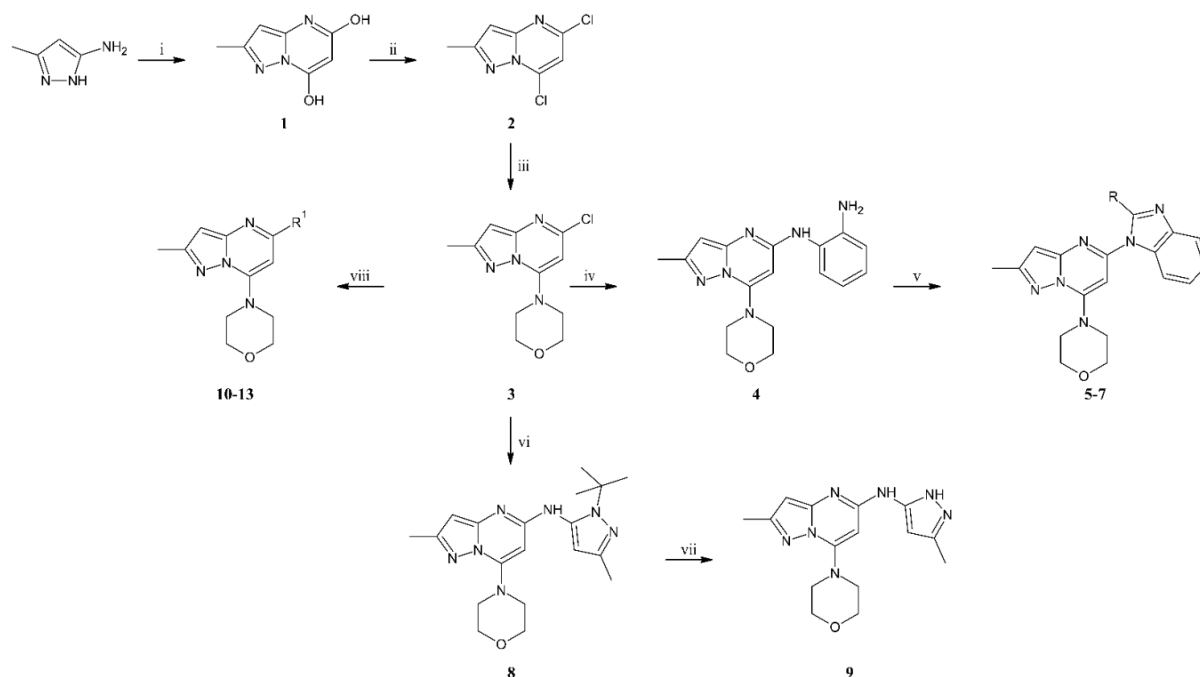
2.1. Chemistry

The final compounds of our design were obtained in three different multistage approaches. The appropriate aminopyrazole derivatives (available commercially or synthesized) were used as the respective starting materials to provide the final inhibitors utilizing mainly the Buchwald–Hartwig reaction, the Suzuki coupling, or the Dess–Martin periodinane oxidation as the crucial synthetic steps.

2.1.1. Synthesis of Compounds 5–3

2-Methyl pyrazolo[1,5-*a*]pyrimidine derivatives were obtained in a multi-step reaction according to Scheme 1. 5-Amino-3-methylpyrazole was reacted with diethyl malonate in the presence of a base (sodium ethanolate) to obtain dihydroxy-heterocycle **1** (89% yield). Then, 2-methylpyrazolo[1,5-*a*]pyrimidine-5,7-diol (**1**) was subjected to the chlorination reaction with phosphorus oxychloride to give 5,7-dichloro-2-methylpyrazolo[1,5-*a*]pyrimidine (**2**) (61% yield). Structure **3** was prepared from **2** in a nucleophilic substitution reaction using morpholine in the presence of potassium carbonate at room temperature (94% yield). The selectivity of the reaction results from the strong reactivity of the chlorine atom at position 7 of the pyrazolo[1,5-*a*]pyrimidine core [50]. 4-{5-Chloro-2-methylpyrazolo[1,5-*a*]pyrimidin-7-yl}morpholine (**3**) is the key intermediate in the preparation of a series of compounds **5–13**. Depending on the R¹ substituent, the final compounds were prepared from **3** using two types of coupling reactions: either the Buchwald–Hartwig or the Suzuki coupling reaction. Benzimidazole derivatives **5–7** were synthesized by carrying out the three-step reaction: again, the Buchwald–Hartwig reaction (average yield of 61%), amidation, following the final cyclization step. The corresponding

amides **5-7** were prepared in the presence of EDCI and HOBt from the appropriate carboxylic acids and amine **4**, resulting from the Buchwald–Hartwig synthesis by the heterocycle ring closure in the presence of glacial acetic acid. Since this synthetic route requires no intermediate purification, the observed yields are satisfactory in the 74–77% range. A separate synthetic route was chosen for compound **9**, obtained in two steps by the Buchwald–Hartwig reaction with a masked aminopyrazole (54% yield), followed by the final deprotection of intermediate **8** (89% yield). Derivatives **10-13** were prepared by the Suzuki reaction of compound **3** with the respective esters or boronic acids in the presence of a palladium catalyst with yields in the range of 55–61%.

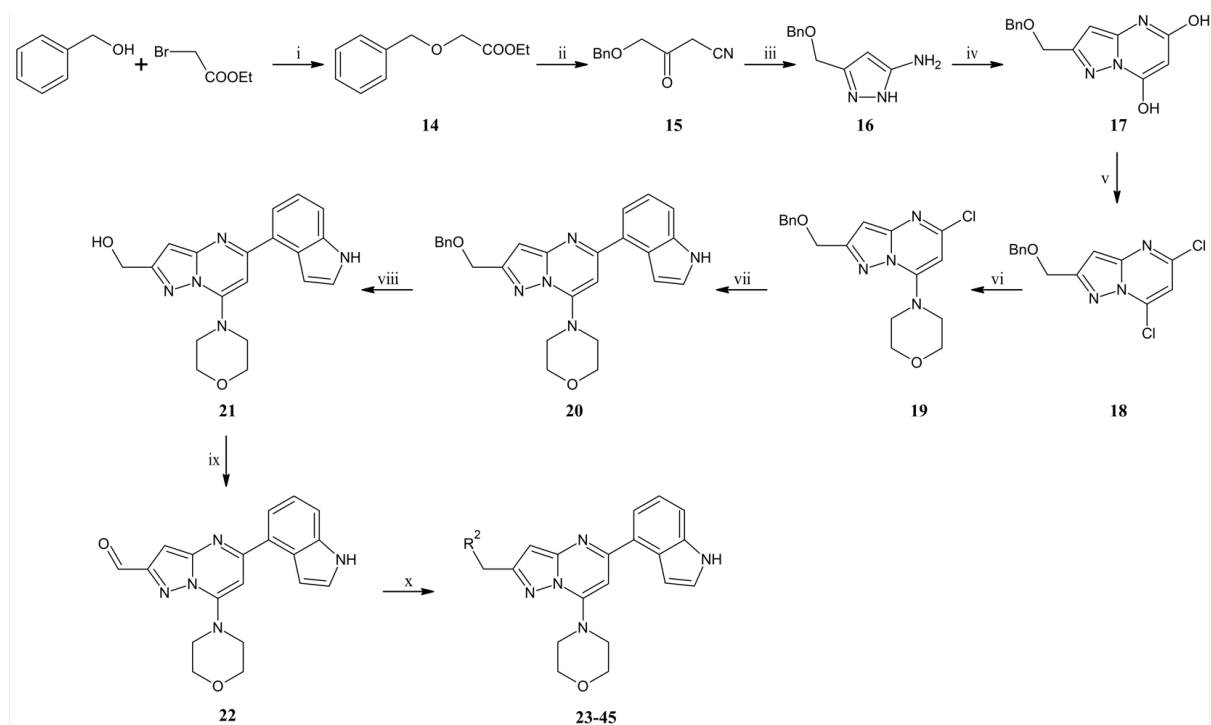


Scheme 1. Synthesis of 2-methylpyrazolo[1,5-*a*]pyrimidine derivatives. Reagents and conditions: (i) diethyl malonate, EtONa, reflux, 24 h, 89%; (ii) POCl₃, reflux, 24 h, 61%; (iii) morpholine, K₂CO₃, acetone, RT, 1.5 h, 94%; (iv) benzene-1,2-diamine, tris(dibenzylideneacetone)dipalladium(0), Xantphos, Cs₂CO₃, toluene, 110 °C, 24 h, 61%; (v) (a) carboxylic acid, EDCI x HCl, HOBt x H₂O, TEA, DCM, RT, 48 h, (b) AcOH, reflux, 24 h, 74–77%; (vi) 1-tert-butyl-3-methyl-1H-pyrazol-5-amine, tris(dibenzylideneacetone)dipalladium(0), Xantphos, Cs₂CO₃, toluene, 100 °C, 18 h, 54%; (vii) TFA, H₂O, reflux, 20 h, 89%; (viii) boronic acid pinacol ester or boronic acid, tetrakis(triphenylphosphino)palladium(0), 2M aq Na₂CO₃, DME, reflux, overnight, 55–61%.

2.1.2. Synthesis of Compounds **23-45**

The synthesis of compounds **23-45** was more complicated and required several additional steps. The first three steps leading to compound **16** were performed based on the available literature data [51–54]. Initially, the reaction of benzyl alcohol with ethyl bromoacetate in the presence of sodium hydride gave the corresponding ether **14** (Scheme 2) with a 76% yield. Then the beta-ketoester derivative **15** was prepared by reaction with acetonitrile under basic conditions using 2,5 M *n*-butyllithium solution at a lower temperature of –78 °C. Compound **15** was subsequently condensed with hydrazine to give the corresponding aminopyrazole derivative **16** in satisfying 87% yield after two steps, as depicted in Scheme 2. The experiences gained in the previous synthetic route could be successfully extrapolated to accomplish the next four steps of the synthesis. Reaction of diethyl malonate with the aminopyrazole derivative **16** gave 2-[(benzyloxy)methyl]pyrazolo[1,5-*a*]pyrimidine-5,7-diol (**17**, 84% yield). Chlorination of **17** with phosphorus oxychloride provided the corresponding dichloro-derivative: 2-[(benzyloxy)methyl]-5,7-dichloropyrazolo[1,5-*a*]pyrimidine (**18**) in 38% yield. A selective and efficient (92% yield) substitution of the C(7)-chlorine atom in the heteroaromatic core with morpholine gave the analog of **3** (Scheme 1) as intermediate **19**. Applying the Suzuki coupling conditions to **19** with indole-4-boronic acid pinacol ester led to benzyl masked alcohol **20** in 83% yield. Classical deprotection conditions (gaseous hydrogen over palladium catalyst on activated charcoal) of the benzyloxy group provided compound **21** in 66% yield. The subsequent oxidation reaction of primary alcohol **21** to the

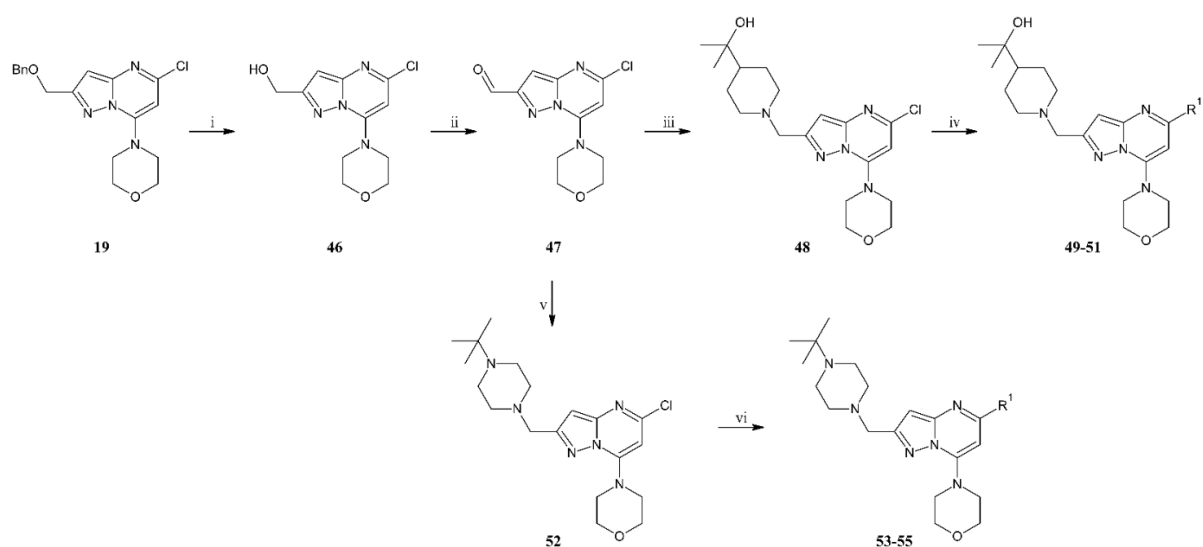
crucial aldehyde **22** was easily accomplished using the Dess–Martin reagent (Scheme 2) with a yield of 78%. A series of the reductive amination reactions utilizing compound **22** as a key intermediate with the appropriate cyclic amines gave additional contributors (**23** to **45**) to the growing library of PI3K δ inhibitors in un-optimized yields varying from 25 to 93%.



Scheme 2. Synthesis of 5-(indol-4-yl)pyrazolo[1,5-*a*]pyrimidine derivatives. Reagents and conditions: (i) 60% NaH, toluene, RT, 5 h, 76%; (ii) acetonitrile, 2.5 M *n*-BuLi, THF, -78 °C, 3 h; (iii) hydrazine monohydrate, EtOH, reflux, 16 h, 87% after two steps; (iv) diethyl malonate, EtONa, reflux, 24 h, 84%; (v) POCl₃, acetonitrile, 80 °C, 5 h, 38%; (vi) morpholine, K₂CO₃, acetone, RT, 1.5 h, 92%; (vii) indole-4-boronic acid pinacol ester, tetrakis(triphenylphosphino)palladium (0), 2M aq Na₂CO₃, DME, reflux, 16h, 83%; (viii) H₂, 10% Pd/C, DMF/EtOH, 60 °C, 24 h, 66%; (ix) Dess–Martin reagent, DMF, RT, 2 h, 78%; (x) amine, sodium triacetoxyborohydride, DCM, RT, 2 h, 25–93%.

2.1.3. Synthesis of Compounds **49–51** and **53–55**

An essential intermediate **19** (Scheme 2) was also successfully used to prepare another set of compounds functionalized at the C(5) position to explore more deeply the structure-activity relationship of this particular core. The synthesis of another subset of substituted pyrazolo[1,5-*a*]pyrimidines is shown in Scheme 3. Due to the same reaction types, the synthesis pathways of examples **49–51** and **53–55** were similar to the synthesis of the previous compounds (**23–45**, Scheme 2), the difference being the order of the Suzuki reaction and the reductive amination reaction sequence in the multistage synthesis pathway. After deprotection of the hydroxyl group of **19**, compound **46** was oxidized to aldehyde **47** (Scheme 3). The following steps included a reductive amination reaction with the carefully selected, based on *in silico* calculations, amines: (2-(4-piperidyl)-2-propanol or *N*-*t*-butylpiperazine followed by a Suzuki coupling to provide **49–51** and **53–55**, respectively (Scheme 3).



Scheme 3. Synthesis of pyrazolo[1,5-*a*]pyrimidine derivatives. Reagents and conditions: (i) methanesulfonic acid, CHCl_3 , RT, 2 h, 97%; (ii) Dess–Martin periodinane, DMF, RT, 2 h, 46%; (iii) 2-(4-piperidyl)-2-propanol, sodium triacetoxyborohydride, DCM, RT, 16 h, 63%; (iv) boronic acid pinacol ester, tetrakis(triphenylphosphino)palladium (0), 2M aq Na_2CO_3 , DME, reflux, 16 h, 60–72%; (v) *N*-*t*-butylpiperazine, sodium triacetoxyborohydride, DCM, RT, 16 h, 53%; (vi) boronic acid pinacol ester, tetrakis(triphenylphosphino)palladium (0), 2M aq Na_2CO_3 , DME, reflux, 16 h, 68–77%.

2.2. Docking Study

Several approaches have been described leading to various structural docking theories explaining the selectivity of PI3K δ inhibitors [25,27]. Opening the specificity pocket between the two amino acids, Trp-812 and Met-804, and adopting the appropriate shape within the protein combined with additional correlations, allows the identification of much more selective PI3K δ inhibitors from all PI3K Class I isoforms [25,27,34]. It was reported that there are many meaningful interactions between ligand and protein in the enzyme's active site [6,24,27]. First is the hydrogen bond of the morpholine from pyrazolo[1,5-*a*]pyrimidine derivative in the hinge-binding motif [6,24–26]. More precisely, the hydrogen bonding between the oxygen atom from the morpholine mentioned above the ring and amino acid Val-828 was crucial in the hinge region. It has been suggested that indole derivatives in the C(5) position of the core of pyrazolo[1,5-*a*]pyrimidine may form an additional hydrogen bond with Asp-787 (another important interaction in many selective inhibitors, most with the affinity pocket) [25]. For this reason, indole heterocycle-based inhibitors are more selective for PI3K δ than other PI3K isoforms. In addition, a suitable substituent of this structure, which can extend into the solvent, can improve the solubility, ADME properties, and potency of the final compounds [25].

Our work is focused on the pyrazolo[1,5-*a*]pyrimidine scaffold and appropriate further optimization with different C(5) substituents.

An example of our approach showing the possible binding site of compound **13** with the kinase is presented in Figure 2. The docking procedure utilizes the PI3K δ protein (PDB: 2WXP) and the AutoDock Vina program [55]. Compound **13** (magenta) binds similarly to protein as referent compound GDC-0941 (orange, Figure 2). More specifically, the oxygen atom in the morpholine ring forms a hydrogen bond with the amino acid (Val-828) in the hinge region of the enzyme (the importance of this interaction has been explained before). Moreover, the indole system's hydrogen atom (NH) is involved in forming the hydrogen bond with the carbonyl oxygen in Asp-787 in the affinity pocket of the kinase (Figure 2).

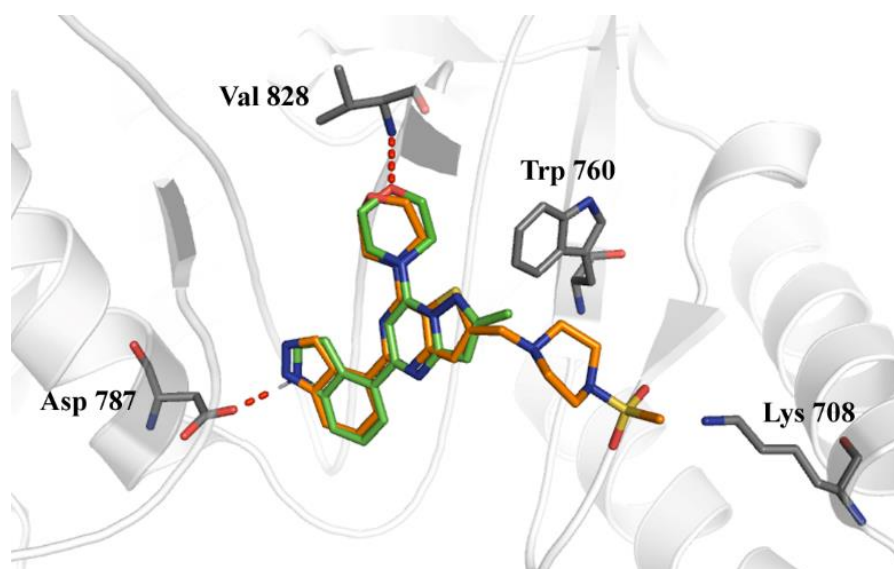


Figure 2. Example of 3D modeling of a possible binding mode of compound **13** (green) and reference compound GDC-0941 (orange) in 2WXP. No protons were added, but the appropriate protonation state was maintained.

Among the structures **24**, **36**, and **37** additional features were found in our *in silico* model compared to **13** and similars. Compared to compound **23**, higher activity and selectivity can be explained by interactions with the tryptophan shelf (2WXP: Trp-760) in PI3K δ , as described by Sutherland et al. [25]. For those compounds, the distance between the R² substituent and the tryptophan's indole ring is significantly shorter (Figure 3A). Moreover, the additional hydrogen bond of the hydroxyl group in (2-(piperidin-4-yl) propan-2-ol) (**36**) with Lys-708 was observed (Figure 3B). On the other hand, for a derivative containing *tert*-butylpiperazine (**37**), strong hydrophobic interactions with tryptophan (Trp-760) were found, which may cause the withdrawal of the indole ring of **37** from the enzyme affinity pocket. Most likely, this situation is observed due to the lack of interaction with tyrosine (Tyr-813) and aspartic acid (Asp-787) in the mentioned pocket (Figure 3B).

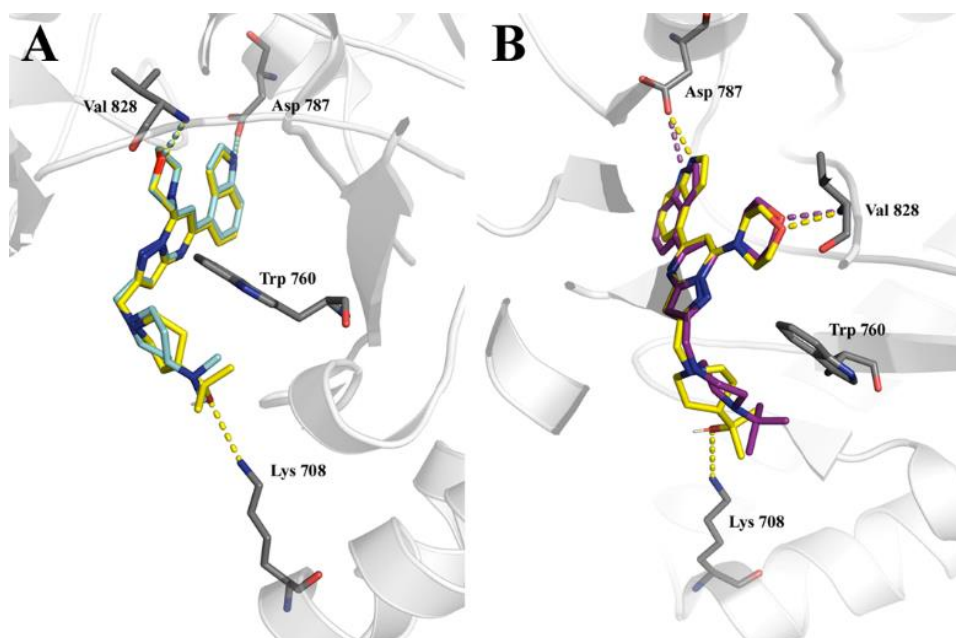


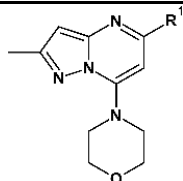
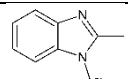
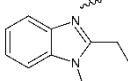
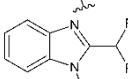
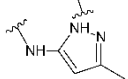
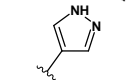
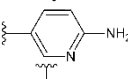
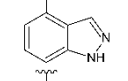
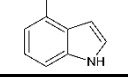
Figure 3. (A,B)—examples of 3D modeling of a possible binding mode of compounds **24** (gray), **36** (yellow) and **37** (magenta) in 2WXP. No protons were added, but the appropriate state of protonation was maintained.

2.3. Biological Evaluation

2.3.1. In Vitro PI3 Kinase Inhibition Assays

To verify whether the 7-(morpholin-4-yl) pyrazolo [1,5-*a*] pyrimidine system can inhibit PI3 δ kinase, the synthesized compounds **6–13** were tested for inhibition of selected PI3K δ and PI3K α kinases activity. Enzymatic tests have been used, and the results are presented in Table 1.

Table 1. Inhibition of PI3K δ and PI3K α by 2-methylpyrazolo[1,5-*a*]pyrimidine derivatives.

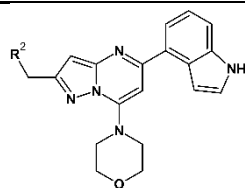
Compound	R ¹			
		IC ₅₀ PI3K δ [μ M]	IC ₅₀ PI3K α [μ M]	Fold Selectivity α/δ
5		3.56	35.1	9.9
6		2.30	25.9	11
7		0.475	1.06	2.2
9		43.6	>60	>1.4
10		12.7	36.2	2.9
11		6.86	4.64	0.7
12		3.85	4.81	1.2
13		0.772	23.5	30

IC₅₀ values were determined as the mean based on two independent experiments.

The activity of these compounds ranged from 45 μ M to 0.5 μ M for the PI3K δ isoform and from over 60 μ M to 1.06 μ M for the PI3K α isoform, and thus the α/δ selectivity ranged from 1 to 30 (Table 1). Among all benzimidazole derivatives synthesized, the most promising activity with the low PI3K δ IC₅₀ value was measured for compound **7** (IC₅₀=0.47 μ M) (Table 1). On the other hand, compounds **5** and **6**, keeping benzimidazole derivatives within their structures, show significantly lower activity against the PI3K δ isoform than compound **7** (IC₅₀ value of 3.56 μ M and 2.30 μ M, respectively), regardless of better selectivity against the PI3K α isoform (α/δ) (9.9 for **5** and 11 for **6**). We observed that compounds with a monocyclic 5- or 6-membered heteroaromatic ring (**9–11**) turned out to be less active and thus showed a lower enzyme inhibition potential than the other bicyclic structures. Structures **12** and **13** bearing conjugated bicyclic system as the R¹ substituent presented a similar activity to the benzimidazole derivatives. The most active were compounds having R¹ substituents in the form of 2-difluoromethylbenzimidazole (**7**) and indole (**13**). Specifically, their IC₅₀ value against PI3K δ was 0.475 μ M and 0.772 μ M, respectively. Due to the much better α/δ selectivity of compound **13** over compound **7** (α/δ = 30 and α/δ = 2.2, respectively), we have chosen the indole derivatives for further optimization.

Compared to compound **13**, significantly more sterically demanding derivatives were designed and synthesized as the next optimization step. While the indole fragments were preserved, many different cyclic amines were linked to the scaffold core through a methylene linkage as an R² substituent (Table 2).

Table 2. Inhibition of PI3K isoforms by 5-(indol-4-yl)pyrazolo[1,5-*a*]pyrimidine derivatives.

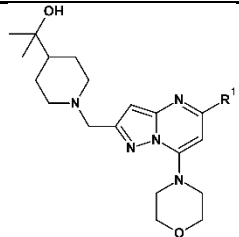


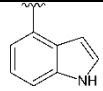
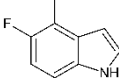
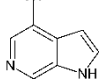
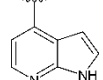
Compound	R ¹	IC ₅₀ PI3K δ [nM]	IC ₅₀ PI3K α [nM]	IC ₅₀ PI3K β [nM]	IC ₅₀ PI3K γ [nM]	Fold Selectivity		
						α/δ	β/δ	γ/δ
23		402	2351			5.8		
24		37	6380	14,400	49,300	172	389	1332
25		1992						
26		2207						
27		266	8650			33		
28		1072						
29		52	15,630			301		
30		360	14,200			39		
31		559						
32		177	8790			50		
33		193	42,400			220		
34		43	34,300	10,900	>60,000	798	253	>1395
35		138	8,460			61		
36		13	15,820	4,310	15,900	1217	332	1223
37		6.6	12,470	5470	>60,000	1889	829	>9091
38		41	17,740	5990	17,550	433	146	428
39		58	25,300	15,000		436	259	
40		42	13,800			329		
41		51	12,300	3170	9730	241	62	191
42		56	18,680			334		
43		71	22,600			318		
44		22	1270	7 310	846	58	332	38
45		29	6320			218		

IC₅₀ values were determined as the mean based on two independent experiments. For compounds with PI3K δ IC₅₀ above 0.5 μ M, the activity for the remaining isoforms was not determined. Compounds with PI3K δ IC₅₀ above 50 nM were additionally checked for the potency of the PI3K α isoform.

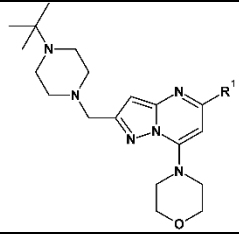
The synthesis of the new group of pyrazolo[1,5-*a*] pyrimidine derivatives (depicted in Scheme 2) required additional steps related to the functionalization of the C(2)-position of the heteroaromatic core. Firstly, a group of derivatives with differing sizes of heterocycle rings and different chemical properties of substituents (**23-31**) was synthesized (Table 2). We noted that structures containing monocyclic five-membered rings (**25-26**) and morpholine (**28**) turned out to be less potent PI3K δ inhibitors than compound **13** (Table 1). The mesylpiperazine group present in the GDC0941 Reference [34] did not significantly improve the activity of structurally similar compound **23** from our library (the IC₅₀ value of that example for PI3K δ and PI3K α was 0.4 μ M and 2.35 μ M, respectively). Urea-derivatives, **30** and **31**, also showed moderate activity. The most potent compounds in this group (Table 2) turn out to be the analogs of *N,N*-dimethyl-4-aminopiperidine (**24**), and 4-(*N*-methylpiperazin-1-yl)piperidine (**29**). Both, **24** and **29**, showed promising inhibitory activity against PI3K δ (37 nM and 52 nM respectively) and selectivity against other isoforms ($\alpha/\delta = 172$; $\beta/\delta = 389$; $\gamma/\delta = 1332$ for **24** and $\alpha/\delta = 301$ for **29**). Careful structural analysis around the R² substituent of the examples provided in Table 2 led us to several conclusions. Relatively modest activities of the compounds containing the methyl group, aromatic ring, or ester group at the C(4)-position of the heterocyclic ring misled us towards the synthesis of piperazine and piperidine analogs(**32-45**) (Table 2). Moreover, the presence of the second ring within the R² substituent (compounds **39-40** and **42-45**) did not improve PI3K δ activity compared to previously obtained compounds **24** or **29**. Finally, only large aliphatic substituents within piperazine or piperidine rings gain the PI3K δ potency and respective selectivity.

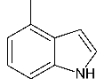
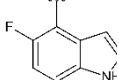
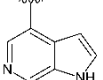
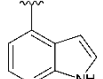
We observed that the best results were achieved for two compounds being the representatives of two different modifications. More specifically 2- (piperidin-4-yl) propan-2-ol (compound **36** of piperidine modification series) and *N-tert*-butylpiperazine (compound **37** of piperazine modification series) exhibit high activities towards the PI3K δ (IC₅₀ = 6.6 and 13.0 nM, respectively) and appreciable selectivities towards other isoforms ($\alpha/\delta = 1217$; $\beta/\delta = 332$; $\gamma/\delta = 1223$ for **36** and $\alpha/\delta = 1889$; $\beta/\delta = 829$; $\gamma/\delta > 9091$ for **37**; Table 2). As the hit to lead optimization route continued, several indole and azaindole derivatives at the C(5) position were introduced to the existing scaffold. While preserving the most active amino groups, we prepared the piperidine derivatives series (summarized in Table 3) and piperazine derivatives series (covered in Table 4). From all the synthesized structures, the *N-tert*-butylpiperazine derivatives (**37**, **53**, **54**, **55**, Table 4) show the highest PI3K δ activity, greater than the piperidyl–propanol analogs shown in Table 3 (**36**, **49**, **50**, **51**). The presence of the fluorine atom in the C(5)-position of the indol fragment causes a slight decrease in activity against the PI3K δ isoform in both groups without affecting the selectivity toward other isoforms. The introduction of the nitrogen atom to the indole ring at position 7 caused a slight decrease in the activity of compound **51** (Table 3), which was almost doubled in the case of **55** (Table 4). Moreover, slight decreases in activity related to the PI3K α isoform were observed for these structures. An introduction of a nitrogen atom in the 6-position of the indole caused a decrease in activity derivate **50** but a 10-fold improvement for **54**. Decreased selectivity against the PI3K α isoform was also observed for the azaindole structures (**50**, **51**, **53**, **54**) despite the good activity in the nanomolar range (IC₅₀ value: 2.8–45 nM).

Table 3. Inhibition of PI3K δ by pyrazolo[1,5-*a*]pyrimidine derivatives.


Compound	R ¹	IC ₅₀ PI3K δ	IC ₅₀ PI3K α	IC ₅₀ PI3K β	IC ₅₀ PI3K γ	Fold Selectivity		
		[nM]	[nM]	[nM]	[nM]	α/δ	β/δ	γ/δ
36		13	15,820	4310	15,900	1217	332	1223
49		40	34,400	11,300	47,800	860	283	1195
50		28	3650	5260		130	188	
51		23	9750	26,800		424	1165	

IC₅₀ values were determined as the mean based on two independent experiments.

Table 4. Inhibition of PI3K δ by pyrazolo[1,5-*a*]pyrimidine derivatives.


Compound	R ¹	IC ₅₀ PI3K δ	IC ₅₀ PI3K α	IC ₅₀ PI3K β	IC ₅₀ PI3K γ	Fold Selectivity			IC ₅₀ CD19 [nM]
		[nM]	[nM]	[nM]	[nM]	α/δ	β/δ	γ/δ	
37		6.6	12,470	5470	>60,000	1889	829	>9091	20
53		11	19,300	19,450	>60,000	1754	1768	>5455	
54		2.8	2670	21,600	34,400	954	7714	12,286	19
55		45	2960	32,000		66	711		

IC₅₀ values were determined as the mean based on two independent experiments.

We have found that two compounds: **37** and **54**, from the entire synthesized library showed the best activity and selectivity for PI3K δ . Based on all parameters, these structures showed the highest selectivity, the lowest IC₅₀ values, and the most promising other parameters [15]. Consequently, those two selected examples were tested by flow cytometry towards the proliferation of B lymphocytes capabilities. Both showed very high potency in inhibiting B cell proliferation with IC₅₀ values of 20 nM and 19 nM, respectively (Table 5). Moreover, compound **54** had better kinetic solubility at pH 7.4 than compound **37** (>500 and 444 μ M respectively) (Table 5). We also observed that the presence of nitrogen

atom in the 6-azaindole ring of **54** molecule results in higher metabolic stability in murine and human microsomes (for details, see Table 5).

Table 5. Comparison of the selected properties of compounds **37** and **54**.

Compound	Solubility [μM]	MLM $t_{1/2}$ [min]	MLM CI [$\text{ml} \times \text{min}^{-1} \times \text{mg}^{-1}$]	HLM $t_{1/2}$ [min]	HLM CI [$\text{ml} \times \text{min}^{-1} \times \text{mg}^{-1}$]
37	444	126	13.7	76	22.8
54	>500	198	7.0	370	3.7

3. Materials and Methods

3.1. Chemistry

3.1.1. General Information

Chemicals (at least 95% purity) were purchased from ABCR (Karlsruhe, Germany), Acros (Geel, Belgium), Alfa Aesar (Haverhill, MA, USA), Combi-Blocks (San Diego, CA, USA), Fluorochem (Hadfield, UK), Fluka (Charlotte, NC, USA), Merck (Rahway, NJ, USA), and Sigma Aldrich (St. Louis, MO, USA) and were used without additional purification. Solvents were purified according to standard procedures if required. Air or moisture-sensitive reactions were carried out under an argon atmosphere. All reaction progresses were routinely checked by thin-layer chromatography (TLC). TLC was performed using silica gel coated plates (Kieselgel F254) and visualized using UV light. Flash chromatography was performed using Merck silica gel 60 (230–400 mesh ASTM). ^1H NMR spectra were acquired on a Varian Inova 300 MHz NMR spectrometer, JOEL JNMR-ECZS 400 MHz spectrometer, JOEL JNMR-ECZR 600 MHz spectrometer, and Bruker DRX 500 NMR spectrometer with ^1H being observed at 300 MHz, 400 MHz, 600 MHz, and 500 MHz, respectively. ^{13}C NMR spectra were recorded similarly at 75 MHz, 101 MHz, 151 MHz, and 126 MHz, frequencies for ^{13}C , respectively. Due to the poor solubility of some final compounds, usual characterization by ^{13}C NMR was omitted. Chemical shifts for ^1H and ^{13}C NMR spectra were reported in δ (ppm) using tetramethylsilane as an internal standard or according to the residual undeuterated solvent signal (2.50 ppm for DMSO- d_6 , and 7.26 ppm for CDCl_3). The abbreviations for spin interaction coupled ^1H signals are as follows: s (singlet), d (doublet), t (triplet), m (multiplet), dd (doublet of doublets), dt (doublet of triplet), q (quartet). Coupling constants (J) are expressed in Hertz. Mass spectra (Atmospheric Pressure Ionization Electrospray, API-ES, and Electrospray Ionization, ESI-MS) were obtained using Agilent 6130 LC/MSD spectrometer or Agilent 1290 UHPLC coupled with Agilent QTOF 6545 mass spectrometer.

3.1.2. Synthesis

Procedure for 5,7-dihydroxy-2-methylpyrazolo[1,5-*a*]pyrimidine (**1**)

To the flask with sodium ethoxide solution (obtained from sodium (4.73 g, 0.21 mol) and ethanol (175 mL) a solution of 3-amino-5-methylpyrazole (10.0 g, 0.10 mol) in ethanol (100 mL) and diethyl malonate (23.5 mL, 0.15 mol) were added. The reaction was carried out at reflux for 24 h. The reaction mixture was cooled to room temperature, and then the solvent was evaporated under reduced pressure. The residue was dissolved in 1200 mL of water and acidified with concentrated hydrochloric acid to a pH of about 2. Creamy solid precipitated from the solution was filtered off, washed, and dried. The title compound **1** (15.2 g, 0.08 mol) was obtained as an off-white solid with 89% yield. MS-ESI: m/z calcd for $\text{C}_7\text{H}_7\text{N}_3\text{O}_2$ [$\text{M}+\text{Na}$] $^+$: 188.04; found 187.9.

Procedure for 5,7-dichloro-2-methylpyrazolo[1,5-*a*]pyrimidine (2)

To the cooled to 0 °C POCl₃ (90 mL, 0.963 mol), compound 1 (15.2 g, 0.092 mol) was added. The reaction was carried out at reflux for 24 h. The reaction mixture was cooled to room temperature and poured into the water with ice. The mixture was quenched with a 6 M sodium hydroxide solution to pH 6. The aqueous phase was extracted with ethyl acetate, and after separation, the organic phase was dried with anhydrous sodium sulfate. After filtration of the drying agent and evaporation of the solvent, the residue was purified by column chromatography (0–40% ethyl acetate gradient in heptane) to give compound 2 (11.4 g, 0.056 mol) obtained as an off-white solid with 61% yield. ¹H NMR (300 MHz, CDCl₃) δ: 6.90 (s, 1H, Ar-H), 6.53 (s, 1H, Ar-H), 2.56 (s, 3H, CH₃). MS-ESI: *m/z* calcd for C₇H₅Cl₂N₃ [M+H]⁺: 201.99; found 201.9.

Procedure for 5-chloro-2-methyl-7-morpholin-4-yl-pyrazolo[1,5-*a*]pyrimidine (3)

To the solution of compound 2 (2.0 g, 9.9 mmol) in acetone (50 mL), potassium carbonate (1.64 g, 11.9 mmol), and morpholine (1.35 mL, 15.5 mmol) were added. The reaction was carried out at room temperature for 1.5 h. Then water (100 mL) was added to the reaction mixture, and the precipitated white solid was filtered off. The obtained solid was washed with water (50 mL) and water/acetone mixture (2/1, *v/v*) (50 mL), then dried. Compound 3 (2.36 g, 0.09 mol) was obtained as a white solid with 94% yield. ¹H NMR (300 MHz, CDCl₃) δ: 6.29 (s, 1H, Ar-H), 6.01 (s, 1H, Ar-H), 4.00–3.92 (m, 4H, morph.), 3.81–3.72 (m, 4H, morph.), 2.46 (s, 3H, CH₃). MS-ESI: *m/z* calcd for C₁₁H₁₃ClN₄O [M+H]⁺: 253.09; found 253.0.

Procedure for *N*-(2-methyl-7-(morpholin-4-yl)pyrazolo[1,5-*a*]pyrimidin-5-yl)benzene-1,2-diamine (4)

The mixture of compound 3 (1.0 g, 3.96 mmol), benzene-1,2-diamine (1.31 g, 11.9 mmol), cesium carbonate (3.87 g, 11.9 mmol), tris(dibenzylideneacetone)dipalladium(0) (0.181 g, 0.20 mmol), 9,9-dimethyl-4,5-bis(diphenylphosphine)xanthene (0.229 g, 0.40 mmol) and dry toluene (40 mL) were introduced to the reaction Schlenk flask. The mixture was flushed with argon and stirred at 110 °C for 24 h. After cooling to room temperature, the reaction mixture was filtered through Celite®, and the solid was washed with ethyl acetate. The filtrate was concentrated under reduced pressure using an evaporator. The residue was resolved and purified by column chromatography (50–100% ethyl acetate gradient in heptane) to give the title compound 4 (0.78 g, 2.4 mmol) with 61% yield. ¹H NMR (300 MHz, CDCl₃) δ 7.23–7.17 (m, 1H, Ar-H), 7.16–7.09 (m, 1H, Ar-H), 6.88–6.76 (m, 2H, Ar-H), 6.37 (s, 1H, Ar-H), 5.92–5.86 (m, 1H), 5.30 (s, 1H), 4.01–3.81 (m, 4H, morph.), 3.58–3.45 (m, 4H, morph.), 2.39 (s, 3H, CH₃). MS-ESI: *m/z* calcd for C₁₇H₂₀N₆O [M+H]⁺: 325.18; found 325.1.

General Procedure for the Synthesis of Benzimidazole Derivatives (5-7)

In the solution of compound 4 (1.0 eq) dissolved in dry DCM (10 mL/1g of compound 4), the carboxylic acid (2.0 eq), HOBt × H₂O (1.2 eq), EDCI × HCl (2.4 eq), and TEA (3.0 eq) were added. The whole reaction mixture was stirred at room temperature for 48 h. To the reaction, mixture water was added, and organic and water phases were separated. The aqueous phase was washed three times with DCM. Combined organic phases were dried over anhydrous sodium sulfate. After the drying agent was filtered off and the solvent evaporated, the reaction mixture was dissolved in glacial acetic acid. The reaction mixture was refluxed for 24 h. Then the reaction mixture was cooled and concentrated under reduced pressure. The residue was diluted with water and neutralized with a saturated sodium bicarbonate solution. The aqueous phase was extracted three times with ethyl acetate. Combined organic phases were dried over sodium sulfate. Once the drying agent was filtered off, the solvent was evaporated under reduced pressure using an evaporator. The reaction mixture was purified by column chromatography.

2-methyl-5-(2-methylbenzimidazol-1-yl)-7-(morpholin-4-yl)pyrazolo[1,5-*a*]pyrimidine (5)

Compound 5 was prepared from compound 4 (0.20 g, 0.62 mmol), acetic acid (70 μL, 74 mg, 1.23 mmol), HOBt (0.10 g, 0.74 mmol), EDCI (0.28 g, 1.48 mmol), TEA (0.26 mL, 0.19 g, 1.85 mmol) and DCM (6.0 mL). The crude product was purified by flash chromatography to give 5 (0.16 g, 0.46 mmol) as a light yellow solid with 73% yield. ¹H NMR (300 MHz, CDCl₃) δ 7.78–7.72 (m, 1H, Ar-H), 7.50–7.45 (m,

1H, Ar-H), 7.34–7.22 (m, 2H, Ar-H), 6.42 (s, 1H, Ar-H), 6.16 (s, 1H, Ar-H), 4.03–3.97 (m, 4H, morph.), 3.88–3.82 (m, 4H, morph.), 2.76 (s, 3H, CH₃), 2.53 (s, 3H, CH₃). ¹³C NMR (75 MHz, CDCl₃) δ 155.0, 151.6, 151.2, 150.4, 148.5, 142.7, 134.5, 123.0, 122.9, 119.4, 110.4, 96.1, 87.5, 66.2, 48.4, 15.6, 14.8. MS-ESI: *m/z* calcd for C₁₉H₂₀N₆O [M+H]⁺: 349.18; found 349.1.

2-methyl-5-(2-ethylbenzimidazol-1-yl)-7-(morpholin-4-yl)pyrazolo[1,5-*a*]pyrimidine (6)

Compound 6 was prepared from compound 4 (0.20 g, 0.62 mmol), propionic acid (92 μL, 91 mg, 1.23 mmol), HOBt (0.10 g, 0.74 mmol), EDCI (0.28 g, 1.48 mmol), TEA (0.26 mL, 0.19 g, 1.85 mmol) and DCM (6.0 mL). The crude product was purified by flash chromatography to give 6 (0.17 g, 0.47 mmol) as a white solid with 75% yield. ¹H NMR (300 MHz, CDCl₃) δ 7.83–7.76 (m, 1H, Ar-H), 7.47–7.41 (m, 1H, Ar-H), 7.34–7.21 (m, 2H, Ar-H), 6.42 (s, 1H, Ar-H), 6.15 (s, 1H, Ar-H), 4.03–3.97 (m, 4H, morph.), 3.88–3.82 (m, 4H, morph.), 3.11 (q, *J* = 7.5 Hz, 2H, CH₂), 2.53 (s, 3H, CH₃), 1.41 (t, *J* = 7.5 Hz, 3H, CH₃). ¹³C NMR (75 MHz, CDCl₃) δ 156.2, 155.0, 151.2, 150.4, 148.4, 142.7, 134.6, 123.0, 122.7, 119.5, 110.2, 96.2, 87.7, 66.2, 48.4, 22.1, 14.8, 11.9. MS-ESI: *m/z* calcd for C₂₀H₂₂N₆O [M+H]⁺: 363.19; found 363.1.

2-methyl-5-(2-difluoromethylbenzimidazol-1-yl)-7-(morpholin-4-yl)pyrazolo[1,5-*a*]pyrimidine (7)

Compound 7 was prepared from compound 4 (0.20 g, 0.62 mmol), difluoroacetic acid (77 μL, 0.12 g, 1.23 mmol), HOBt (0.10 g, 0.74 mmol), EDCI (0.28 g, 1.48 mmol), TEA (0.26 mL, 0.19 g, 1.85 mmol) and DCM (6.0 mL). The crude product was purified by flash chromatography to give 7 (0.18 g, 0.47 mmol) as a white solid with 76% yield. ¹H NMR (300 MHz, CDCl₃) δ 7.92 (d, *J* = 7.1 Hz, 1H, Ar-H), 7.65 (d, *J* = 7.4 Hz, 1H, Ar-H), 7.47–7.38 (m, 2H, Ar-H), 7.24 (t, *J* = 26.8 Hz, 1H, CHF₂), 6.42 (s, 1H, Ar-H), 6.28 (s, 1H, Ar-H), 4.02–3.97 (m, 4H, morph.), 3.92–3.87 (m, 4H, morph.), 2.53 (s, 3H, CH₃). MS-ESI: *m/z* calcd for C₁₉H₁₈F₂N₆O [M+H]⁺: 385.16; found 385.0.

Procedure for 1-*tert*-butyl-3-methyl-*N*-[2-methyl-7-(morpholin-4-yl)pyrazolo[1,5-*a*]pyrimidin-5-yl]-1*H*-pyrazol-5-amine (8)

The mixture of compound 3 (0.64 g, 2.53 mmol), 1-*tert*-butyl-3-methyl-1*H*-pyrazol-5-amine (0.59 g, 3.86 mmol), cesium carbonate (1.70 g, 5.16 mmol), tris(dibenzylideneacetone)dipalladium(0) (0.13 g, 0.12 mmol), 9,9-dimethyl-4,5-bis(diphenylphosphine)xanthene (0.15 g, 0.25 mmol) and dry toluene (30 mL) were introduced to the reaction Schlenk flask. The whole mixture was flushed with argon and stirred at 100 °C for 18 h. After cooling to room temperature, the reaction mixture was filtered through the Celite®, and the solid was washed with CHCl₃ (50 mL). The filtrate was concentrated under reduced pressure. The residue was resolved on a chromatographic column (amine-functionalized silica gel) (0–10% ethyl acetate gradient in heptane) to give compound 8 (0.51 g, 1.38 mmol) with 54% yield. ¹H NMR (300 MHz, CDCl₃) δ 7.02 (s, 1H, Ar-H), 6.01 (s, 1H, Ar-H), 5.77 (s, 1H), 3.96–3.86 (m, 4H, morph.), 3.59–3.49 (m, 4H, morph.), 2.38 (s, 3H, CH₃), 2.29 (s, 3H, CH₃), 1.60 (s, 9H, *t*-Bu.). ¹³C NMR (75 MHz, CDCl₃) δ 156.9, 154.3, 151.9, 151.0, 146.1, 137.3, 104.6, 92.1, 79.2, 66.5, 59.8, 48.8, 30.3, 15.0, 14.6. MS-ESI: *m/z* calcd for C₁₉H₂₇N₇O [M+H]⁺: 370.24; found 370.1.

Procedure for 3-methyl-*N*-[2-methyl-7-(morpholin-4-yl)pyrazolo[1,5-*a*]pyrimidin-5-yl]-1*H*-pyrazol-5-amine (9)

Compound 8 (0.20 g, 0.545 mmol), trifluoroacetic acid (1.0 mL), and water (4.0 mL) were refluxed for 20 h. Then, the reaction mixture was cooled to room temperature, water (10 mL) was added and the whole mixture was alkalinized with saturated sodium carbonate solution (12 mL). Precipitation was observed and obtained solid was filtered off, washed with water (5 mL), and dried. The title compound 9 (0.15 g, 0.48 mmol) was isolated as a white solid with 89% yield. ¹H NMR (400 MHz, DMSO-*d*₆) δ 11.86 (s, 1H, NH), 9.41 (s, 1H, NH), 6.30 (s, 1H, Ar-H), 6.06 (s, 1H, Ar-H), 5.85 (s, 1H, Ar-H), 3.80–3.78 (m, 4H, morph.), 3.52–3.50 (m, 4H, morph.), 2.27 (s, 3H, CH₃), 2.20 (s, 3H, CH₃). ¹³C NMR (101 MHz, DMSO-*d*₆) δ 153.6, 151.6, 150.7, 150.1, 95.1, 91.4, 81.8, 65.6, 48.0, 14.4, 10.9. MS-ESI: *m/z* calcd for C₁₅H₁₉N₇O [M+H]⁺: 314.17; found 314.1.

General Procedure for the Suzuki Reaction

To the solution of compound **3** (1.0 eq) dissolved in 1,2-dimethoxyethane (DME) (10 mL/1 g of compound **3**), boronic acid pinacol ester or boronic acid (1.5 eq), tetrakis(triphenylphosphino)palladium(0) (0.2 eq) and 2M aqueous sodium carbonate solution (2.0 eq) were added. The reaction mixture was refluxed overnight. Then, the reaction mixture was cooled to room temperature, filtered through the pad of Celite®, and obtained solid washed with ethyl acetate. The filtrate was concentrated under reduced pressure using an evaporator and the residue was purified by column chromatography.

2-methyl-7-(morpholin-4-yl)-5-(1*H*-pyrazol-4-yl)pyrazolo[1,5-*a*]pyrimidine (**10**)

Synthesized from compound **3** (0.15 g, 0.594 mmol), 4-(4,4,5,5-tetramethyl-1,3,2-dioxaborolan-2-yl)-1*H*-pyrazole-1-carboxylic acid tert-butyl ester (0.26 g, 0.890 mmol), tetrakis(triphenylphosphine)palladium(0) (0.14 g, 0.119 mmol), 2M aqueous sodium carbonate solution (0.59 mL, 1.19 mmol) and DME (6 mL). The crude product was purified by flash chromatography (0–100% ethyl acetate gradient in heptane) to give **10** (0.095 g, 0.33 mmol) with 56% yield. ¹H NMR (300 MHz, DMSO-*d*₆) δ 13.18 (s, 1H, NH), 8.49 (s, 1H, Ar-H), 8.13 (s, 1H, Ar-H), 6.60 (s, 1H, Ar-H), 6.24 (s, 1H, Ar-H), 3.90–3.78 (m, 4H, morph.), 3.78–3.63 (m, 4H, morph.), 2.37 (s, 3H, CH₃). ¹³C NMR (75 MHz, DMSO-*d*₆) δ 152.8, 151.7, 151.4, 149.8, 138.1, 128.7, 121.7, 93.9, 89.3, 65.9, 48.3, 14.7. MS-ESI: *m/z* calcd for C₁₄H₁₆N₆O [M+H]⁺: 285.15; found 284.9.

2-methyl-7-(morpholin-4-yl)-5-(2-aminopyridin-5-yl)pyrazolo[1,5-*a*]pyrimidine (**11**)

Synthesized from compound **3** (0.10 g, 0.396 mmol), 2-aminopyridine-5-boronic acid pinacol ester (0.14 g, 0.594 mmol), tetrakis(triphenylphosphine)palladium(0) (91 mg, 0.079 mmol), 2M aqueous sodium carbonate solution (0.40 mL, 0.791 mmol) and DME (4 mL). The crude product was purified by flash chromatography (0–100% ethyl acetate gradient in heptane) to give **11** (0.075 g, 0.032 mol) with 61% yield. ¹H NMR (300 MHz, CDCl₃+CD₃OD) δ 8.58 (d, *J* = 1.8 Hz, 1H), 8.11 (dd, *J* = 8.8, 1.8 Hz, 1H), 6.68 (d, *J* = 8.8 Hz, 1H, Ar-H), 6.47 (s, 1H, Ar-H), 6.34 (s, 1H), 4.04–3.98 (m, 4H, morph.), 3.80–3.75 (m, 4H, morph.), 2.49 (s, 3H, CH₃). ¹³C NMR (75 MHz, CDCl₃+CD₃OD) δ 146.6, 136.8, 108.8, 100.2, 94.7, 88.7, 74.8, 70.2, 66.1, 29.5, 16.55, 14.0. MS-ESI: *m/z* calcd for C₁₆H₁₈N₆O [M+H]⁺: 311.16; found 311.0.

2-methyl-7-(morpholin-4-yl)-5-(1*H*-indazole-4-yl)pyrazolo[1,5-*a*]pyrimidine (**12**)

Synthesized from compound **3** (0.10 g, 0.396 mmol), 1*H*-indazole-4-boronic acid (0.10 g, 0.594 mmol), tetrakis(triphenylphosphine)palladium(0) (91 mg, 0.079 mmol), 2M aqueous sodium carbonate solution (0.40 mL, 0.791 mmol) and DME (4 mL). The crude product was purified by flash chromatography (0–100% ethyl acetate gradient in heptane) to give **12** (0.077 g, 0.23 mmol) with 58% yield. ¹H NMR (300 MHz, CDCl₃) δ 8.76–8.74 (m, 1H, NH), 7.69–7.65 (m, 1H), 7.61–7.57 (m, 1H, Ar-H), 7.53–7.46 (m, 1H), 6.59 (s, 1H, Ar-H), 6.50 (s, 1H, Ar-H), 4.06–3.98 (m, 4H, morph.), 3.85–3.76 (m, 4H, morph.), 2.54 (s, 3H, CH₃). ¹³C NMR (75 MHz, CDCl₃) δ 156.8, 154.8, 151.9, 150.6, 141.2, 135.8, 132.3, 128.9, 126.9, 121.0, 111.7, 96.3, 91.2, 66.6, 48.7, 15.2. MS-ESI: *m/z* calcd for C₁₈H₁₈N₆O [M+H]⁺: 335.16; found 335.1.

2-methyl-7-(morpholin-4-yl)-5-(1*H*-indole-4-yl)pyrazolo[1,5-*a*]pyrimidine (**13**)

Synthesized from compound **3** (0.10 g, 0.404 mmol), indole-4-boronic acid pinacol ester (0.15 g, 0.606 mmol), tetrakis(triphenylphosphine)palladium(0) (93 mg, 0.081 mmol), 2M aqueous sodium carbonate solution (0.40 mL, 0.80 mmol) and DME (5 mL). The crude product was purified by flash chromatography (0–50% ethyl acetate gradient in heptane) to give **13** (0.074 g, 0.22 mmol) with 55% yield. ¹H NMR (300 MHz, CDCl₃) δ 8.68 (s, 1H, NH), 7.63–7.55 (m, 1H, Ar-H), 7.48–7.39 (m, 1H, Ar-H), 7.33–7.21 (m, 2H, Ar-H), 7.10–7.04 (m, 1H, Ar-H), 6.61 (s, 1H, Ar-H), 6.45 (s, 1H, Ar-H), 4.05–3.93 (m, 4H, morph.), 3.82–3.70 (m, 4H, morph.), 2.52 (s, 3H, CH₃). ¹³C NMR (75 MHz, CDCl₃) δ 158.4, 154.1, 151.7, 150.1, 136.6, 131.3, 125.9, 125.4, 121.9, 120.2, 112.6, 102.6, 95.5, 92.1, 66.3, 48.4, 14.8. MS-ESI: *m/z* calcd for C₁₉H₁₉N₅O [M+H]⁺: 334.17; found 334.0.

Procedure for Ethyl 2-benzyloxyacetate (**14**)

To the suspension of 60% NaH (21.8 g, 0.545 mol) in dry toluene (1000 mL), benzyl alcohol (47 mL, 0.454 mol) was added dropwise over 30 min. The whole mixture was stirred at room temperature for 4 h. The suspension was cooled in a water-ice bath and ethyl bromoacetate (66 mL, 0.595 mol) was added dropwise for 45 min. The reaction mixture was heated to room temperature and stirred for one h. The whole mixture was poured onto ice water (1200 mL) acidified with concentrated hydrochloric acid (10 mL) to pH 4. Phases were separated and the aqueous phase was extracted three times with diethyl ether (200 mL). Combined organic phases were washed with brine and dried over anhydrous magnesium sulfate. After filtration of the drying agent, organic solvents were evaporated under reduced pressure. The residue was separated by distillation under reduced pressure to give (66.7 g, 0.34 mol) ethyl 2-benzyloxyacetate (**14**) with 76% yield as a colorless liquid ($T_b = 104\text{--}106^\circ\text{C} / 0.7\text{ tor}$). $^1\text{H NMR}$ (500 MHz, CDCl_3) δ : 7.39–7.28 (m; 5H, Ar-H), 4.63 (s; 2H, CH_2), 4.23 (q; $J = 7.1\text{ Hz}$; 2H, CH_2), 4.09 (s; 2H, CH_2), 1.28 (t; $J = 7.1\text{ Hz}$; 3H, CH_3). MS-ESI: m/z calcd for $\text{C}_{11}\text{H}_{14}\text{O}_3$ [$\text{M}+\text{H}$] $^+$: 195.23; found 195.1.

Procedure for 4-benzyloxy-3-oxobutyronitrile (**15**)

A flask filled with dry THF (750 mL) under an argon atmosphere was cooled to -78°C , then 2.5 M *n*-BuLi hexane solution (200 mL, 0.5 mol) was added, and after that acetonitrile (28 mL, 0.533 mol) was added dropwise. The whole mixture was stirred at -78°C for 2 h. The mixture was transferred dropwise to the suspension of ethyl 2-benzyloxyacetate (77.7 g, 0.4 mol) dropwise, and stirring was continued at -78°C for one h. The reaction was quenched with ammonium chloride solution (500 mL). The reaction mixture was poured onto ice water and acidified with 6 M hydrochloric acid (250 mL) to pH 3. The aqueous phase was extracted twice with diethyl ether (400 mL). Combined organic phases were washed with brine and dried over anhydrous magnesium sulfate. The drying agent was filtered off, and the solvent was evaporated under reduced pressure. Compound **15** was used in the next step without additional purification. MS-ESI: m/z calcd for $\text{C}_{11}\text{H}_{11}\text{NO}_2$ [$\text{M}+\text{H}$] $^+$: 190.22; found 190.1.

Procedure for 3-(benzyloxymethyl)-1*H*-pyrazol-5-amine (**16**)

To compound **15** (75.7 g, 0.4 mol, obtained above), ethanol (500 mL) and hydrazine monohydrate (100 mL, 2.1 mol) were added. The mixture was refluxed for 16 h. After concentration, the residue was dissolved with chloroform and dried over anhydrous sodium sulfate. Then, the drying agent was filtered off, and the solvent was evaporated. The crude product was purified by column chromatography (0–5% methanol gradient in ethyl acetate) to give **16** (70.4 g, 0.34 mol) with 87% yield after two steps as a brown oil. $^1\text{H NMR}$ (300 MHz; CDCl_3) δ : 7.39–7.28 (m; 5H, Ar-H); 5.59 (s; 1H); 4.53 (s; 2H, CH_2); 4.50 (s; 2H, CH_2). MS-ESI: m/z calcd for $\text{C}_{11}\text{H}_{13}\text{N}_3\text{O}$ [$\text{M}+\text{H}$] $^+$: 204.25; found 204.1.

Procedure for 2-(benzyloxymethyl)pyrazolo[1,5-*a*]pyrimidin-5,7-diol (**17**)

To the flask containing sodium ethanolate solution (obtained from sodium ethanolate (53 g, 0.74 mol) and ethanol (700 mL)), compound **16** (70.4 g, 0.35 mol) dissolved in ethanol (200 mL) and diethyl malonate (80 mL, 0.53 mol) was added. The reaction was refluxed for 24 h. Then the reaction mixture was cooled to room temperature, and the solvent was evaporated under reduced pressure. The residue was dissolved in water (1200 mL) and acidified with concentrated hydrochloric acid (250 mL). Creamy solid precipitated from the solution was filtered off, washed, and dried to give **17** (79.0 g, 0.27 mol) with 84% yield as a creamy solid. MS-ESI: m/z calcd for $\text{C}_{14}\text{H}_{13}\text{N}_3\text{O}_3$ [$\text{M}+\text{Na}$] $^+$: 294.26; found 294.1.

Procedure for 2-(benzyloxymethyl)-5,7-dichloropyrazolo[1,5-*a*]pyrimidine (**18**)

The suspension of compound **17** (30 g, 0.11 mol) in acetonitrile (270 mL) was cooled to 0°C in a water-ice bath, and POCl_3 (206 mL, 2.2 mol) was added. The reaction was heated at 80°C for five h. The reaction mixture was concentrated under reduced pressure to remove acetonitrile and POCl_3 . The residue was poured onto the water with ice and alkalized to pH 5 with saturated sodium hydrogen carbonate solution (350 mL). The aqueous phase was extracted with ethyl acetate, and after separation, the organic phase was dried over anhydrous sodium sulfate. After filtration of the drying agent and evaporation of the solvent, the residue was purified by column chromatography (0–20% ethyl acetate gradient in heptane) to give **18** (13 g, 42.3 mmol) with 38% yield as a slightly yellow oil. $^1\text{H NMR}$ (300

MHz, CDCl₃) δ : 7.41–7.27 (m; 5H, Ar-H); 6.96 (s; 1H, Ar-H); 6.80 (s; 1H, Ar-H); 4.81 (s; 2H, CH₂); 4.65 (s; 2H, CH₂). MS-ESI: m/z calcd for C₁₄H₁₁Cl₂N₃O [M+H]⁺: 309.17; found 308.0.

Procedure for 2-(benzyloxymethyl)-5-chloro-7-(morpholin-4-yl)pyrazolo[1,5-*a*]pyrimidine (**19**)

To the solution of compound **18** (13 g, 42.3 mmol) dissolved in acetone (450 mL), sodium carbonate (5.38 g, 50.8 mmol), and morpholine (6.65 mL, 76.2 mmol) were added. The reaction was carried out at room temperature for 1.5 h. 500 mL of water were added to the reaction mixture, and the precipitated white solid was filtered off. The solid was washed with water (300 mL) and water/acetone mixture (2/1, *v/v*) (200 mL), then dried to give **19** (14 g, 39.01 mmol) with 92% yield as a white solid. ¹H NMR (300 MHz, CDCl₃) δ : 7.41–7.27 (m; 5H, Ar-H); 6.56 (s; 1H, Ar-H); 6.06 (s; 1H, Ar-H); 4.73 (s; 2H, CH₂); 4.62 (s; 2H, CH₂); 3.98–3.90 (m; 4H, morph.); 3.82–3.74 (m; 4H, morph.). MS-ESI: m/z calcd for C₁₈H₁₉ClN₄O₂ [M+H]⁺: 359.83; found 359.2.

Procedure for 2-(benzyloxymethyl)-5-(1H-indol-4-yl)-7-(morpholin-4-yl)pyrazolo[1,5-*a*]pyrimidine (**20**)

To the solution of compound **19** (1.88 g, 5.24 mmol) dissolved in 1,2-dimethoxyethane (DME) (52 mL), indole-4-boronic acid pinacol ester (1.97 g, 7.87 mmol), tetrakis(triphenylphosphino)palladium (0) (0.61 g, 0.52 mmol) and 2M aqueous sodium carbonate solution (5.2 mL) were added. The reaction was refluxed for 16 h. Then, the reaction mixture was cooled to room temperature, filtered through the Celite®, and the solid was washed with ethyl acetate (50 mL). The filtrate was concentrated under reduced pressure using an evaporator. The crude product was purified by column chromatography (0–70% ethyl acetate gradient in heptane) to obtain compound **20** (1.91 g, 4.34 mmol) with an 83% yield. ¹H NMR (300 MHz, CDCl₃) δ : 8.61 (s; 1H); 7.61 (dd; *J* = 7.4; 0.8 Hz; 1H, Ar-H); 7.50–7.23 (m; 8H); 7.13–7.07 (m; 1H, Ar-H); 6.74 (s; 1H, Ar-H); 6.66 (s; 1H, Ar-H); 4.81 (s; 2H, CH₂); 4.67 (s; 2H, CH₂); 4.02–3.95 (m; 4H, morph.); 3.81–3.73 (m; 4H, morph.). MS-ESI: m/z calcd for C₂₆H₂₅N₅O₂ [M+H]⁺: 440.21; found 440.1.

Procedure for [5-(1H-indol-4-yl)-7-(morpholin-4-yl)pyrazolo[1,5-*a*]pyrimidin-2-yl]methanol (**21**)

To the solution of compound **20** (5.0 g, 9.1 mmol) in DMF (120 mL) and EtOH (60 mL), 10% Pd/C (11.3 g) and formic acid (100 μ L) were added. The reaction was heated to 60 °C under hydrogen pressure for 24 h. After cooling the reaction mixture to room temperature, the catalyst was filtered-off on a Celite®, washed with EtOH (50 mL), and the filtrate was then concentrated under reduced pressure using an evaporator. The crude product was purified by column chromatography (0–100% ethyl acetate gradient in heptane) to give **21** (2.08 g, 5.95 mmol) with 66% yield. ¹H NMR (300 MHz, DMSO-*d*₆) δ 11.36 (s; 1H, NH); 7.70–7.63 (m; 1H, Ar-H); 7.59–7.52 (m; 1H, Ar-H); 7.52–7.46 (m; 1H, Ar-H); 7.28–7.20 (m; 1H, Ar-H); 7.14–7.09 (m; 1H, Ar-H); 6.78 (s; 1H, Ar-H); 6.55 (s; 1H, Ar-H); 5.36 (t; *J* = 6.0 Hz; 1H, OH); 4.66 (d; *J* = 6.0 Hz; 2H, CH₂); 3.90–3.83 (m; 4H, morph.); 3.83–3.75 (m; 4H, morph.). MS-ESI: m/z calcd for C₁₉H₁₉N₅O₂ [M+H]⁺: 350.39; found 350.2.

Procedure for 5-(1H-indol-4-yl)-7-(morpholin-4-yl)pyrazolo[1,5-*a*]pyrimidin-2-carboxyaldehyde (**22**)

To the solution of compound **21** (0.90 g, 2.58 mmol) in dry DMF (26 mL), Dess–Martin reagent (1.31 g, 3.09 mmol) was added. The whole mixture was stirred at room temperature for one h. The obtained solid was filtered off and then washed with ethyl acetate (35 mL). The obtained solution was concentrated under reduced pressure. The crude product was purified by flash chromatography (0–70% ethyl acetate gradient in heptane) to give **22** (0.70 g, 2.01 mmol) with 78% yield. ¹H NMR (300 MHz, CDCl₃) δ 10.22 (s; 1H, CHO); 8.47 (s; 1H); 7.66–7.59 (m; 1H, Ar-H); 7.57–7.50 (m; 1H, Ar-H); 7.39–7.29 (m; 2H, Ar-H); 7.18–7.09 (m; 2H, Ar-H); 6.83 (s; 1H, Ar-H); 4.08–4.00 (m; 4H, morph.); 3.86–3.77 (m; 4H, morph.). MS-ESI: m/z calcd for C₁₉H₁₇N₅O₂ [M+H]⁺: 348.38; found 348.1.

General Procedure for the Reductive Amination Reaction (**23–45**)

To the solution of compound **22** (1.0 eq) in dry DCM (10 mL/1 g of compound **22**), amine derivative (1.2 eq) was added and then stirred at room temperature. After 1 h sodium triacetoxyborohydride (1.5 eq) was added and the mixture was stirred at room temperature for 15 h. To the reaction mixture was added water and phases were separated. The aqueous phase was extracted three times with DCM.

Combined organic phases were dried over anhydrous sodium sulfate, filtered, and evaporated under reduced pressure. The residue was purified by flash chromatography.

5-(1*H*-indol-4-yl)-2-((4-(methylsulfonyl)piperazin-1-yl)methyl)-7-(morpholin-4-yl)pyrazolo[1,5-*a*]pyrimidine (**23**)

Compound **23** was prepared from aldehyde **22** (0.39 g, 0.65 mmol), 1-methanesulfonylpiperazine (0.13 g, 0.78 mmol), DCM (4.0 mL) and sodium triacetoxyborohydride (0.25 g, 1.18 mmol). The crude product was purified by flash chromatography (0–10% MeOH gradient in AcOEt) to give **23** (0.27 mg, 0.54 mmol) as a light yellow solid with 84% yield. ¹H NMR (600 MHz, DMSO-*d*₆) δ 11.31 (s, 1H, NH), 7.64 (dd, *J* = 7.4, 0.8 Hz, 1H, Ar-H), 7.53 (dt, *J* = 8.0, 0.8 Hz, 1H, Ar-H), 7.47 (t, *J* = 2.8 Hz, 1H, Ar-H), 7.22 (t, *J* = 7.7 Hz, 1H, Ar-H), 7.10–7.09 (m, 1H, Ar-H), 6.77 (s, 1H, Ar-H), 6.51 (s, 1H, Ar-H), 3.86–3.84 (m, 4H, morph.), 3.79–3.77 (m, 4H, morph.), 3.74 (s, 2H, CH₂), 3.14–3.13 (m, 4H), 2.86 (s, 3H, CH₃), 2.58–2.57 (m, 4H). ¹³C NMR (151 MHz, DMSO-*d*₆) δ 157.9, 153.5, 151.0, 149.5, 136.7, 129.9, 126.4, 125.6, 120.7, 119.5, 113.2, 101.8, 94.7, 91.5, 65.6, 55.5, 51.8, 47.8, 45.4, 33.7. HRMS (ESI): *m/z* calcd for C₂₄H₂₉N₇O₃S [M+H]⁺: 496.2125; found 496.2134.

2-((4-(dimethylamino)piperidin-1-yl)methyl)-5-(1*H*-indol-4-yl)-7-(morpholin-4-yl)pyrazolo[1,5-*a*]pyrimidine (**24**)

Compound **24** was prepared from aldehyde **22** (0.18 g, 0.52 mmol), 4-(dimethylamino)piperidine dihydrochloride (0.13 g, 0.62 mmol), DCM (3.5 mL), triethylamine (0.17 mL, 1.24 mmol) and sodium triacetoxyborohydride (0.17 g, 0.78 mmol). The crude product was purified by flash chromatography (0–20% MeOH gradient in AcOEt) to give **24** (0.18 g, 0.39 mmol) as a light yellow solid with 76% yield. ¹H NMR (300 MHz, CDCl₃) δ: 8.85 (s, 1H, NH); 7.60 (d; *J* = 7.2 Hz; 1H, Ar-H); 7.51 (d; *J* = 8.2 Hz; 1H, Ar-H); 7.36–7.28 (m; 2H, Ar-H); 7.12–7.08 (m; 1H, Ar-H); 6.65 (s; 1H, Ar-H); 6.61 (s; 1H, Ar-H); 4.04–3.94 (m; 4H, morph.); 3.80 (s; 2H, CH₂); 3.79–3.72 (m; 4H, morph.); 3.19–3.07 (m; 2H, CH₂); 2.60–2.49 (m; 1H, CH); 2.44 (s; 6H, 2xCH₃); 2.22–2.09 (m; 2H, CH₂); 1.98–1.86 (m; 2H); 1.76–1.59 (m; 2H) HRMS (ESI): *m/z* calcd for C₂₆H₃₃N₇O [M+H]⁺: 460.2819; found 460.2842.

5-(1*H*-indol-4-yl)-2-((3*R*)-1-methylpyrrolidin-3-ol)methyl)-7-(morpholin-4-yl)pyrazolo[1,5-*a*]pyrimidine (**25**)

Compound **25** was prepared from aldehyde **22** (0.17 g, 0.48 mmol), (*R*)-(+)-3-pyrrolidinol (53 mg, 0.58 mmol), DCM (2.0 mL) and sodium triacetoxyborohydride (0.18 mg, 0.86 mmol). The crude product was purified by flash chromatography (0–30% MeOH gradient in AcOEt) to give **25** (50 mg, 0.12 mmol) as a light yellow solid with 25% yield. ¹H NMR (600 MHz, DMSO-*d*₆) δ 11.31 (s, 1H, NH), 7.64 (dd, *J* = 7.4, 0.6 Hz, 1H, Ar-H), 7.53 (d, *J* = 8.0 Hz, 1H, Ar-H), 7.46 (t, *J* = 2.8 Hz, 1H, Ar-H), 7.21 (t, *J* = 7.7 Hz, 1H, Ar-H), 7.09 (t, *J* = 2.1 Hz, 1H, Ar-H), 6.76 (s, 1H, Ar-H), 6.50 (s, 1H, Ar-H), 4.21–4.19 (m, 1H), 3.86–3.84 (m, 4H, morph.), 3.82–3.72 (m, 6H), 2.80–2.77 (m, 1H), 2.71–2.67 (m, 1H), 2.55–2.52 (m, 1H), 2.44–2.42 (m, 1H), 2.01–1.98 (m, 1H), 1.57–1.54 (m, 1H). ¹³C NMR (151 MHz, DMSO-*d*₆) δ 157.8, 154.6, 150.9, 149.5, 136.7, 130.0, 126.4, 125.6, 120.7, 119.5, 113.1, 101.8, 94.6, 91.4, 69.4, 65.6, 62.5, 53.3, 52.3, 47.8, 34.5. HRMS (ESI): *m/z* calcd for C₂₃H₂₆N₆O₂ [M+H]⁺: 419.2190; found 419.2191.

5-(1*H*-indol-4-yl)-2-((3*S*)-1-methylpyrrolidin-3-ol)methyl)-7-(morpholin-4-yl)pyrazolo[1,5-*a*]pyrimidine (**26**)

Compound **26** was prepared from aldehyde **22** (0.17 mg, 0.48 mmol), (*S*)-3-pyrrolidinol (52 mg, 0.58 mmol), DCM (2.0 mL) and sodium triacetoxyborohydride (0.18 mg, 0.86 mmol). The crude product was purified by flash chromatography (0–30% MeOH gradient in AcOEt) to give **26** (70 mg, 0.17 mmol) as a light yellow solid with 35% yield. ¹H NMR (600 MHz, DMSO-*d*₆) δ 11.33 (s, 1H, NH), 7.64 (dd, *J* = 7.4, 0.7 Hz, 1H, Ar-H), 7.53 (d, *J* = 8.0 Hz, 1H, Ar-H), 7.47 (t, *J* = 2.8 Hz, 1H, Ar-H), 7.22–7.20 (m, 1H, Ar-H), 7.09–7.08 (m, 1H, Ar-H), 6.76 (s, 1H, Ar-H), 6.50 (s, 1H, Ar-H), 4.21–4.19 (m, 1H), 3.86–3.84 (m, 4H, morph.), 3.78–3.72 (m, 6H), 2.78 (m, 1H), 2.68 (m, 1H), 2.54–2.50 (m, 1H), 2.43 (m, 1H), 2.03–1.97 (m, 1H), 1.57–1.54 (m, 1H). ¹³C NMR (151 MHz, DMSO-*d*₆) δ 157.8, 154.6, 150.9, 149.6, 136.8, 130.0, 126.5, 125.6, 120.8, 119.6, 113.2, 101.8, 94.6, 91.5, 69.5, 65.6, 62.6, 53.4, 52.4, 47.9, 34.5. HRMS (ESI): *m/z* calcd for C₂₃H₂₆N₆O₂ [M+H]⁺: 419.2190; found 419.2200.

2-((1,1-dioxothiomorpholin-1-yl)-methyl)-5-(1*H*-indol-4-yl)-7-(morpholin-4-yl)pyrazolo[1,5-*a*]pyrimidine (**27**)

Compound **27** was prepared from aldehyde **22** (85 mg, 0.25 mmol), thiomorpholine-1,1-dioxide (40 mg, 0.29 mmol), DCM (3.0 mL) and sodium triacetoxyborohydride (78 mg, 0.37 mmol). The crude product was purified by flash chromatography (0–10% MeOH gradient in AcOEt) to give **27** (48 mg, 0.10 mmol) as a light yellow solid with 42% yield. ¹H NMR (400 MHz, DMSO-*d*₆) δ 11.33 (s, 1H, NH), 7.62 (dd, *J* = 7.4, 0.8 Hz, 1H, Ar-H), 7.51 (d, *J* = 8.1 Hz, 1H, Ar-H), 7.44 (t, *J* = 2.8 Hz, 1H, Ar-H), 7.19 (t, *J* = 7.7 Hz, 1H, Ar-H), 7.07–7.06 (m, 1H, Ar-H), 6.75 (s, 1H, Ar-H), 6.54 (s, 1H, Ar-H), 3.87 (s, 2H), 3.83–3.81 (m, 3H), 3.75–3.74 (m, 3H), 3.12–3.09 (m, 4H), 2.98–2.95 (m, 4H). ¹³C NMR (101 MHz, DMSO-*d*₆) δ 158.0, 153.3, 151.0, 149.6, 136.8, 129.9, 126.5, 125.6, 120.8, 119.6, 113.3, 101.8, 94.8, 91.7, 65.6, 54.2, 50.6, 50.2, 47.9. HRMS (ESI): *m/z* calcd for C₂₃H₂₆N₆O₃S [M+H]⁺: 467.1860; found 467.1866.

5-(1*H*-indol-4-yl)-7-(morpholin-4-yl)-2-((morpholin-4-yl)methyl)pyrazolo[1,5-*a*]pyrimidine (**28**)

Compound **28** was prepared from aldehyde **22** (0.20 g, 0.23 mmol), morpholine (24 mL, 24 mg, 0.27 mmol), DCM (3.0 mL) and sodium triacetoxyborohydride (95 mg, 0.45 mmol). The crude product was purified by flash chromatography (0–10% MeOH gradient in AcOEt) to give **28** (55 mg, 0.13 mmol) as a light yellow solid with 59% yield. ¹H NMR (500 MHz, DMSO-*d*₆) δ 11.32 (s, 1H, NH), 7.65 (d, *J* = 7.4 Hz, 1H, Ar-H), 7.54 (d, *J* = 7.4 Hz, 1H, Ar-H), 7.49–7.45 (m, 1H, Ar-H), 7.25–7.19 (m, 1H, Ar-H), 7.12–7.08 (m, 1H, Ar-H), 6.77 (s, 1H, Ar-H), 6.52 (s, 1H, Ar-H), 3.89–3.83 (m, 4H, morph.), 3.81–3.76 (m, 4H, morph.), 3.68 (s, 2H, CH₂), 3.63–3.57 (m, 4H, morph.), 2.49–2.45 (m, 4H, morph.). ¹³C NMR (126 MHz, DMSO-*d*₆) δ: 157.9, 153.6, 151.0, 149.6, 136.8, 129.9, 126.5, 125.6, 120.8, 119.6, 113.2, 101.8, 94.8, 91.5, 66.2, 65.6, 56.4, 53.2, 47.9. HRMS (ESI): *m/z* calcd for C₂₃H₂₆N₆O₂ [M+H]⁺: 419.2190; found 419.2196.

5-(1*H*-indol-4-yl)-2-((4-(4-methylpiperazin-1-yl)piperidin-1-yl)methyl)-7-(morpholin-4-yl)pyrazolo[1,5-*a*]pyrimidine (**29**)

Compound **29** was prepared from aldehyde **22** (0.17 g, 0.50 mmol), 1-methyl-4-(piperidin-4-yl)piperazine (0.11 g, 0.6 mmol), DCM (3.5 mL) and sodium triacetoxyborohydride (0.16 g, 0.75 mmol). The crude product was purified by flash chromatography (0–15% MeOH gradient in AcOEt) to give **29** (0.23 g, 0.45 mmol) as a yellow solid with 89% yield. ¹H NMR (300 MHz, CDCl₃) δ: 9.56 (s; 1H); 7.62–7.55 (m; 1H, Ar-H); 7.47–7.1 (m; 1H, Ar-H); 7.31–7.21 (m; 2H, Ar-H); 7.11–7.02 (m; 1H, Ar-H); 6.64 (s; 1H, Ar-H); 6.62 (s; 1H, Ar-H); 4.00–3.90 (m; 4H, morph.); 3.86–3.62 (m; 6H); 3.19–3.05 (m; 2H); 2.81–2.45 (m; 8H); 2.34 (s; 3H); 2.39–2.29 (m; 1H); 2.21–2.08 (m; 2H); 1.91–1.79 (m; 2H); 1.75–1.54 (m; 2H). ¹³C NMR (75 MHz, CDCl₃) δ 158.8, 154.2, 151.6, 150.2, 136.8, 131.1, 126.1, 125.8, 121.8, 120.1, 113.0, 102.4, 96.0, 92.5, 66.3, 61.9, 56.5, 54.8, 53.0, 48.5, 48.4, 45.6, 27.9. HRMS (ESI): *m/z* calcd for C₂₉H₃₈N₈O [M+H]⁺: 515.3241; found 515.3224.

3-ethyl-1-(1-((5-(1*H*-indol-4-yl)-7-(morpholin-4-yl)pyrazolo[1,5-*a*]pyrimidin-2-yl)methyl)piperidin-4-yl)urea (**30**)

The 3-ethyl-1-(piperidin-4-yl)urea was synthesized according to the van Duzer et al. procedure [56]. The urea derivative was used in the reductive amination reaction (next step) as is, without additional purification.

Compound **30** was prepared from aldehyde **22** (0.20 g, 0.58 mmol), 3-ethyl-1-(piperidin-4-yl)urea hydrochloride (0.14 g, 0.69 mmol), DCM (4.0 mL), triethylamine (0.194 mL, 1.38 mmol) and sodium triacetoxyborohydride (0.19 g, 0.86 mmol). The crude product was purified by flash chromatography (0–15% MeOH gradient in AcOEt) to give **30** (0.15 g, 0.30 mmol) as a light yellow solid with 52% yield. ¹H NMR (400 MHz, DMSO-*d*₆) δ 11.33 (s, 1H), 7.64 (d, *J* = 7.4 Hz, 1H), 7.53 (d, *J* = 8.0 Hz, 1H), 7.47 (t, *J* = 2.7 Hz, 1H), 7.21 (t, *J* = 7.7 Hz, 1H, Ar-H), 7.09–7.09 (m, 1H, Ar-H), 6.76 (s, 1H, Ar-H), 6.48 (s, 1H, Ar-H), 5.71 (d, *J* = 7.8 Hz, 1H), 5.65 (t, *J* = 5.5 Hz, 1H), 3.86–3.84 (m, 4H), 3.78–3.77 (m, 4H), 3.64 (s, 2H), 3.36–3.36 (m, 1H), 3.01–2.94 (m, 2H), 2.81–2.78 (m, 2H), 2.15–2.10 (m, 2H), 1.74–1.72 (m, 2H, CH₂), 1.38–1.32 (m, 2H, CH₂), 0.96 (t, *J* = 7.1 Hz, 3H, CH₃). ¹³C NMR (101 MHz, DMSO-*d*₆) δ 157.9, 157.3, 154.3, 151.0, 149.5, 136.8, 130.0, 126.5, 125.6, 120.8, 119.6, 113.2, 101.8, 94.7, 91.5, 65.6, 56.2, 52.0, 47.9, 46.1, 33.9, 32.5, 15.7. HRMS (ESI): *m/z* calcd for C₂₇H₃₄N₈O₂ [M+H]⁺: 503.2877; found 503.2882.

1-phenyl-3-(1-((5-(1H-indol-4-yl)-7-(morpholin-4-yl)pyrazolo[1,5-a]pyrimidin-2-yl)methyl)piperidin-4-yl)urea (**31**)

The synthesis of 1-phenyl-3-(piperidin-4-yl)urea was conducted according to the van Duzer et al. procedure [56]. The urea derivative was used in the reductive amination reaction (next step) as is, without additional purification.

Compound **31** was prepared from aldehyde **22** (0.20 g, 0.58 mmol), 1-phenyl-3-(piperidin-4-yl)urea hydrochloride (0.18 g, 0.69 mmol), DCM (4.0 mL), triethylamine (0.194 mL, 1.38 mmol) and sodium triacetoxyborohydride (0.19 g, 0.86 mmol). The crude product was purified by flash chromatography (0–15% MeOH gradient in AcOEt) to give **31** (0.18 g, 0.33 mmol) as a light yellow solid with 58% yield. ¹H NMR (400 MHz, DMSO-*d*₆) δ 11.33 (s, 1H, NH), 8.30 (s, 1H), 7.65 (dd, *J* = 7.4, 0.8 Hz, 1H), 7.53 (d, *J* = 8.1 Hz, 1H), 7.47 (t, *J* = 2.8 Hz, 1H), 7.37–7.34 (m, 2H), 7.24–7.16 (m, 3H), 7.10–7.09 (m, 1H, Ar-H), 6.88–6.84 (m, 1H, Ar-H), 6.76 (s, 1H, Ar-H), 6.51 (s, 1H, Ar-H), 6.11 (d, *J* = 7.7 Hz, 1H), 3.86–3.84 (m, 4H, morph.), 3.79–3.78 (m, 4H, morph.), 3.67 (s, 2H, CH₂), 3.49–3.48 (m, 1H), 2.83–2.80 (m, 2H, CH₂), 2.22–2.17 (m, 2H, CH₂), 1.98–1.80 (m, 2H, CH₂), 1.47–1.38 (m, 2H, CH₂). ¹³C NMR (101 MHz, DMSO-*d*₆) δ 157.9, 154.5, 154.2, 151.0, 149.6, 140.5, 136.8, 130.0, 128.6, 126.5, 125.6, 120.9, 120.8, 119.6, 117.5, 113.2, 101.8, 94.7, 91.5, 65.6, 56.2, 51.7, 47.9, 46.0, 32.2. HRMS (ESI): *m/z* calcd for C₃₁H₃₄N₈O₂ [M+H]⁺: 551.2887; found 551.2880.

5-(1H-indol-4-yl)-2-((4-(4-methoxyphenyl)piperazin-1-yl)-methyl)-7-(morpholin-4-yl)pyrazolo[1,5-*a*]pyrimidine (**32**)

Compound **32** was prepared from aldehyde **22** (0.18 g, 0.52 mmol), 1-(4-methoxyphenyl)piperazine (0.12 g, 0.63 mmol), DCM (3.5 mL) and sodium triacetoxyborohydride (0.17 g, 0.79 mmol). The crude product was purified by flash chromatography (0–5% MeOH gradient in AcOEt) to give **32** (0.22 g, 0.42 mmol) as a light yellow solid with 81% yield. ¹H NMR (300 MHz, CDCl₃) δ: 8.52 (s; 1H, NH); 7.61 (d; *J* = 7.4 Hz; 1H, Ar-H); 7.49 (d; *J* = 8.1 Hz; 1H, Ar-H); 7.35–7.27 (m; 2H, Ar-H); 7.14–7.09 (m; 1H, Ar-H); 6.96–6.80 (m; 4H); 6.67 (s; 1H, Ar-H); 6.65 (s; 1H, Ar-H); 4.04–3.95 (m; 4H, morph.); 3.88 (s; 2H, CH₂); 3.82–3.76 (m; 4H, morph.); 3.77 (s; 3H, CH₃); 3.19–3.11 (m; 4H, piperaz.); 2.84–2.74 (m; 4H, piperaz.). ¹³C NMR (75 MHz, CDCl₃) δ 158.8, 154.3, 153.8, 151.7, 150.3, 145.8, 136.8, 131.3, 126.1, 125.6, 122.0, 120.3, 118.3, 114.5, 112.9, 102.7, 96.1, 92.5, 66.4, 56.8, 55.7, 53.4, 50.7, 48.6. HRMS (ESI): *m/z* calcd for C₃₀H₃₃N₇O₂ [M+H]⁺: 524.2769; found 524.2770.

5-(1H-indol-4-yl)-2-((4-methyl-piperazin-1-yl)methyl)-7-(morpholin-4-yl)pyrazolo[1,5-*a*]pyrimidine (**33**)

Compound **33** was prepared from aldehyde **22** (85 mg, 0.24 mmol), 1-methylpiperazine, (33 mL, 29 mg, 0.29 mmol), DCM (4.0 mL) and sodium triacetoxyborohydride (78 mg, 0.37 mmol). The crude product was purified by flash chromatography (0–20% MeOH gradient in AcOEt) to give **33** (91 mg, 0.21 mmol) as a light yellow solid with 86% yield. ¹H NMR (400 MHz, DMSO-*d*₆) δ 11.41 (s, 1H, NH), 7.64 (d, *J* = 7.4 Hz, 1H, Ar-H), 7.53 (d, *J* = 8.1 Hz, 1H, Ar-H), 7.46 (t, *J* = 2.7 Hz, 1H, Ar-H), 7.21 (t, *J* = 7.7 Hz, 1H, Ar-H), 7.09 (t, *J* = 2.0 Hz, 1H, Ar-H), 6.76 (s, 1H, Ar-H), 6.48 (s, 1H, Ar-H), 3.85–3.83 (m, 4H, morph.), 3.78–3.76 (m, 4H, morph.), 3.65 (s, 2H, CH₂), 2.50–2.45 (m, 4H, piperaz.), 2.32–2.32 (m, 4H, piperaz.), 2.14 (s, 3H, CH₃). ¹³C NMR (101 MHz, DMSO-*d*₆) δ 157.9, 154.0, 151.0, 149.6, 136.8, 129.9, 126.5, 125.6, 120.7, 119.6, 113.2, 101.8, 94.7, 91.5, 65.6, 56.0, 54.7, 52.6, 47.9, 45.7. HRMS (ESI): *m/z* calcd for C₂₄H₂₉N₇O [M+H]⁺: 432.2506; found 432.2511.

2-((4-ethylpiperazin-1-yl)methyl)-5-(1H-indol-4-yl)-7-(morpholin-4-yl)pyrazolo[1,5-*a*]pyrimidine (**34**)

Compound **34** was prepared from aldehyde **22** (85 mg, 0.24 mmol), 1-ethylpiperazine (37 mL, 33 mg, 0.29 mmol), DCM (4.0 mL) and sodium triacetoxyborohydride (78 mg, 0.37 mmol). The crude product was purified by flash chromatography (0–20% MeOH gradient in AcOEt) to give **34** (85 mg, 0.19 mmol) as a light yellow solid with 78% yield. ¹H NMR (400 MHz, DMSO-*d*₆) δ 11.37 (s, 1H, NH), 7.64 (d, *J* = 7.4 Hz, 1H, Ar-H), 7.53 (d, *J* = 8.1 Hz, 1H, Ar-H), 7.46 (t, *J* = 2.7 Hz, 1H, Ar-H), 7.21 (t, *J* = 7.7 Hz, 1H, Ar-H), 7.09–7.08 (m, 1H, Ar-H), 6.76 (s, 1H, Ar-H), 6.49 (s, 1H, Ar-H), 3.86–3.84 (m, 4H, morph.), 3.78–3.77 (m, 4H, morph.), 3.67 (s, 2H, CH₂), 2.63–2.44 (m, 8H, piperaz.), 2.39 (q, *J* = 7.2 Hz, 2H, CH₂), 1.00 (t, *J* = 7.2 Hz, 3H, CH₃). ¹³C NMR (101 MHz, DMSO-*d*₆) δ 172.0, 157.9, 153.8, 151.0, 149.6, 136.8, 129.9,

126.5, 125.6, 120.7, 119.6, 113.2, 101.8, 94.8, 91.5, 65.6, 55.9, 52.1, 51.4, 47.9, 21.1. HRMS (ESI): m/z calcd for $C_{25}H_{31}N_7O$ $[M+H]^+$: 446.2663; found 446.2661.

Methyl 1-((5-(1*H*-indol-4-yl)-7-(morpholin-4-yl)pyrazolo[1,5-*a*]pyrimidin-2-yl)methyl)piperidin-4-carboxylate (**35**)

Compound **35** was prepared from aldehyde **22** (85 mg, 0.24 mmol), methyl isonipecotate, (42 mg, 0.29 mmol), DCM (4.0 mL) and sodium triacetoxyborohydride (78 mg, 0.37 mmol). The crude product was purified by flash chromatography (0–10% MeOH gradient in $CHCl_3$) to give **35** (76 mg, 0.16 mmol) as a light yellow solid with 65% yield. 1H NMR (400 MHz, $DMSO-d_6$) δ 11.35 (s, 1H, NH), 7.64 (dd, $J = 7.4, 0.7$ Hz, 1H, Ar-H), 7.53 (d, $J = 8.1$ Hz, 1H, Ar-H), 7.47 (t, $J = 2.8$ Hz, 1H, Ar-H), 7.21 (t, $J = 7.7$ Hz, 1H, Ar-H), 7.10–7.09 (m, 1H, Ar-H), 6.76 (s, 1H, Ar-H), 6.49 (s, 1H, Ar-H), 3.86–3.83 (m, 4H, morph.), 3.78–3.77 (m, 4H, morph.), 3.65 (s, 2H, CH_2), 3.58 (s, 3H, CH_3), 2.87–2.84 (m, 2H, CH_2), 2.32–2.27 (m, 1H, CH), 2.11–2.06 (m, 2H, CH_2), 1.82–1.79 (m, 2H, CH_2), 1.63–1.57 (m, 2H). ^{13}C NMR (101 MHz, $DMSO-d_6$) δ 174.8, 157.9, 154.0, 151.0, 149.5, 136.8, 130.0, 126.5, 125.6, 120.7, 119.6, 113.2, 101.8, 94.7, 91.5, 65.6, 56.2, 52.2, 51.3, 47.9, 40.1, 28.0. HRMS (ESI): m/z calcd for $C_{26}H_{30}N_6O_3$ $[M+H]^+$: 475.2452; found 475.2458.

2-((4-(2-hydroxypropan-2-yl)piperidin-1-yl)methyl)-5-(1*H*-indol-4-yl)-7-(morpholin-4-yl)pyrazolo[1,5-*a*]pyrimidine (**36**)

Compound **36** was prepared from aldehyde **22** (0.18 g, 0.52 mmol), 2-(4-piperidyl)-2-propanol (93 mg, 0.62 mmol), DCM (3.5 mL) and sodium triacetoxyborohydride (0.17 g, 0.78 mmol). The crude product was purified by flash chromatography (0–5% MeOH gradient in AcOEt) to give **36** (0.183 g, 0.39 mmol) as an off-white solid with 74% yield. 1H NMR (300 MHz, $CDCl_3$) δ : 8.57 (s; 1H, NH); 7.64–7.58 (m; 1H, Ar-H); 7.52–7.46 (m; 1H, Ar-H); 7.36–7.25 (m; 2H, Ar-H); 7.14–7.09 (m; 1H, Ar-H); 6.64 (s; 1H, Ar-H); 6.64 (s; 1H, Ar-H); 4.03–3.95 (m; 4H, morph.); 3.82 (s; 2H, CH_2); 3.81–3.71 (m; 4H, morph.); 3.20–3.10 (m; 2H, CH_2); 2.18–2.03 (m; 2H, CH_2); 1.81–1.69 (m; 2H, CH_2); 1.56–1.38 (m; 2H, CH_2); 1.35–1.30 (m; 1H); 1.18 (s; 6H). ^{13}C NMR (75 MHz, $CDCl_3$) δ 158.7, 151.7, 150.2, 136.8, 131.3, 126.1, 125.6, 122.0, 120.3, 112.9, 102.7, 96.2, 92.4, 72.7, 66.4, 56.9, 54.2, 48.6, 47.3, 27.1, 27.0. HRMS (ESI): m/z calcd for $C_{27}H_{34}N_6O_6$ $[M+H]^+$: 475.2816; found 475.2815.

2-((4-*tert*-butylpiperazin-1-yl)methyl)-5-(1*H*-indol-4-yl)-7-(morpholin-4-yl)pyrazolo[1,5-*a*]pyrimidine (**37**)

Compound **37** was prepared from aldehyde **22** (0.12 g, 0.35 mmol), *N-tert*-butylpiperazine (59 mg, 0.42 mmol), DCM (2.0 mL) and sodium triacetoxyborohydride (0.11 g, 0.52 mmol). The crude product was purified by flash chromatography (0–20% MeOH gradient in AcOEt) to give **37** (0.15 g, 0.32 mmol) as a yellow solid with 93% yield. 1H NMR (400 MHz, $DMSO-d_6$) δ 11.33 (s, 1H, NH), 7.64 (dd, $J = 7.4, 0.9$ Hz, 1H, Ar-H), 7.53 (dt, $J = 8.1, 0.8$ Hz, 1H, Ar-H), 7.46 (t, $J = 2.8$ Hz, 1H, Ar-H), 7.21 (t, $J = 7.7$ Hz, 1H, Ar-H), 7.10–7.08 (m, 1H, Ar-H), 6.76 (s, 1H, Ar-H), 6.48 (s, 1H, Ar-H), 3.86–3.84 (m, 4H, morph.), 3.78–3.76 (m, 4H, morph.), 3.63 (s, 2H, CH_2), 2.53–2.45 (m, 8H, piperaz.), 0.98 (s, 9H, *t*-Bu.). ^{13}C NMR (101 MHz, $DMSO-d_6$) δ 157.8, 154.0, 151.0, 149.5, 136.8, 130.0, 126.5, 125.6, 120.7, 119.6, 113.2, 101.8, 94.8, 91.5, 65.6, 56.0, 53.5, 53.1, 47.9, 45.2, 25.7. HRMS (ESI): m/z calcd for $C_{27}H_{35}N_7O$ $[M+H]^+$: 474.2976; found 474.2976.

2-(4-((5-(1*H*-indol-4-yl)-7-(morpholin-4-yl)pyrazolo[1,5-*a*]pyrimidin-2-yl)methyl)piperazin-1-yl)-2-methylpropanamide (**38**)

Compound **38** was prepared from aldehyde **22** (0.20 g, 0.58 mmol), 2-methyl-2-(piperazin-1-yl)propanamide dihydrochloride (0.18 g, 0.69 mmol), DCM (3.0 mL), triethylamine (0.194 mL, 1.38 mmol) and sodium triacetoxyborohydride (0.18 g, 0.86 mmol). The crude product was purified by flash chromatography (0–10% MeOH gradient in AcOEt) to give **38** (0.21 g, 0.42 mmol) as a light yellow solid with 73% yield. 1H NMR (500 MHz, $DMSO-d_6$) δ 11.32 (s, 1H, NH), 7.65 (d, $J = 7.3$ Hz, 1H, Ar-H), 7.54 (d, $J = 8.0$ Hz, 1H, Ar-H), 7.49–7.45 (m, 1H, Ar-H), 7.22 (t, $J = 7.7$ Hz, 1H, Ar-H), 7.12–7.08 (m, 1H, Ar-H), 7.07–7.01 (m, 1H, Ar-H), 6.95–6.90 (m, 1H), 6.77 (s, 1H), 6.50 (s, 1H), 3.89–3.82 (m, 4H, morph.), 3.82–3.76 (m, 4H, morph.), 3.68 (s, 2H, CH_2), 2.57–2.51 (m, 4H), 2.49–2.40 (m, 4H), 1.06 (s, 6H). ^{13}C NMR (126 MHz,

DMSO-*d*₆) δ 178.1, 157.9, 153.9, 151.0, 149.5, 136.8, 130.0, 126.5, 125.6, 120.8, 119.6, 113.2, 101.8, 94.8, 91.5, 65.6, 62.4, 56.0, 53.2, 47.9, 46.1, 20.4. HRMS (ESI): *m/z* calcd for C₂₇H₃₄N₈O₂ [M+H]⁺: 503.2877; found 503.2901.

2-((4-cyclopropylpiperazin-1-yl)methyl)-5-(1*H*-indol-4-yl)-7-(morpholin-4-yl)pyrazolo[1,5-*a*]pyrimidine (**39**)

Compound **39** was prepared from aldehyde **22** (85 mg, 0.25 mmol), 1-cyclopropylpiperazine (35 mL, 37 mg, 0.29 mmol), DCM (3.0 mL) and sodium triacetoxymethylborohydride (78 mg, 0.37 mmol). The crude product was purified by flash chromatography (0–15% MeOH gradient in AcOEt) to give **39** (84 mg, 0.18 mmol) as a light yellow solid with 75% yield. ¹H NMR (400 MHz, DMSO-*d*₆) δ 11.32 (s, 1H, NH), 7.64 (dd, *J* = 7.4, 0.7 Hz, 1H, Ar-H), 7.53 (d, *J* = 8.1 Hz, 1H, Ar-H), 7.47 (t, *J* = 2.8 Hz, 1H, Ar-H), 7.21 (t, *J* = 7.7 Hz, 1H, Ar-H), 7.09 (t, *J* = 2.1 Hz, 1H), 6.76 (s, 1H, Ar-H), 6.48 (s, 1H, Ar-H), 3.85–3.83 (m, 4H, morph.), 3.78–3.76 (m, 4H, morph.), 3.64 (s, 2H, CH₂), 2.54 (s, 4H, piperaz.), 2.43 (s, 4H, piperaz.), 1.58 (s, 1H, CH), 0.38–0.36 (m, 2H, CH₂), 0.26–0.24 (m, 2H, CH₂). ¹³C NMR (101 MHz, DMSO-*d*₆) δ 157.9, 154.0, 151.0, 149.5, 136.8, 130.0, 126.5, 125.6, 120.7, 119.6, 113.2, 101.8, 94.7, 91.5, 65.6, 56.0, 52.7, 52.7, 47.9, 38.0, 5.6. HRMS (ESI): *m/z* calcd for C₂₆H₃₁N₇O [M+H]⁺: 458.2663; found 458.2666.

2-((4-cyclopentylpiperazin-1-yl)methyl)-5-(1*H*-indol-4-yl)-7-(morpholin-4-yl)pyrazolo[1,5-*a*]pyrimidine (**40**)

Compound **40** was prepared from aldehyde **22** (70 mg, 0.20 mmol), 1-cyclopentylpiperazine (39 mL, 38 mg, 0.24 mmol), DCM (4.0 mL) and sodium triacetoxymethylborohydride (64 mg, 0.30 mmol). The crude product was purified by flash chromatography (0–15% MeOH gradient in AcOEt) to give **40** (84 mg, 0.17 mmol) as a light yellow solid with 86% yield. ¹H NMR (400 MHz, DMSO-*d*₆) δ 11.34 (s, 1H, NH), 7.64 (dd, *J* = 7.4, 0.7 Hz, 1H, Ar-H), 7.53 (d, *J* = 8.1 Hz, 1H, Ar-H), 7.46 (t, *J* = 2.8 Hz, 1H, Ar-H), 7.21 (t, *J* = 7.7 Hz, 1H, Ar-H), 7.09 (t, *J* = 2.1 Hz, 1H, Ar-H), 6.76 (s, 1H, Ar-H), 6.48 (s, 1H, Ar-H), 3.86–3.83 (m, 4H, morph.), 3.78–3.76 (m, 4H, morph.), 3.64 (s, 2H, CH₂), 2.53–2.42 (m, 9H), 1.75–1.72 (m, 2H, CH₂), 1.59–1.55 (m, 2H), 1.48–1.44 (m, 2H), 1.31–1.26 (m, 2H). ¹³C NMR (101 MHz, DMSO-*d*₆) δ 157.9, 153.9, 151.0, 149.5, 136.8, 130.0, 126.4, 125.6, 120.7, 119.6, 113.2, 101.8, 94.7, 91.5, 66.7, 65.6, 56.0, 52.7, 51.6, 47.9, 29.8, 23.6. HRMS (ESI): *m/z* calcd for C₂₈H₃₅N₇O [M+H]⁺: 486.2976; found 486.2973.

2-((4-*tert*-butylpiperidin-1-yl)methyl)-5-(1*H*-indol-4-yl)-7-(morpholin-4-yl)pyrazolo[1,5-*a*]pyrimidine (**41**)

Compound **41** was prepared from aldehyde **22** (0.10 g, 0.29 mmol), 4-(*tert*-butyl)piperidine hydrochloride (61 mg, 0.35 mmol), DCM (4.0 mL), triethylamine (0.097 mL, 0.69 mmol) and sodium triacetoxymethylborohydride (94 mg, 0.43 mmol). The crude product was purified by flash chromatography (0–20% MeOH gradient in CHCl₃) to give **41** (0.10 g, 0.21 mmol) as a light yellow solid with 76% yield. ¹H NMR (400 MHz, DMSO-*d*₆) δ 11.32 (s, 1H, NH), 7.64 (dd, *J* = 7.4, 0.7 Hz, 1H, Ar-H), 7.53 (d, *J* = 8.1 Hz, 1H, Ar-H), 7.46 (t, *J* = 2.8 Hz, 1H, Ar-H), 7.21 (t, *J* = 7.7 Hz, 1H, Ar-H), 7.10–7.09 (m, 1H, Ar-H), 6.75 (s, 1H, Ar-H), 6.48 (s, 1H, Ar-H), 3.85–3.83 (m, 4H, morph.), 3.78–3.76 (m, 4H, morph.), 3.61 (s, 2H, CH₂), 2.98–2.95 (m, 2H, CH₂), 1.95–1.89 (m, 2H, CH₂), 1.59–1.56 (m, 2H, CH₂), 1.27–1.17 (m, 2H, CH₂), 0.96–0.90 (m, 1H, CH), 0.81 (s, 9H, *t*-Bu.). ¹³C NMR (101 MHz, DMSO-*d*₆) δ 157.8, 154.3, 151.0, 149.5, 136.8, 130.0, 126.4, 125.6, 120.7, 119.5, 113.2, 101.9, 94.7, 91.4, 65.6, 56.4, 54.0, 47.9, 45.8, 31.8, 27.2, 26.4. HRMS (ESI): *m/z* calcd for C₂₈H₃₆N₆O [M+H]⁺: 473.3023; found 473.3028.

5-(1*H*-indol-4-yl)-2-((4-(oxetan-3-yl)piperidin-1-yl)methyl)-7-(morpholin-4-yl)pyrazolo[1,5-*a*]pyrimidine (**42**)

The multistep preparation of compound **42** started from 1-(oxetan-3-yl)piperazine.

Step 1.

To the solution of 3-oxetanone (0.23 mL, 0.28 g, 3.9 mmol) in dry DCM (39.0 mL), 1-Boc-piperazine (0.60 g, 3.2 mmol) was added, and then the mixture was stirred at room temperature. After four h, sodium triacetoxymethylborohydride (1.35 g, 6.4 mmol) was added, and stirring was continued at room temperature overnight. Then, water (30 mL) was added to the reaction mixture, and the phases were separated. The aqueous phase was extracted three times with chloroform (25 mL). Combined organic

phases were dried over anhydrous sodium sulfate, filtrated the drying agent, and the solvent was evaporated under reduced pressure to obtain *tert*-butyl 4-(oxetan-3-yl)piperazin-1-carboxylate (0.61 g, 2.52 mmol) with 65% yield without purification. ¹H NMR (300 MHz, CDCl₃) δ 4.68–4.52 (m; 4H, piperaz.); 3.50–3.32 (m; 5H); 2.31–2.09 (m; 4H); 1.43 (s; 9H, *t*-Bu.). MS-ESI: (*m/z*) calcd for C₁₂H₂₂N₂O₃ [M+H]⁺: 243.17; found 243.2.

Step 2.

To the solution of the product of Step 1 (0.55 g, 2.8 mmol) in DCM (28 mL), trifluoroacetic acid (16.8 mL) was added. The reaction was carried out at room temperature for two h. Then, the water was added (30 mL), and the reaction mixture was alkalized with saturated sodium carbonate solution (10 mL). Phases were separated, and the aqueous phase was extracted three times with chloroform (25 mL). Combined organic phases were dried over anhydrous sodium sulfate. The drying agent was filtered off and the solvent evaporated under reduced pressure to obtain 1-(oxetan-3-yl)piperazine (0.23 g, 1.61 mmol) with 57% yield without purification. ¹H NMR (300 MHz, CDCl₃) δ 4.66–4.56 (m; 4H); 3.66–3.56 (m; 1H); 3.30–3.12 (m; 4H); 2.68–2.51 (m; 4H). MS-ESI: (*m/z*) calcd for C₇H₁₄N₂O [M+H]⁺: 143.12; found 143.1.

Compound **42** was prepared from aldehyde **22** (0.20 g, 0.58 mmol), 1-(oxetan-3-yl)piperazine (98 mg, 0.69 mmol), DCM (4.0 mL) and sodium triacetoxyborohydride (0.19 g, 0.86 mmol). The crude product was purified by flash chromatography (0–10% MeOH gradient in AcOEt) to give **42** (0.15 g, 0.32 mmol) as a light yellow solid with 54% yield. ¹H NMR (400 MHz, DMSO-*d*₆) δ 11.33 (s, 1H, NH), 7.64 (dd, *J* = 7.5, 0.8 Hz, 1H, Ar-H), 7.54–7.52 (m, 1H, Ar-H), 7.47 (t, *J* = 2.8 Hz, 1H, Ar-H), 7.21 (t, *J* = 7.7 Hz, 1H, Ar-H), 7.10–7.08 (m, 1H, Ar-H), 6.76 (s, 1H, Ar-H), 6.49 (s, 1H, Ar-H), 4.50 (t, *J* = 6.5 Hz, 2H, CH₂), 4.39 (t, *J* = 6.1 Hz, 2H, CH₂), 3.86–3.84 (m, 4H, morph.), 3.78–3.76 (m, 4H, morph.), 3.67 (s, 2H, CH₂), 3.40–3.33 (m, 1H, CH), 2.53–2.48 (m, 4H, piperaz.), 2.27–2.27 (m, 4H, piperaz.). ¹³C NMR (101 MHz, DMSO-*d*₆) δ 157.9, 153.9, 151.0, 149.5, 136.8, 130.0, 126.5, 125.6, 120.7, 119.6, 113.2, 101.8, 94.8, 91.5, 74.4, 65.6, 58.5, 56.0, 52.3, 49.0, 47.9. HRMS (ESI): *m/z* calcd for C₂₆H₃₁N₇O₂ [M+H]⁺: 474.2612; found 474.2616.

5-(1*H*-indol-4-yl)-2-(((1*S*, 4*S*)-2-(oxetan-3-yl)-2,5-diaza-bicyclo[2.2.1]hept-2-yl)methyl)-7-(morpholin-4-yl)pyrazolo[1,5-*a*]pyrimidine (**43**)

The preparation of compound **43** started from (1*S*, 4*S*)-2-(oxetan-3-yl)-2,5-diazabicyclo [2.2.1] heptane, which was prepared analogously, as described for the synthesis of 1-(oxetan-3-yl) piperazine.

Compound **43** was prepared from aldehyde **22** (0.20 g, 0.58 mmol), (1*S*, 4*S*)-2-(oxetan-3-yl)-2,5-diazabicyclo[2.2.1]heptane (0.11 g, 0.69 mmol), DCM (4.0 mL) and sodium triacetoxyborohydride (0.19 g, 0.86 mmol). The crude product was purified by flash chromatography (0–10% MeOH gradient in AcOEt) to give **43** (0.18 g, 0.37 mmol) as a light yellow solid with 63% yield. ¹H NMR (600 MHz, DMSO-*d*₆) δ 11.34 (s, 1H, NH), 7.63 (dd, *J* = 7.4, 0.7 Hz, 1H, Ar-H), 7.53 (d, *J* = 8.0 Hz, 1H, Ar-H), 7.46 (t, *J* = 2.8 Hz, 1H, Ar-H), 7.21 (t, *J* = 7.7 Hz, 1H, Ar-H), 7.09–7.08 (m, 1H, Ar-H), 6.75 (s, 1H, Ar-H), 6.50 (s, 1H, Ar-H), 4.59–4.51 (m, 2H, CH₂), 4.41–4.34 (m, 2H, CH₂), 3.89–3.82 (m, 6H), 3.79–3.75 (m, 5H), 3.40 (s, 1H, CH), 3.22 (s, 1H), 2.84 (d, *J* = 9.4 Hz, 1H), 2.65–2.59 (m, 2H, CH₂), 2.54–2.53 (m, 1H), 1.65–1.54 (m, 2H, CH₂). ¹³C NMR (151 MHz, DMSO-*d*₆) δ 157.8, 150.9, 149.5, 136.8, 130.0, 126.4, 125.6, 120.7, 119.5, 113.2, 101.8, 94.3, 91.4, 75.8, 75.3, 65.6, 61.6, 59.4, 57.3, 55.0, 52.7, 52.2, 47.8, 32.7. HRMS (ESI): *m/z* calcd for C₂₇H₃₁N₇O₂ [M+H]⁺: 486.2612; found 486.2614.

2-((4-(cyclopropanecarbonyl)piperazin-1-yl)methyl)-5-(1*H*-indol-4-yl)-7-(morpholin-4-yl)pyrazolo[1,5-*a*]pyrimidine (**44**)

Compound **44** was prepared from aldehyde **22** (0.12 g, 0.36 mmol), 1-(cyclopropylcarbonyl)piperazine (64 μL, 70 mg, 0.43 mmol), DCM (4.0 mL) and sodium triacetoxyborohydride (0.11 g, 0.54 mmol). The crude product was purified by flash chromatography (0–10% MeOH gradient in AcOEt) to give **44** (0.14 g, 0.29 mmol) as a light yellow solid with 78% yield. ¹H NMR (500 MHz, CDCl₃) δ 8.67 (s, 1H, NH), 7.60 (d, *J* = 7.3 Hz, 1H, Ar-H), 7.48 (d, *J* = 8.1 Hz, 1H, Ar-H), 7.33–7.27 (m, 2H, Ar-H), 7.10 (s, 1H, Ar-H), 6.65 (s, 1H, Ar-H), 6.64 (s, 1H, Ar-H), 4.01–3.95 (m, 4H, morph.), 3.84 (s, 2H, CH₂), 3.80–3.75 (m, 4H, morph.), 3.75–3.65 (m, 4H), 2.69–2.55 (m, 4H), 1.75–1.69 (m, 1H, CH), 1.01–0.95 (m, 2H, CH₂), 0.77–0.72 (m, 2H, CH₂). ¹³C NMR (126 MHz, CDCl₃) δ 174.81, 153.02,

139.60, 128.89, 128.34, 124.80, 123.14, 115.62, 105.57, 98.80, 95.28, 69.17, 59.40, 51.37, 13.80, 10.22. HRMS (ESI): m/z calcd for $C_{27}H_{31}N_7O_2$ $[M+H]^+$: 486.2612; found 486.2619.

2-((4-(cyclopropylmethyl)piperazin-1-yl)methyl)-5-(1H-indol-4-yl)-7-(morpholin-4-yl)pyrazolo[1,5-a]pyrimidine (**45**)

Compound **45** was prepared from aldehyde **22** (85 mg, 0.25 mmol), 1-(cyclopropylmethyl)piperazine (44 μ L, 41 mg, 0.29 mmol), DCM (3.0 mL) and sodium triacetoxymethylborohydride (78 mg, 0.37 mmol). The crude product was purified by flash chromatography (0–20% MeOH gradient in AcOEt) to give **45** (97 mg, 0.21 mmol) as a light yellow solid with 84% yield. 1H NMR (400 MHz, DMSO- d_6) δ 11.34 (s, 1H, NH), 7.65–7.63 (m, 1H, Ar-H), 7.53 (d, J = 8.1 Hz, 1H, Ar-H), 7.47–7.46 (m, 1H, Ar-H), 7.21 (t, J = 7.7 Hz, 1H, Ar-H), 7.10–7.09 (m, 1H, Ar-H), 6.76 (s, 1H, Ar-H), 6.48 (s, 1H, Ar-H), 3.86–3.84 (m, 4H, morph.), 3.78–3.77 (m, 4H, morph.), 3.65 (s, 2H, CH₂), 2.53–2.45 (m, 8H, piperaz.), 2.15 (d, J = 6.6 Hz, 2H, CH₂), 0.84–0.77 (m, 1H, CH), 0.45–0.40 (m, 2H, CH₂), 0.06–0.02 (m, 2H, CH₂). ^{13}C NMR (101 MHz, DMSO- d_6) δ 157.9, 154.0, 151.0, 149.5, 136.8, 130.0, 126.4, 125.6, 120.7, 119.5, 113.2, 101.8, 94.7, 91.5, 65.6, 62.8, 56.1, 52.7, 52.7, 47.9, 8.2, 3.7. HRMS (ESI): m/z calcd for $C_{27}H_{33}N_7O$ $[M+H]^+$: 472.2819; found 472.2825.

Procedure for [5-chloro-7-(morpholin-4-yl)pyrazolo[1,5-a]pyrimidin-2-yl]methanol (**46**)

To the solution of compound **19** (16.6 g, 46.3 mmol) in $CHCl_3$ (150 mL), methanesulfonic acid (61 mL, 925 mmol) was added, and then the reaction mixture was stirred at room temperature. After two h, the reaction mixture was poured onto the water containing ice and alkalized with 15% sodium hydroxide solution (25 mL). The aqueous phase was extracted with ethyl acetate (35 mL), and after separation, the organic phase was dried over anhydrous sodium sulfate. After filtration of the drying agent and evaporation of the solvent, the residue was purified by column chromatography (0–80% ethyl acetate gradient in heptane) to give **46** (12 g, 44.76 mmol) with 97% yield as an off-white solid. 1H NMR (300 MHz, $CDCl_3$) δ : 6.49 (s, 1H, Ar-H), 6.07 (s, 1H, Ar-H), 4.87 (s, 2H, CH₂), 4.00–3.90 (m, 4H, morph.), 3.83–3.73 (m, 4H, morph.). MS-ESI: m/z calcd for $C_{11}H_{13}ClN_4O_2$ $[M+H]^+$: 269.08; found 269.0.

Procedure for 5-chloro-7-(morpholin-4-yl)pyrazolo[1,5-a]pyrimidine-2-carbaldehyde (**47**)

To a solution of compound **46** (3.00 g, 10.9 mmol) in DMF (30.0 mL) in argon atmosphere was added Dess–Martin periodinane (97%, 5.74 g, 13.1 mmol). The resulting mixture was stirred at room temperature for 2 h. The solvent was evaporated. The residue was washed with AcOEt and filtered. The filtrate was concentrated, and the crude product was purified by flash chromatography (0–100% AcOEt gradient in heptane) to give **47** (1.34 g, 5.02 mmol) with 46% yield. 1H NMR (500 MHz, DMSO- d_6) δ 10.09 (s, 1H, CHO), 6.97 (s, 1H, Ar-H), 6.63 (s, 1H, Ar-H), 3.90–3.85 (m, 4H, morph.), 3.86–3.78 (m, 4H, morph.).

Procedure for 2-(1-[[5-chloro-7-(morpholin-4-yl)pyrazolo[1,5-a]pyrimidin-2-yl]methyl]piperidin-4-yl)propan-2-ol (**48**)

To the solution of compound **47** (3.4 g, 12.5 mmol) in dry DCM (30 mL), 2-(4-piperidyl)-2-propanol (2.24 g, 15.0 mmol) was added and then stirred at room temperature. After one hour, sodium triacetoxymethylborohydride (4.59 g, 21.2 mmol) was added, stirring the mixture at room temperature for a further 15 h. Then, water (45 mL) was added to the reaction mixture, and water-organic phases were separated. The aqueous phase was extracted three times with DCM (30 mL). Combined organic phases were dried over anhydrous sodium sulfate, filtered, and evaporated under reduced pressure. The residue was purified by flash chromatography (0–10% methanol gradient in ethyl acetate) to give **48** (3.1 g, 7.88 mmol) with a 63% yield as a slightly yellow solid. 1H NMR (500 MHz, $CDCl_3$) δ 6.47 (s, 1H, Ar-H), 6.01 (s, 1H, Ar-H), 3.96–3.91 (m, 4H, morph.), 3.81–3.76 (m, 4H, morph.), 3.71 (s, 2H), 3.11–3.00 (m, 2H), 2.09–1.98 (m, 2H), 1.78–1.67 (m, 2H), 1.48–1.35 (m, 2H), 1.30–1.23 (m, 1H), 1.17 (s, 6H, 2 \times CH₃). MS-ESI: m/z calcd for $C_{19}H_{28}ClN_5O_2$ $[M+H]^+$: 394.20; found 394.1.

Procedure for 2-((4-(2-hydroxypropan-2-yl)piperidin-1-yl)methyl)-5-(5-fluoro-1H-indol-4-yl)-7-(morpholin-4-yl)pyrazolo[1,5-a]pyrimidine (**49**)

Compound **49** was prepared according to the general procedure for the Suzuki reaction. Synthesized from **48** (0.15 g, 0.381 mmol), 5-fluoro-4-(4,4,5,5-tetramethyl-1,3,2-dioxaborolan-2-yl)-1*H*-indole (0.16 g, 0.571 mmol), tetrakis(triphenylphosphine)palladium(0) (90 mg, 0.076 mmol), 2M aqueous sodium carbonate solution (0.38 mL, 0.762 mmol) and DME (6 mL). The crude product was purified by flash chromatography (50–100% ethyl acetate gradient in heptane) to give **49** (0.11 g, 0.22 mmol) with 60% yield. ¹H NMR (400 MHz, DMSO-*d*₆) δ 11.34 (s, 1H, NH), 7.50–7.46 (m, 2H, Ar-H), 7.07–7.02 (m, 1H, Ar-H), 6.72–6.71 (m, 1H, Ar-H), 6.56 (d, *J* = 1.7 Hz, 1H, Ar-H), 6.49 (s, 1H), 4.02 (bs, 1H), 3.84–3.80 (m, 4H, morph.), 3.77–3.73 (m, 4H, morph.), 3.63 (s, 2H), 2.98–2.95 (m, 2H), 1.95–1.90 (m, 2H), 1.65–1.62 (m, 2H), 1.31–1.23 (m, 3H), 1.01 (s, 6H, 2xCH₃). ¹³C NMR (101 MHz, DMSO-*d*₆) δ 154.5, 154.2, 153.6, 150.8, 149.2, 132.8, 128.0, 126.9, 116.6, 113.5, 109.6, 101.8, 94.8, 93.9, 70.2, 65.6, 56.4, 53.9, 47.8, 46.9, 26.9, 26.6. HRMS (ESI): *m/z* calcd for C₂₇H₃₃FN₆O₂ [M+H]⁺: 493.2722; found 493.724.

Procedure for 2-((4-(2-hydroxypropan-2-yl)piperidin-1-yl)methyl)-5-(1*H*-pyrrolo[2,3-*c*]pyridin-4-yl)-7-(morpholin-4-yl)pyrazolo[1,5-*a*]pyrimidine (**50**)

Compound **50** was prepared according to the general procedure for the Suzuki reaction. Synthesized from **48** (0.15 g, 0.381 mmol), 6-azaindole-4-boronic acid pinacol ester (0.15 g, 0.571 mmol), tetrakis(triphenylphosphine)palladium(0) (88 mg, 0.076 mmol), 2M aqueous sodium carbonate solution (0.38 mL, 0.762 mmol) and DME (6 mL). The crude product was purified by flash chromatography (0–2% methanol gradient in ethyl acetate) to give **50** (0.13 g, 0.27 mmol) with 72% yield. ¹H NMR (300 MHz, CDCl₃) δ 10.43 (bs, 1H, NH); 8.80–8.78 (m; 1H, Ar-H); 8.72 (s; 1H, Ar-H); 7.51 (d; *J* = 3.1 Hz; 1H, Ar-H); 7.18 (d; *J* = 2.6 Hz; 1H, Ar-H); 6.65 (s; 1H, Ar-H); 6.61 (s; 1H, Ar-H); 4.02–3.90 (m; 4H, morph.); 3.84–3.72 (m; 6H); 3.20–3.09 (m; 2H, CH₂); 2.16–2.03 (m; 2H, CH₂); 1.80–1.70 (m; 2H); 1.53–1.31 (m; 3H); 1.18 (s; 6H, 2xCH₃). ¹³C NMR (75 MHz, CDCl₃) δ 156.4, 154.9, 151.7, 150.5, 138.2, 135.1, 133.8, 131.2, 130.0, 126.6, 102.7, 96.3, 91.5, 72.6, 66.4, 57.0, 54.3, 48.6, 47.4, 27.1, 27.1. HRMS (ESI): *m/z* calcd for C₂₆H₃₃N₇O₂ [M+H]⁺: 476.2769; found 476.2775.

Procedure for 2-((4-(2-hydroxypropan-2-yl)piperidin-1-yl)methyl)-5-(1*H*-pyrrolo[2,3-*b*]pyridin-4-yl)-7-(morpholin-4-yl)pyrazolo[1,5-*a*]pyrimidine (**51**)

Compound **51** was prepared according to the general procedure for the Suzuki reaction. Synthesized from **48** (0.15 g, 0.381 mmol), 4-(4,4,5,5-tetramethyl-1,3,2-dioxaborolan-2-yl)-1*H*-pyrrolo[2,3-*b*]pyridine (0.14 g, 0.571 mmol), tetrakis(triphenylphosphine) palladium(0) (88 mg, 0.076 mmol), 2M aqueous sodium carbonate solution (0.38 mL, 0.762 mmol) and DME (6 mL). The crude product was purified by flash chromatography (0–5% methanol gradient in ethyl acetate) to give **51** (0.12 g, 0.25 mmol) with 67% yield. ¹H NMR (400 MHz, DMSO-*d*₆) δ 11.85 (s, 1H, NH), 8.34 (d, *J* = 5.0 Hz, 1H, Ar-H), 7.67 (d, *J* = 5.0 Hz, 1H, Ar-H), 7.61–7.59 (m, 1H, Ar-H), 7.10–7.09 (m, 1H, Ar-H), 6.84 (s, 1H, Ar-H), 6.55 (s, 1H, Ar-H), 4.02 (s, 1H), 3.84–3.83 (m, 8H), 3.63 (s, 2H), 2.97–2.94 (m, 2H), 1.95–1.89 (m, 2H), 1.65–1.62 (m, 2H), 1.27–1.20 (m, 3H), 1.01 (s, 6H, 2xCH₃). ¹³C NMR (101 MHz, DMSO-*d*₆) δ 155.5, 154.8, 150.9, 149.8, 149.7, 142.5, 137.0, 127.4, 117.1, 114.1, 100.8, 95.2, 91.1, 70.2, 65.6, 56.4, 53.9, 47.9, 46.8, 26.9, 26.6. HRMS (ESI): *m/z* calcd for C₂₆H₃₃N₇O₂ [M+H]⁺: 476.2769; found 476.2776.

Procedure for 4-{2-[(4-*tert*-butylpiperazin-1-yl)methyl]-5-chloropyrazolo[1,5-*a*]pyrimidin-7-yl}morpholine (**52**)

To the solution of compound **47** (4.1 g, 15.4 mmol) in dry DCM (60 mL), *N*-*t*-butylpiperazine (2.62 g, 18.4 mmol) was added and then stirred at room temperature. After one h, sodium triacetoxyborohydride (5.54 g, 26.1 mmol) was added, and the mixture was stirred at room temperature for a further 15 h. Then, water (50 mL) was added to the reaction mixture, and the phases were separated. The aqueous phase was extracted three times with DCM (45 mL). Combined organic phases were dried over anhydrous sodium sulfate, filtered, and evaporated under reduced pressure. The residue was purified by flash chromatography (0–10% methanol gradient in ethyl acetate) to give **52** (3.2 g, 8.15 mmol) with 53% yield as a slightly yellow solid. ¹H NMR (300 MHz, CDCl₃) δ 6.47 (s, 1H, Ar-H), 6.03 (s, 1H, Ar-H), 3.99–3.89 (m, 4H, morph.), 3.84–3.76 (m, 4H, morph.), 3.74 (s, 2H, CH₂), 2.63 (s, 8H, piperaz.), 1.08 (s, 9H, *t*-Bu.). MS-ESI: *m/z* calcd for C₁₉H₂₉ClN₆O [M+H]⁺: 393.22; found 393.1.

Procedure for 2-((4-tert-butylpiperazin-1-yl)methyl)-5-(5-fluoro-1H-indol-4-yl)-7-(morpholin-4-yl)pyrazolo[1,5-a]pyrimidine (**53**)

Compound **53** was prepared according to the general procedure for the Suzuki reaction. Synthesized from **52** (0.12 g, 0.305 mmol), 5-fluoro-4-(4,4,5,5-tetramethyl-1,3,2-dioxaborolan-2-yl)-1H-indole (0.13 g, 0.458 mmol), tetrakis(triphenylphosphine)palladium(0) (72 mg, 0.061 mmol), 2M aqueous sodium carbonate solution (0.31 mL, 0.611 mmol) and DME (5 mL). The crude product was purified by flash chromatography (0–5% methanol gradient in ethyl acetate) to give **53** (0.10 g, 0.20 mmol) with 68% yield. ¹H NMR (600 MHz, DMSO-*d*₆) δ 11.36 (s, 1H, NH), 7.50–7.48 (m, 1H, Ar-H), 7.47–7.46 (m, 1H, Ar-H), 7.06–7.03 (m, 1H, Ar-H), 6.71–6.70 (m, 1H, Ar-H), 6.57–6.57 (m, 1H, Ar-H), 6.51 (s, 1H, Ar-H), 3.83–3.82 (m, 4H, morph.), 3.75–3.74 (m, 4H, morph.), 3.67 (s, 2H, CH₂), 2.65–2.37 (m, 8H, piperaz.), 1.03 (s, 9H, *t*-Bu.). ¹³C NMR (151 MHz, DMSO-*d*₆) δ 154.9, 153.7, 153.4, 150.8, 149.2, 132.8, 128.0, 126.9, 116.6, 113.6, 109.7, 101.8, 95.0, 94.0, 65.6, 55.8, 53.3, 47.8, 45.3, 40.0, 25.5. HRMS (ESI): *m/z* calcd for C₂₇H₃₄FN₇O [M+H]⁺: 492.2881; found 492.2886.

Procedure for 2-((4-tert-butylpiperazin-1-yl)methyl)-5-(1H-pyrrolo[2,3-c]pyridin-4-yl)-7-(morpholin-4-yl)pyrazolo[1,5-a]pyrimidine (**54**)

Compound **54** was prepared according to the general procedure for the Suzuki reaction. Synthesized from **52** (0.12 g, 0.305 mmol), 6-azaindole-4-boronic acid pinacol ester (0.12 g, 0.458 mmol), tetrakis(triphenylphosphine)palladium(0) (71 mg, 0.061 mmol), 2M aqueous sodium carbonate solution (0.305 mL, 0.611 mmol) and DME (5 mL). The crude product was purified by flash chromatography (0–5% methanol gradient in ethyl acetate) to give **54** (0.11 g, 0.23 mmol) with 77% yield. ¹H NMR (600 MHz, DMSO-*d*₆) δ 11.84 (s, 1H, NH), 8.83–8.83 (m, 1H, Ar-H), 8.76–8.75 (m, 1H, Ar-H), 7.73–7.73 (m, 1H, Ar-H), 7.17–7.16 (m, 1H, Ar-H), 6.84 (s, 1H, Ar-H), 6.51 (s, 1H, Ar-H), 3.85–3.84 (m, 5H), 3.82–3.81 (m, 4H), 3.63 (s, 2H, CH₂), 2.54–2.46 (m, 8H, piperaz.), 0.97 (s, 9H, *t*-Bu.). ¹³C NMR (151 MHz, DMSO-*d*₆) δ 155.8, 154.1, 151.0, 149.6, 137.9, 133.6, 130.6, 129.8, 125.1, 101.7, 94.9, 90.9, 65.6, 56.0, 53.6, 52.9, 47.9, 45.2, 40.0, 25.7. HRMS (ESI): *m/z* calcd for C₂₆H₃₄N₈O [M+H]⁺: 475.2928; found 472.2929.

Procedure for 2-((4-tert-butylpiperazin-1-yl)methyl)-5-(1H-pyrrolo[2,3-b]pyridin-4-yl)-7-(morpholin-4-yl)pyrazolo[1,5-a]pyrimidine (**55**)

Compound **55** prepared according to the general procedure for the Suzuki reaction. Synthesized from **52** (0.15 g, 0.382 mmol), 4-(4,4,5,5-tetramethyl-1,3,2-dioxaborolan-2-yl)-1H-pyrrolo[2,3-*b*]pyridine (0.14 g, 0.573 mmol), tetrakis(triphenylphosphine) palladium(0) (88 mg, 0.076 mmol), 2M aqueous sodium carbonate solution (0.38 mL, 0.763 mmol) and DME (5 mL). The crude product was purified by flash chromatography (0–5% methanol gradient in ethyl acetate) to give **55** (0.13 g, 0.27 mmol) with 72% yield. ¹H NMR (400 MHz, DMSO-*d*₆) δ 11.85 (s, 1H, NH), 8.34 (d, *J* = 5.0 Hz, 1H, Ar-H), 7.67 (d, *J* = 5.1 Hz, 1H, Ar-H), 7.61–7.59 (m, 1H, Ar-H), 7.10–7.08 (m, 1H, Ar-H), 6.85 (s, 1H, Ar-H), 6.56 (s, 1H, Ar-H), 3.84–3.83 (m, 8H, morph.), 3.64 (s, 2H, CH₂), 2.50–2.43 (m, 8H, piperaz.), 0.97 (s, 9H, *t*-Bu.). ¹³C NMR (101 MHz, DMSO-*d*₆) δ 155.5, 154.4, 150.9, 149.8, 142.5, 137.0, 127.4, 117.1, 114.1, 100.8, 95.3, 91.2, 65.6, 55.9, 53.5, 53.1, 47.9, 45.2, 40.2, 25.7. HRMS (ESI): *m/z* calcd for C₂₆H₃₄N₈O [M+H]⁺: 475.2928; found 472.2936.

3.2. Docking Study

The docking procedure was performed in the PI3K δ protein from Protein Data Bank (PDB: 2WXP) using the Auto-Dock Vina program [55]. All figures with examples of 3D modeling of a possible binding mode of selected compounds were prepared based on the calculated pK_a from the Instant JChem 21.13.0 program [57]. More specifically, all structures depicted in the respective figures have not had protons added, but the appropriate protonation state has been maintained.

3.3. Biology

3.3.1. In Vitro Kinase Inhibition Assay for PI3K

Tested compounds were dissolved in 100% DMSO, and obtained solutions were serially diluted in 1x reaction buffer. The recombinant kinase solution was diluted in a reaction mixture comprising 5x reaction buffer, respective compound solution (1 mM sodium diacetate 4,5-bisphosphate phosphatidylinositol (PIP2) solution in 40 mM Tris buffer), and water. In a 96-wells plate, 5 μL of

compound solutions and 15 μL of the kinase solution in the reaction mixture were added per well. To initiate the interaction of chemical compounds to be tested with the enzyme, the plate was incubated for 10 min at a suitable temperature in a plate thermostat with orbital shaking at 600 rpm. Negative control wells contained all the above reagents except tested compound and kinase, and positive control wells contained all the above reagents except tested compounds. The enzymatic reaction was initiated by adding 5 μL of 150 μM ATP solution. Subsequently, the plate was incubated for 1 h at 25 or 30 $^{\circ}\text{C}$ (depending on the PI3K isoform tested) in a plate thermostat with orbital shaking of the plate contents at 600 rpm. The reaction conditions are combined in the table below (Table 6).

Table 6. Reaction conditions and compositions of reaction mixtures for kinases.

KINASE	Kinase Concentration [ng per Reaction]	Reaction Temperature and Time	Substrate PIP2 [Final Concentration μM]	Reaction Buffer
PI3K α (Carna Biosciences)	7.5 ng	25 $^{\circ}\text{C}$, 1 h	30 μM	50 mM HEPES pH 7.5 50 mM NaCl 3 mM MgCl ₂ 0.025 mg/mL BSA
PI3K δ (Merck Millipore)	10 ng	25 $^{\circ}\text{C}$, 1 h	30 μM	50 mM HEPES pH 7.5 50 mM NaCl 3 mM MgCl ₂ 0.025 mg/mL BSA
PI3K β (Merck Millipore)	15 ng	30 $^{\circ}\text{C}$, 1 h	50 μM	50 mM HEPES pH 7.5 50 mM NaCl 3 mM MgCl ₂ 0.025 mg/mL BSA
PI3K α (Merck Millipore)	30 ng	30 $^{\circ}\text{C}$, 1 h	50 μM	40 nM Tris pH 7.5 20 mM MgCl ₂ 0.1 mg/mL BSA 1 mM DTT

Detection of ADP formed in the enzymatic reaction was then performed using ADP-Glo Kinase AssayTM (Promega, Madison, WI, USA). To the wells of a 96-well plate, 25 μL of ADP-Glo ReagentTM was added, and the plate was incubated for 40 min at 25 $^{\circ}\text{C}$ in a plate thermostat with orbital shaking at 600 rpm. Then 50 μL of Kinase Detection Reagent were added to each well, and the plate was incubated for 40 min at 25 $^{\circ}\text{C}$ in a plate thermostat with orbital shaking at 600 rpm. Once the incubation was complete, the luminescence intensity was measured using a Victor Light luminometer (Perkin Elmer, Inc., Waltham, MA, USA). IC₅₀ values were determined based on luminescence intensity measured in wells containing tested compounds at different concentrations in relation to control wells. These values were calculated with Graph Pad 5.03 software by fitting the curve using non-linear regression. Each compound was tested at least in quadruplicates (4 wells) on two 96-well plates utilizing at least 4 wells for each control. Averaged results of inhibition activity respective to specific isoforms of PI3K kinases for tested compounds are presented as IC₅₀ values in Tables 1–4.

3.3.2. Influence of Selected Compounds on B Cells Proliferation

CD19 cells were isolated from PBMC using magnetic beads (Stem Cell, Cambridge, MA, USA) and then labeled with 2 μM CFSE (Invitrogen, Waltham, MA, USA).

1×10^5 cells were seeded on 96-well plate, activated by 2 $\mu\text{g}/\text{mL}$ αIgM (Jackson ImmunoResearch, Ely, UK) and 1 $\mu\text{g}/\text{mL}$ ODN2006 (InvivoGen, San Diego, CA, USA), and incubated with increasing concentrations of drugs (0.1, 0.3, 1.0, 3.3, 10, 33, 100, 333, 1000, 3333, 10,000 nM). After four days, cells were stained with LIVE/DEADTM kit (Invitrogen, Waltham, MA, USA). Samples were acquired using Attune NxT Flow Cytometer (Invitrogen, Waltham, MA, USA) and analyzed using FlowJo software.

Each biological assay was performed with cells isolated from a different donor. The presented results constitute the average value of the percentage of proliferating cells from 3 independent experiments.

3.4. Metabolic Stability and Solubility

3.4.1. Metabolic Stability Assay

Assessment of metabolic phase I stability in mouse (CD-1TM) and human microsomes (Thermo-Fisher Scientific, Waltham, MA, USA) was performed on 96-well non-binding plates (Greiner, Frickenhausen, Germany) at 1 μ M concentration for verapamil (positive control) and donepezil (negative control) and tested compounds. Unless otherwise stated, all chemicals and materials were ordered from Merck Life Science (Palo Alto, CA, USA). Each biological replicate was prepared in triplicates. Briefly, mixtures were incubated in 100 mM potassium phosphate buffer with microsomes (0.5 mg/mL) and NADPH (1–1.2 mM) on a plate shaker (500 rpm) in the dark at 37 °C. A 4 \times solution of NADPH, a cofactor for metabolic enzymes, was prepared directly prior to the experiment by reducing NADP with G6P dehydrogenase (13.2 mM MgCl₂, 13.2 mM G6P, 5.2 mM NADP, 3.2 U/mL G6P dehydrogenase, 20 min at 30 °C, 500 rpm). The negative control contained buffer instead of NADPH solution. Samples were collected at 0, 10, 20, and 40 min or 0 and 40 min for the negative and double negative controls. The reaction was stopped by protein precipitation in 2 volumes of ice-cold MeOH with 200 nM imipramine (an internal standard for LC-MS analysis). Then, the extract was mixed (1 min, 1000 rpm), filtered through a 0.22 μ m filter on a 96-well plate vacuum manifold, and subjected to LC-MS analysis.

3.4.2. Kinetic Stability Assay

Kinetic solubility was determined by the shake-flask protocol [58,59]. Appropriate compounds (500 μ M) were incubated in an aqueous buffer (0.1 M phosphate-buffered saline pH 7.4) at 25 °C with stirring at 500 rpm. The samples were taken at the start time and after 24 h of incubation, filtered through 0.22 μ m filters, and diluted with two volumes of acetonitrile. UHPLC-UV/Vis determined sample concentrations. A calibration curve was prepared to quantify the compound's contents in the test solution.

4. Conclusions

Based on the 2-methyl-pyrazolo[1,5-*a*]pyrimidine system, the most promising R¹ (Scheme 1) substituent in terms of activity and selectivity was selected, and appropriate structures were designed and synthesized in multi-step synthesis. Among various derivatives obtained, two amino groups were identified as the most promising concerning the PI3K δ activity and other PI3K isoforms selectivity: 2-(piperidin-4-yl) propan-2-ol and *N*-*tert*-butylpiperazine located at the C(2) position of the pyrazolo[1,5-*a*]pyrimidine. The most selective compounds turned out to be 4-{2-[(4-*tert*-butylpiperazin-1-yl)methyl]-7-(morpholin-4-yl)pyrazolo[1,5-*a*]pyrimidin-5-yl}-1*H*-indole (**37**) and 4-{2-[(4-*tert*-butylpiperazin-1-yl)methyl]-5-{1*H*-pyrrolo[2,3-*c*]pyridin-4-yl}pyrazolo[1,5-*a*]pyrimidin-7-yl}morpholine (**54**), bearing the indol or azaindole system as the R¹ substituent and *N*-*tert*-butylpiperazine as the R² (Scheme 2) residue. Molecular calculations and docking studies supported the strong tryptophan shelf (Trp-760) mechanism in which the lipophilic *tert*-butyl substituent is possibly engaged. Compound **54** (CPL302253) showed promising additional properties such as suitable kinetic solubility or higher metabolic stability (Table 6) compared to compound **37**. For these reasons, CPL302253 was selected as a promising clinical candidate for the treatment of asthma. Additional, biological studies supporting this selection have been published by Gunerka et al. [15].

Author Contributions: Synthesis, M.S., M.Z., S.M., N.O. and M.D.; biological evaluation B.D., P.S., J.H.-K., P.T., P.G., D.Z.-B., A.S. and K.D. (Karolina Dzwonek); analytical evaluation K.M., D.S., L.G.-B. and A.L.; investigation, M.S., M.Z., P.G., D.Z.-B. and B.D.; writing—original draft preparation, M.S., M.Z. and S.M.; writing—review and editing, M.M., P.G., D.Z.-B. and Z.O.; visualization, F.S.; supervision, M.W. and Z.O.; project administration, M.Z., P.G., A.S., K.D. (Karolina Dzwonek), K.D. (Krzysztof Dubiel), M.L.-P., M.W. and Z.O.; funding acquisition, M.W. All authors have read and agreed to the published version of the manuscript.

Funding: This research was co-financed by Celon Pharma S.A. and the National Centre for Research and Development “Narodowe Centrum Badan i Rozwoju”, project “PIKCEL—Preclinical and clinical development of

innovative lipid kinases inhibitor as a candidate for the treatment of steroid-resistant and severe inflammatory lung diseases”, granted under number POIR.01.01.01-00-1341/15.

Institutional Review Board Statement: Not applicable.

Informed Consent Statement: Not applicable.

Data Availability Statement: Data sharing not applicable.

Acknowledgments: We would like to thank Aleksandra Świdorska (Celon Pharma) for NMR analyses and practical suggestions. Moreover, we would like to thank Wojciech Pietruś for docking study suggestions and docking figures. This work was supported by The National Centre for Research and Development (POIR.01.01.01-00-1341/15) in Poland.

Conflicts of Interest: The authors declare the following financial interests/personal relationships which may be considered as potential competing interests: All contributors to this work at the time of their direct involvement in the project were the full-time employees of Celon Pharma S.A. A patent application WO 2016/157091 A1, based on the present observations, has been filed. M. Wiczorek is the CEO of Celon Pharma S.A. Some of the authors are the shareholders of Celon Pharma S.A.

References.

1. Okkenhaug, K.; Vanhaesebroeck, B. PI3K-Signalling in B- and T-Cells: Insights from Gene-Targeted Mice. *Biochem. Soc. Trans.* **2003**, *31*, 270–274. <https://doi.org/10.1042/bst0310270>.
2. Okkenhaug, K.; Vanhaesebroeck, B. PI3K in Lymphocyte Development, Differentiation, and Activation. *Nat. Rev. Immunol.* **2003**, *3*, 317–330. <https://doi.org/10.1038/nri1056>.
3. Rommel, C.; Camps, M.; Ji, H. PI3K δ and PI3K γ : Partners in Crime in Inflammation in Rheumatoid Arthritis and Beyond? *Nat. Rev. Immunol.* **2007**, *7*, 191–201. <https://doi.org/10.1038/nri2036>.
4. Thomas, M.; Owen, C. Inhibition of PI-3 Kinase for Treating Respiratory Disease: Good Idea or Bad Idea? *Curr. Opin. Pharmacol.* **2008**, *8*, 267–274. <https://doi.org/10.1016/j.coph.2008.02.004>.
5. Williams, O.; Houseman, B.T.; Kunkel, E.J.; Aizenstein, B.; Hoffman, R.; Knight, Z.A.; Shokat, K.M. Discovery of Dual Inhibitors of the Immune Cell PI3Ks P110 δ and P110 γ : A Prototype for New Anti-Inflammatory Drugs. *Chem. Biol.* **2010**, *17*, 123–134. <https://doi.org/10.1016/j.chembiol.2010.01.010>.
6. Perry, M.W.D.; Abdulai, R.; Mogemark, M.; Petersen, J.; Thomas, M.J.; Valastro, B.; Westin Eriksson, A. Evolution of PI3K γ and δ Inhibitors for Inflammatory and Autoimmune Diseases. *J. Med. Chem.* **2019**, *62*, 4783–4814. <https://doi.org/10.1021/acs.jmedchem.8b01298>.
7. Zhang, T.; Makondo, K.J.; Marshall, A.J. P110 δ Phosphoinositide 3-Kinase Represses IgE Switch by Potentiating BCL6 Expression. *J. Immunol.* **2012**, *188*, 3700–3708. <https://doi.org/10.4049/jimmunol.1103302>.
8. Puri, K.D.; Gold, M.R. Selective Inhibitors of Phosphoinositide 3-Kinase Delta: Modulators of B-Cell Function with Potential for Treating Autoimmune Inflammatory Diseases and B-Cell Malignancies. *Front. Immunol.* **2012**, *3*, 256. <https://doi.org/10.3389/fimmu.2012.00256>.
9. Suárez-Fueyo, A.; Rojas, J.M.; Cariaga, A.E.; García, E.; Steiner, B.H.; Barber, D.F.; Puri, K.D.; Carrera, A.C. Inhibition of PI3K δ Reduces Kidney Infiltration by Macrophages and Ameliorates Systemic Lupus in the Mouse. *J. Immunol.* **2014**, *193*, 544–554. <https://doi.org/10.4049/jimmunol.1400350>.
10. Haselmayer, P.; Camps, M.; Muzerelle, M.; el Bawab, S.; Waltzinger, C.; Bruns, L.; Abba, N.; Polokoff, M.A.; Jond-Necand, C.; Gaudet, M.; et al. Characterization of Novel PI3K δ Inhibitors as Potential Therapeutics for SLE and Lupus Nephritis in Pre-Clinical Studies. *Front. Immunol.* **2014**, *5*, 233. <https://doi.org/10.3389/fimmu.2014.00233>.
11. Suárez-Fueyo, A.; Barber, D.F.; Martínez-Ara, J.; Zea-Mendoza, A.C.; Carrera, A.C. Enhanced Phosphoinositide 3-Kinase δ Activity Is a Frequent Event in Systemic Lupus Erythematosus That Confers Resistance to Activation-Induced T Cell Death. *J. Immunol.* **2011**, *187*, 2376–2385. <https://doi.org/10.4049/jimmunol.1101602>.
12. Cushing, T.D.; Metz, D.P.; Whittington, D.A.; McGee, L.R. PI3K δ and PI3K γ as Targets for Autoimmune and Inflammatory Diseases. *J. Med. Chem.* **2012**, *55*, 8559–8581. <https://doi.org/10.1021/jm300847w>.
13. Wright, H.L.; Moots, R.J.; Bucknall, R.C.; Edwards, S.W. Neutrophil Function in Inflammation and Inflammatory Diseases. *Rheumatology* **2010**, *49*, 1618–1631. <https://doi.org/10.1093/rheumatology/keq045>.
14. Ali, K.; Camps, M.; Pearce, W.P.; Ji, H.; Rückle, T.; Kuehn, N.; Pasquali, C.; Chabert, C.; Rommel, C.; Vanhaesebroeck, B. Isoform-Specific Functions of Phosphoinositide 3-Kinases: P110 δ but Not P110 γ Promotes Optimal Allergic Responses In Vivo. *J. Immunol.* **2008**, *180*, 2538–2544. <https://doi.org/10.4049/jimmunol.180.4.2538>.

15. Gunerka, P.; Gala, K.; Banach, M.; Dominowski, J.; Hucz-Kalitowska, J.; Mulewski, K.; Hajnal, A.; Mikus, E.G.; Smuga, D.; Zagozda, M.; et al. Preclinical Characterization of CPL302-253, a Selective Inhibitor of PI3K δ , as the Candidate for the Inhalatory Treatment and Prevention of Asthma. *PLoS ONE* **2020**, *15*, e0236159. <https://doi.org/10.1371/journal.pone.0236159>.
16. Barnes, P.J. Immunology of Asthma and Chronic Obstructive Pulmonary Disease. *Nat. Rev. Immunol.* **2008**, *8*, 183–192. <https://doi.org/10.1038/nri2254>.
17. Lambrecht, B.N.; Hammad, H. The Immunology of Asthma. *Nat. Immunol.* **2015**, *16*, 45–56. <https://doi.org/10.1038/ni.3049>.
18. Jeong, J.S.; Kim, J.S.; Kim, S.R.; Lee, Y.C. Defining Bronchial Asthma with Phosphoinositide 3-Kinase Delta Activation: Towards Endotype-Driven Management. *Int. J. Mol. Sci.* **2019**, *20*, 3525. <https://doi.org/10.3390/ijms20143525>.
19. Zirlik, K.; Veelken, H. Idelalisib. *Rec. Res. Canc. Res.* **2018**, *212*, 243–264. https://doi.org/10.1007/978-3-319-91439-8_12.
20. Blair, H.A. Duvelisib: First Global Approval. *Drugs* **2018**, *78*, 1847–1853. <https://doi.org/10.1007/s40265-018-1013-4>.
21. Okabe, S.; Tanaka, Y.; Tauchi, T.; Ohyashiki, K. Copanlisib, a Novel Phosphoinositide 3-Kinase Inhibitor, Combined with Carfilzomib Inhibits Multiple Myeloma Cell Proliferation. *Ann. Hematol.* **2019**, *98*, 723–733. <https://doi.org/10.1007/s00277-018-3547-7>.
22. Greenwell, I.B.; Ip, A.; Cohen, J.B. PI3K Inhibitors: Understanding Toxicity Mechanisms and Management. *Oncology (Williston Park)* **2017**, *31*, 821–828.
23. Barnes, P.J. New Therapies for Asthma: Is There Any Progress? *Trends Pharmacol. Sci.* **2010**, *31*, 335–343. <https://doi.org/10.1016/j.tips.2010.04.009>.
24. Murray, J.M.; Sweeney, Z.K.; Chan, B.K.; Balazs, M.; Bradley, E.; Castanedo, G.; Chabot, C.; Chantry, D.; Flagella, M.; Goldstein, D.M.; et al. Potent and Highly Selective Benzimidazole Inhibitors of PI3-Kinase Delta. *J. Med. Chem.* **2012**, *55*, 7686–7695. <https://doi.org/10.1021/jm300717c>.
25. Sutherland, D.P.; Baker, S.; Bisconte, A.; Blaney, P.M.; Brown, A.; Chan, B.K.; Chantry, D.; Castanedo, G.; DePledge, P.; Goldsmith, P.; et al. Potent and Selective Inhibitors of PI3K δ : Obtaining Isoform Selectivity from the Affinity Pocket and Tryptophan Shelf. *Bioorg. Med. Chem. Lett.* **2012**, *22*, 4296–4302. <https://doi.org/10.1016/j.bmcl.2012.05.027>.
26. Safina, B.S.; Baker, S.; Baumgardner, M.; Blaney, P.M.; Chan, B.K.; Chen, Y.-H.; Cartwright, M.W.; Castanedo, G.; Chabot, C.; Cheguillaume, A.J.; et al. Discovery of Novel PI3-Kinase δ Specific Inhibitors for the Treatment of Rheumatoid Arthritis: Taming CYP3A4 Time-Dependent Inhibition. *J. Med. Chem.* **2012**, *55*, 5887–5900. <https://doi.org/10.1021/jm3003747>.
27. Stark A.K., Sriskantharajah S., Hessel E.M., Okkenhaug K. PI3K inhibitors in inflammation, autoimmunity and cancer. *Curr Opin Pharmacol* 2015, *23*: 82-91. <https://doi.org/10.1016/j.coph.2015.05.017>.
28. Knight, Z.A.; Gonzalez, B.; Feldman, M.E.; Zunder, E.R.; Goldenberg, D.D.; Williams, O.; Loewith, R.; Stokoe, D.; Balla, A.; Toth, B.; et al. A Pharmacological Map of the PI3-K Family Defines a Role for P110 α in Insulin Signaling. *Cell* **2006**, *125*, 733–747. <https://doi.org/10.1016/j.cell.2006.03.035>.
29. Berndt, A.; Miller, S.; Williams, O.; Le, D.D.; Houseman, B.T.; Pacold, J.I.; Gorrec, F.; Hon, W.-C.; Ren, P.; Liu, Y.; et al. Erratum: Corrigendum: The P110 δ Structure: Mechanisms for Selectivity and Potency of New PI(3)K Inhibitors. *Nat. Chem. Biol.* **2010**, *6*, 244–244. <https://doi.org/10.1038/nchembio0310-244b>.
30. Garces, A.E.; Stocks, M.J. Class 1 PI3K Clinical Candidates and Recent Inhibitor Design Strategies: A Medicinal Chemistry Perspective. *J. Med. Chem.* **2019**, *62*, 4815–4850. <https://doi.org/10.1021/acs.jmedchem.8b01492>.
31. Vanhaesebroeck, B.; Perry, M.W.D.; Brown, J.R.; André, F.; Okkenhaug, K. PI3K Inhibitors Are Finally Coming of Age. *Nat. Rev. Drug Discov.* **2021**, *20*, 741–769. <https://doi.org/10.1038/s41573-021-00209-1>.
32. Hayakawa, M.; Kaizawa, H.; Moritomo, H.; Koizumi, T.; Ohishi, T.; Yamano, M.; Okada, M.; Ohta, M.; Tsukamoto, S.; Raynaud, F.I.; et al. Synthesis and Biological Evaluation of Pyrido[3',2':4,5]Furo[3,2-d]Pyrimidine Derivatives as Novel PI3 Kinase P110 α Inhibitors. *Bioorg. Med. Chem. Lett.* **2007**, *17*, 2438–2442. <https://doi.org/10.1016/j.bmcl.2007.02.032>.
33. Kawashima, S.; Matsuno, T.; Yaguchi, S.; Sasahara, H.; Watanabe, T. Heterocyclic Compound and Antitumor Agent Containing the Same as Active Ingredient. EP1389617, 2002, *June*, 26.
34. Folkes, A.J.; Ahmadi, K.; Alderton, W.K.; Alix, S.; Baker, S.J.; Box, G.; Chuckowree, I.S.; Clarke, P.A.; Depledge, P.; Eccles, S.A.; et al. The Identification of 2-(1*H*-Indazol-4-yl)-6-(4-Methanesulfonyl-Piperazin-1-ylmethyl)-4-Morpholin-4-yl-Thieno[3,2-*d*]Pyrimidine (GDC-0941) as a Potent, Selective, Orally Bioavailable Inhibitor of Class I PI3 Kinase for the Treatment of Cancer. *J. Med. Chem.* **2008**, *51*, 5522–5532. <https://doi.org/10.1021/jm800295d>.
35. Scott, W.J.; Hentemann, M.F.; Rowley, R.B.; Bull, C.O.; Jenkins, S.; Bullion, A.M.; Johnson, J.; Redman, A.; Robbins, A.H.; Esler, W.; et al. Discovery and SAR of Novel 2,3-Dihydroimidazo[1,2-*c*]Quinazoline PI3K Inhibitors: Identification of Copanlisib (BAY 80-6946). *ChemMedChem* **2016**, *11*, 1517–1530. <https://doi.org/10.1002/cmdc.201600148>.

36. Burger, M.T.; Pecchi, S.; Wagman, A.; Ni, Z.-J.; Knapp, M.; Hendrickson, T.; Atallah, G.; Pfister, K.; Zhang, Y.; Bartulis, S.; et al. Identification of NVP-BKM120 as a Potent, Selective, Orally Bioavailable Class I PI3 Kinase Inhibitor for Treating Cancer. *ACS Med. Chem. Lett.* **2011**, *2*, 774–779. <https://doi.org/10.1021/ml200156t>.
37. Sutherland, D.P.; Bao, L.; Berry, M.; Castanedo, G.; Chuckowree, I.; Dotson, J.; Folks, A.; Friedman, L.; Goldsmith, R.; Gunzner, J.; et al. Discovery of a Potent, Selective, and Orally Available Class I Phosphatidylinositol 3-Kinase (PI3K)/Mammalian Target of Rapamycin (MTOR) Kinase Inhibitor (GDC-0980) for the Treatment of Cancer. *J. Med. Chem.* **2011**, *54*, 7579–7587. <https://doi.org/10.1021/jm2009327>.
38. Zhang J.Q., Luo Y. J., Xiong Y. S., Yu Y., Tu Z. C., Long Z. J., Lai X. J., Chen H. X., Luo Y., Weng J., Lu G. J. *Med. Chem.* 2016, 59, 15, 7268–7274. <https://doi.org/10.1021/acs.jmedchem.6b00235>.
39. Ren, P.; Liu, Y.; Wilson, T.E.; Chan, K.; Rommel, C.; Li, L. Certain Chemical Entities, Compositions and Methods. WO2009088986, 2009. *July*, 16.
40. Down, K.; Amour, A.; Baldwin, I.R.; Cooper, A.W.J.; Deakin, A.M.; Felton, L.M.; Guntrip, S.B.; Hardy, C.; Harrison, Z.A.; Jones, K.L.; et al. Optimization of Novel Indazoles as Highly Potent and Selective Inhibitors of Phosphoinositide 3-Kinase δ for the Treatment of Respiratory Disease. *J. Med. Chem.* **2015**, *58*, 7381–7399. <https://doi.org/10.1021/acs.jmedchem.5b00767>.
41. King-Underwood, J.; Ito, K.; Murray, J.; Hardy, G.; Brookfield, F.A.; Brown, C.J. Compounds. WO2011048111, 2011 *April*, 28.
42. Erra, M.; Taltavull, J.; Bernal, F.J.; Caturla, J.F.; Carrascal, M.; Pagès, L.; Mir, M.; Espinosa, S.; Gràcia, J.; Domínguez, M.; et al. Discovery of a Novel Inhaled PI3K δ Inhibitor for the Treatment of Respiratory Diseases. *J. Med. Chem.* **2018**, *61*, 9551–9567. <https://doi.org/10.1021/acs.jmedchem.8b00873>.
43. Perry, M.W.D.; Björhall, K.; Bold, P.; Brülls, M.; Börjesson, U.; Carlsson, J.; Chang, H.-F.A.; Chen, Y.; Eriksson, A.; Fihn, B.-M.; et al. Discovery of AZD8154, a Dual PI3K γ δ Inhibitor for the Treatment of Asthma. *J. Med. Chem.* **2021**, *64*, 8053–8075. <https://doi.org/10.1021/acs.jmedchem.1c00434>.
44. A Study to Evaluate the Safety, Tolerability and Absorption to the Blood After Administration of Single and Multiple Doses of AZD8154 in Healthy Participants. Available online: <https://clinicaltrials.gov/show/NCT03436316> (accessed on 31 May 2022).
45. Dose Finding Study of Nemiralisib (GSK2269557) in Subjects with an Acute Moderate or Severe Exacerbation of Chronic Obstructive Pulmonary Disease (COPD). Available online: <https://clinicaltrials.gov/ct2/show/NCT03345407> (accessed on 31 May 2022).
46. Safety, Tolerability and Pharmacokinetics of Single and Repeat Doses of GSK2292767 in Healthy Participants Who Smoke Cigarettes. Available online: <https://clinicaltrials.gov/ct2/show/study/NCT03045887> (accessed on 31 May 2022).
47. Rao, V.K.; Webster, S.; Dalm, V.A.S.H.; Šedivá, A.; van Hagen, P.M.; Holland, S.; Rosenzweig, S.D.; Christ, A.D.; Sloth, B.; Cabanski, M.; et al. Effective “Activated PI3K δ Syndrome”-Targeted Therapy with the PI3K δ Inhibitor Leniolisib. *Blood* **2017**, *130*, 2307–2316. <https://doi.org/10.1182/blood-2017-08-801191>.
48. Study of Efficacy of CDZ173 in Patients with APDS/PASLI. Available online: <https://clinicaltrials.gov/ct2/show/NCT02435173> (accessed on 31 May 2022).
49. Sun, J.; Feng, Y.; Huang, Y.; Zhang, S.-Q.; Xin, M. Research Advances on Selective Phosphatidylinositol 3 Kinase δ (PI3K δ) Inhibitors. *Bioorg. Med. Chem. Lett.* **2020**, *30*, 127457. <https://doi.org/10.1016/j.bmcl.2020.127457>.
50. Hayakawa, N.; Noguchi, M.; Takeshita, S.; Eviyanti, A.; Seki, Y.; Nishio, H.; Yokoyama, R.; Noguchi, M.; Shuto, M.; Shima, Y.; et al. Structure–Activity Relationship Study, Target Identification, and Pharmacological Characterization of a Small Molecular IL-12/23 Inhibitor, APY0201. *Bioorg. Med. Chem.* **2014**, *22*, 3021–3029. <https://doi.org/10.1016/j.bmc.2014.03.036>.
51. Michrowska-Piankowska, A.; Kordes, M.; Hutzler, J.; Newton, T.; Evans, R.R.; Kreuz, K.; Grossmann, K.; Seitz, T.; van der Kloet, A.; Witschel, M.; et al. Herbicidal Isoxazolo[5,4-b]Pyridines. WO2013104561A1, 2013., *June*, 3.
52. Moszczyński-Pętkowski, R.; Bojarski, Ł.; Stefaniak, F.; Wieczorek, M.; Dubiel, K.; Lamparska-Przybysz, M. Pyrazolo[3,4-d]Pyrimidin-4(5h)-One Derivatives as Pde9 Inhibitors. WO2014016789A1, *Jan.* 30, 2014.
53. Yamada, S.; Goto, T.; Mashiko, T.; Kogi, K.; Oguchi, Y.; Narita, S. Thiazolopyridine derivative, their production and cardiovascular treating agents containing tchem. EP277701A1, 1989.
54. Oakley, P.; Press, N.; Spanka, C.; Watson, J. Heterocyclic Compounds as Inhibitors of Cxcr2. WO2009106539A1, *Sept.* 9, 2009
55. Trott, O.; Olson, A.J. AutoDock Vina: Improving the Speed and Accuracy of Docking with a New Scoring Function, Efficient Optimization, and Multithreading. *J. Comput. Chem.* **2009**, *31*, 455–461. <https://doi.org/10.1002/jcc.21334>.
56. Duzer, J.; Michaelis, A.; Geiss William; Stafford, D.; Raker, J.; Yu, X.; Siedlecki, J.; Yang, Y. Rifamycin Analogs and Uses Thereof. US020070155715A1, 2006, *March*, 1.
57. Instant JChem, Available online: <https://chemaxon.com/products/instant-jchem> (accessed on 31 May 2022).

58. Sugano, K.; Okazaki, A.; Sugimoto, S.; Tavornvipas, S.; Omura, A.; Mano, T. Solubility and Dissolution Profile Assessment in Drug Discovery. *Drug Metab. Pharm.* **2007**, *22*, 225–254. <https://doi.org/10.2133/dmpk.22.225>.
59. Guha, R.; Dexheimer, T.S.; Kestranek, A.N.; Jadhav, A.; Chervenak, A.M.; Ford, M.G.; Simeonov, A.; Roth, G.P.; Thomas, C.J. Exploratory Analysis of Kinetic Solubility Measurements of a Small Molecule Library. *Bioorg. Med. Chem.* **2011**, *19*, 4127–4134. <https://doi.org/10.1016/j.bmc.2011.05.005>.

12.2. Publikacja 2 – P2

Article

Design, Synthesis, and Development of Pyrazolo[1,5-*a*]pyrimidine Derivatives as a Novel Series of Selective PI3K δ Inhibitors. Part II-benzimidazole Derivatives

Mariola Stypik ^{1,2,*}, Stanisław Michałek ^{1,2}, Nina Orłowska ^{1,2}, Marcin Zagozda ¹, Maciej Dziachan ¹, Martyna Banach ¹, Paweł Turowski ¹, Paweł Gunerka ¹, Daria Zdżalik-Bielecka ¹, Aleksandra Stańczak ¹,

Urszula Kędzierska ¹, Krzysztof Mulewski ¹, Damian Smuga ¹, Wioleta Maruszak ¹, Lidia Gurba-Bryśkiewicz ¹, Arkadiusz Leniak ¹, Wojciech Pietruś ¹, Zbigniew Ochal ², Mateusz Mach ¹, Beata Zygmunt ¹, Jerzy Pieczykolan ¹, Krzysztof Dubiel ¹, and Maciej Wiczorek ¹

Citation: Stypik, M.; Michałek, S.; Orłowska, N.; Zagozda, M.; Dziachan, M.; Banach, M.; Turowski, P.; Gunerka, P.; Zdżalik-Bielecka, D.; Stańczak, A.; et al. Design, Synthesis, and Development of Pyrazolo[1,5-*a*]pyrimidine Derivatives as a Novel Series of Selective PI3K δ Inhibitors. Part II—Benzimidazole Derivatives. *Pharmaceuticals* **2022**, *15*, x. <https://doi.org/10.3390/xxxxx>

Academic Editor: Paweł Kafarski

Received: 22 June 2022

Accepted: 18 July 2022

Published: date

Publisher's Note: MDPI stays neutral with regard to jurisdictional claims in published maps and institutional affiliations.



Copyright: © 2022 by the authors.

Submitted for possible open access

publication under the terms and

conditions of the Creative Commons

Attribution (CC BY) license

(<https://creativecommons.org/licenses/by/4.0/>).

by/4.0/).

As a lead compound synthesized on a relatively large scale, this structure is considered a potential future candidate for clinical trials in SLE treatment.

¹ Celon Pharma S.A., ul. Marymoncka 15, 05-152, Kazun Nowy, Poland; stanislaw.michalek@celonpharma.com (S.M.); orlowska.nina@gmail.com (N.O.); marcin.zagozda@celonpharma.com (M.Z.); maciejdziachan@gmail.com (M.D.); martyna.banach@celonpharma.com (M.B.); tupaw@wp.pl (P.T.); pgunerka@gmail.com (P.G.); dzdzalik@iimcb.gov.pl (D.Z.-B.); apstanczak@gmail.com (A.S.); ulak54@gmail.com (U.K.); kmulewski91@gmail.com (K.M.); damian.smuga@celonpharma.com (D.S.); wioleta.maruszak@celonpharma.com (W.M.); lidia.gurba@celonpharma.com (L.G.-B.); arkadiusz.leniak@celonpharma.com (A.L.); wojciech.pietrus@celonpharmra.com (W.P.); mateusz.mach@celonpharma.com (M.M.); beata.zygmunt@celonpharma.com (B.Z.); jerzy.pieczykolan@celonpharma.com (J.P.); krzysztof.dubiel@celonpharma.com (K.D.); maciej.wiczorek@celonpharma.com (M.W.)

² Faculty of Chemistry, Warsaw University of Technology, ul. Noakowskiego 3, 00-664 Warsaw, Poland; zbigniew.ochal@pw.edu.pl

* Correspondence: mariola.stypik@celonpharma.com

Abstract: Phosphoinositide 3-kinase (PI3K) is the family of lipid kinases participating in vital cellular processes such as cell proliferation, growth, migration, or cytokines production. Due to the high expression of these proteins in many human cells and their involvement in metabolism regulation, normal embryogenesis, or maintaining glucose homeostasis, the inhibition of PI3K (especially the first class which contains four subunits: α , β , γ , δ) is considered to be a promising therapeutic strategy for the treatment of inflammatory and autoimmune diseases such as systemic lupus erythematosus (SLE) or multiple sclerosis. In this work, we synthesized a library of benzimidazole derivatives of pyrazolo[1,5-*a*]pyrimidine representing a collection of new, potent, active, and selective inhibitors of PI3K δ , displaying IC₅₀ values ranging from 1.892 to 0.018 μ M. Among all compounds obtained, CPL302415 (**6**) showed the highest activity (IC₅₀ value of 18 nM for PI3K δ), good selectivity (for PI3K δ relative to other PI3K isoforms: PI3K α / δ = 79; PI3K β / δ = 1415; PI3K γ / δ = 939), and promising physicochemical properties.

1. Introduction

Phosphoinositide 3-kinase delta (PI3K δ), the lipid kinase, is a member of the family of PI3K enzymes divided into three classes: I (PI3K α , PI3K β , PI3K γ , PI3K δ), II, and III. Due to their involvement in catalyzing the phosphorylation of phosphatidylinositol-4,5-diphosphate (PIP2) to phosphatidylinositol-3,4,5-triphosphate (PIP3), PI3Ks start a cascade of downstream activities to induce various types of biological processes such as cell growth, survival, proliferation, or differentiation [1-6]. All class I PI3K isoforms occur as a heterodimer of one regulatory subunit (p85) with the corresponding catalytic subunit (p110 α , p110 β , and p110 δ). The p110 subunits of PI3K isoforms have been thoroughly characterized [7]. The ATP-binding site of p110 δ in PI3K δ comprises a few functionalities such as a hinge pocket, an affinity pocket, and a hydrophobic region, which lies below a non-conserved rim of the active site. Interaction with the large and flat hydrophobic face of a conserved tyrosine residue (Tyr-876) was reported for most PI3K inhibitors. Moreover, many of them also have additional hydrophobic interactions with the affinity pocket for the enzyme, where they can form hydrogen bonds with Lys-833 or other hydrophilic residues caused by the presence of adequate heteroatom [8,9]. Most selective PI3K δ inhibitors exhibit interaction between crucial amino acids (Trp-760 and Met-752) while entering the active pocket [9-11]. Interaction with the tryptophan shelf (Trp-760) impacts the PI3K δ selectivity. Steric blockage in the tryptophan region leads to selectivity for PI3K δ because of the disfavored binding to other PI3K isoforms. It has been proven that these structural determinants are crucial in the activity and selectivity of PI3K δ and thus are used for designing PI3K δ inhibitors [5,8,10, 11].

In this study, we designed, developed, and described a family of PI3K δ inhibitor structures, based on the pyrazolo[1,5-*a*]pyrimidine core with different modifications, which can occupy the affinity pocket of the enzyme.

The basis for inflammatory and autoimmune diseases, such as systemic lupus erythematosus (SLE) or rheumatoid arthritis (RA), is dysregulation, including overactivity of the immune system [8]. These alterations are typically progressive and cause much burdensomeness for the patients. The overproduction of autoantibodies manifests in SLE due to uncontrolled cellular action in which T lymphocytes and B lymphocytes play a crucial role [4,12-17]. The activity of PI3K δ in T cells of SLE diagnosed patients is risen by approximately 70% [15]. Due to the engagement of the p110 δ subunit of the PI3K δ in human Th17 cells for the production of IL-17, this PI3K subfamily can be viewed as a promising molecular target for future therapies, including SLE [18-21]. Moreover, a well-recognized mechanism of the PI3K δ interaction at the molecular level can be efficiently utilized for the rational design, synthesis, and development of new anti-inflammatory drugs [18-20,22].

Selective PI3K δ inhibitors can be obtained by appropriate modifications of a heterocycle that occupies the affinity pocket of the enzyme [5,10,23]. Despite the formation of hydrogen bonds between the indazole group of well-known inhibitor GDC-0941 (Figure 1) [24] and two amino acids Asp-787 and Tyr-813, the PI3K γ/δ selectivity was poor [10]. It was reported that changing the indazole group of GDC-0941 for 2-methylbenzimidazole group helped to obtain a more selective inhibitor of PI3K δ (PI3K γ/δ = 29) which demonstrated good potency in cellular assays [5,10]. Moreover, it was shown that optimization of interactions with Trp-760 helped to improve the selectivity of PI3K δ inhibitors as candidates for further development with good pharmacokinetic properties [10,11,25,26]. The new compounds with different substituents at the benzimidazole ring's C(2) position were obtained and described [10]. It was reported that the inclusion of large, bulky groups at the benzimidazole's C(2) position could reduce the inhibition of PI3K δ [10]. These structure-activity relationships highlight the crucial role of the amine and benzimidazole subunit in determining PI3K δ activity and selectivity for an obtained series of compounds.

Many bicyclic cores-based compounds were reported as effective and active PI3K inhibitors. Most of them, including thienopyrimidines [23,27] or pyridopyrimidines [10,23,24], were described as pan-PI3K inhibitors. Due to the problems with time-dependent CYP inhibition [5,23], selectivity, bioavailability, or solubility [23,28], other bicyclic cores such as isoxazolopyrimidines [23,29], imidazopyrimidines [23,30], or pyrazolopyrimidines [23,31] have also been designed, synthesized, and

reported. A large number of PI3K inhibitors showed the potential of applying morpholine moiety as a *H*-bond acceptor in the hinge-binding motif [23,24]. In our docking studies in the previous paper [25], the crucial role of binding between the morpholine system and Val-828 was observed. Since 2012, many morpholine-based inhibitors of the PI3K kinase have been published [23]. Moreover, in 2012, a group of 2-(difluoromethyl)-1*H*-benzimidazole derivatives enriched a library of known PI3K inhibitors [23,32–34]. These structures are based on the 1,3,5-triazine monocyclic core and a morpholine ring in the hinge region. Evaluation of mono-, bi-, or higher-cyclic cores with a different arrangement of the substituents allowed for more active and selective compounds [10,23,28].

In our work, we focused on the pyrazolo[1,5-*a*]pyrimidine core with various amine substituents in position C(2) and different benzimidazole groups in the C(5) position at the core region. It was reported that pyrazolo[1,5-*a*]pyrimidines are promising medical pharmacophores in structures as potential drugs in the treatment of cancer, as well as inflammatory or viral diseases [35,36]. Our previous study [25] described the development of pyrazolo[1,5-*a*] pyrimidine derivatives with different substituents (heteroaromatic systems) at position 5 of the mentioned core. It was reported that 5-indole-pyrazolo[1,5-*a*] pyrimidines as inhibitors of PI3K δ were the most selective structures of the obtained series. On the other hand, we identified a 2-difluoromethylbenzimidazole derivative **1** as the most active compound (Figure 1). It was identified as a moderate PI3K δ inhibitor (IC_{50} = 475 nM) with poor selectivity toward the alpha isoform. We reported that modifications of a mentioned core with many different substituents could contribute to inhibitors' activity and selectivity enhancement. In this work, we synthesized and described more than thirty new, active, and potent selective PI3K δ inhibitors in the extended structure–active relationship (SAR) study, keeping the scaffold of **1** as a starting point.

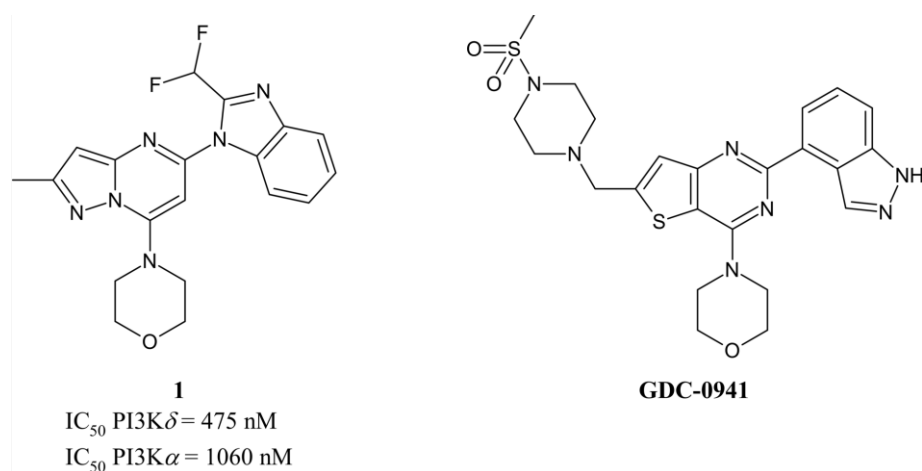


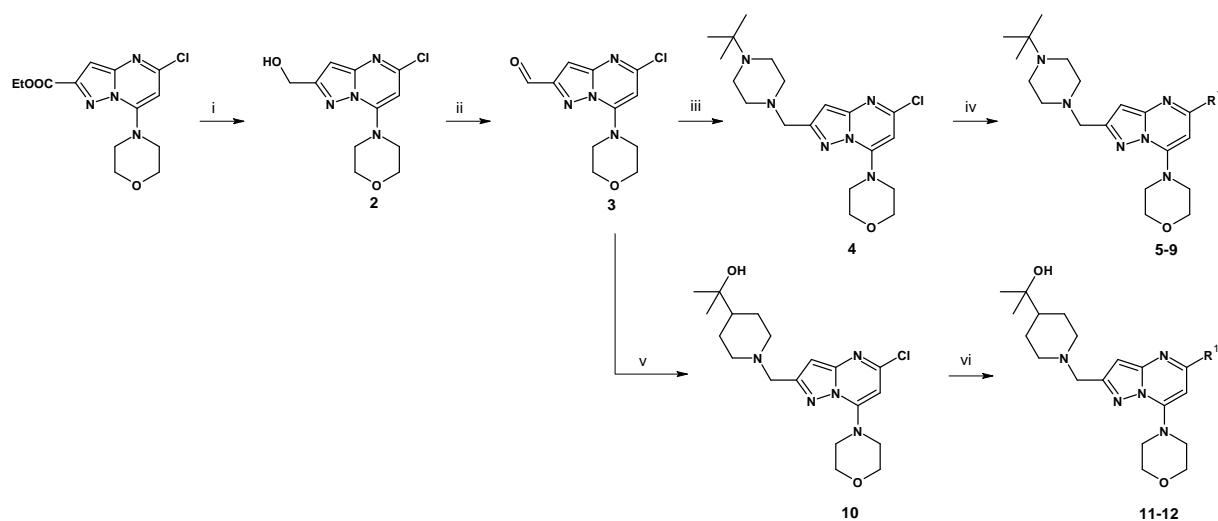
Figure 1. Structure of the PI3K δ active inhibitor and GDC-0941.

2. Results and Discussion

2.1. Chemistry

2.1.1. Synthesis of Compounds 5–9 and 11–12

Our research shows that modifications of benzimidazole groups and amine subunits play a crucial role in the activity and selectivity of PI3K δ inhibitors. During the SAR exploration and docking calculations, we found two amine subunits at the C(2) position of the pyrazolo[1,5-*a*]pyrimidine core, *N*-*tert*-butylpiperazin-1-ylmethyl and 2-(4-piperidin-1-ylmethyl)-2-propanol, have the most promising potency in PI3K δ inhibition. Due to the observed high activity of the mentioned families of compounds against PI3K δ and unexplored chemical space, new benzimidazole derivatives were synthesized according to Scheme 1.

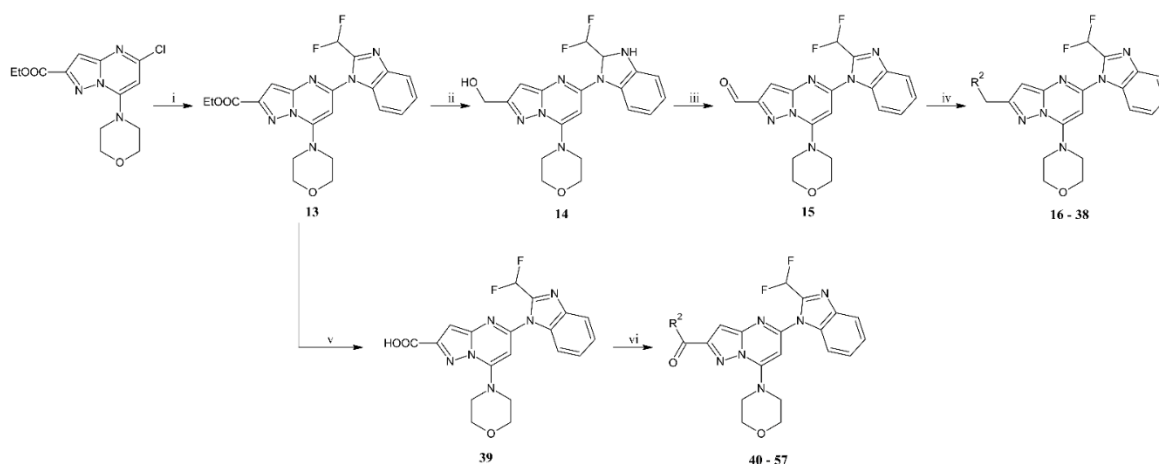


Scheme 1. Synthesis of benzimidazole derivatives. Reagents and conditions: (i) CaCl_2 , NaBH_4 , EtOH, reflux, 3 h, 99%; (ii) Dess–Martin periodinane, DMF, RT, 2 h, 46%; (iii) 1-*tert*-butylpiperazine, sodium triacetoxyborohydride, DCM, RT, 18 h, 84%; (iv) benzimidazole derivative, tris(dibenzylideneacetone)dipalladium(0), 9,9-dimethyl-4,5-bis(diphenylphosphino)xanthene, Cs_2CO_3 , toluene, 150 °C, 6 h, 200 W, MW, 4–93%; (v) 2-(4-piperidyl)-2-propanol, sodium triacetoxyborohydride, DCM, RT, 63%; (vi) benzimidazole derivative, tris(dibenzylideneacetone)dipalladium(0), 9,9-Dimethyl-4,5-bis(diphenylphosphino)xanthene, Cs_2CO_3 , toluene, 150 °C, 6 h, 200 W, MW, 52–66%.

Starting from ethyl 5-chloro-7-(morpholin-4-yl)pyrazolo[1,5-*a*]pyrimidine-2-carboxylate, structures 5–9 and 11–12 were obtained after four-step synthesis. In the first step, alcohol 2 was synthesized by the ester group reduction with sodium borohydride and an almost quantitative yield (99%, Scheme 1). Next, alcohol 2 was oxidized into the corresponding aldehyde 3 using Dess–Martin periodinane (46% yield). Subsequently, the amine subunits derivatives 4 and 10 were obtained in reductive amination reactions by engaging appropriate amine in the presence of sodium triacetoxyborohydride (good, 84%, and 63% yields, respectively). In the last step, the received substituted 5-chloro-pyrazolo[1,5-*a*]pyrimidines 4 and 10 were transferred into the final structures by utilizing the Buchwald–Hartwig reaction conditions with corresponding benzimidazoles. This palladium-catalyzed reaction, conducted under microwave irradiation, gave compounds 5–9 and 11–12 (un-optimized yields in the range of 34–93%).

2.1.2. Synthesis of Compounds 16–38 and 40–54

Benzimidazole derivatives were prepared in a multistep synthesis that branched into two pathways depending on the group selected in the core C(2) position (Scheme 2).



Scheme 2. Synthesis of 5-(2-difluoromethylbenzimidazo-1-yl)pyrazolo[1,5-*a*]pyrimidine derivatives. Reagents and conditions: (i) 2-(difluoromethyl)-1*H*-benzimidazole, TEACl, K₂CO₃, DMA, 160 °C, 3 h, 89%; (ii) LiAlH₄, THF, 0 °C, 3 h, 89%, (iii) Dess–Martin periodinane, DMF, RT, 1 h, 78% or MnO₂, toluene:buthyl acetate, reflux 1.5 h, 68%; (iv) amine, sodium triacetoxyborohydride, DCM, 18 h, 38–93%; (v) LiOH, MeOH, H₂O, 98%; (vi) amine, HATU, TEA, RT, 2 h, 33–81%.

Structures **16–38** and **40–57** were synthesized according to the general pathway depicted in Scheme 2. Compounds **16–38** were obtained after four-step synthesis from 5-chloro-7-(morpholin-4-yl)pyrazolo[1,5-*a*]pyrimidine-2-carboxylate (commercially available) which was coupled with 2-(difluoromethyl)-1*H*-benzimidazole in the presence of tetraethylammonium chloride and potassium carbonate to provide ethyl 5-[2-(difluoromethyl)-1*H*-1,3-benzimidazol-1-yl]-7-(morpholin-4-yl)pyrazolo[1,5-*a*]pyrimidine-2-carboxylate (**13**) as a crucial intermediate (89% yield). Then, the resulting product **13** was reduced to alcohol **14** under treatment with a lithium aluminum hydride solution (89% yield). We observed that the double bond within the imidazole ring of benzimidazole substituent was reduced concomitantly with the ester group. Interestingly, the oxidation of alcohol **14** to aldehyde **15** with Dess–Martin periodinane (or with activated manganese(IV) oxide) was accompanied by full restoration of aromaticity within the benzimidazole heterocycle. Final structures **16–38** were obtained by reductive amination reactions (Scheme 2) with different amines such as *N*-*tert*-butylpiperazine, morpholine, or 4-methylpiperidin-4-ol (see tables below for details) with un-optimized yields (38–93%). Based on our previous SAR studies, we observed that the carbonyl group in position C(2) of pyrazolo[1,5-*a*]pyrimidine derivatives may enhance the activity of the obtained structures. While keeping this in mind, further research focused on the replacement of the (-CH₂) group with a (-CO) group leading to structures **40–57** in two steps from intermediate **13**. Unlike for compounds **16–38** synthesis, the ester group of **13** was hydrolyzed with the lithium hydroxide to 5-[2-(difluoromethyl)-1*H*-benzimidazol-1-yl]-7-(morpholin-4-yl)pyrazolo[1,5-*a*]pyrimidine-2-carboxylic acid (**39**, 98% yield). Subsequently, carboxyl derivatives were converted into a series of final amides **40–57** (see tables below to trace the selection of substituents) using 2-(7-aza-1*H*-benzotriazole-1-yl)-1,1,3,3-tetramethyluronium hexafluorophosphate (HATU) and triethylamine as a base (un-optimized 33–81% yields).

2.2. Docking Study

Crystal structure analysis, combined with data from biochemical and cellular assays, has been used to understand the molecular basis of observed inhibitors' activities and selectivities. Utilizing the Auto-Dock Vina program for docking studies [35], we wished to investigate the binding mode of our compounds with the PI3K δ isoform. Based on the available crystallographic structures of PI3K (for example PDB ID: 2WXL) and reference papers regarding in silico calculations [5,8,10,23,24], we gained valuable information about protein–ligand interactions in the active site and chose to focus on the pyrazolo[1,5-*a*]pyrimidine core.

Over the course of our computer-assisted studies, we found that the morpholine ring at position 7 of pyrazolo[1,5-*a*]pyrimidine core is required for interaction with PI3K at the catalytic

site. More specifically, the most crucial interaction is the critical hydrogen bond between the oxygen atom of the morpholine group and Val-828 in the hinge region of the enzyme. In our previous work [25], we observed an existing hydrogen bond between the C(5)-indole pyrazolo[1,5-*a*]pyrimidine derivatives and the Asp-787. However, benzimidazole derivatives, presented in this work, lack that interaction when targeted toward this region. Instead, we observed the possibility of hydrogen bond formation between the nitrogen atom at the third position of the benzimidazole ring system and Lys-779.

In addition, several regions have been identified in the active site of the enzyme that have a profound impact on the activity and selectivity toward PI3K δ . Due to critical structural determinants, depending on the substituent type (R¹, R², Scheme 1 and Scheme 2, respectively), we observed different interactions of our structures with the tryptophan shelf (Trp-760) and selected amino acids within the active pocket. For example, 2-hydroxypropyl residue of compound **11** keeps close proximity to Trp-760 (the tryptophan shelf interaction, Figure 2A) by locating the hydroxyl group conformationally away from the amino acid. On the other hand, the piperazine fragment of compound **17** (Figure 2B) takes the most distant position from the tryptophan shelf, supported by the polar amide group bond with aspartic acid (Asp-897). Moreover, among some structures showing no Trp-760 interaction, due to different types of the amine substituents, a shift towards other amino acids, e.g., Ser-831, was observed.

Compounds containing a donor fragment, such as hydroxyl, amine, or the amide group near the piperazine or piperidine ring (such as **11**, **35**, or **36**), are found to have higher IC₅₀ values and therefore lower potential for activity due to the poor interaction between the aliphatic fragment and the tryptophan shelf (Trp-760). A similar situation is observed for structure **30** (Figure 2C), in which the aliphatic component targets the Trp-760 indole ring, but the hydroxyl group is too far to form a hydrogen bond with the polar amino acids located at the opposite side of the enzyme pocket.

A shift beyond the tryptophan region of the piperidine ring was also observed for compound **49**, with the carboxyl group introduced in place of the methylene group. Such arrangement is additionally supported by the formation of a hydrogen bond between the hydroxyl group of the 4-hydroxy-4-methylpiperidinyl subunit and aspartic acid (Asp-832, Figure 2D).

In connection with the described dependencies, our research suggests that due to the shift of the amine ring relative to the Trp-760 and the formation of a hydrogen bonding with the aforementioned Asp-832 and Asp-897, compounds with a carboxyl group in the C(2) position of the pyrazolo[1,5-*a*]pyrimidine (linking the amine group) are more preferred in terms of kinase activity and selectivity than compounds with a methylene group at the same position.

Compound **6** (Figure 2E), containing the *tert*-butyl piperazine ring, gave different outcomes in our docking studies. Interaction between that aliphatic fragment and Trp-760 translates into the properties of this compound, such as potency, activity, and selectivity towards PI3K δ . Moreover, in this structure, we observed the characteristic bond between the oxygen atom located at the morpholine ring (playing the role of an *H*-bond acceptor in the hinge-binding motif) and Val-828. Interaction of the benzimidazole residue nitrogen atom and Lys-779 has also been recognized.

A mix of conformational interactions was assigned to compound **40** (Figure 2F), which binds to Val-828 and Lys-779, including compound **6**. However, the replacement of the methylene bridge with the carbonyl function was associated with the loss of Trp-760 interaction and the simultaneous loss of biological activity.

As a result of all relationships described, compound **6** turned out to be the most active and promising structure of the entire library obtained.

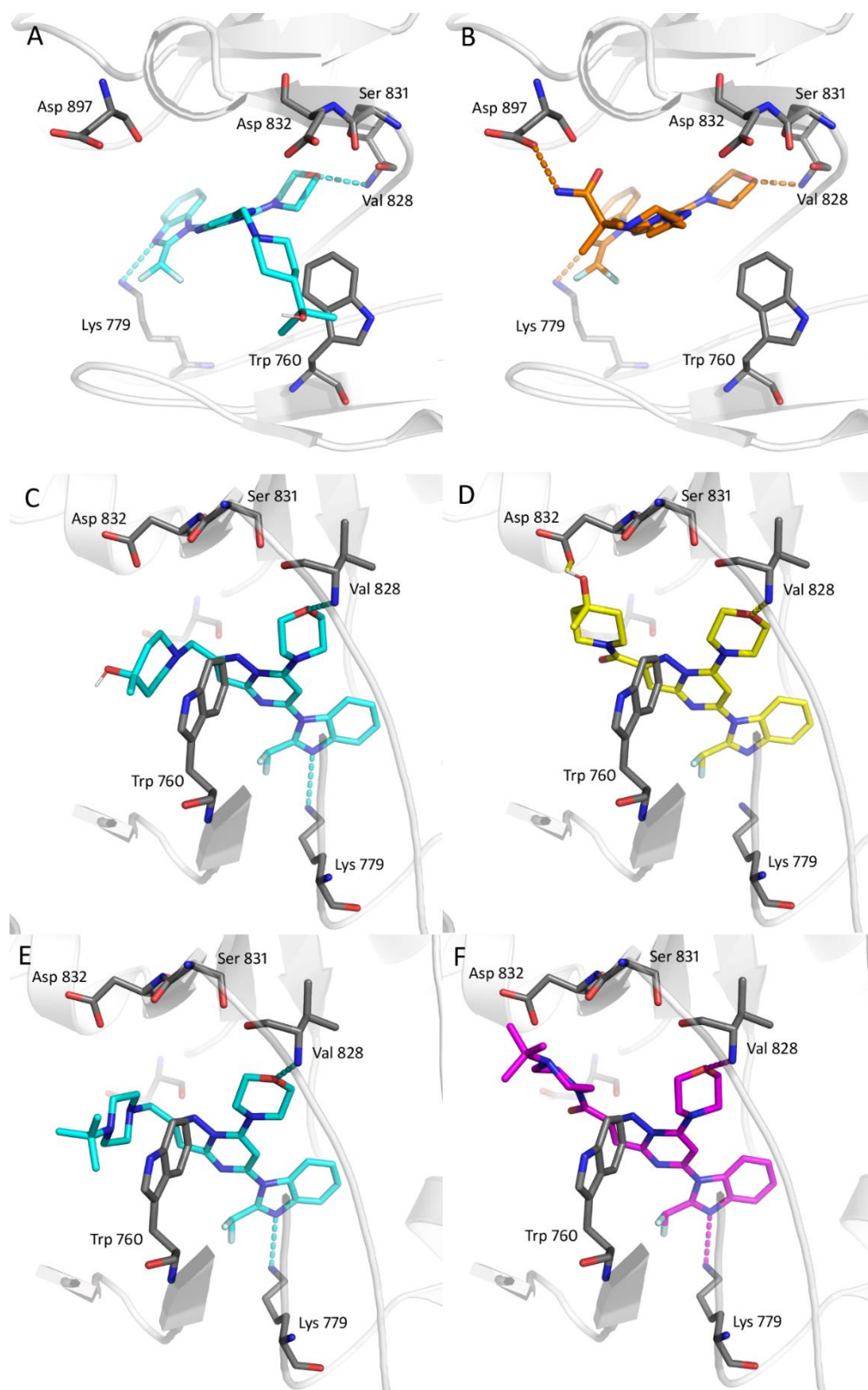


Figure 2. The most important interactions in the PI3K binding site for selected structures. An example of 3D modeling possible interaction found for selected compounds (PDB ID:2WXL): (A)—compound 11; (B)—compound 17; (C)—compound 30; (D)—compound 49; (E)—compound 6; (F)—compound 40. No protons were added, but the appropriate state of protonation was maintained.

2.3. Biological Evaluation

In Vitro PI3 Kinase Inhibition Assays

All compounds were tested in a biochemical assay that measured the inhibition of phosphatidylinositol (4,5)-bisphosphate (PIP2) production by PI3K isoforms using the ADP-Glo kinase assay (Promega). In addition, the effects of synthesized compounds on B cell proliferation were measured.

All newly synthesized compounds proved to be active PI3K δ inhibitors (IC_{50} = 1.892–0.018 μ M) and, additionally, eleven of obtained structures turned out to be highly active, reaching the value of IC_{50} below 100 nM. For this reason, PI3K δ final inhibitors, which are very potent with drug-like physical properties, are considered drug candidates in SLE and other autoimmune and inflammatory diseases.

Two positions of the pyrazolo[1,5-*a*]pyrimidine core: C(2) (R^1) and C(5) (R^2) were optimized and described in this paper. Regarding the first C(2) optimization, many benzimidazole derivatives (for two chosen amine subunits: piperazines and piperidines) were designed and synthesized (Table 1). It was observed that within the nano- and micro-molar IC_{50} value range, the potency of obtained inhibitors is different despite the substituent size at the C(2) position, for example in pairs **5** and **8** or **6** and **9**. On the other hand, a selected pair of examples (compounds **11** and **12**) indicates that the selectivity against PI3K δ activity is relatively insensitive to the steric bulkiness of the substituent placed at the C(5) core's position. Of the whole series of PI3K δ inhibitors obtained, compounds **6** and **11** turned out to be the most potent, with IC_{50} values of 18 and 52 nM, respectively. Moreover, structure **6** shows the best selectivity towards other PI3K isoforms among all the compounds tested. For the above reasons, 2-(difluoromethyl)-1*H*-benzimidazole was selected as the most optimal and promising R^1 substituent in pyrazolo[1,5-*a*]pyrimidine ring. The next step of our studies was the expansion of the compound library with the determination of R^2 groups keeping the constant 2-(difluoromethyl)-1*H*-benzimidazole R^1 substituent at C(5) position.

Table 1. Activity and selectivity of benzimidazole derivatives (5–12).

Compound	R ¹	R ²	IC ₅₀ PI3K δ	IC ₅₀ PI3K α	IC ₅₀ PI3K β	IC ₅₀ PI3K γ	Fold Selectivity		
			[nM]	[nM]	[nM]	[nM]	α/δ	β/δ	γ/δ
5			236	10,642	298,400	175,187	45	1264	742
6			18	1428	25,475	16,904	79	1415	939
7			385	28,677	265,699	258,277	74	690	671
8			1072	82,502	259,143	271,097	77	242	253
9			907			135,500			149
11			52	1729		6347	33		122
12			878	30,511	194,624	119,254	35	222	136

IC₅₀ values were determined as the mean based on two independent experiments.

The R² substituent has been optimized using different substituents which aim to simultaneously increase selectivity and activity. Optimization focused on modifying the amine subunit; thus, piperazines, piperidines, five-member rings, bulky amine groups, and other available amines were used (Table 2). Among all modifications, we found the piperazine and piperidine derivatives as the most promising. Compounds containing an amine group with a five-membered ring showed the IC₅₀ values in the 1892–96 nM range; however, their PI3K γ/δ selectivities remained lower than for the other amine groups with a six-membered ring in their structure (Table 2). This observation suggests that replacing the five- with a six-membered ring is more favorable for PI3K δ inhibition. Moreover, heterocycles based on the six-membered ring as R², with a nitrogen atom in the 1- or 1- and 4-position(s), are generally more active and selective. As an excellent example, this thesis can serve compound **27**, with the nitrogen atom shifted outside the six-membered ring. In this individual case, a significant potency drop against PI3K δ below 1000 nM threshold was noted (Table 2). Modifications of substituted amine heterocycles are significant because they directly affect the PI3K δ enzyme's affinity pocket interactions. Our preliminary research suggested that the presence of the 2-(4-piperidinyl)-2-propanol hydroxylic group could play a crucial role in gaining the inhibition of PI3K δ . We believed, based on *in silico* studies, that the bond formed between the hydroxyl group and amine group of Ser-831 within the selectivity pocket of the enzyme should increase both the activity and selectivity. Therefore, a set of compounds containing proton donor groups was synthesized. Unfortunately, this rationale failed, as it can be clearly seen while searching the IC₅₀ values of compounds: **29–31** and **34–36** (Table 2). The observed loss of potency could be explained by the conformational freedom provided by the methylene linkage, allowing the escape from the tryptophan shelf position and simultaneous polar interactions with side amino

acids within the active pocket. To confront this possibility, the methylene bridge was converted into carbonyl function, leading to conformationally restrained cyclic amide derivatives which lack possible conformational changes in the C(2) position of pyrazolo[1,5-*a*]pyrimidine.

Table 2. PI3K δ and PI3K γ activity of pyrazolo[1,5-*a*]pyrimidine derivatives with (-CH₂) groups.

Compound	R ²	IC ₅₀ PI3K δ [nM]	IC ₅₀ PI3K γ [nM]	Fold Selectivity γ/δ
16		43	111	2.6
17		31	2197	71
18		24	156	6.5
19		1070	4474	4.2
20		1892	22,134	12
21		956	10,944	11
22		979	8420	8.6
23		135	1380	10
24		254	588	2.3
25		647	1972	3.0
26		203	4283	21
27		1805	20,526	11
28		443	1709	3.9
29		240	1855	7.7
30		615	7553	12
31		593	8318	14

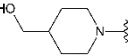
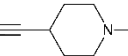
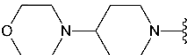
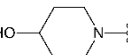
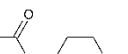
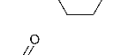
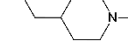
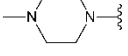
32		192	3155	16
33		276	4800	17
34		561	4317	7.7
35		445	1503	3.4
36		63	1247	20
37		351	17,658	50
38		38	13,330	351

IC₅₀ values were determined as the mean based on two independent experiments.

For that reason, a library of compounds with multiple amine substituents was designed and synthesized (Table 3). Within this set, the lowest IC₅₀ values were observed for examples 40, 42, 43, and 55, (measured at 84, 74, 63, and 82 nM, respectively). These structures also had good PI3K γ/δ selectivity.

Table 3. PI3K δ and PI3K γ activity of pyrazolo[1,5-*a*]pyrimidine derivatives with (-CO) groups.

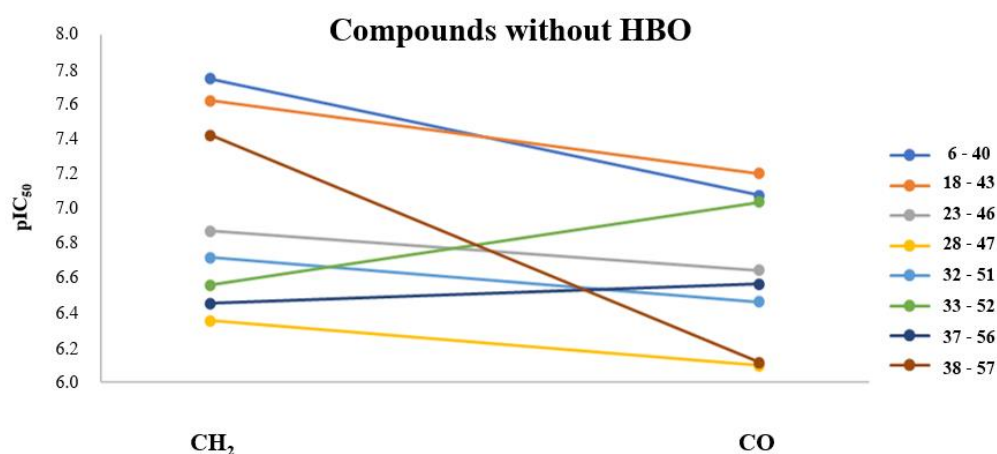
Compound	R ²	IC ₅₀ PI3K δ [nM]	IC ₅₀ PI3K γ [nM]	Fold Selectivity γ/δ
40		84	48,777	581
41		101	2483	25
42		74	3593	48
43		63	3831	61
44		459	2024	4.4
45		1704	23,290	14
46		226	8536	38
47		801	35,750	45
48		314	2793	9

49		213	1818	8.5
50		90	1782	20
51		344	1629	4.7
52		92	5946	65
53		195	2081	11
54		141	1689	12
55		82	2170	26
56		768	11,397	94
57		271	25,527	15

IC₅₀ values were determined as the mean based on two independent experiments.

The consequence of the methylene bridge to carbonyl group interchange can be tracked separately in groups of compounds divided into those with or without hydrogen bond donor (HBD) capabilities within the R² substituent.

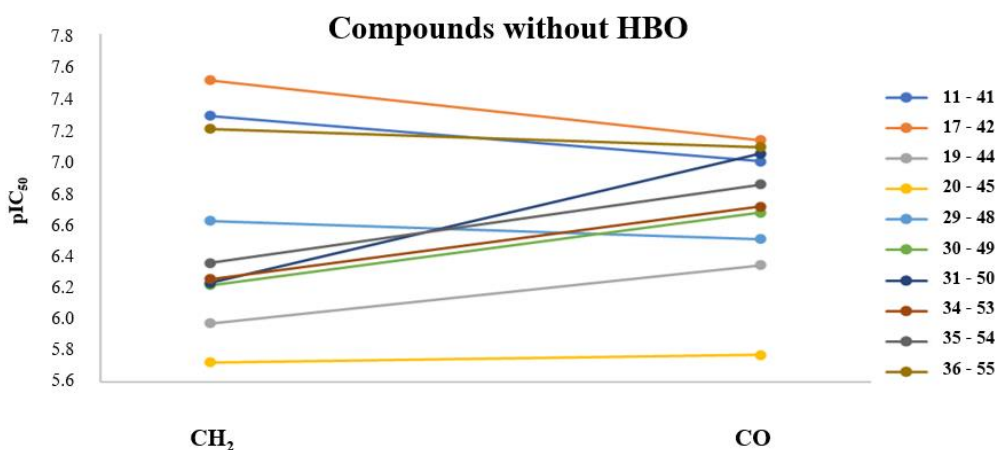
The compounds lacking the HBD functionally tend to have better potency when the methylene bridge at the C(2) core position is present within a stable substituent environment. Although some exceptions have been found, including the pairs **33** and **52** or **37** and **56**, for all other pairs, such as **6** and **40** or **38** and **57**, the PI3K δ activity drops when the methylene bridge is replaced with its carbonyl structural equivalent (Scheme 3). The measured potency is positively correlated with the increasing spherical lipophilic volume present at position 4 in the six-membered heterocyclic ring of the amino substituent. As an example, compounds **37**, **38** (Table 2), and **6** (Table 1), bearing methyl, *iso*-propyl, and *tert*-butyl motif, can be named, for which the IC₅₀ value at concentrations of 351, 38, and 18 nM was measured, respectively.



Scheme 3. The correlation of the potencies given for the compounds lacking HBD interaction within the heterocyclic system.

The activity dependence on the relationship between the methylene bridge and carbonyl interchange is not so clear for the compounds with structural capabilities of HBD interaction

within the R² substituent. Since it is challenging to isolate the bulkiness of the substituent alone and the accompanying HBD interplay with the surrounding polar environment, both those elements might affect the IC₅₀ value. As seen in Scheme 4, there is only a slight prevalence of increased activity toward the carbonyl (amide) functionality. Therefore, both structural motifs (the methylene bridge and the carbonyl function) should be considered equally essential modifications for SAR exploration.

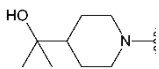
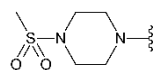
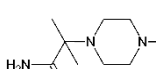
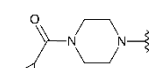


Scheme 4. The correlation of the potencies given for the compounds lacking HBD interaction within the heterocyclic system.

A detailed analysis of the entire library of synthesized compounds led to the selection of five the most promising structures: **6**, **11**, **16**, **17**, and **18** (Table 4). All of them turned out to be the derivatives of 2-(difluoromethyl)-1*H*-benzimidazole at the C(5) position of pyrazolo[1,5-*a*]pyrimidine core bearing amines of the six-membered ring as the R² can substitute a methylene bridge (CH₂) as a linkage (Table 4). Their IC₅₀ values against PI3K δ were found in the nanomolar range (18–52 nM), good selectivity in relation to other PI3K isoforms, and preserved CD19 cellular activity (for details see Table 4).

Table 4. Activity and selectivity of the most promising compounds.

Compound	R ²	IC ₅₀ PI3K δ [nM]	IC ₅₀ PI3K α [nM]	IC ₅₀ PI3K β [nM]	IC ₅₀ PI3K γ [nM]	α/δ	β/δ	γ/δ	IC ₅₀ CD19 [nM]
6		18	1428	25,475	16,904	79	1415	939	41

11		52	1729		6347	33	122		
16		43	44	13,577	111	1.0	316	2.6	114
17		31	624	44,753	2197	20	1444	71	52
18		24	73	47,360	156	3.0	1973	6.5	58

IC₅₀ values were determined as the mean based on two independent experiments.

Besides the best enzymatic and cellular activity, compound **6** was chosen for further development based on acceptable solubility, microsomal stability, permeability, and the plasma protein binding range (for details see Table 5). Attempts to scale up the synthesis turned out to be chemically and economically viable. As a result, the lead compound **6** (CPL302415) was obtained in the amount exceeding one kilogram and purity suitable for future toxicological studies.

Due to the prediction of metabolism, the calculation of in vitro clearance, or the identification of the correlation of metabolites with hepatic stability in the ADMET studies [37,38], many important parameters were determined for our lead compound CPL302415 (Table 5). The metabolic stability was evaluated by measuring the intrinsic clearance and t_{1/2} in mice and human liver microsomes (MLM and HLM), which were reported as very promising for CPL302415 (details in Table 5). Moreover, this structure has good solubility, permeability, and optimistic plasma protein binding parameters ((PPBs) in the range of 79–83% depending on the species; Table 5). Additionally, CPL302415 (**6**) was checked for bioavailability in mice (F > 55%) and dogs (F > 90%), depending on the formulation form. All these parameters make CPL302415 ready for toxicological studies and, hopefully, for future clinical trials.

Table 5. Selected parameters measured for CPL302415 (**6**).

	Kinetic Solubility pH 7.4 [mM]	Metabolic Stability				PAMPA [10 ⁻⁶ cm × s ⁻¹]	Plasma Protein Binding [%]			
		MLM t _{1/2} [min]	MLM CL [mL × mn ⁻¹ × mg ⁻¹]	HLM t _{1/2} [min]	HLM CL [mL × min ⁻¹ × mg ⁻¹]		Human	Monkey	Mice	Rat
6	>500	378	3.7	145	9.6	13.3	79	81	83	82

3. Materials and Methods

3.1. Chemistry

3.1.1. General Information

Chemicals (at least 95% purity) were purchased from ABCR (Dallas, USA), Acros (Geel, Belgium), Alfa Aesar (Haverhill, USA), Combi-Blocks (San Diego, USA), Fluorochem (Hadfield, United Kingdom), (Buchs, Switzerland), Merck (Darmstadt, Germany), and Sigma Aldrich (Saint Louis, USA), and were used without additional purification. Solvents were purified according to standard procedures if required. Air- or moisture-sensitive reactions were carried out under an argon atmosphere. All reaction progresses were routinely checked by thin-layer chromatography (TLC). TLC was performed using silica-gel-coated plates (Kieselgel F254) and

visualized using UV light. Flash chromatography was performed using Merck silica gel 60 (230–400 mesh ASTM). ^1H NMR spectra were acquired using a Varian Inova 300 MHz NMR spectrometer, a JOEL JNMR-ECZS 400 MHz spectrometer, a JOEL JNMR-ECZR 600 MHz spectrometer, and a Bruker DRX 500 NMR spectrometer with ^1H being observed at 300 MHz, 400 MHz, 600 MHz, and 500 MHz, respectively. ^{13}C NMR spectra were recorded similarly at 75 MHz, 101 MHz, 151 MHz, and 126 MHz frequencies for ^{13}C , respectively. Due to the poor solubility of some final compounds, usual characterization was omitted using ^{13}C NMR. Chemical shifts for ^1H and ^{13}C NMR spectra were reported in δ (ppm) using tetramethylsilane as an internal standard or according to the residual undeuterated solvent signal (2.50 ppm for $\text{DMSO-}d_6$ and 7.26 ppm for CDCl_3). The abbreviations for spin interaction coupled ^1H signals are as follows: s (singlet), d (doublet), t (triplet), m (multiplet), dd (doublet of doublets), dt (doublet of triplet), and q (quartet). Coupling constants (J) are expressed in Hertz. The ^{13}C NMR spectrum was recorded with the use of the JEOL Royal HFX probehead that allows measurements to be taken with the simultaneous decoupling of both ^1H and ^{19}F nuclei [39]. Mass spectra (atmospheric pressure ionization electrospray (API-ES) and electrospray ionization (ESI-MS)) were obtained using the Agilent 6130 LC/MSD spectrometer or Agilent 1290 UHPLC coupled with the Agilent QTOF 6545 mass spectrometer. All spectra of final compounds are in Supplementar Materials.

3.1.2. Synthesis

Procedure for 5-chloro-7-(morpholin-4-yl)pyrazolo[1,5-a]pyrimidin-2-yl]methanol (**2**)

Calcium chloride (10.4 g, 93.6 mmol) and sodium borohydride (7.56 g, 190 mmol) were added to the suspension of ethyl 5-chloro-7-(morpholin-4-yl)pyrazolo[1,5-a]pyrimidine-2-carboxylate (10.0 g, 31.2 mmol) in EtOH (150 mL). The mixture was stirred and heated to reflux for 3 h. Then, the reaction was cooled to RT and quenched with $\text{NH}_4\text{Cl}_{\text{aq}}$ (150 mL) and 1 M HCl (150 mL). The aqueous phase was extracted three times with AcOEt. The combined extracts were washed with water and dried over Na_2SO_4 , filtered, and concentrated to give **2** as a white solid (8.36 g, 31.1 mmol) with a 99% yield. ^1H NMR (600 MHz, $\text{DMSO-}d_6$) δ 6.43 (s, 1H, Ar-H), 6.35 (s, 1H, Ar-H), 5.32 (t, $J = 5.9$ Hz, 1H, -OH), 4.59 (dd, $J = 5.9, 0.3$ Hz, 2H, CH_2), 3.82–3.80 (m, 4H, morph.), 3.78–3.77 (m, 4H, morph.).

Procedure for 5-chloro-7-(morpholin-4-yl)pyrazolo[1,5-a]pyrimidine-2-carbaldehyde (**3**)

To a solution of compound **2** (3.00 g, 10.9 mmol) in DMF (30.0 mL) in argon atmosphere, Dess–Martin periodinane (97%, 5.74 g, 13.1 mmol) was added. The resulting mixture was stirred at room temperature for 2 h. The solvent was evaporated. The residue was washed with AcOEt and filtered. The filtrate was concentrated and the crude product was purified by flash chromatography (0–100% AcOEt gradient in heptane) to give **3** (1.34 g, 5.02 mmol) with a 46% yield. ^1H NMR (500 MHz, $\text{DMSO-}d_6$) δ 10.09 (s, 1H, -CHO), 6.97 (s, 1H, Ar-H), 6.63 (s, 1H, Ar-H), 3.90–3.85 (m, 4H, morph.), 3.86–3.78 (m, 4H, morph.).

General Procedure for the Reductive Amination Reaction

Amine derivative (1.2 eq) was added to the solution of the corresponding aldehyde (1.0 eq) in dry DCM (10 mL/1 g corresponding aldehyde) and then stirred at room temperature. After 1 h, sodium triacetoxyborohydride (1.5 eq) was added and the mixture was stirred at room temperature for a further 15 h. Water was added to the reaction mixture and phases were separated. The aqueous phase was extracted three times with DCM. Combined organic phases were dried over anhydrous sodium sulfate, filtered, and concentrated. The residue was purified by flash chromatography.

4-{2-[(4-*tert*-butylpiperazin-1-yl)methyl]-5-chloropyrazolo[1,5-a]pyrimidin-7-yl}morpholine (**4**)

Compound **4** was prepared from aldehyde **3** (1.70 g, 2.15 mmol), 1-*tert*-butylpiperazine (0.36 g, 2.58 mmol), and DCM (17.0 mL) with sodium triacetoxyborohydride (0.68 g, 3.22 mmol), according to the general procedure for the reductive amination reaction. The crude product was purified by flash chromatography (0–10% MeOH gradient in AcOEt) to give **4** (1.42 g, 3.61 mmol)

as a white solid with a 84% yield. ^1H NMR (600 MHz, DMSO- d_6) δ 6.38 (s, 1H, Ar-H), 6.36 (s, 1H, Ar-H), 3.83–3.80 (m, 4H, morph.), 3.80–3.78 (m, 4H, morph.), 3.59 (s, 2H, -CH $_2$), 2.50–2.46 (m, 4H, piperaz.), 2.45–2.37 (m, 4H, piperaz.), 0.98 (s, 9H, t-Bu.).

General Procedure for the Buchwald–Hartwig Reaction

To a pressure, microwave vessel 5-chloro-pyrazolo[1,5-*a*]pyrimidine (1.0 eq), amine (1.5 eq), tris(dibenzylideneacetone)dipalladium (0.05 eq), 9,9-dimethyl-4,5-bis(diphenylphosphino)xanthene (0.1 eq), cesium carbonate (2.0 eq), and solvent (10 mL/1 g pyrazolo[1,5-*a*]pyrimidine) were simultaneously added. The reaction vessel was then sealed and heated to 150 °C for 6 h in a microwave (power 200 W). Then, the reaction mixture was filtered through Celite® and concentrated, and the crude product was purified using flash chromatography.

1-{2-[(4-*tert*-butylpiperazin-1-yl)methyl]-7-(morpholin-4-yl)pyrazolo[1,5-*a*]pyrimidin-5-yl}-2-methyl-1*H*-benzimidazole (5)

Compound 5 was synthesized from 4 (0.22 g, 0.56 mmol) and 2-methyl-benzimidazole (0.11 g, 0.83 mmol) as an amine, tris(dibenzylideneacetone)dipalladium (26.3 mg, 0.027 mmol), 9,9-dimethyl-4,5-bis(diphenylphosphino)xanthene (33.9 mg, 0.055 mmol), cesium carbonate (0.37 g, 1.11 mmol), and *o*-xylene (2.20 mL), according to the general procedure for the Buchwald–Hartwig reaction. The crude product was purified by flash chromatography (0–100% AcOEt gradient in heptane) to give the title compound 5 as a white solid (0.19 g, 0.38 mmol) with a 69% yield. ^1H NMR (300 MHz, CDCl $_3$) δ 7.79–7.70 (m, 1H, Ar-H), 7.50–7.43 (m, 1H, Ar-H), 7.35–7.21 (m, 2H, Ar-H), 6.60 (s, 1H, Ar-H), 6.17 (s, 1H, Ar-H), 4.02–3.95 (m, 4H, morph.), 3.90–3.83 (m, 4H, morph.), 3.82 (s, 2H, CH $_2$), 2.76 (s, 3H, CH $_3$), 2.71–2.59 (m, 8H, piperaz.), 1.08 (s, 9H, t-Bu.). $^{13}\text{C}\{^1\text{H}\}$ NMR (75 MHz, CDCl $_3$) δ 155.1, 151.4, 151.2, 151.0, 150.2, 148.5, 142.7, 134.5, 122.9, 119.4, 110.3, 96.5, 87.6, 66.1, 56.3, 53.6, 48.4, 45.5, 25.8, 15.6. HRMS (ESI/MS): *m/z* calculated for C $_{27}$ H $_{36}$ N $_8$ O [M+H] $^+$ 489.3084 found 489.3088.

1-{2-[(4-*tert*-butylpiperazin-1-yl)methyl]-7-(morpholin-4-yl)pyrazolo[1,5-*a*]pyrimidin-5-yl}-2-(difluoromethyl)-1*H*-benzimidazole (6)

Compound 6 was synthesized from 4 (0.27 g, 0.68 mmol), 2-(difluoromethyl)benzimidazole (0.17 g, 1.01 mmol), tris(dibenzylideneacetone)dipalladium (31.8 mg, 0.033 mmol), 9,9-dimethyl-4,5-bis(diphenylphosphino)xanthene (39.0 mg, 0.067 mmol), cesium carbonate (0.44 g, 1.35 mmol), and *o*-xylene (2.70 mL), according to the general procedure for the Buchwald–Hartwig reaction. The crude product was purified by flash chromatography (0–100% AcOEt gradient in heptane; amino-functionalized gel column) and crystallization (AcOEt) to give 6 (0.33 g, 0.63 mmol) as a white solid with a 93% yield. ^1H NMR (600 MHz, CDCl $_3$) δ 7.92–7.90 (m, 1H, Ar-H), 7.65–7.64 (m, 1H, Ar-H), 7.43–7.38 (m, 2H, Ar-H), 7.25 (t, *J* = 53.5 Hz, 1H, CHF $_2$), 6.59 (s, 1H, Ar-H), 6.29 (s, 1H, Ar-H), 3.99–3.97 (m, 4H, morph.), 3.90–3.89 (m, 4H, morph.), 3.80 (s, 2H, CH $_2$), 2.64 (s, 8H), 1.07 (s, 9H, t-Bu.). $^{13}\text{C}\{^1\text{H}, ^{19}\text{F}\}$ NMR (151 MHz, CDCl $_3$) δ 155.5, 151.3, 150.0, 147.5, 144.7, 141.8, 134.6, 125.7, 124.1, 121.5, 111.7, 109.2 (CF $_2$), 96.7, 87.2, 66.2, 56.3, 53.9, 53.6, 48.5, 45.6, 25.9 (t-Bu.). HRMS (ESI/MS): *m/z* calculated for C $_{27}$ H $_{34}$ F $_2$ N $_8$ O [M+H] $^+$ 525.2896 found 525.2904.

1-{2-[(4-*tert*-butylpiperazin-1-yl)methyl]-7-(morpholin-4-yl)pyrazolo[1,5-*a*]pyrimidin-5-yl}-2-ethyl-1*H*-benzimidazole (7)

Compound 7 was synthesized from 4 (0.17 g, 0.42 mmol), 2-ethyl-benzimidazole (93.0 mg, 0.64 mmol), tris(dibenzylideneacetone)dipalladium (20.0 mg, 0.021 mmol), 9,9-dimethyl-4,5-bis(diphenylphosphino)xanthene (25.8 mg, 0.042 mmol), cesium carbonate (0.28 g, 0.85 mmol), and *o*-xylene (1.7 mL), according to the general procedure for the Buchwald–Hartwig reaction. The crude product was purified by flash chromatography (0–100% AcOEt gradient in heptane; amino-functionalized gel column) to give the title compound 7 as a white solid (85.0 mg, 0.17 mmol) with a 40% yield. ^1H NMR (300 MHz, CDCl $_3$) δ 7.77 (dd, *J* = 6.9, 1.6 Hz, 1H, Ar-H), 7.42 (dd, *J* = 6.8, 1.5 Hz, 1H, Ar-H), 7.26 (qd, *J* = 7.3, 3.7 Hz, 2H, Ar-H), 6.57 (s, 1H, Ar-H), 6.16 (s, 1H, Ar-H), 4.00–3.94 (m, 4H, morph.), 3.87–3.79 (m, 6H), 3.10 (q, *J* = 7.5 Hz, 2H, CH $_2$), 2.77 (s, 8H), 1.40 (t, *J* = 7.5 Hz, 3H, CH $_3$), 1.17 (s, 9H, t-Bu.). $^{13}\text{C}\{^1\text{H}\}$ NMR (75 MHz, CDCl $_3$) δ 156.2, 154.9, 151.2,

150.3, 148.6, 142.7, 134.6, 122.9, 119.5, 110.2, 99.8, 96.4, 87.9, 66.1, 56.0, 52.5, 48.4, 45.6, 25.4, 22.1, 11.9. HRMS (ESI/MS): m/z calculated for $C_{28}H_{38}N_8O$ $[M+H]^+$ 503.3241 found 503.3242.

1-{2-[(4-*tert*-butylpiperazin-1-yl)methyl]-7-(morpholin-4-yl)pyrazolo[1,5-*a*]pyrimidin-5-yl}-2-cyclopropyl-1*H*-benzimidazole (**8**)

Compound **8** was synthesized from **4** (100 mg, 0.25 mmol), 2-cyclopropyl-benzimidazole (59.2 mg, 0.37 mmol), tris(dibenzylideneacetone)dipalladium (11.8 mg, 0.012 mmol), 9,9-dimethyl-4,5-bis(diphenylphosphino)xanthene (15.2 mg, 0.025 mmol), cesium carbonate (168 mg, 0.51 mmol), and *o*-xylene (1.0 mL), according to the general procedure for the Buchwald–Hartwig reaction. The crude product was purified by flash chromatography (0–20% MeOH gradient in AcOEt) to give the title compound **8** as a white solid (93.0 mg, 0.18 mmol) with a 72% yield. 1H NMR (400 MHz, $CDCl_3$) δ 7.70–7.68 (m, 1H, Ar-H), 7.53–7.51 (m, 1H, Ar-H), 7.29–7.20 (m, 2H, Ar-H), 6.61 (s, 1H, Ar-H), 6.28 (s, 1H, Ar-H), 3.99–3.97 (m, 4H, morph.), 3.87–3.84 (m, 4H, morph.), 3.82 (s, 2H, CH_2), 2.66 (s, 8H), 2.39–2.32 (m, 1H, CH), 1.39–1.35 (m, 2H, CH_2), 1.12–1.06 (m, 11H). $^{13}C\{^1H\}$ NMR (101 MHz, $CDCl_3$) δ 156.4, 155.1, 151.2, 150.4, 148.8, 142.7, 134.9, 123.0, 122.8, 119.2, 110.6, 96.6, 88.4, 66.2, 56.3, 53.7, 48.5, 45.7, 25.8 (t-Bu.), 9.8, 8.9. HRMS (ESI/MS): m/z calculated for $C_{29}H_{38}N_8O$ $[M+H]^+$ 515.3241 found 515.3239.

1-{2-[(4-*tert*-butylpiperazin-1-yl)methyl]-7-(morpholin-4-yl)pyrazolo[1,5-*a*]pyrimidin-5-yl}-2-(trifluoromethyl)-1*H*-benzimidazole (**9**)

Compound **9** was synthesized from **4** (0.20 g, 0.51 mmol), 2-(trifluoromethyl)-benzimidazole (0.14 g, 0.76 mmol), tris(dibenzylideneacetone)dipalladium (24.1 mg, 0.025 mmol), 9,9-dimethyl-4,5-bis(diphenylphosphino)xanthene (29.5 mg, 0.051 mmol), cesium carbonate (0.34 g, 1.02 mmol), and toluene (2.0 mL), according to the general procedure for the Buchwald–Hartwig reaction. The crude product was purified by flash chromatography (0–100% AcOEt gradient in heptane; amino-functionalized gel column) to give the title compound **9** as a white solid (12.0 mg, 0.02 mmol) with a 4% yield. 1H NMR (600 MHz, $CDCl_3$) δ 7.94–7.93 (m, 1H, Ar-H), 7.55–7.53 (m, 1H, Ar-H), 7.46–7.42 (m, 2H, Ar-H), 6.63 (s, 1H, Ar-H), 6.16 (s, 1H, Ar-H), 3.98–3.97 (m, 4H, morph.), 3.90–3.89 (m, 4H, morph.), 3.82 (s, 2H, CH_2), 2.67 (d, $J = 2.1$ Hz, 8H), 1.13–1.06 (m, 9H, t-Bu.). $^{13}C\{^1H, ^{19}F\}$ NMR (151 MHz, $CDCl_3$) δ 151.2, 150.2, 147.0, 141.0, 139.9, 135.4, 126.3, 124.5, 121.7, 119.7, 118.0, 111.9, 97.2, 88.1, 66.2, 56.3, 53.8, 48.6, 45.7, 45.0, 29.7, 25.9, 25.8. HRMS (ESI/MS): m/z calculated for $C_{27}H_{33}F_3N_8O$ $[M+H]^+$ 543.2802 found 543.2806.

2-(1-([5-chloro-7-(morpholin-4-yl)pyrazolo[1,5-*a*]pyrimidin-2-yl)methyl]piperidin-4-yl)propan-2-ol (**10**)

Compound **10** was prepared from **3** (3.4 g, 12.5 mmol), 2-(4-piperidyl)-2-propanol (2.24 g, 15.0 mmol) as an amine, DCM (34.0 mL), and sodium triacetoxyborohydride (4.09 g, 18.7 mmol), according to the general procedure for the reductive amination reaction. The crude product was purified by flash chromatography (0–10% MeOH gradient in AcOEt) to give **10** (3.1 g, 7.87 mmol) with a 63% yield. 1H NMR (300 MHz, $CDCl_3$) δ 6.48 (s, 1H, Ar-H), 6.03 (s, 1H, Ar-H), 3.94 (dd, $J = 5.9, 3.6$ Hz, 4H), 3.78 (dd, $J = 5.9, 3.6$ Hz, 4H), 3.72 (s, 2H, CH_2), 3.11–3.02 (m, 2H, CH_2), 2.09–1.98 (m, 2H, CH_2), 1.78–1.66 (m, 4H), 1.50–1.21 (m, 4H), 1.16 (s, 6H, $2 \times CH_3$).

2-[1-([5-[2-(difluoromethyl)-1*H*-benzimidazol-1-yl]-7-(morpholin-4-yl)pyrazolo[1,5-*a*]pyrimidin-2-yl)methyl]piperidin-4-yl]propan-2-ol (**11**)

Compound **11** was synthesized from **10** (0.50 g, 1.24 mmol), 2-(difluoromethyl)-benzimidazole (0.31 g, 1.87 mmol), tris(dibenzylideneacetone)dipalladium (58.7 mg, 0.63 mmol), 9,9-dimethyl-4,5-bis(diphenylphosphino)xanthene (75.8 mg, 0.12 mmol), cesium carbonate (0.82 g, 2.49 mmol), and toluene (5.0 mL), according to the general procedure for the Buchwald–Hartwig reaction. The crude product was purified by flash chromatography (0–15% MeOH gradient in AcOEt) and crystallization (AcOEt) to give **11** (0.43 g, 0.81 mmol) as a white solid with a 66% yield. 1H NMR (300 MHz, $DMSO-d_6$) δ 7.85 (dd, $J = 20.1, 7.3$ Hz, 2H, Ar-H), 7.55 (s, $J = 54.0$, 1H, Ar-H), 7.51–7.40 (m, 2H), 6.66 (s, 1H, Ar-H), 6.53 (s, 1H, Ar-H), 3.94 (s, 4H, morph.), 3.84 (s, 4H, morph.), 3.65 (s, 2H, CH_2), 2.97 (d, $J = 10.5$ Hz, 2H, CH_2), 1.93 (d, $J = 10.8$ Hz, 1H), 1.65 (d, $J = 11.8$ Hz, 2H), 1.36–1.10 (m, 3H), 1.02 (s, 6H, $2 \times CH_3$). $^{13}C\{^1H\}$ NMR (75 MHz, $DMSO-d_6$) δ 155.4, 150.8, 149.6, 146.9, 144.6 (t, $J = 47.5$ Hz), 141.1, 134.0, 125.4, 123.8, 120.6, 112.3,

108.5 (t, $J = 177.7$ Hz), 95.2, 87.6, 70.1, 65.5, 56.1, 53.8, 48.1, 46.8, 26.8, 26.5. HRMS (ESI/MS): m/z calculated for $C_{27}H_{33}F_2N_7O_2$ $[M+H]^+$ 526.2736 found 526.2741.

2-(1-([5-(2-methyl-1*H*-1,3-benzimidazol-1-yl)-7-(morpholin-4-yl)pyrazolo[1,5-*a*]pyrimidin-2-yl)methyl]piperidin-4-yl)propan-2-ol (**12**)

Compound **12** was synthesized from **10** (0.15 g, 0.38 mmol), 2-methyl-benzimidazole (75.5 mg, 0.57 mmol), tris(dibenzylideneacetone)dipalladium (18.0 mg, 0.019 mmol), 9,9-dimethyl-4,5-bis(diphenylphosphino)xanthene (23.2 mg, 0.038 mmol), cesium carbonate (0.25 g, 0.56 mmol), and *o*-xylene (1.5 mL), according to the general procedure for the Buchwald–Hartwig reaction. The crude product was purified by flash chromatography (0–20% MeOH gradient in AcOEt) to give the title compound **12** as a white solid (97.0 mg, 0.20 mmol) with a 52% yield. 1H NMR (300 MHz, $CDCl_3$) δ 7.79–7.72 (m, 1H, Ar-H), 7.52–7.45 (m, 1H, Ar-H), 7.34–7.20 (m, 2H), 6.61 (s, 1H, Ar-H), 6.18 (s, 1H, Ar-H), 4.04–3.95 (m, 4H, morph.), 3.91–3.82 (m, 4H, morph.), 3.79 (s, 2H, CH_2), 3.18–3.09 (m, 2H), 2.77 (s, 3H, CH_3), 2.16–2.03 (m, 2H, CH_2), 1.82–1.71 (m, 2H, CH_2), 1.55–1.37 (m, 2H), 1.37–1.23 (m, 1H), 1.19 (s, 6H, $2 \times CH_3$). $^{13}C\{^1H\}$ NMR (75 MHz, $CDCl_3$) δ 155.2, 151.5, 151.2, 150.2, 148.5, 142.6, 134.4, 123.0, 119.3, 110.3, 96.5, 87.6, 72.3, 66.1, 56.4, 53.9, 48.4, 47.0, 29.6, 26.7, 15.5. HRMS (ESI/MS): m/z calculated for $C_{27}H_{35}N_7O_2$ $[M+H]^+$ 490.2925 found 490.2956.

Procedure for 5-[2-(difluoromethyl)-1*H*-1,3-benzimidazol-1-yl]-7-(morpholin-4-yl)pyrazolo[1,5-*a*]pyrimidine-2-carboxylate (**13**)

Compound **13** was synthesized from ethyl 5-chloro-7-(morpholin-4-yl)pyrazolo[1,5-*a*]pyrimidine-2-carboxylate (100 mg, 0.31 mmol), 2-(difluoromethyl)-1*H*-benzimidazole (79.5 mg, 0.47 mmol), tris(dibenzylideneacetone)dipalladium (14.4 mg, 0.015 mmol), 9,9-dimethyl-4,5-bis(diphenylphosphino)xanthene (19.2 mg, 0.03 mmol), cesium carbonate (0.21 g, 0.63 mmol), and toluene (2.0 mL), according to the general procedure for the Buchwald–Hartwig reaction. The crude product was purified by flash chromatography (0–50% AcOEt gradient in heptane; amino-functionalized gel column) to give the title compound **13** as a light yellow solid (65.0 mg, 0.31 mmol) with a 47% yield.

Alternatively, **13** can be synthesized as follows. Ethyl 5-chloro-7-(morpholin-4-yl)pyrazolo[1,5-*a*]pyrimidine-2-carboxylate (100 g, 312 mmol), 2-(difluoromethyl)-1*H*-benzimidazole (79.5 g, 473 mmol), tetra ethyl ammonium chloride (78.0 g, 471 mmol), potassium carbonate (87.0 g, 623 mmol), and DMF (1000 mL) were added to a reactor (2000 mL volume). The reaction was heated at 160 °C for 3 h. Then, the reaction was cooled to room temperature, filtered through Celite®, and washed with AcOEt (1.5 l). Water (3.0 mL) was added to the filtrate and phases were separated. The organic layer was concentrated. The solid was dissolved in 20% MeOH in DCM and the crude product was then purified by filtration through silica gel (0.72 kg) (20% MeOH in DCM) and macerated in TBME to give **13** (123 g, 312 mmol) as a light yellow solid with an 89% yield. 1H NMR (300 MHz, $CDCl_3$) δ 7.95–7.89 (m, 1H, Ar-H), 7.71–7.65 (m, 1H, Ar-H), 7.46–7.39 (m, 2H, Ar-H), 7.30 (t, $J = 54.0$ Hz, 1H, CHF_2), 7.11 (s, 1H, Ar-H), 6.47 (s, 1H, Ar-H), 4.48 (q, $J = 7.1$ Hz, 2H, CH_2), 4.03–3.99 (m, 4H, morph.), 3.98–3.93 (m, 4H, morph.), 1.45 (dd, $J = 8.1, 6.2$ Hz, 3H, CH_3).

Procedure for {5-[2-(difluoromethyl)-2,3-dihydro-1*H*-1,3-benzodiazol-1-yl]-7-(morpholin-4-yl)pyrazolo[1,5-*a*]pyrimidin-2-yl}methanol (**14**)

Lithium aluminum hydride solution (1M in THF, 8.00 mL, 7.20 g, 8.00 mmol) was added to the suspension of **13** (2.40 g, 5.30 mmol) in dry THF (28.0 mL) at 0 °C. The suspension was stirred at 0 °C for 3 h. The reaction was quenched with 1.0 M HCl (14.0 mL). Then, water (70 mL) and AcOEt (90 mL) were added and the mixture was then allowed to warm to room temperature and stirred for 0.5 h. The organic layer was separated, dried over Na_2SO_4 , and filtered. The solvent was removed under reduced pressure. The solid was macerated with DCM to give the title compound **14** (1.90 g, 4.72 mmol) as a light yellow solid with an 89% yield. 1H NMR (300 MHz, $DMSO-d_6$) δ 7.70 (d, $J = 7.7$ Hz, 1H, Ar-H), 6.74 (td, $J = 7.6, 1.2$ Hz, 1H), 6.62 (ddd, $J = 8.7, 6.9, 2.4$ Hz, 3H), 6.12 (s, $J = 54.0$ Hz, 1H, Ar-H), 6.10 (s, 1H, Ar-H), 5.13 (t, $J = 5.9$ Hz, 1H, OH), 4.47 (d, $J = 5.9$ Hz, 2H, CH_2), 3.74 (t, $J = 4.5$ Hz, 4H, morph.), 3.65–3.54 (m, 4H, morph.).

Procedure for 5-[2-(difluoromethyl)-1*H*-1,3-benzimidazol-1-yl]-7-(morpholin-4-yl)pyrazolo[1,5-*a*]pyrimidine-2-carbaldehyde (**15**)

Dess–Martin reagent (2.90 g, 6.63 mmol) was added to the solution of **14** (1.30 g, 3.23 mmol) in dry DMF (33 mL). The whole mixture was stirred at room temperature for 1 h. The solid was filtered off and then washed with ethyl acetate (25 mL). The obtained solution was concentrated under reduced pressure. The crude product was purified by flash chromatography (0–70% ethyl acetate gradient in heptane) to give **15** (1.02 g, 2.56 mmol) as a white solid with a 78% yield.

Alternatively, **15** can be synthesized as follows. Activated toluene:butyl acetate 1:1 (700 mL) manganese(IV) oxide (58.4 g, 667 mmol) was added to the solution of **14** (27.2 g, 67.1 mmol). The mixture was stirred at reflux (set temp: 120 °C) for 1.5 h. The reaction was then filtered through Celite®. Celite® was washed with DCM (200 mL). Organic phases were combined, and concentrated to give **15** (18.2g, 45.7 mmol) as a creamy solid with a 68% yield. ¹H NMR (300 MHz, CDCl₃) δ 10.21 (s, 1H, CHO), 7.97–7.90 (m, 1H, Ar-H), 7.73–7.67 (m, 1H, Ar-H), 7.48–7.42 (m, 2H, Ar-H), 7.29 (t, *J* = 54.0 Hz, 1H, CHF₂), 7.11 (s, 1H, Ar-H), 6.53 (s, 1H, Ar-H), 4.03 (dd, *J* = 6.1, 2.7 Hz, 4H, morph.), 3.96 (dd, *J* = 6.3, 2.9 Hz, 4H, morph.).

General Procedure for the Amidation Reaction

Corresponding amine (1.05 eq), 2-(7-aza-1*H*-benzotriazole-1-yl)-1,1,3,3-tetramethyluronium hexafluorophosphate (HATU) (1.1 eq), and triethylamine (1.5 eq) were added to the solution of substituted 5-chloro-pyrazolo[1,5-*a*]pyrimidine derivative (1.0 eq) in solvent (10 mL/1 g pyrazolo[1,5-*a*]pyrimidine derivative). The mixture was stirred at room temperature for 2 h. Water was added to the reaction mixture and phases were separated. The aqueous phase was extracted three times with the solvent. Combined organic phases were dried over anhydrous sodium sulfate, filtered, and concentrated. The residue was purified by flash chromatography.

2-(difluoromethyl)-1-[2-[(4-methanesulfonylpiperazin-1-yl)methyl]-7-(morpholin-4-yl)pyrazolo[1,5-*a*]pyrimidin-5-yl]-1*H*-1,3-benzimidazole (**16**)

Compound **16** was prepared from aldehyde **15** (0.48 g, 1.18 mmol), 1-methanesulfonylpiperazine (0.24 g, 1.42 mmol) as an amine, DCM (4.80 mL), and sodium triacetoxyborohydride (0.38 g, 1.87 mmol), according to the general procedure for the reductive amination reaction. The crude product was purified by flash chromatography (0–100% AcOEt gradient in heptane) and crystallization (AcOEt) to give the title compound **16** (0.35 g, 0.63 mmol) as a white solid with a 54% yield. ¹H NMR (600 MHz, CDCl₃) δ 7.93–7.91 (m, 1H, Ar-H), 7.66–7.65 (m, 1H, Ar-H), 7.45–7.40 (m, 2H, Ar-H), 7.29 (t, *J* = 52.6 Hz, 1H, CHF₂), 6.58 (s, 1H, Ar-H), 6.33 (s, 1H, Ar-H), 4.00–3.98 (m, 4H, morph.), 3.91–3.89 (m, 4H, morph.), 3.83 (s, 2H, CH₂), 3.29 (t, *J* = 4.6 Hz, 4H), 2.78 (s, 3H, CH₃), 2.70 (t, *J* = 4.8 Hz, 4H). ¹³C{¹H, ¹⁹F}NMR (151 MHz, CDCl₃) δ 155.1, 151.4, 150.2, 147.7, 144.6, 141.9, 134.6, 125.7, 124.2, 121.6, 111.7, 109.3 (CF₂), 96.3, 87.5, 66.2, 56.2, 52.4, 48.6, 45.9, 34.3. HRMS (ESI/MS): *m/z* calculated for C₂₄H₂₈F₂N₈O₃S [M+H]⁺ 547.2045 found 547.2048.

2-[4-([5-[2-(difluoromethyl)-1*H*-1,3-benzimidazol-1-yl]-7-(morpholin-4-yl)pyrazolo[1,5-*a*]pyrimidin-2-yl)methyl]piperazin-1-yl]-2-methylpropanamide (**17**)

Compound **17** was prepared from aldehyde **15** (0.50 g, 1.23 mmol), 2-methyl-2-(piperazin-1-yl)propanamide dihydrochloride (0.38 g, 1.48 mmol) as an amine, DCM (5.0 mL), and sodium triacetoxyborohydride (0.40 g, 1.85 mmol), according to the general procedure for the reductive amination reaction. The crude product was purified by flash chromatography (0–15% MeOH gradient in AcOEt) to give **17** (0.49 g, 0.88 mmol) as a light yellow solid with a 72% yield. ¹H NMR (400 MHz, CDCl₃) δ 7.93–7.90 (m, 1H, Ar-H), 7.67–7.63 (m, 1H, Ar-H), 7.45–7.39 (m, 2H, Ar-H), 7.23 (t, *J* = 53.6 Hz, 1H, CHF₂), 7.13 (d, *J* = 5.2 Hz, 1H), 6.59 (s, 1H, Ar-H), 6.32 (s, 1H, Ar-H), 5.46 (d, *J* = 5.1 Hz, 1H), 4.00–3.96 (m, 4H, morph.), 3.93–3.89 (m, 4H, morph.), 3.79 (s, 2H), 2.60 (s, 8H), 1.22 (s, 6H, 2xCH₃). ¹³C{¹H, ¹⁹F}NMR (101 MHz, CDCl₃) δ 180.1, 155.5, 151.3, 150.1, 147.6, 144.7, 141.8, 134.5, 125.7, 124.2, 121.6, 111.7, 109.3 (CF₂), 96.5, 87.3, 66.2, 63.5, 56.4, 53.9, 48.5, 46.6, 20.6. HRMS (ESI/MS): *m/z* calculated for C₂₇H₃₃F₂N₉O₂ [M+H]⁺ 554.2798 found 554.2800.

2-{2-[(4-cyclopropanecarbonylpiperazin-1-yl)methyl]-7-(morpholin-4-yl)pyrazolo[1,5-*a*]pyrimidin-5-yl}-2-(difluoromethyl)-1*H*-1,3-benzimidazole (**18**)

Compound **18** was prepared from aldehyde **15** (0.50 g, 1.23 mmol), 1-(cyclopropylcarbonyl)piperazine (0.21 mL, 0.23 g, 1.48 mmol) as an amine, DCM (5.0 mL), and sodium triacetoxyborohydride (0.40 g, 1.85 mmol), according to the general procedure for the reductive amination reaction. The crude product was purified by flash chromatography (0–15% MeOH gradient in AcOEt) and crystallization (AcOEt) to give **18** (0.45 g, 0.84 mmol) as a white solid with a 68% yield. ¹H NMR (400 MHz, CDCl₃) δ 7.93–7.90 (m, 1H, Ar-H), 7.67–7.64 (m, 1H, Ar-H), 7.46–7.39 (m, 2H, Ar-H), 7.23 (t, *J* = 53.6 Hz, 1H, CHF₂), 6.61 (s, 1H, Ar-H), 6.33 (s, 1H, Ar-H), 4.00–3.96 (m, 4H, morph.), 3.93–3.89 (m, 4H, morph.), 3.82 (s, 2H, CH₂), 3.73–3.69 (m, 4H), 2.60 (d, *J* = 24.3 Hz, 4H), 1.76–1.70 (m, 1H, CH), 1.00–0.96 (m, 2H, CH₂), 0.77–0.73 (m, 2H, CH₂). ¹³C{¹H, ¹⁹F}NMR (101 MHz, CDCl₃) δ 171.9, 155.3, 151.4, 150.1, 147.7, 144.6, 141.9, 134.6, 125.7, 124.2, 121.6, 111.7, 109.3 (CF₂), 96.4, 87.4, 66.2, 56.4, 48.5, 10.9, 7.4. HRMS (ESI/MS): *m/z* calculated for C₂₇H₃₀F₂N₈O₂ [M+H]⁺ 537.2532 found 537.2541.

[1-({5-[2-(difluoromethyl)-1*H*-1,3-benzimidazol-1-yl]-7-(morpholin-4-yl)pyrazolo[1,5-*a*]pyrimidin-2-yl)methyl}pyrrolidin-2-yl)methanol (**19**)

Compound **19** was prepared from aldehyde **15** (0.50 g, 1.23 mmol), 2-pyrrolidinylmethanol (0.14 mL, 0.15 g, 1.48 mmol) as an amine, DCM (5.0 mL), and sodium triacetoxyborohydride (0.40 g, 1.85 mmol), according to the general procedure for the reductive amination reaction. The crude product was purified by flash chromatography (0–20% MeOH gradient in AcOEt) to give **19** (0.33 g, 0.68 mmol) as a white solid with a 55% yield. ¹H NMR (400 MHz, CDCl₃) δ 7.93–7.90 (m, 1H, Ar-H), 7.67–7.65 (m, 1H, Ar-H), 7.45–7.38 (m, 2H, Ar-H), 7.29 (t, *J* = 53.6 Hz, 1H, CHF₂), 6.56 (s, 1H, Ar-H), 6.33 (s, 1H, Ar-H), 4.14 (d, *J* = 14.3 Hz, 1H, OH), 4.00–3.98 (m, 4H), 3.90–3.82 (m, 6H), 3.70 (dd, *J* = 11.0, 3.5 Hz, 1H), 3.47 (dd, *J* = 11.0, 3.2 Hz, 1H), 3.20–3.16 (m, 1H), 2.90–2.85 (m, 1H), 2.73–2.72 (m, 1H), 2.59–2.54 (m, 1H), 1.97–1.92 (m, 1H), 1.82–1.75 (m, 2H, CH₂). ¹³C{¹H, ¹⁹F}NMR (101 MHz, CDCl₃) δ 156.5, 151.4, 150.1, 147.6, 144.7, 141.8, 134.5, 125.7, 124.2, 121.6, 111.7, 109.3 (CF₂), 96.2, 87.5, 66.2, 64.3, 62.3, 54.8, 51.7, 48.6, 27.7, 25.3, 23.5. HRMS (ESI/MS): *m/z* calculated for C₂₄H₂₇F₂N₇O₂ [M+H]⁺ 484.2267 found 484.2271.

1-({5-[2-(difluoromethyl)-1*H*-1,3-benzimidazol-1-yl]-7-(morpholin-4-yl)pyrazolo[1,5-*a*]pyrimidin-2-yl)methyl}pyrrolidin-3-amine (**20**)

Compound *tert*-butyl *N*-[1-({5-[2-(difluoromethyl)-1*H*-1,3-benzodiazol-1-yl]-7-(morpholin-4-yl)pyrazolo[1,5-*a*]pyrimidin-2-yl)methyl}pyrrolidin-3-yl]carbamate (**Boc-20**) was prepared from aldehyde **15** (0.50 g, 1.23 mmol), 3-(Boc-amino)pyrrolidine (0.27 g, 1.48 mmol) as an amine, DCM (5.0 mL), and sodium triacetoxyborohydride (0.40 g, 1.85 mmol), according to the general procedure for the reductive amination reaction. The crude product was purified by flash chromatography (0–10% MeOH gradient in AcOEt) to give **Boc-20** (0.50 g, 0.88 mmol) as a white solid with a 71% yield. ¹H NMR (400 MHz, CDCl₃) δ 7.93–7.91 (m, 1H, Ar-H), 7.67–7.65 (m, 1H, Ar-H), 7.45–7.39 (m, 2H, Ar-H), 7.23 (t, *J* = 52.5 Hz, 1H, CHF₂), 6.58 (s, 1H, Ar-H), 6.32 (s, 1H, Ar-H), 4.91–4.90 (m, 1H), 4.20 (d, *J* = 3.4 Hz, 1H), 4.00–3.96 (m, 4H), 3.93–3.82 (m, 6H), 2.97 (d, *J* = 3.0 Hz, 1H), 2.72 (s, 2H, CH₂), 2.47 (d, *J* = 8.0 Hz, 1H), 2.32–2.27 (m, 1H), 1.67–1.63 (m, 1H), 1.43 (s, 9H, *t*-Bu.). ¹³C{¹H, ¹⁹F}NMR (101 MHz, CDCl₃) δ 156.0, 155.4, 151.4, 150.1, 147.6, 144.7, 141.8, 134.6, 125.7, 124.2, 121.5, 111.7, 109.3 (CF₂), 96.2, 87.4, 66.2, 61.0, 53.4, 52.8, 48.5, 32.7, 28.4 (*t*-Bu). HRMS (ESI/MS): *m/z* calculated for C₂₈H₃₄F₂N₈O₃ [M+H]⁺ 569.2794 found 569.2803.

The solution of **Boc-20** (0.40 g, 0.69 mmol) in trifluoroacetic acid (2.08 mL, 3.09 g, 26.9 mmol) was heated at 50 °C for 3 h. The reaction was then cooled to room temperature, stopped with 15% NaOH (15 mL). The aqueous mixture was extracted with DCM (3 × 15 mL). The combined organic extracts were washed with water and dried over Na₂SO₄, filtered, and concentrated to give **20** as a white solid (0.30 g, 0.64 mmol) with a 93% yield. ¹H NMR (400 MHz, DMSO-*d*₆) δ 8.04 (s, 2H, NH₂), 7.89–7.87 (m, 1H, Ar-H), 7.81 (dd, *J* = 6.9, 1.4 Hz, 1H, Ar-H), 7.59 (t, *J* = 52.6 Hz, 1H, CHF₂), 7.49–7.41 (m, 2H, Ar-H), 6.69 (s, 1H, Ar-H), 6.66 (s, 1H, Ar-H), 3.94–3.89 (m, 6H), 3.84–3.82 (m, 5H), 3.73 (d, *J* = 5.0 Hz, 1H), 2.80 (s, 2H, CH₂), 2.13–2.23 (1H), 1.68–1.80 (1H), 1.22 (s, 1H). ¹³C{¹H, ¹⁹F}NMR (101 MHz, DMSO-*d*₆) δ 158.0, 150.9, 149.7, 147.2, 144.7,

141.2, 134.1, 125.5, 124.0, 120.7, 117.3, 112.4, 108.6, 95.5, 88.0, 65.6, 51.9, 48.3, 29.2. HRMS (ESI/MS): m/z calculated for $C_{23}H_{26}F_2N_8O$ $[M+H]^+$ 469.2270 found 469.2273.

(3*S*)-1-({5-[2-(difluoromethyl)-1*H*-1,3-benzimidazol-1-yl]-7-(morpholin-4-yl)pyrazolo[1,5-*a*]pyrimidin-2-yl)methyl}pyrrolidin-3-ol (**21**)

Compound **21** was prepared from aldehyde **15** (0.50 g, 1.23 mmol), (*S*)-3-pyrrolidinol (0.16 mL, 0.17 g, 1.85 mmol) as an amine, DCM (5.0 mL), and sodium triacetoxyborohydride (0.40 g, 1.85 mmol), according to the general procedure for the reductive amination reaction. The crude product was purified by flash chromatography (0–100% AcOEt gradient in heptane, amino-functionalized gel column) to give **21** (0.22 g, 0.47 mmol) as a light yellow solid with a 38% yield. 1H NMR (400 MHz, $CDCl_3$) δ 7.94–7.90 (m, 1H, Ar-H), 7.67–7.64 (m, 1H, Ar-H), 7.45–7.39 (m, 2H, Ar-H), 7.23 (t, $J = 52.5$ Hz, 1H, CHF_2), 6.60 (s, 1H, Ar-H), 6.32 (s, 1H, Ar-H), 4.41–4.37 (m, 1H, OH), 4.00–3.96 (m, 4H, morph.), 3.93–3.89 (m, 6H), 3.07–3.01 (m, 1H), 2.84 (dd, $J = 10.1, 1.6$ Hz, 1H, CH), 2.74 (dd, $J = 10.1, 5.2$ Hz, 1H), 2.53 (td, $J = 8.9, 6.2$ Hz, 1H), 2.46–2.31 (m, 1H), 2.27–2.19 (m, 1H), 1.84–1.77 (m, 1H). $^{13}C\{^1H, ^{19}F\}$ NMR (101 MHz, $CDCl_3$) δ 156.0, 151.4, 150.1, 147.6, 144.7, 141.8, 134.6, 125.7, 124.2, 121.6, 111.7, 109.3 (CF_2), 96.3, 87.4, 71.5, 66.2, 62.8, 53.3, 52.4, 48.5, 35.1. HRMS (ESI/MS): m/z calculated for $C_{23}H_{25}F_2N_7O_2$ $[M+H]^+$ 470.2110 found 470.2134.

(3*R*)-1-({5-[2-(difluoromethyl)-1*H*-1,3-benzimidazol-1-yl]-7-(morpholin-4-yl)pyrazolo[1,5-*a*]pyrimidin-2-yl)methyl}pyrrolidin-3-ol (**22**)

Compound **22** was prepared from aldehyde **15** (0.50 mg, 1.23 mmol), (*R*)-3-pyrrolidinol (0.16 mL, 0.17 g, 1.85 mmol) as an amine, DCM (5.0 mL), and sodium triacetoxyborohydride (0.40 g, 1.85 mmol), according to the general procedure for the reductive amination reaction. The crude product was purified by flash chromatography (0–100% AcOEt gradient in heptane, amine gel column) to give **22** (0.34 g, 0.73 mmol) as a white solid with a 60% yield. 1H NMR (400 MHz, $CDCl_3$) δ 7.94–7.90 (m, 1H, Ar-H), 7.68–7.63 (m, 1H, Ar-H), 7.45–7.39 (m, 2H, Ar-H), 7.23 (t, $J = 52.5$ Hz, 1H, CHF_2), 6.60 (s, 1H, Ar-H), 6.31 (s, 1H, Ar-H), 4.40–4.36 (m, 1H, OH), 4.00–3.97 (m, 4H, morph.), 3.92–3.88 (m, 6H), 3.04–2.99 (m, 1H), 2.82 (dd, $J = 10.0, 2.1$ Hz, 1H), 2.73 (dd, $J = 10.1, 5.1$ Hz, 1H), 2.51 (td, $J = 8.9, 6.2$ Hz, 1H), 2.27–2.18 (m, 2H), 1.83–1.75 (m, 1H). $^{13}C\{^1H, ^{19}F\}$ NMR (101 MHz, $CDCl_3$) δ 156.2, 151.4, 150.1, 147.6, 144.7, 141.8, 134.6, 125.7, 124.2, 121.5, 111.7, 109.3 (CF_2), 96.3, 87.4, 71.5, 66.2, 62.9, 53.4, 52.4, 48.5, 35.1. HRMS (ESI/MS): m/z calculated for $C_{23}H_{25}F_2N_7O_2$ $[M+H]^+$ 470.2110 found 470.2115.

2-(difluoromethyl)-1-[7-(morpholin-4-yl)-2-(morpholin-4-ylmethyl)pyrazolo[1,5-*a*]pyrimidin-5-yl]-1*H*-1,3-benzimidazole (**23**)

Compound **23** was prepared from aldehyde **15** (0.50 g, 1.23 mmol), morpholine (0.13 mL, 0.13 g, 1.48 mmol) as an amine, DCM (5.00 mL), and sodium triacetoxyborohydride (0.40 g, 1.85 mmol), according to the general procedure for the reductive amination reaction. The crude product was purified by flash chromatography (0–15% AcOEt gradient in heptane, amino-functionalized gel column) and crystallization (AcOEt) to give the title compound **23** (0.28 g, 0.60 mmol) as a white solid with a 50% yield. 1H NMR (300 MHz, $CDCl_3$) δ 7.89–7.81 (m, 1H, Ar-H), 7.63–7.54 (m, 1H, Ar-H), 7.38–7.30 (m, 2H, Ar-H), 7.23 (d, $J = 54.0$ Hz, 1H, CHF_2), 6.55 (s, 1H, Ar-H), 6.25 (s, 1H, Ar-H), 3.92 (dd, $J = 6.0, 2.9$ Hz, 4H, morph.), 3.83 (dd, $J = 6.1, 3.0$ Hz, 4H, morph.), 3.72 (s, 2H, CH_2), 3.71–3.66 (m, 4H, morph.), 2.58–2.49 (m, 4H, morph.). $^{13}C\{^1H\}$ NMR (75 MHz, $CDCl_3$) δ 155.6, 151.5, 150.3, 147.8, 144.84 (t, $J = 26.2$ Hz), 142.1, 134.8, 125.0, 124.3, 121.7, 111.9, 109.5 (t, $J = 238.5$ Hz) (CF_2), 96.7, 87.5, 77.6, 77.2, 76.7, 67.1, 66.4, 57.1, 53.8, 48.7, 31.0. HRMS (ESI/MS): m/z calculated for $C_{23}H_{25}F_2N_7O_2$ $[M+H]^+$ 470.2110 found 470.2113.

2-(difluoromethyl)-1-(2-[[3*S*]-3-methylmorpholin-4-yl)methyl]-7-(morpholin-4-yl)pyrazolo[1,5-*a*]pyrimidin-5-yl)-1*H*-1,3-benzimidazole (**24**)

Compound **24** was prepared from aldehyde **15** (0.50 g, 1.23 mmol), (*R*)-3-methylmorpholine (0.15 g, 1.48 mmol) as an amine, DCM (5.0 mL), and sodium triacetoxyborohydride (0.40 g, 1.85 mmol), according to the general procedure for the reductive amination reaction. The crude product was purified by flash chromatography (0–100% AcOEt gradient in heptane) and crystallization (AcOEt) to give **24** (0.32 g, 0.67 mmol) as a white solid with a 54% yield. 1H NMR (400 MHz, $CDCl_3$) δ 7.93–7.90 (m, 1H, Ar-H), 7.67–7.64 (m, 1H, Ar-

H), 7.45–7.39 (m, 2H, Ar-H), 7.23 (t, $J = 52.5$ Hz, 1H, CHF₂), 6.57 (s, 1H, Ar-H), 6.32 (s, 1H, Ar-H), 4.07 (d, $J = 14.4$ Hz, 1H, CH), 4.00–3.97 (m, 4H, morph.), 3.93–3.89 (m, 4H, morph.), 3.84 (d, $J = 14.4$ Hz, 1H), 3.79 (dt, $J = 11.2, 2.6$ Hz, 1H), 3.73–3.63 (m, 2H), 3.30 (dd, $J = 11.2, 9.3$ Hz, 1H), 2.78 (dt, $J = 11.8, 2.5$ Hz, 1H), 2.60–2.51 (m, 2H), 1.15 (d, $J = 6.3$ Hz, 3H, CH₃). ¹³C{¹H, ¹⁹F}NMR (101 MHz, CDCl₃) δ 155.1, 151.2, 150.0, 147.6, 144.7, 141.9, 134.5, 125.7, 124.2, 121.6, 111.7, 109.3 (CF₂), 96.8, 87.3, 73.0, 67.4, 66.2, 54.5, 51.7, 51.6, 49.3, 48.5, 14.4. HRMS (ESI/MS): m/z calculated for C₂₄H₂₇F₂N₇O₂ [M+H]⁺ 484.2267 found 484.2269.

2-(difluoromethyl)-1-(2-[(3*R*)-3-methylmorpholin-4-yl]methyl)-7-(morpholin-4-yl)pyrazolo[1,5-*a*]pyrimidin-5-yl)-1*H*-1,3-benzimidazole (**25**)

Compound **25** was prepared from aldehyde **15** (0.50 g, 1.23 mmol), (*S*)-3-methylmorpholine (0.16 g, 1.51 mmol) as an amine, DCM (5.0 mL), and sodium triacetoxymethylborohydride (0.40 g, 1.85 mmol), according to the general procedure for the reductive amination reaction. The crude product was purified by flash chromatography (0–100% AcOEt gradient in heptane) and crystallization (AcOEt) to give **25** (0.33 g, 0.68 mmol) as a white solid with a 55% yield. ¹H NMR (400 MHz, CDCl₃) δ 7.93–7.90 (m, 1H, Ar-H), 7.68–7.64 (m, 1H, Ar-H), 7.45–7.39 (m, 2H, Ar-H), 7.23 (t, $J = 52.5$ Hz, 1H, CHF₂), 6.58 (s, 1H, Ar-H), 6.32 (s, 1H, Ar-H), 4.07 (d, $J = 14.4$ Hz, 1H, CH), 4.00–3.97 (m, 4H, morph.), 3.93–3.89 (m, 4H, morph.), 3.85 (d, $J = 14.4$ Hz, 1H), 3.81–3.77 (m, 1H), 3.73–3.63 (m, 2H), 3.30 (dd, $J = 11.1, 9.3$ Hz, 1H), 2.78 (dt, $J = 11.8, 2.5$ Hz, 1H), 2.61–2.51 (m, 2H, CH₂), 1.15 (d, $J = 6.3$ Hz, 3H, CH₃). ¹³C{¹H, ¹⁹F}NMR (101 MHz, CDCl₃) δ 155.1, 151.3, 150.0, 147.6, 144.7, 141.9, 134.6, 125.7, 124.2, 121.6, 111.7, 109.3 (CF₂), 96.8, 87.3, 73.0, 67.4, 66.2, 54.5, 51.7, 51.6, 48.5, 14.4. HRMS (ESI/MS): m/z calculated for C₂₄H₂₇F₂N₇O₂ [M+H]⁺ 484.2267 found 484.2268.

1-({5-[2-(difluoromethyl)-1*H*-1,3-benzodiazol-1-yl]-7-(morpholin-4-yl)pyrazolo[1,5-*a*]pyrimidin-2-yl}methyl)piperidine-3-carboxylate (**26**)

Compound **26** was prepared from aldehyde **15** (0.50 g, 1.23 mmol), ethyl piperidine-3-carboxylate (0.23 mL, 0.24 g, 1.48 mmol) as an amine, DCM (5.0 mL), and sodium triacetoxymethylborohydride (0.40 g, 1.85 mmol), according to the general procedure for the reductive amination reaction. The crude product was purified by flash chromatography (0–100% AcOEt gradient in heptane) to give **26** (0.56 g, 1.04 mmol) as a white solid with a 84% yield. ¹H NMR (400 MHz, CDCl₃) δ 7.93–7.91 (m, 1H, Ar-H), 7.67–7.64 (m, 1H, Ar-H), 7.45–7.40 (m, 2H, Ar-H), 7.24 (t, $J = 53.6$ Hz, 1H, CHF₂), 6.59 (s, 1H, Ar-H), 6.30 (s, 1H, Ar-H), 4.15–4.10 (m, 2H, CH₂), 4.00–3.98 (m, 4H, morph.), 3.91–3.89 (m, 4H, morph.), 3.80 (s, 2H), 3.09 (dd, $J = 10.9, 2.9$ Hz, 1H), 2.88–2.86 (m, 1H), 2.65–2.58 (m, 1H), 2.38–2.33 (m, 1H), 2.20 (td, $J = 10.9, 2.9$ Hz, 1H), 1.98–1.93 (m, 1H), 1.80–1.73 (m, 1H), 1.69–1.58 (m, 1H), 1.26–1.23 (m, 3H, CH₃). ¹³C{¹H, ¹⁹F}NMR (101 MHz, CDCl₃) δ 174.1, 156.0, 151.3, 150.0, 147.5, 144.7, 141.9, 134.6, 125.7, 124.1, 121.5, 111.7, 109.2 (CF₂), 96.4, 87.2, 66.2, 60.3, 56.8, 55.4, 53.8, 48.5, 41.9, 26.8, 24.6, 14.2. HRMS (ESI/MS): m/z calculated for C₂₈H₃₄F₂N₈O₂ [M+H]⁺ 540.2529 found 540.2536.

N-({5-[2-(difluoromethyl)-1*H*-1,3-benzimidazol-1-yl]-7-(morpholin-4-yl)pyrazolo[1,5-*a*]pyrimidin-2-yl}methyl)oxan-4-amine (**27**)

Compound **27** was prepared from aldehyde **15** (0.50 g, 1.23 mmol), 4-aminotetrahydropyran (0.16 mL, 0.16 g, 1.51 mmol) as an amine, DCM (5.0 mL), and sodium triacetoxymethylborohydride (0.40 g, 1.85 mmol), according to the general procedure for the reductive amination reaction. The crude product was purified by flash chromatography (0–10% MeOH gradient in AcOEt) to give **27** (0.45 g, 0.95 mmol) as a white solid with a 77% yield. ¹H NMR (600 MHz, DMSO-*d*₆) δ 7.88 (d, $J = 7.6$ Hz, 1H, Ar-H), 7.82–7.80 (m, 1H, Ar-H), 7.58 (t, $J = 52.6$ Hz, 1H, CHF₂), 7.47–7.42 (m, 2H, Ar-H), 6.64 (s, 1H, Ar-H), 6.60 (s, 1H, Ar-H), 3.93 (d, $J = 7.7$ Hz, 7H), 3.84–3.81 (m, 6H), 3.26 (td, $J = 11.4, 2.1$ Hz, 2H, CH₂), 2.71–2.66 (m, 1HCH), 1.80 (dd, $J = 12.5, 1.7$ Hz, 2H, CH₂), 1.32–1.26 (m, 2HCH₂). ¹³C{¹H, ¹⁹F}NMR (151 MHz, DMSO-*d*₆) δ 157.9, 150.9, 149.6, 146.9, 144.7, 141.2, 134.1, 125.5, 123.9, 120.7, 112.4, 108.6, 94.5, 87.6, 65.7, 65.6, 52.4, 48.1, 43.6, 33.0. HRMS (ESI/MS): m/z calculated for C₂₄H₂₇F₂N₇O₂ [M+H]⁺ 484.2267 found 484.2266.

2-(difluoromethyl)-1-[2-[(4,4-difluoropiperidin-1-yl)methyl]-7-(morpholin-4-yl)pyrazolo[1,5-*a*]pyrimidin-5-yl]-1*H*-1,3-benzimidazole (**28**)

Compound **28** was prepared from aldehyde **15** (0.50 g, 1.23 mmol), 4,4-difluoropiperidine (0.24 g, 1.48 mmol) as an amine, DCM (5.0 mL), and sodium triacetoxyborohydride (0.40 g, 1.85 mmol), according to the general procedure for the reductive amination reaction. The crude product was purified by flash chromatography (0–100% AcOEt gradient in heptane) and crystallization (AcOEt) to give **28** (0.41 g, 0.81 mmol) as a white solid with a 66% yield. ¹H NMR (400 MHz, CDCl₃) δ 7.93–7.91 (m, 1H, Ar-H), 7.67–7.65 (m, 1H, Ar-H), 7.46–7.39 (m, 2H, Ar-H), 7.23 (t, *J* = 54.0 Hz, 1H, CHF₂), 6.59 (s, 1H, Ar-H), 6.33 (s, 1H, Ar-H), 4.00–3.98 (m, 4H, morph.), 3.91–3.89 (m, 4H, morph.), 3.84 (s, 2H, CH₂), 2.70 (t, *J* = 5.6 Hz, 4H), 2.09–1.99 (m, 4H). ¹³C{¹H, ¹⁹F}NMR (101 MHz, CDCl₃) δ 155.9, 151.5, 150.3, 147.8, 144.8, 142.0, 134.7, 125.9, 124.4, 121.8, 111.9, 109.5 (CF₂), 96.5, 96.4, 87.6, 66.4, 55.9, 50.2, 48.7, 34.2. HRMS (ESI/MS): *m/z* calculated for C₂₄H₂₅F₄N₇O [M+H]⁺ 504.2194 found 504.2131.

1-([5-[2-(difluoromethyl)-1H-1,3-benzimidazol-1-yl]-7-(morpholin-4-yl)pyrazolo[1,5-*a*]pyrimidin-2-yl)methyl)piperidine-4-carboxamide (**29**)

Compound **29** was prepared from aldehyde **15** (0.50 g, 1.23 mmol), 4-piperidinecarboxamide (0.19 g, 1.48 mmol) as an amine, DCM (5.0 mL) and sodium triacetoxyborohydride (0.40 g, 1.85 mmol), according to the general procedure for the reductive amination reaction. The crude product was purified by crystallization (AcOEt/DCM, 90:10, *v/v*) to give **29** (0.40 g, 0.78 mmol) as a white solid with a 64% yield. ¹H NMR (300 MHz, CDCl₃) δ 7.95–7.88 (m, 1H, Ar-H), 7.70–7.62 (m, 1H, Ar-H), 7.46–7.37 (m, 2H, Ar-H), 7.30 (t, *J* = 54.0 Hz, 1H, CHF₂), 6.59 (s, 1H, Ar-H), 6.31 (s, 1H, Ar-H), 5.48 (s, 2H, NH₂), 3.98 (m, 4H, morph.), 3.90 (m, 4H, morph.), 3.78 (s, 2H, CH₂), 3.06 (d, *J* = 11.7 Hz, 2H, CH₂), 2.18 (t, *J* = 11.3 Hz, 3H), 1.96–1.73 (m, 4H). ¹³C{¹H}NMR (75 MHz, CDCl₃) δ 177.3, 156.1, 151.5, 150.3, 147.7, 144.8 (t, *J* = 26.2 Hz), 142.0, 134.8, 125.9, 124.3, 121.7, 111.9, 109.5 (t, *J* = 237.0 Hz, CF₂), 96.6, 87.5, 66.4, 56.8, 53.3, 48.7, 31.7, 29.1, 22.8. HRMS (ESI/MS): *m/z* calculated for C₂₅H₂₈F₂N₈O₂ [M+H]⁺ 511.2376 found 511.2377.

1-([5-[2-(difluoromethyl)-1H-1,3-benzimidazol-1-yl]-7-(morpholin-4-yl)pyrazolo[1,5-*a*]pyrimidin-2-yl)methyl)-4-methylpiperidin-4-ol (**30**)

Compound **30** was prepared from aldehyde **15** (0.50 g, 1.23 mmol), 4-methylpiperidin-4-ol (0.18 g, 1.48 mmol) as an amine, DCM (5.0 mL), and sodium triacetoxyborohydride (0.40 g, 1.85 mmol), according to the general procedure for the reductive amination reaction. The crude product was purified by flash chromatography (50–100% AcOEt gradient in heptane) and crystallization (AcOEt) to give **30** (0.33 g, 0.66 mmol) as a white solid with a 54% yield. ¹H NMR (400 MHz, CDCl₃) δ 7.93–7.91 (m, 1H, Ar-H), 7.67–7.65 (m, 1H, Ar-H), 7.45–7.40 (m, 2H, Ar-H), 7.23 (t, *J* = 54.0 Hz, 1H, CHF₂), 6.60 (s, 1H, Ar-H), 6.30 (s, 1H, Ar-H), 4.00–3.96 (m, 4H, morph.), 3.93–3.89 (m, 4H, morph.), 3.81 (s, 2H, CH₂), 2.74–2.69 (m, 2H, CH₂), 2.57–2.51 (m, 2H, CH₂), 1.77–1.70 (m, 2H, CH₂), 1.63 (d, *J* = 13.2 Hz, 2H, CH₂), 1.26 (s, 3H, CH₃). ¹³C{¹H, ¹⁹F} NMR (101 MHz, CDCl₃) δ 156.1, 151.3, 150.1, 147.5, 144.7, 141.9, 134.6, 125.7, 124.1, 121.6, 111.7, 109.3 (CF₂), 96.5, 87.2, 67.7, 66.2, 56.6, 49.8, 48.5, 38.8. HRMS (ESI/MS): *m/z* calculated for C₂₅H₂₉F₂N₇O₂ [M+H]⁺ 498.2423 found 498.2422.

[1-([5-[2-(difluoromethyl)-1H-1,3-benzimidazol-1-yl]-7-(morpholin-4-yl)pyrazolo[1,5-*a*]pyrimidin-2-yl)methyl)piperidin-4-yl]methanol (**31**)

Compound **31** was prepared from aldehyde **15** (0.50 g, 1.23 mmol), 4-piperidinemethanol (0.17 g, 1.48 mmol) as an amine, DCM (5.0 mL), and sodium triacetoxyborohydride (0.40 g, 1.85 mmol), according to the general procedure for the reductive amination reaction. The crude product was purified by flash chromatography (0–10% MeOH gradient in AcOEt) and crystallization (*i*-PrOH) to give **31** (0.34 g, 0.68 mmol) as a white solid with a 56% yield. ¹H NMR (600 MHz, CDCl₃) δ 7.93–7.91 (m, 1H, Ar-H), 7.67–7.64 (m, 1H, Ar-H), 7.44–7.39 (m, 2H, Ar-H), 7.26 (t, *J* = 26.8 Hz, 1H, CHF₂), 6.60 (s, 1H, Ar-H), 6.30 (s, 1H, OH), 3.99–3.98 (m, 4H, morph.), 3.91–3.89 (m, 4H, morph.), 3.78 (s, 2H, CH₂), 3.51 (d, *J* = 6.5 Hz, 2H, CH₂), 3.04 (d, *J* = 11.5 Hz, 2H, CH₂), 2.16–2.11 (m, 2H, CH₂), 1.76–1.74 (m, 2H, CH₂), 1.70–1.59 (m, 1H), 1.56–1.48 (m, 1H), 1.37–1.31 (m, 2H). ¹³C{¹H, ¹⁹F} NMR (151 MHz, CDCl₃) δ 156.2, 151.3, 150.1, 147.5, 144.7, 141.8, 134.6, 125.7, 124.1, 121.5, 111.7, 109.3 (CF₂), 96.5, 87.2, 67.9, 66.2, 56.9, 53.6, 48.5, 38.4, 28.8. HRMS (ESI/MS): *m/z* calculated for C₂₅H₂₉F₂N₇O₂ [M+H]⁺ 498.2423 found 498.2426.

1-((5-[2-(difluoromethyl)-1*H*-1,3-benzimidazol-1-yl]-7-(morpholin-4-yl)pyrazolo[1,5-*a*]pyrimidin-2-yl)methyl)piperidine-4-carbonitrile (**32**)

Compound **32** was prepared from aldehyde **15** (0.50 g, 1.23 mmol), 4-cyanopiperidine (0.17 mL, 0.16 g, 1.48 mmol) as an amine, DCM (5.0 mL), and sodium triacetoxyborohydride (0.40 g, 1.85 mmol), according to the general procedure for the reductive amination reaction. The crude product was purified by flash chromatography (0–100% AcOEt gradient in heptane) and crystallization (AcOEt) to give **32** (0.50 g, 1.01 mmol) as a white solid with a 82% yield. ¹H NMR (600 MHz, CDCl₃) δ 7.93–7.91 (m, 1H, Ar-H), 7.67–7.65 (m, 1H, Ar-H), 7.45–7.41 (m, 2H, Ar-H), 7.30 (t, *J* = 53.4 Hz, 1H, CHF₂), 6.58 (s, 1H, Ar-H), 6.32 (s, 1H, Ar-H), 4.00–3.98 (m, 4H, morph.), 3.91–3.89 (m, 4H, morph.), 3.79 (s, 2H, CH₂), 2.79 (s, 2H, CH₂), 2.69 (s, 1H, CH), 2.51 (d, *J* = 1.3 Hz, 2H, CH₂), 2.00–1.89 (m, 4H). ¹³C{¹H, ¹⁹F} NMR (151 MHz, CDCl₃) δ 155.6, 151.4, 150.2, 147.7, 144.7, 141.9, 134.6, 125.7, 124.2, 121.7, 121.6, 111.7, 109.3 (CF₂), 96.4, 87.4, 66.2, 56.7, 51.3, 48.6, 28.8, 26.0. HRMS (ESI/MS): *m/z* calculated for C₂₅H₂₆F₂N₈O [M+H]⁺ 493.2270 found 493.2281.

2-(difluoromethyl)-1-[7-(morpholin-4-yl)-2-[[4-(morpholin-4-yl)piperidin-1-yl]methyl]pyrazolo[1,5-*a*]pyrimidin-5-yl]-1*H*-1,3-benzimidazole (**33**)

Compound **33** was prepared from aldehyde **15** (0.50 g, 1.23 mmol), 4-morpholinopiperidine (0.26 g, 1.48 mmol) as an amine, DCM (5.0 mL), and sodium triacetoxyborohydride (0.40 g, 1.85 mmol), according to the general procedure for the reductive amination reaction. The crude product was purified by flash chromatography (0–20% MeOH gradient in AcOEt) and crystallization (*i*-PrOH) to give **33** (0.37 g, 0.66 mmol) as a white solid with a 54% yield. ¹H NMR (600 MHz, CDCl₃) δ 7.92–7.91 (m, 1H, Ar-H), 7.66–7.65 (m, 1H, Ar-H), 7.44–7.39 (m, 2H, Ar-H), 7.26 (t, *J* = 53.4 Hz, 1H, CHF₂), 6.59 (s, 1H, Ar-H), 6.30 (s, 1H, Ar-H), 3.99–3.98 (m, 4H, morph.), 3.91–3.89 (m, 4H, morph.), 3.77 (s, 2H, CH₂), 3.72 (t, *J* = 4.6 Hz, 4H, morph.), 3.07 (d, *J* = 11.9 Hz, 2H, CH₂), 2.55 (t, *J* = 4.6 Hz, 4H, morph.), 2.21 (t, *J* = 11.4, 3.8 Hz, 1H, CH), 2.13 (td, *J* = 11.8, 2.1 Hz, 2H, CH₂), 1.84–1.82 (m, 2H, CH₂), 1.64–1.57 (m, 2H, CH₂). ¹³C{¹H, ¹⁹F} NMR (151 MHz, CDCl₃) δ 156.2, 151.3, 150.1, 147.5, 144.7, 141.9, 134.6, 125.7, 124.2, 121.6, 111.7, 109.3 (CF₂), 96.5, 87.3, 67.3, 66.2, 62.1, 56.5, 53.2, 49.8, 48.5, 28.2. HRMS (ESI/MS): *m/z* calculated for C₂₈H₃₄F₂N₈O₂ [M+H]⁺ 553.2845 found 553.2846.

1-((5-[2-(difluoromethyl)-1*H*-1,3-benzimidazol-1-yl]-7-(morpholin-4-yl)pyrazolo[1,5-*a*]pyrimidin-2-yl)methyl)piperidin-4-ol (**34**)

Compound **34** was prepared from aldehyde **15** (0.50 g, 1.23 mmol), 4-hydroxypiperidine (0.15 g, 1.48 mmol) as an amine, DCM (5.0 mL), and sodium triacetoxyborohydride (0.40 g, 1.85 mmol), according to the general procedure for the reductive amination reaction. The crude product was purified by flash chromatography (0–20% MeOH gradient in AcOEt) and crystallization (*i*-PrOH) to give **34** (0.32 g, 0.66 mmol) as a white solid with a 54% yield. ¹H NMR (300 MHz, CDCl₃) δ 7.96–7.87 (m, 1H, Ar-H), 7.70–7.60 (m, 1H, Ar-H), 7.46–7.36 (m, 2H, Ar-H), 7.29 (t, *J* = 54.0 Hz, 1H, CHF₂), 6.60 (s, 1H, Ar-H), 6.30 (s, 1H, Ar-H), 4.02–3.94 (m, 4H, morph.), 3.94–3.86 (m, 4H, morph.), 3.79 (s, 2H, CH₂), 3.77–3.66 (m, 1H), 2.95–2.81 (m, 2H, CH₂), 2.40–2.25 (m, 2H, CH₂), 1.99–1.85 (m, 2H, CH₂), 1.74–1.55 (m, 3H). ¹³C{¹H} NMR (75 MHz, CDCl₃) δ 156.3, 151.5, 150.3, 147.7, 144.8 (t, *J* = 27.0 Hz), 142.0, 134.8, 125.8, 124.3, 121.7, 109.4 (t, *J* = 240.0 Hz, CF₂), 96.6, 87.4, 67.9, 66.3, 56.6, 51.2, 48.7, 34.6. HRMS (ESI/MS): *m/z* calculated for C₂₄H₂₇F₂N₇O₂ [M+H]⁺ 484.2267 found 484.2272.

N-[1-((5-[2-(difluoromethyl)-1*H*-1,3-benzimidazol-1-yl]-7-(morpholin-4-yl)pyrazolo[1,5-*a*]pyrimidin-2-yl)methyl)piperidin-4-yl]acetamide (**35**)

Compound **35** was prepared from aldehyde **15** (0.50 g, 1.23 mmol), 4-acetylaminopiperidine (0.22 g, 1.48 mmol) as an amine, DCM (5.0 mL), and sodium triacetoxyborohydride (0.40 g, 1.85 mmol), according to the general procedure for the reductive amination reaction. The crude product was purified by flash chromatography (0–15% MeOH gradient in AcOEt) and crystallization (AcOEt) to give **35** (0.51 g, 0.97 mmol) as a white solid with a 79% yield. ¹H NMR (600 MHz, CDCl₃) δ 7.92–7.91 (m, 1H, Ar-H), 7.66–7.64 (m, 1H, Ar-H), 7.44–7.39 (m, 2H, Ar-H), 7.25 (t, *J* = 53.4 Hz, 1H, CHF₂), 6.58 (s, 1H, Ar-H), 6.31 (s, 1H, Ar-H), 5.39 (d, *J* = 8.0 Hz, 1H, NH), 3.99–3.97 (m, 4H, morph.), 3.90–3.89 (m, 4H, morph.), 3.84–3.78 (m, 1H, CH), 3.76 (s,

2H, CH₂), 2.95 (d, *J* = 11.8 Hz, 2H, CH₂), 2.29–2.25 (m, 2H, CH₂), 1.96 (s, 3H, CH₃), 1.96–1.93 (m, 2H, CH₂), 1.52–1.45 (m, 2H, CH₂). ¹³C{¹H, ¹⁹F} NMR (151 MHz, CDCl₃) δ 169.3, 156.0, 151.3, 150.1, 147.6, 144.7, 141.9, 134.6, 125.7, 124.2, 121.5, 111.7, 109.3 (CF₂), 96.4, 87.3, 66.2, 56.5, 52.5, 48.5, 46.5, 32.4, 23.5. HRMS (ESI/MS): *m/z* calculated for C₂₆H₃₀F₂N₈O₂ [M+H]⁺ 525.2532 found 525.2890.

2-[4-((5-[2-(difluoromethyl)-1*H*-1,3-benzimidazol-1-yl]-7-(morpholin-4-yl)pyrazolo[1,5-*a*]pyrimidin-2-yl)methyl)piperazin-1-yl]-*N*-methylacetamide (**36**)

Compound **36** was prepared from aldehyde **15** (0.50 g, 1.23 mmol), *N*-methyl-2-(1-piperazinyl)acetamide (0.24 g, 1.48 mmol) as an amine, DCM (5.0 mL), and sodium triacetoxyborohydride (0.40 g, 1.85 mmol), according to the general procedure for the reductive amination reaction. The crude product was purified by flash chromatography (0–20% MeOH gradient in AcOEt) and crystallization (AcOEt) to give **36** (0.44 g, 0.82 mmol) as a white solid with a 66% yield. ¹H NMR (600 MHz, CDCl₃) δ 7.92–7.90 (m, 1H, Ar-H), 7.66–7.64 (m, 1H, Ar-H), 7.44–7.39 (m, 2H, Ar-H), 7.25 (t, *J* = 53.4 Hz, 1H, CHF₂), 7.10–7.08 (m, 1H, NH), 6.59–6.58 (m, 1H, Ar-H), 6.32 (s, 1H, Ar-H), 3.99–3.98 (m, 4H, morph.), 3.91–3.89 (m, 4H, morph.), 3.80 (s, 2H, CH₂), 3.02 (s, 2H, CH₂), 2.83 (d, *J* = 5.1 Hz, 3H, CH₃), 2.61 (d, *J* = 17.8 Hz, 8H). ¹³C{¹H, ¹⁹F} NMR (151 MHz, CDCl₃) δ 170.8, 155.6, 151.3, 150.1, 147.6, 144.6, 141.9, 134.6, 125.7, 124.2, 121.6, 111.7, 109.3 (CF₂), 96.5, 87.3, 66.2, 61.5, 56.4, 53.6, 53.2, 48.5, 25.7. HRMS (ESI/MS): *m/z* calculated for C₂₆H₃₁F₂N₉O₂ [M+H]⁺ 540.2641 found 540.2644.

2-(difluoromethyl)-1-[2-[(4-methylpiperazin-1-yl)methyl]-7-(morpholin-4-yl)pyrazolo[1,5-*a*]pyrimidin-5-yl]-1*H*-1,3-benzimidazole (**37**)

Compound **37** was prepared from aldehyde **15** (0.20 g, 0.49 mmol), 1-methylpiperazine (0.066 mL, 59.7 mg, 0.59 mmol) as an amine, DCM (2.0 mL), and sodium triacetoxyborohydride (0.17 g, 0.80 mmol), according to the general procedure for the reductive amination reaction. The crude product was purified by flash chromatography (0–30% AcOEt gradient in heptane, amino-functionalized gel column) to give **37** (0.19 g, 0.40 mmol) as a white solid with a 81% yield. ¹H NMR (600 MHz, CDCl₃) δ 7.92–7.91 (m, 1H, Ar-H), 7.66–7.64 (m, 1H, Ar-H), 7.44–7.39 (m, 2H, Ar-H), 7.29 (t, *J* = 54.0 Hz, 1H, CHF₂), 6.60 (s, 1H, Ar-H), 6.30 (s, 1H, Ar-H), 3.99–3.98 (m, 4H, morph.), 3.91–3.89 (m, 4H, morph.), 3.79 (s, 2H, CH₂), 2.56 (d, *J* = 85.2 Hz, 8H, piperaz.), 2.30 (s, 3H, CH₃). ¹³C{¹H, ¹⁹F} NMR (151 MHz, CDCl₃) δ 155.7, 151.2, 150.0, 147.4, 144.6, 141.7, 134.5, 125.6, 124.0, 121.4, 111.6, 109.1 (CF₂), 96.4, 87.1, 66.1, 56.3, 55.0, 53.0, 48.4, 45.9. HRMS (ESI/MS): *m/z* calculated for C₂₄H₂₈F₂N₈O [M+H]⁺ 483.2426 found 483.2429.

2-(difluoromethyl)-1-[7-(morpholin-4-yl)-2-[[4-(propan-2-yl)piperazin-1-yl)methyl]pyrazolo[1,5-*a*]pyrimidin-5-yl]-1*H*-1,3-benzimidazole (**38**)

Compound **38** was prepared from aldehyde **15** (1.50 g, 3.69 mmol), 1-isopropylpiperazine (0.65 mL, 0.58 g, 4.43 mmol) as an amine, DCM (15.0 mL), and sodium triacetoxyborohydride (1.25 g, 5.90 mmol), according to the general procedure for the reductive amination reaction. The crude product was purified by flash chromatography (0–30% AcOEt gradient in heptane, amino-functionalized gel column) and crystallization (AcOEt) to give **38** (1.30 g, 3.45 mmol) as a white solid with a 93% yield. ¹H NMR (400 MHz, DMSO-*d*₆) δ 7.89–7.87 (m, 1H, Ar-H), 7.82–7.80 (m, 1H, Ar-H), 7.60 (t, *J* = 52.6 Hz, 1H, CHF₂), 7.46–7.40 (m, 2H, Ar-H), 6.65 (s, 1H, Ar-H), 6.52 (s, 1H, Ar-H), 3.94–3.92 (m, 4H, morph.), 3.84–3.82 (m, 4H, morph.), 3.66 (s, 2H, CH₂), 2.58 (t, *J* = 6.5 Hz, 1H, CH), 2.44 (s, 8H, piperaz.), 0.94 (d, *J* = 6.5 Hz, 6H, 2xCH₃). ¹³C{¹H, ¹⁹F} NMR (101 MHz, DMSO-*d*₆) δ 155.0, 150.9, 149.6, 147.0, 144.7, 141.2, 134.0, 125.4, 123.9, 120.7, 112.4, 108.5, 108.5, 95.4, 87.8, 65.6, 55.9, 53.5, 53.1, 48.2, 47.9, 18.2. HRMS (ESI/MS): *m/z* calculated for C₂₆H₃₂F₂N₈O [M+H]⁺ 511.2739 found 511.2743.

Procedure for 5-[2-(difluoromethyl)-1*H*-1,3-benzimidazol-1-yl]-7-(morpholin-4-yl)pyrazolo[1,5-*a*]pyrimidine-2-carboxylic acid (**39**)

The solution of lithium hydroxide monohydrate (28.4 g, 678 mmol) was added to the suspension of **13** (60.0 g, 136 mmol) in MeOH (1000 mL) in water (200 mL). The mixture was stirred at room temperature for 18 h. The solvent was removed under reduced pressure and the reaction was quenched with water (600 mL) and 2.5 M HCl (60 mL). The solid was collected by

filtration and dried to give **39** (52.1 g, 126 mmol) as a white solid with a 93% yield. ¹H NMR (300 MHz, DMSO-*d*₆) δ 7.93–7.81 (m, 2H, Ar-H), 7.56 (t, *J* = 54.0 Hz, 1H, CHF₂), 7.47 (ddd, *J* = 10.4, 5.2, 3.6 Hz, 2H, Ar-H), 7.03 (s, 1H), 6.86 (s, 1H), 4.02–3.96 (m, 4H, morph.), 3.90–3.77 (m, 6H), 3.57 (s, 1H).

1-[2-(4-*tert*-butylpiperazine-1-carbonyl)-7-(morpholin-4-yl)pyrazolo[1,5-*a*]pyrimidin-5-yl]-2-(difluoromethyl)-1*H*-1,3-benzimidazole (**40**)

Compound **40** was prepared from **39** (0.20 g, 0.48 mmol), *N*-*t*-butylpiperazine (0.10 g, 0.72 mmol), HATU (0.21 g, 0.57 mmol), TEA (0.13 mL, 96.5 mg, 0.75 mmol), and DMF (2.0 mL), according to the general procedure for the amidation reaction. The crude product was purified by flash chromatography (0–100% AcOEt gradient in heptane, amino-functionalized gel column) to give **40** (0.13 g, 0.23 mmol) as a white solid with a 51% yield. ¹H NMR (400 MHz, DMSO-*d*₆) δ 7.88 (dd, *J* = 7.1, 1.5 Hz, 1H, Ar-H), 7.84–7.82 (m, 1H, Ar-H), 7.61 (t, *J* = 52.5 Hz, 1H, CHF₂), 7.48–7.41 (m, 2H, Ar-H), 6.83 (s, 1H, Ar-H), 6.80 (s, 1H, Ar-H), 3.93–3.91 (m, 4H), 3.86–3.83 (m, 4H), 3.72–3.64 (m, 4H), 2.59–2.51 (m, 4H), 1.02 (s, 9H, *t*-Bu). ¹³C{¹H, ¹⁹F} NMR (101 MHz, DMSO-*d*₆) δ 161.5, 151.2, 150.4, 149.2, 147.8, 144.7, 141.2, 134.0, 125.6, 124.1, 120.7, 112.4, 108.5, 108.5, 96.7, 89.3, 65.6, 59.7, 48.5, 46.1, 25.6, 20.7, 14.1. HRMS (ESI/MS): *m/z* calculated for C₂₇H₃₂F₂N₈O₂ [M+H]⁺ 539.2689 found 539.2736.

2-(4-{5-[2-(difluoromethyl)-1*H*-1,3-benzimidazol-1-yl]-7-(morpholin-4-yl)pyrazolo[1,5-*a*]pyrimidine-2-carbonyl}piperazin-1-yl)propan-2-ol (**41**)

Compound **41** was prepared from **39** (1.50 g, 3.62 mmol), 2-(4-piperidyl)-2-propanol (0.57 g, 3.83 mmol), HATU (1.51 mg, 3.98 mmol), TEA (0.76 mL, 0.55, 5.44 mmol), and DCM (15.0 mL), according to the general procedure for the amidation reaction. The crude product was purified by flash chromatography (0–10% MeOH gradient in AcOEt) to give **41** (0.66 g, 1.22 mmol) as a light yellow solid with a 34% yield. ¹H NMR (300 MHz, CDCl₃) δ 7.94–7.89 (m, 1H, Ar-H), 7.69–7.65 (m, 1H, Ar-H), 7.46–7.39 (m, 2H, Ar-H), 7.29 (t, *J* = 54.0 Hz, 1H, CHF₂), 6.86 (s, 1H, Ar-H), 6.42 (s, 1H, Ar-H), 4.91 (d, *J* = 13.0 Hz, 1H), 4.49 (d, *J* = 13.5 Hz, 1H), 4.00–3.95 (m, 4H, morph.), 3.94–3.86 (m, 4H, morph.), 3.08 (t, *J* = 11.8 Hz, 1H), 2.76 (td, *J* = 12.8, 2.6 Hz, 1H), 1.97–1.78 (m, 2H, CH₂), 1.68–1.56 (m, 1H, CH), 1.49–1.34 (m, 3H), 1.22 (d, *J* = 6.0 Hz, 6H, 2xCH₃). ¹³C{¹H} NMR (75 MHz, CDCl₃) δ 162.7, 151.6, 149.7, 148.5, 144.7 (t, *J* = 27.0 Hz), 142.0, 134.7, 126.0, 124.5, 121.7, 111.9 (t, *J* = 238.5 Hz, CF₂), 97.8, 88.6, 72.2, 66.3, 48.9, 47.8, 43.2, 27.6 (d, *J* = 16.8 Hz), 26.9 (d, *J* = 5.1 Hz). HRMS (ESI/MS): *m/z* calculated for C₂₇H₃₁F₂N₇O₃ [M+H]⁺ 540.2529 found 540.2533.

2-(4-{5-[2-(difluoromethyl)-1*H*-1,3-benzimidazol-1-yl]-7-(morpholin-4-yl)pyrazolo[1,5-*a*]pyrimidine-2-carbonyl}piperazin-1-yl)-2-methylpropanamide (**42**)

Compound **42** was prepared from **39** (0.20 g, 0.48 mmol), 2-methyl-2-(piperazin-1-yl)propanamide dihydrochloride (0.13 g, 0.49 mmol), HATU (0.20 g, 0.52 mmol), TEA (0.23 mL, 0.16 g, 1.66 mmol), and DCM (2.0 mL), according to the general procedure for the amidation reaction. The crude product was purified by flash chromatography (0–20% MeOH gradient in AcOEt) to give **42** (0.18 g, 0.31 mmol) as a white solid with a 67% yield. ¹H NMR (600 MHz, DMSO-*d*₆) δ 7.89 (d, *J* = 7.6 Hz, 1H, Ar-H), 7.82 (d, *J* = 7.9 Hz, 1H, Ar-H), 7.58 (t, *J* = 52.6 Hz, 1H, CHF₂), 7.49–7.42 (m, 2H), 7.25 (d, *J* = 2.9 Hz, 1H), 6.99 (d, *J* = 2.8 Hz, 1H, Ar-H), 6.84 (s, 1H, Ar-H), 6.80 (s, 1H), 3.93–3.91 (m, 4H, morph.), 3.85–3.84 (m, 4H, morph.), 3.79 (s, 2H, CH₂), 3.73 (s, 2H, CH₂), 2.52–2.50 (m, 2H, CH₂), 2.46 (t, *J* = 4.4 Hz, 2H, CH₂), 1.09 (s, 6H, 2xCH₃). ¹³C{¹H, ¹⁹F} NMR (151 MHz, DMSO-*d*₆) δ 177.7, 161.6, 151.1, 150.3, 149.2, 147.7, 144.6, 141.2, 134.0, 125.5, 124.0, 120.6, 112.3, 108.5, 96.6, 89.2, 79.1, 65.5, 62.6, 48.4, 47.1, 46.4, 42.2, 20.5. HRMS (ESI/MS): *m/z* calculated for C₂₇H₃₁F₂N₉O₃ [M+H]⁺ 568.2590 found 568.2586.

1-[2-(4-cyclopropanecarbonylpiperazine-1-carbonyl)-7-(morpholin-4-yl)pyrazolo[1,5-*a*]pyrimidin-5-yl]-2-(difluoromethyl)-1*H*-1,3-benzimidazole (**43**)

Compound **43** was prepared from **39** (0.30 g, 0.71 mmol), 1-(cyclopropylcarbonyl)piperazine (0.11 mL, 0.11 g, 0.74 mmol), HATU (0.30 g, 0.78 mmol), TEA (0.15 mL, 100 mg, 1.06 mmol), and DCM (3.0 mL), according to the general procedure for the amidation reaction. The crude product was purified by flash chromatography (0–10% MeOH

gradient in AcOEt) to give **43** (0.24 g, 0.44 mmol) as a white solid with a 62% yield. ¹H NMR (600 MHz, DMSO-*d*₆) δ 7.89–7.88 (m, 1H, Ar-H), 7.83 (d, *J* = 7.8 Hz, 1H, Ar-H), 7.59 (t, *J* = 52.5 Hz, 1H, CHF₂), 7.49–7.43 (m, 2H, Ar-H), 6.89 (s, 1H, Ar-H), 6.82 (s, 1H, Ar-H), 3.92 (d, *J* = 4.5 Hz, 4H), 3.85 (s, 4H), 3.78 (s, 4H), 3.67–3.56 (m, 3H), 1.98 (s, 1H, CH), 1.16 (d, *J* = 7.1 Hz, 1H), 0.77–0.73 (m, 4H). ¹³C{¹H, ¹⁹F} NMR (151 MHz, DMSO-*d*₆) δ 171.3, 151.2, 150.1, 149.3, 147.8, 144.7, 141.2, 134.0, 125.6, 124.1, 120.7, 112.4, 108.5, 97.0, 89.4, 65.6, 48.5, 45.8, 10.4, 7.1. HRMS (ESI/MS): *m/z* calculated for C₂₇H₂₈F₂N₈O₃ [M+H]⁺ 551.2332 found 551.2333.

(1-{5-[2-(difluoromethyl)-1*H*-1,3-benzodiazol-1-yl]-7-(morpholin-4-yl)pyrazolo[1,5-*a*]pyrimidine-2-carbonyl}pyrrolidin-2-yl)methanol (**44**)

Compound **44** was prepared from **39** (0.50 g, 1.18 mmol), pyrrolidin-2-ylmethanol (0.13 mL, 0.13 g, 1.31 mmol), HATU (0.49 g, 1.30 mmol), TEA (0.25 mL, 0.18 g, 1.79 mmol), and DCM (5.0 mL), according to the general procedure for the amidation reaction. The crude product was purified by flash chromatography (0–10% MeOH gradient in AcOEt) to give **44** (0.16 g, 0.33 mmol) as a white solid with a 28% yield. ¹H NMR (600 MHz, DMSO-*d*₆) δ 7.89 (d, *J* = 7.8 Hz, 1H, Ar-H), 7.85–7.83 (m, 1H, Ar-H), 7.60 (t, *J* = 52.3 Hz, 1H, CHF₂), 7.49–7.42 (m, 2H, Ar-H), 6.92–6.90 (m, 1H, Ar-H), 6.81 (s, 1H, Ar-H), 4.85–4.81 (m, 1H, OH), 4.24–4.17 (m, 1H), 3.96–3.90 (m, 4H, morph.), 3.87–3.83 (m, 4H, morph.), 3.68–3.59 (m, 1H), 3.54–3.45 (m, 1H), 3.37–3.35 (m, 2H, CH₂), 2.09–1.82 (m, 4H). ¹³C{¹H, ¹⁹F} NMR (151 MHz, DMSO-*d*₆) δ 161.0, 160.7, 151.2, 149.0, 144.7, 141.2, 134.0, 125.6, 124.1, 120.7, 112.4, 108.5, 97.3, 89.2, 65.7, 60.8, 59.7, 59.1, 49.1, 48.5, 26.3, 24.2. HRMS (ESI/MS): *m/z* calculated for C₂₄H₂₅F₂N₇O₃ [M+H]⁺ 498.2059 found 498.2066.

1-{5-[2-(difluoromethyl)-1*H*-1,3-benzodiazol-1-yl]-7-(morpholin-4-yl)pyrazolo[1,5-*a*]pyrimidine-2-carbonyl}pyrrolidin-3-amine (**45**)

Compound *N*-(1-{5-[2-(difluoromethyl)-1*H*-1,3-benzodiazol-1-yl]-7-(morpholin-4-yl)pyrazolo[1,5-*a*]pyrimidine-2-carbonyl}pyrrolidin-3-yl)carbamate (**Boc-45**) was prepared from **39** (0.50 g, 1.18 mmol), 3-(Boc-amino)pyrrolidine (0.24 g, 1.30 mmol), HATU (0.49 g, 1.30 mmol), TEA (0.25 mL, 0.18 g, 1.79 mmol), and DCM (5.0 mL), according to the general procedure for the amidation reaction. The crude product was purified by flash chromatography (0–10% MeOH gradient in AcOEt) to give **Boc-45** (0.37 g, 0.64 mmol) as a light yellow solid with a 55% yield. ¹H NMR (300 MHz, DMSO-*d*₆) δ 7.93–7.82 (m, 2H, Ar-H), 7.56 (t, *J* = 54.0 Hz, 1H, CHF₂), 7.52–7.41 (m, 2H, Ar-H), 6.92 (d, *J* = 0.6 Hz, 1H, Ar-H), 6.82 (s, 1H, Ar-H), 4.87–4.79 (m, 1H), 4.71–4.16 (m, 1H), 3.99–3.77 (m, 11H), 3.71–3.58 (m, 1H), 3.58–3.32 (m, 2H), 2.14–1.79 (m, 9H, *t*-Bu).

The solution of **Boc-45** (0.35 g, 0.60 mmol) in trifluoroacetic acid (2.09 mL, 3.11 g, 27.0 mmol, 45.0 eq) was heated at 50 °C for 3 h. The reaction was then cooled to room temperature, and stopped with 15% NaOH (15.0 mL). The aqueous mixture was extracted with DCM (3 × 15 mL). The combined organic extracts were washed with water and dried over Na₂SO₄, filtered, and concentrated. The crude product was purified by flash chromatography (50–100% AcOEt gradient in heptane, amino-functionalized gel column) to give **45** (0.14 g, 0.29 mmol) as a white solid with a 48% yield. ¹H NMR (600 MHz, DMSO-*d*₆) δ 7.89 (d, *J* = 7.6 Hz, 1H, Ar-H), 7.84–7.83 (m, 1H, Ar-H), 7.60 (t, *J* = 52.5 Hz, 1H, CHF₂), 7.47–7.42 (m, 2H, Ar-H), 6.91 (d, *J* = 3.5 Hz, 1H, Ar-H), 6.80 (s, 1H, Ar-H), 4.00–3.93 (m, 5H), 3.90–3.83 (m, 5H), 3.71–3.66 (m, 1H), 3.62 (dd, *J* = 12.2, 5.8 Hz, 1H), 3.55–3.48 (m, 2H), 3.24–3.15 (m, 1H, CH), 2.03–1.94 (m, 1H, CH), 1.73–1.61 (m, 1H, CH). ¹³C{¹H, ¹⁹F} NMR (151 MHz, DMSO-*d*₆) δ 160.5, 151.1, 148.9, 147.6, 144.6, 141.1, 133.9, 125.4, 123.9, 120.6, 112.3, 108.4, 97.1, 89.1, 65.5, 56.7, 54.8, 51.3, 48.9, 46.7, 45.0, 34.7, 32.0. HRMS (ESI/MS): *m/z* calculated for C₂₃H₂₄F₂N₈O₂ [M+H]⁺ 483.2063 found 483.2063.

2-(difluoromethyl)-1-[7-(morpholin-4-yl)-2-(morpholine-4-carbonyl)pyrazolo[1,5-*a*]pyrimidin-5-yl]-1*H*-1,3-benzimidazole (**46**)

Compound **46** was prepared from **39** (1.50 g, 3.62 mmol), morpholine (0.34 mL, 0.34 g, 3.90 mmol), HATU (1.52 mg, 3.99 mmol), TEA (0.76 mL, 0.55 g, 5.44 mmol), and DCM (15.0 mL), according to the general procedure for the amidation reaction. The crude product was purified by flash chromatography (50–100% AcOEt gradient in heptane) to give **46** (937.0 mg, 1.94 mmol) as a light yellow solid with a 53% yield. ¹H NMR (600 MHz, CDCl₃) δ 7.93–7.91 (m, 1H, Ar-H), 7.68–7.66 (m, 1H, Ar-H), 7.46–7.41 (m, 2H, Ar-H), 7.28 (t, *J* = 54.0 Hz, 1H, CHF₂), 6.91 (s, 1H, Ar-

H), 6.45 (s, 1H, Ar-H), 3.98–3.96 (m, 4H, morph.), 3.92–3.86 (m, 8H, morph.), 3.84–3.82 (m, 2H, morph.), 3.73–3.72 (m, 2H, morph.). ¹³C{¹H, ¹⁹F} NMR (151 MHz, CDCl₃) δ 162.9, 151.7, 150.9, 149.9, 148.7, 144.7, 142.1, 134.7, 126.2, 124.6, 121.8, 112.0, 109.7 (CF₂), 98.4, 89.0, 67.2, 66.4, 48.9, 43.1. HRMS (ESI/MS): *m/z* calculated for C₂₃H₂₃F₂N₇O₃ [M+H]⁺ 484.1903 found 484.1912.

2-(difluoromethyl)-1-[2-(4,4-difluoropiperidine-1-carbonyl)-7-(morpholin-4-yl)pyrazolo[1,5-*a*]pyrimidin-5-yl]-1*H*-1,3-benzimidazole (**47**)

Compound **47** was prepared from **39** (1.50 g, 3.62 mmol), 4,4-difluoropiperidine (0.63 g, 3.99 mmol), HATU (1.52 mg, 3.99 mmol), TEA (1.31 mL, 0.95 g, 9.35 mmol), and DCM (15.0 mL), according to the general procedure for the amidation reaction. The crude product was purified by flash chromatography (0–50% AcOEt gradient in heptane, amino-functionalized gel column) to give **47** (934.0 mg, 1.80 mmol) as a light yellow solid with a 50% yield. ¹H NMR (300 MHz, CDCl₃) δ 7.96–7.88 (m, 1H, Ar-H), 7.71–7.66 (m, 1H, Ar-H), 7.48–7.41 (m, 2H, Ar-H), 7.29 (t, *J* = 54.0 Hz, 1H, CHF₂), 6.93 (s, 1H, Ar-H), 6.47 (s, 1H, Ar-H), 4.03–3.95 (m, 8H), 3.93–3.87 (m, 4H, morph.), 2.22–1.98 (m, 4H). ¹³C{¹H} NMR (75 MHz, CDCl₃) δ 163.3, 152.1, 150.3, 149.1, 145.1 (t, *J* = 27.0 Hz), 142.5, 135.2, 126.5, 125.0, 122.0 (t, *J* = 240.7 Hz), 112.4, 110.1 (t, *J* = 238.5 Hz), 98.9, 89.6, 66.7, 49.3, 44.4, 40.1, 35.6 (t, *J* = 24.7 Hz), 34.5 (t, *J* = 22.5 Hz). HRMS (ESI/MS): *m/z* calculated for C₂₄H₂₃F₄N₇O₂ [M+H]⁺ 518.1922 found 518.1924.

1-[5-[2-(difluoromethyl)-1*H*-1,3-benzimidazol-1-yl]-7-(morpholin-4-yl)pyrazolo[1,5-*a*]pyrimidine-2-carbonyl]piperidine-4-carboxamide (**48**)

Compound **48** was prepared from **39** (1.50 g, 3.62 mmol), 4-piperidinecarboxamide (0.51 g, 3.90 mmol), HATU (1.52 mg, 3.99 mmol), TEA (0.76 mL, 0.55 g, 5.44 mmol), and DCM (15.0 mL), according to the general procedure for the amidation reaction. The crude product was purified by flash chromatography (0–20% MeOH gradient in AcOEt) to give **48** (0.73 g, 1.39 mmol) as a light yellow solid with a 39% yield. ¹H NMR (600 MHz, DMSO-*d*₆) δ 7.89–7.88 (m, 1H, Ar-H), 7.84–7.82 (m, 1H, Ar-H), 7.59 (t, *J* = 52.5 Hz, 1H, CHF₂), 7.49–7.42 (m, 2H), 7.31 (s, 1H, Ar-H), 6.83 (s, 1H, Ar-H), 6.82 (s, 1H), 6.80 (s, 1H), 4.48 (d, *J* = 13.0 Hz, 2H, CH₂), 4.25 (d, *J* = 13.6 Hz, 2H, CH₂), 3.93–3.91 (m, 4H, morph.), 3.84 (t, *J* = 4.7 Hz, 4H, morph.), 3.18 (s, 2H), 2.90 (d, *J* = 2.5 Hz, 2H), 2.43 (s, 1H). ¹³C{¹H, ¹⁹F} NMR (151 MHz, DMSO-*d*₆) δ 175.8, 161.8, 151.2, 150.6, 149.2, 147.7, 144.7, 141.2, 134.0, 125.5, 124.0, 120.7, 112.4, 108.5, 96.4, 89.3, 65.6, 48.4, 46.2, 41.4, 29.0, 28.2. HRMS (ESI/MS): *m/z* calculated for C₂₅H₂₆F₂N₈O₃ [M+H]⁺ 525.2168 found 525.2171.

1-[5-[2-(difluoromethyl)-1*H*-1,3-benzimidazol-1-yl]-7-(morpholin-4-yl)pyrazolo[1,5-*a*]pyrimidine-2-carbonyl]-4-methylpiperidin-4-ol (**49**)

Compound **49** was prepared from **39** (1.50 g, 3.62 mmol), 4-methylpiperidin-4-ol (0.47 g, 3.89 mmol), HATU (1.52 mg, 3.99 mmol), TEA (0.76 mL, 0.55 g, 5.44 mmol), and DCM (15.0 mL), according to the general procedure for the amidation reaction. The crude product was purified by flash chromatography (0–10% MeOH gradient in AcOEt) to give **49** (0.90 g, 1.76 mmol) as a light yellow solid with a 49% yield. ¹H NMR (600 MHz, CDCl₃) δ 7.93–7.91 (m, 1H, Ar-H), 7.67 (dd, *J* = 7.4, 1.8 Hz, 1H, Ar-H), 7.46–7.41 (m, 2H, Ar-H), 7.29 (t, *J* = 54.0 Hz, 1H, CHF₂), 6.87 (s, 1H, Ar-H), 6.42 (s, 1H, Ar-H), 4.45–4.41 (m, 1H), 4.12–4.09 (m, 1H), 3.98–3.96 (m, 4H, morph.) 3.91–3.90 (m, 4H, morph.), 3.65–3.61 (m, 1H), 3.42–3.38 (m, 1H), 1.78–1.71 (m, 2H, CH₂), 1.68–1.62 (m, 3H, CH₃), 1.36 (s, 1H), 1.34 (s, 3H). ¹³C{¹H, ¹⁹F} NMR (151 MHz, CDCl₃) δ 162.8, 151.7, 149.8, 148.5, 144.8, 142.1, 134.8, 126.1, 124.5, 121.8, 112.0, 109.7 (CF₂), 97.9, 88.8, 68.4, 66.4, 48.9, 43.8, 39.5, 39.1, 38.6, 30.6. HRMS (ESI/MS): *m/z* calculated for C₂₅H₂₇F₂N₇O₃ [M+H]⁺ 512.2216 found 512.2222.

(1-[5-[2-(difluoromethyl)-1*H*-1,3-benzimidazol-1-yl]-7-(morpholin-4-yl)pyrazolo[1,5-*a*]pyrimidine-2-carbonyl]piperidin-4-yl)methanol (**50**)

Compound **50** was prepared from **39** (1.50 g, 3.62 mmol), 4-piperidinemethanol (0.46 g, 3.95 mmol), HATU (1.52 mg, 3.99 mmol), TEA (0.76 mL, 0.55 g, 5.44 mmol), and DCM (15.0 mL), according to the general procedure for the amidation reaction. The crude product was purified by flash chromatography (0–10% MeOH gradient in AcOEt) to give **50** (0.76 g, 1.54 mmol) as a light yellow solid with a 43% yield. ¹H NMR (600 MHz, DMSO-*d*₆) δ 7.90–7.87 (m, 1H, Ar-H), 7.83 (dd, *J* = 7.0, 1.3 Hz, 1H, Ar-H), 7.61 (t, *J* = 52.5 Hz, 1H, CHF₂), 7.49–7.41 (m, 2H, Ar-H), 6.81

(s, 1H, Ar-H), 6.80 (s, 1H), 4.53 (t, $J = 5.3$ Hz, 2H, CH₂), 4.24 (d, $J = 13.3$ Hz, 1H), 3.92–3.91 (m, 4H, morph.), 3.85–3.83 (m, 5H), 3.30–3.28 (m, 2H), 3.15–3.08 (m, 1H), 2.85–2.78 (m, 1H), 1.78 (d, $J = 13.1$ Hz, 1H), 1.70 (d, $J = 10.4$ Hz, 2H), 1.12–1.09 (m, 1H). ¹³C{¹H, ¹⁹F} NMR (151 MHz, DMSO-*d*₆) δ 170.6, 161.9, 151.4, 149.5, 148.0, 144.9, 141.4, 134.2, 125.8, 124.3, 120.9, 112.7, 108.7, 96.6, 89.4, 65.8, 60.0, 49.0, 46.9, 42.0, 38.6, 29.5, 28.7. HRMS (ESI/MS): m/z calculated for C₂₅H₂₇F₂N₇O₃ [M+H]⁺ 512.2216 found 512.2218.

1-[5-[2-(difluoromethyl)-1H-1,3-benzimidazol-1-yl]-7-(morpholin-4-yl)pyrazolo[1,5-*a*]pyrimidine-2-carbonyl]piperidine-4-carbonitrile (**51**)

Compound **51** was prepared from **39** (1.50 g, 3.62 mmol), 4-cyanopiperidine (0.44 mL, 0.43 g, 3.96 mmol), HATU (1.52 mg, 3.99 mmol), TEA (0.76 mL, 0.55 g, 5.44 mmol), and DCM (15.0 mL), according to the general procedure for the amidation reaction. The crude product was purified by flash chromatography (50–100% AcOEt gradient in heptane) to give **51** (0.86 g, 1.69 mmol) as a light yellow solid with a 47% yield. ¹H NMR (400 MHz, CDCl₃) δ 7.93–7.91 (m, 1H, Ar-H), 7.69–7.66 (m, 1H, Ar-H), 7.47–7.40 (m, 2H, Ar-H), 7.28 (t, $J = 54.0$ Hz, 1H, CHF₂), 6.90 (s, 1H, Ar-H), 6.46 (s, 1H, Ar-H), 4.08–3.97 (m, 6H), 3.91–3.83 (m, 6H), 3.02–2.98 (m, 1H, CH), 2.08–1.92 (m, 4H). ¹³C{¹H, ¹⁹F} NMR (101 MHz, CDCl₃) δ 162.6, 151.5, 150.6, 149.7, 148.5, 144.5, 141.8, 134.5, 126.0, 124.4, 121.6, 120.6, 111.8, 109.5 (CF₂), 98.1, 88.9, 66.1, 48.7, 45.1, 40.4, 29.3, 28.3, 26.4. HRMS (ESI/MS): m/z calculated for C₂₅H₂₄F₂N₈O₂ [M+H]⁺ 507.2063 found 507.2068.

2-(difluoromethyl)-1-[7-(morpholin-4-yl)-2-[4-(morpholin-4-yl)piperidine-1-carbonyl]pyrazolo[1,5-*a*]pyrimidin-5-yl]-1H-1,3-benzimidazole (**52**)

Compound **52** was prepared from **39** (1.50 g, 3.62 mmol), 4-morpholinopiperidine (0.68 g, 3.90 mmol), HATU (1.52 mg, 3.99 mmol), TEA (0.76 mL, 0.55 g, 5.44 mmol), and DCM (15.0 mL), according to the general procedure for the amidation reaction. The crude product was purified by flash chromatography (0–20% MeOH gradient in AcOEt) to give **52** (0.70 g, 1.23 mmol) as a light yellow solid with a 34% yield. ¹H NMR (400 MHz, DMSO-*d*₆) δ 7.90–7.88 (m, 1H, Ar-H), 7.83 (dd, $J = 7.2, 1.3$ Hz, 1H, Ar-H), 7.61 (t, $J = 52.5$ Hz, 1H, CHF₂), 7.49–7.44 (m, 2H), 6.85 (s, 1H, Ar-H), 6.82 (s, 1H, Ar-H), 4.21–4.65 (m, 2H, CH₂), 3.92 (d, $J = 3.3$ Hz, 5H), 3.86–3.84 (m, 5H), 3.66–3.61 (m, 4H, morph.), 3.15–3.07 (m, 4H, morph.), 2.86 (d, $J = 1.2$ Hz, 1H, CH), 1.78–2.06 (m, 2H, CH₂), 1.37–1.57 (m, 2H, CH₂). ¹³C{¹H, ¹⁹F} NMR (101 MHz, DMSO-*d*₆) δ 161.6, 151.2, 149.2, 147.8, 144.7, 141.2, 134.0, 125.5, 124.1, 120.7, 112.4, 108.5, 108.5, 89.3, 65.6, 48.7, 48.4, 45.7, 26.8, 8.6. HRMS (ESI/MS): m/z calculated for C₂₈H₃₂F₂N₈O₃ [M+H]⁺ 567.2638 found 567.2643.

1-[5-[2-(difluoromethyl)-1H-1,3-benzimidazol-1-yl]-7-(morpholin-4-yl)pyrazolo[1,5-*a*]pyrimidine-2-carbonyl]piperidin-4-ol (**53**)

Compound **53** was prepared from **39** (1.50 g, 3.62 mmol), 4-hydroxypiperidine (0.41 g, 4.06 mmol), HATU (1.52 mg, 3.99 mmol), TEA (0.76 mL, 0.55 g, 5.44 mmol), and DCM (15.0 mL), according to the general procedure for the amidation reaction. The crude product was purified by flash chromatography (0–15% MeOH gradient in AcOEt) to give **53** (0.86 g, 1.72 mmol) as a light yellow solid with a 48% yield. ¹H NMR (600 MHz, DMSO-*d*₆) δ 7.90–7.88 (m, 1H, Ar-H), 7.84–7.82 (m, 1H, Ar-H), 7.59 (t, $J = 52.5$ Hz, 1H, CHF₂), 7.49–7.43 (m, 2H, Ar-H), 6.83 (s, 1H, Ar-H), 6.81 (s, 1H, Ar-H), 4.83 (d, $J = 4.0$ Hz, 1H, OH), 4.08–4.03 (m, 2H, CH₂), 4.02–3.97 (m, 2H, CH₂), 3.93–3.92 (m, 4H, morph.), 3.85–3.84 (m, 4H, morph.), 3.81–3.77 (m, 1H, CH), 3.44–3.37 (m, 2H, CH₂), 3.32–3.28 (m, 2H, CH₂). ¹³C{¹H, ¹⁹F} NMR (151 MHz, DMSO-*d*₆) δ 162.0, 151.5, 150.9, 149.5, 148.0, 145.0, 141.5, 134.3, 125.8, 124.3, 121.0, 112.7, 108.8, 96.7, 89.5, 65.9, 65.7, 48.7, 44.3, 35.0, 34.2. HRMS (ESI/MS): m/z calculated for C₂₄H₂₅F₂N₇O₃ [M+H]⁺ 498.2059 found 498.2060.

N-(1-[5-[2-(difluoromethyl)-1H-1,3-benzimidazol-1-yl]-7-(morpholin-4-yl)pyrazolo[1,5-*a*]pyrimidine-2-carbonyl]piperidin-4-yl)acetamide (**54**)

Compound **54** was prepared from **39** (1.50 g, 3.62 mmol), 4-acetylaminopiperidine (0.57 g, 3.89 mmol), HATU (1.52 mg, 3.99 mmol), TEA (0.76 mL, 0.55 g, 5.44 mmol), and DCM (15.0 mL), according to the general procedure for amidation reaction. The crude product was purified by flash chromatography (0–20% MeOH gradient in AcOEt) to give **54** (0.80 g, 1.48 mmol) as a light yellow solid with a 41% yield. ¹H NMR (600 MHz, CDCl₃) δ 7.93–7.91 (m, 1H, Ar-H), 7.68–7.66 (m, 1H, Ar-H), 7.46–7.42 (m, 2H, Ar-H), 7.29 (t, $J = 54.0$ Hz, 1H, CHF₂), 6.87 (s, 1H, Ar-H), 6.44

(s, 1H, Ar-H), 5.55 (d, $J = 7.8$ Hz, 1H, NH), 4.74 (d, $J = 13.7$ Hz, 2H, CH₂), 4.43 (d, $J = 15.1$ Hz, 2H, CH₂ 4.13–4.07 (m, 1H, CH), 3.98–3.96 (m, 4H, morph.), 3.91–3.89 (m, 4H, morph.), 3.31–3.27 (m, 1H), 3.03–2.99 (m, 1H), 2.10–2.05 (m, 1H), 2.00 (s, 3H, CH₃), 1.55–1.40 (m, 1H). ¹³C{¹H, ¹⁹F} NMR (151 MHz, CDCl₃) δ 169.3, 162.6, 151.4, 150.9, 149.5, 148.3, 144.4, 141.7, 134.4, 125.8, 124.2, 121.5, 111.7, 109.4 (CF₂), 97.8, 88.6, 66.1, 48.6, 46.7, 45.9, 41.4, 32.9, 31.7, 23.3. HRMS (ESI/MS): m/z calculated for C₂₆H₂₈F₂N₈O₃ [M+H]⁺ 539.2352 found 539.2325.

2-(4-{5-[2-(difluoromethyl)-1H-1,3-benzimidazol-1-yl]-7-(morpholin-4-yl)pyrazolo[1,5-*a*]pyrimidine-2-carbonyl}piperazin-1-yl)-N-methylacetamide (**55**)

Compound **55** was prepared from **39** (1.50 g, 3.62 mmol), N-methyl-2-(1-piperazinyl)acetamide (0.65 g, 3.97 mmol), HATU (1.52 mg, 3.99 mmol), TEA (0.76 mL, 0.55 g, 5.44 mmol), and DCM (15.0 mL), according to the general procedure for the amidation reaction. The crude product was purified by flash chromatography (0–15% MeOH gradient in AcOEt) to give **55** (0.66 g, 1.18 mmol) as a light yellow solid with a 33% yield. ¹H NMR (600 MHz, DMSO-*d*₆) δ 7.89–7.88 (m, 1H, Ar-H), 7.83–7.82 (m, 1H, Ar-H), 7.79 (s, 1H, Ar-H), 7.59 (t, $J = 52.5$ Hz, 1H, CHF₂), 7.49–7.42 (m, 2H, Ar-H), 6.84 (s, 1H, Ar-H), 6.81 (s, 1H, Ar-H), 3.92–3.91 (m, 4H, morph.), 3.85–3.83 (m, 4H), 3.80–3.73 (m, 4H), 2.98 (s, 2H), 2.62 (d, $J = 4.7$ Hz, 3H, CH₃), 2.54 (s, 2H, CH₂), 1.09 (s, 2H, CH₂). ¹³C{¹H, ¹⁹F} NMR (151 MHz, DMSO-*d*₆) δ 161.6, 151.0, 150.1, 149.1, 147.6, 144.5, 141.1, 133.9, 125.4, 123.9, 120.6, 112.3, 108.4, 96.6, 89.2, 71.9, 65.4, 53.0, 52.4, 48.6, 48.3, 45.7, 26.6, 25.2. HRMS (ESI/MS): m/z calculated for C₂₆H₂₉F₂N₉O₃ [M+H]⁺ 554.2434 found 554.2434.

2-(difluoromethyl)-1-[2-(4-methylpiperazine-1-carbonyl)-7-(morpholin-4-yl)pyrazolo[1,5-*a*]pyrimidin-5-yl]-1H-1,3-benzimidazole (**56**)

Compound **56** was prepared from **39** (0.20 g, 0.48 mmol), 1-methylpiperazine (0.05 mL, 50.2 mg, 0.49 mmol), HATU (0.20 g, 0.52 mmol), TEA (0.09 mL, 72.2 mg, 0.71 mmol), and DCM (2.0 mL), according to the general procedure for the amidation reaction. The crude product was purified by flash chromatography (0–35% MeOH gradient in AcOEt) to give **56** (0.13 g, 0.27 mmol) as a white solid with a 57% yield. ¹H NMR (600 MHz, DMSO-*d*₆) δ 7.89 (m, 1H, Ar-H), 7.83–7.81 (m, 1H, Ar-H), 7.58 (t, $J = 52.4$ Hz, 1H, CHF₂), 7.49–7.42 (m, 2H, Ar-H), 6.83 (s, 1H, Ar-H), 6.81 (s, 1H, Ar-H), 3.92 (t, $J = 4.7$ Hz, 4H, morph.), 3.84 (t, $J = 4.7$ Hz, 4H, morph.), 3.76–3.69 (m, 4H, morph.), 2.43–2.37 (m, 4H, morph.), 2.23 (s, 3H, CH₃). ¹³C{¹H, ¹⁹F} NMR (151 MHz, DMSO-*d*₆) δ 161.7, 151.1, 150.3, 149.2, 147.7, 144.6, 141.2, 134.0, 125.5, 124.0, 120.6, 112.3, 108.5, 96.6, 89.2, 65.5, 54.8, 48.4, 46.5, 45.5, 41.7, 30.8. HRMS (ESI/MS): m/z calculated for C₂₄H₂₆F₂N₈O₂ [M+H]⁺ 497.2219 found 497.2229.

2-(difluoromethyl)-1-[7-(morpholin-4-yl)-2-[4-(propan-2-yl)piperazine-1-carbonyl]pyrazolo[1,5-*a*]pyrimidin-5-yl]-1H-1,3-benzimidazole (**57**)

Compound **57** was prepared from **39** (0.20 g, 0.48 mmol), 1-isopropylpiperazine (0.07 mL, 65.7 mg, 0.49 mmol), HATU (0.20 g, 0.52 mmol), TEA (0.09 mL, 72.2 mg, 0.71 mmol), and DCM (2.0 mL), according to the general procedure for the amidation reaction. The crude product was purified by flash chromatography (0–30% MeOH gradient in AcOEt) to give **57** (0.20 g, 0.38 mmol) as a white solid with a 81% yield. ¹H NMR (600 MHz, DMSO-*d*₆) δ 7.89–7.88 (m, 1H, Ar-H), 7.83–7.82 (m, 1H, Ar-H), 7.58 (t, $J = 52.5$ Hz, 1H, CHF₂), 7.49–7.42 (m, 2H, Ar-H), 6.83 (s, 1H, Ar-H), 6.80 (s, 1H, Ar-H), 3.93–3.91 (m, 4H, morph., morph.), 3.85–3.84 (m, 4H, morph.), 3.73–3.71 (m, 2H, CH₂), 3.67–3.66 (m, 2H, CH₂), 2.72–2.68 (m, 1H, CH), 2.53–2.50 (m, 2H, CH₂), 2.47 (d, $J = 4.8$ Hz, 2H, CH₂), 0.98 (d, $J = 6.6$ Hz, 6H, 2xCH₃). ¹³C NMR (151 MHz, DMSO-*d*₆) δ 161.6, 151.1, 150.4, 149.2, 147.7, 144.6, 141.2, 134.0, 125.5, 124.0, 120.6, 112.3, 108.4, 96.6, 89.2, 65.5, 53.6, 48.5, 48.4, 47.9, 47.0, 42.2, 18.0. HRMS (ESI/MS): m/z calculated for C₂₆H₃₀F₂N₈O₂ [M+H]⁺ 525.2532 found 525.2544.

3.2. Docking Study

The docking procedure was performed using the PI3K δ protein from the Protein Data Bank (PDB: 2WXL) with the Auto-Dock Vina program [40]. All figures with examples of 3D modeling of a possible binding mode of selected compounds were prepared based on the calculated pK_a from the Instant JChem 21.13.0 program [39]. More specifically, all structures depicted in the

respective figures have not had protons added, but the appropriate state of protonation has been maintained.

3.3. Biology

3.3.1. In Vitro PI3K Inhibition Assays

The potency and selectivity of compounds were assessed by measuring the ability of PI3K kinases to convert ATP to ADP during an enzymatic reaction in the presence of decreasing doses of tested compounds. The experiments were carried out using the ADP-Glo kinase assay kit (Promega), according to the manufacturer's protocol. PI3K α , PI3K β , PI3K δ , and PI3K γ have been purchased from Merck Millipore and phosphoinositol-4,5-bisphosphate (PIP2) lipid vesicles with phosphoserine from ThermoFisher Scientific were used as a substrate in the enzymatic reaction. The composition of the reaction mixture and reaction conditions for individual kinases are listed in the table below (Table 6).

Table 6. Reaction conditions and compositions of mixtures for individual kinases.

KINASE	Kinase Concentration [ng per Reaction]	Reaction Temperature and Time	Substrate PIP2 [Final Concentration μ M]	Reaction Buffer
PI3K α (Carna Biosciences)	7.5 ng	25 °C, 1 h	30 μ M	50 mM of HEPES pH 7.5 50 mM of NaCl 3 mM of MgCl ₂ 0.025 mg/mL of BSA
PI3K δ (Merck Millipore)	10 ng	25 °C, 1 h	30 μ M	50 mM of HEPES pH 7.5 50 mM of NaCl 3 mM of MgCl ₂ 0.025 mg/mL of BSA
PI3K β (Merck Millipore)	15 ng	30 °C, 1 h	50 μ M	50 mM of HEPES pH 7.5 50 mM of NaCl 3 mM of MgCl ₂ 0.025 mg/mL of BSA
PI3K α (Merck Millipore)	30 ng	30 °C, 1 h	50 μ M	40 nM of Tris pH 7.5 20 mM of MgCl ₂ 0.1 mg/mL of BSA 1 mM of DTT

After the reaction, the ADP-Glo reagent and the kinase detection reagent were added sequentially with 40 min of incubation (25 °C, 600 rpm) after adding each reagent. Finally, the luminescence intensity was measured and the IC₅₀ was calculated using GraphPad Prism 7 software. The presented results are the mean value of IC₅₀ from at least two independent experiments.

3.3.2. Influence of Selected Compounds on B Cells Proliferation

CD19 cells were isolated from PBMCs using magnetic beads (Stem Cell (Vancouver, Canada)) and then labeled with 2 μ M of CFSE (Invitrogen (Waltham, USA)).

Then, 1 \times 10⁵ cells were seeded on 96-well plates, activated by 2 μ g/mL of α IgM (Jackson ImmunoResearch (West Grove, USA)) and 1 μ g/mL of ODN2006 (InvivoGen (San Diego, USA)), and incubated with increasing concentrations of drugs (0.1, 0.3, 1.0, 3.3, 10, 33, 100, 333, 1000, 3333, and 10000 nM). After 4 days, cells were stained with LIVE/DEAD™ kit (Invitrogen (Waltham, USA)). Samples were acquired using Attune NxT flow cytometer (Invitrogen) and analyzed using FlowJo software. Each biological assay was performed with cells isolated from a different donor. The presented results constitute the average percentage values of proliferating cells from 3 independent experiments.

3.4. Metabolic Stability and Solubility

3.4.1. Metabolic Stability Assay

The metabolic phase I stability in mouse (CD-1TM) and human microsomes (Thermo-Fisher Scientific (Waltham, USA)) was assessed on 96-well non-binding plates (Greiner (Kremsmuster, Austria)) at a 1 μ M concentration for verapamil (positive control) and donepezil (negative control) and tested compounds. Unless otherwise stated, all chemicals and materials were ordered from Merck Life Science (Sheboygan, USA). Each biological replicate was prepared in triplicates [40-41]. Briefly, compounds were incubated in 100 mM potassium phosphate buffer with microsomes (0.5 mg/mL) and NADPH (1–1.2 mM) on a plate shaker (500 rpm) in the dark at 37 °C. On a 4 \times solution of NADPH, the cofactor for metabolic enzymes was prepared directly prior to the experiment by reducing NADP with G6P dehydrogenase (13.2 mM MgCl₂, 13.2 mM G6P, 5.2 mM NADP, 3.2 U/mL G6P dehydrogenase, 20 min at 30 °C, 500 rpm). The negative control contained buffer instead of NADPH solution. Samples were collected at 0, 10, 20, and 40 min or 0 and 40 min for the negative and double negative controls. The reaction was stopped by protein precipitation in 2 volumes of ice-cold MeOH with 200 nM of imipramine (as an internal standard for LC-MS analysis). Then, the extract was mixed (1 min, 1000 rpm), filtered through a 0.22 μ m filter on a 96-well plate vacuum manifold, and subjected to LC-MS analysis.

3.4.2. Lymphocyte B Proliferation Assessment

Human PBMCs were isolated from buffy coats of healthy donors obtained from the Regional Blood Donation and Blood Medicine Center in Warsaw. Lymphocytes B: CD19⁺ cells were isolated from PBMCs on magnetic beads (Stem Cell), labeled with 2 μ M CFSE (Invitrogen), and seeded on a 96-well plate (1 \times 10⁵ cells/well). B cells were activated by 2 μ g/mL of α IgM (Jackson ImmunoResearch) and 1 μ g/mL of ODN2006 (InvivoGen). Cells were incubated with increasing concentrations of compounds (range 0.03–10000 nM). After 4 days, B cells were stained with LIVE/DEADTM kit (Invitrogen), acquired using the Attune NxT flow cytometer (Invitrogen), and analyzed using FlowJo10 software. For data normalization, the percentage value of proliferating cells in each sample was divided by the average percentage value of positive control in a single experiment. IC₅₀ values were calculated using a three-parameter dose–response inhibition function in GraphPad Prism.

3.4.3. Kinetic Stability Assay

The kinetic solubility was determined using the shake-flask protocol [42-43]. The appropriate compounds (500 μ M) were incubated in an aqueous buffer (0.1 M phosphate-buffered saline pH 7.4) at 25 °C with stirring at 500 rpm. The samples were taken at the start time and after 24 h of incubation, filtered through 0.22 μ m filters, and diluted with 2 volumes of acetonitrile. Sample concentrations were determined by UHPLC-UV/Vis. A calibration curve was prepared in order to quantify the contents of the compound in the test solution.

4. Conclusions

A new family of substituted pyrazolo[1,5-*a*]pyrimidines was prepared in multi-step synthesis utilizing the Buchwald–Hartwig reaction or reductive amination as the crucial synthetic steps. The SAR studies were performed firstly at the C(5) position of the pyrazolo[1,5-*a*]pyrimidine and then the final optimization was turned up using a careful sterical amino group at the C(2) position adjustment. The biological activities were measured for each new compound against four PI3K isoforms: α , β , γ , and δ , providing comprehensive information on the selectivity of the obtained structures. Eleven compounds with an IC₅₀ value below the 100 nM threshold within the new compounds' library were synthesized in this work. Five of them, with an IC₅₀ value below or equal to 52 nM, were assumed as hits. Molecular modeling studies provide a rational explanation for the interaction of active structures within the PI3K δ ATP binding site. CPL302415 (1-[2-[(4-*tert*-butylpiperazin-1-yl)methyl]-7-(morpholin-4-yl)pyrazolo[1,5-*a*]pyrimidin-5-yl]-2-(difluoromethyl)-1*H*-benzimidazole, compound 6) proved to be the most potent structure with excellent activity (IC₅₀ = 18 nM), good selectivity

(PI3K α /PI3K δ = 79; PI3K β / δ = 1415; PI3K γ /PI3K δ = 939), and other promising parameters (Table 5). Therefore, CPL302415 was selected as a lead compound for toxicological studies and as a candidate for further development in phase I clinical trials in SLE treatment. More detailed biological and physicochemical studies and their outcomes are the subjects of a separate paper under preparation.

Supplementary Materials: The following supporting information can be downloaded at: www.mdpi.com/xxx/s1, 1H NMR, 13C NMR and HRMS supplementary figures of the final compounds 5-9, 11-12, 16-38, and 40-54.,

Author Contributions: Synthesis, M.S., M.Z., S.M., N.O., and M.D.; biological evaluation M.B., P.T., P.G., D.Z.-B., A.S., U.K., and B.Z.; analytical evaluation K.M., D.S., W.M., L.G.-B., and A.L.; investigation, M.S., M.Z., P.G., D.Z.-B., and B.Z.; writing—original draft preparation, M.S., M.Z., and S.M.; writing—review and editing, M.M., P.G., D.Z.-B., and Z.O.; visualization, W.P.; supervision, M.W. and Z.O.; project administration, M.Z., P.G., A.S., B.Z., K.D., J.P., M.W., and Z.O.; funding acquisition, M.W. All authors have read and agreed to the published version of the manuscript.

Funding: This research was co-financed by Celon Pharma S.A. and the National Centre for Research and Development “Narodowe Centrum Badan i Rozwoju”, project “KICHAI—Pre-clinical and clinical development of an innovative PI3 delta kinase inhibitor of as a candidate for the treatment of inflammatory disorders”, grant number POIR.01.02.00-00-0085/18.

Institutional Review Board Statement: Not applicable.

Informed Consent Statement: Not applicable.

Data Availability Statement: Data is contained within the article and supplementary material.

Acknowledgments: We would like to thank Aleksandra Świdorska (Celon Pharma S.A.) for NMR analyses and practical suggestions. This work was supported by The National Centre for Research and Development (POIR.01.01.01-00-1341/15) in Poland.

Conflicts of Interest: The authors declare the following financial interests/personal relationships which may be considered as potential competing interests. All contributors to this work at the time of their direct involvement in the project were the full-time employees of Celon Pharma S.A. A patent application WO 2016/157091 A1, based on the present observations, has been filed. M. Wiczorek is the CEO of Celon Pharma S.A. Some of the authors are the shareholders of Celon Pharma S.A. This work was financially supported by The National Centre for Research and Development (POIR.01.01.01-00-1341/15).

References

1. Saurat, T.; Buron, F.; Rodrigues, N.; de Tauzia, M.-L.; Colliandre, L.; Bourg, S.; Bonnet, P.; Guillaumet, G.; Akssira, M.; Corlu, A.; et al. Design, Synthesis, and Biological Activity of Pyridopyrimidine Scaffolds as Novel PI3K/MTOR Dual Inhibitors. *J. Med. Chem.* **2014**, *57*, 613–631. <https://doi.org/10.1021/jm401138v>.
2. Parker, P.J. The Ubiquitous Phosphoinositides. *Biochem. Soc. Trans.* **2004**, *32*, 893–898. <https://doi.org/10.1042/BST0320893>.
3. Engelman, J.A.; Luo, J.; Cantley, L.C. The Evolution of Phosphatidylinositol 3-Kinases as Regulators of Growth and Metabolism. *Nat. Rev. Genet.* **2006**, *7*, 606–619. <https://doi.org/10.1038/nrg1879>.
4. Foster, J.G.; Blunt, M.D.; Carter, E.; Ward, S.G. Inhibition of PI3K Signaling Spurs New Therapeutic Opportunities in Inflammatory/Autoimmune Diseases and Hematological Malignancies. *Pharmacol. Rev.* **2012**, *64*, 1027–1054. <https://doi.org/10.1124/pr.110.004051>.
5. Safina, B.S.; Baker, S.; Baumgardner, M.; Blaney, P.M.; Chan, B.K.; Chen, Y.-H.; Cartwright, M.W.; Castanedo, G.; Chabot, C.; Cheguillaume, A.J.; et al. Discovery of Novel PI3-Kinase δ Specific Inhibitors for the Treatment of Rheumatoid Arthritis: Taming CYP3A4 Time-Dependent Inhibition. *J. Med. Chem.* **2012**, *55*, 5887–5900. <https://doi.org/10.1021/jm3003747>.
6. Cantley, L.C. The Phosphoinositide 3-Kinase Pathway. *Science* **2002**, *296*, 1655–1657. <https://doi.org/10.1126/science.296.5573.1655>.
7. Liu, P.; Cheng, H.; Roberts, T.M.; Zhao, J.J. Targeting the Phosphoinositide 3-Kinase Pathway in Cancer. *Nat. Rev. Drug Discov.* **2009**, *8*, 627–644. <https://doi.org/10.1038/nrd2926>.
8. Cushing, T.D.; Metz, D.P.; Whittington, D.A.; McGee, L.R. PI3K δ and PI3K γ as Targets for Autoimmune and Inflammatory Diseases. *J. Med. Chem.* **2012**, *55*, 8559–8581. <https://doi.org/10.1021/jm300847w>.

9. Knight, Z.A.; Gonzalez, B.; Feldman, M.E.; Zunder, E.R.; Goldenberg, D.D.; Williams, O.; Loewith, R.; Stokoe, D.; Balla, A.; Toth, B.; et al. A Pharmacological Map of the PI3-K Family Defines a Role for P110 α in Insulin Signaling. *Cell* **2006**, *125*, 733–747. <https://doi.org/10.1016/j.cell.2006.03.035>.
10. Murray, J.M.; Sweeney, Z.K.; Chan, B.K.; Balazs, M.; Bradley, E.; Castanedo, G.; Chabot, C.; Chantry, D.; Flagella, M.; Goldstein, D.M.; et al. Potent and Highly Selective Benzimidazole Inhibitors of PI3-Kinase Delta. *J. Med. Chem.* **2012**, *55*, 7686–7695. <https://doi.org/10.1021/jm300717c>.
11. Berndt, A.; Miller, S.; Williams, O.; Le, D.D.; Houseman, B.T.; Pacold, J.I.; Gorrec, F.; Hon, W.-C.; Ren, P.; Liu, Y.; et al. Erratum: Corrigendum: The P110 δ Structure: Mechanisms for Selectivity and Potency of New PI(3)K Inhibitors. *Nat. Chem. Biol.* **2010**, *6*, 244–244. <https://doi.org/10.1038/nchembio0310-244b>.
12. Puri, K.D.; Gold, M.R. Selective Inhibitors of Phosphoinositide 3-Kinase Delta: Modulators of B-Cell Function with Potential for Treating Autoimmune Inflammatory Diseases and B-Cell Malignancies. *Front. Immunol.* **2012**, *3*, 256. <https://doi.org/10.3389/fimmu.2012.00256>.
13. Suárez-Fueyo, A.; Rojas, J.M.; Cariaga, A.E.; García, E.; Steiner, B.H.; Barber, D.F.; Puri, K.D.; Carrera, A.C. Inhibition of PI3K δ Reduces Kidney Infiltration by Macrophages and Ameliorates Systemic Lupus in the Mouse. *J. Immunol.* **2014**, *193*, 544–554. <https://doi.org/10.4049/jimmunol.1400350>.
14. Haselmayer, P.; Camps, M.; Muzerelle, M.; el Bawab, S.; Waltzinger, C.; Bruns, L.; Abla, N.; Polokoff, M.A.; Jond-Necand, C.; Gaudet, M.; et al. Characterization of Novel PI3K δ Inhibitors as Potential Therapeutics for SLE and Lupus Nephritis in Pre-Clinical Studies. *Front. Immunol.* **2014**, *5*, 1–15. <https://doi.org/10.3389/fimmu.2014.00233>.
15. Banham-Hall, E. The Therapeutic Potential for PI3K Inhibitors in Autoimmune Rheumatic Diseases. *Open Rheumatol. J.* **2012**, *6*, 245–258. <https://doi.org/10.2174/1874312901206010245>.
16. Stark, A.-K.; Srisankarajah, S.; Hessel, E.M.; Okkenhaug, K. PI3K Inhibitors in Inflammation, Autoimmunity and Cancer. *Curr. Opin. Pharmacol.* **2015**, *23*, 82–91. <https://doi.org/10.1016/j.coph.2015.05.017>.
17. Suárez-Fueyo, A.; Barber, D.F.; Martínez-Ara, J.; Zea-Mendoza, A.C.; Carrera, A.C. Enhanced Phosphoinositide 3-Kinase δ Activity Is a Frequent Event in Systemic Lupus Erythematosus That Confers Resistance to Activation-Induced T Cell Death. *J. Immunol.* **2011**, *187*, 2376–2385. <https://doi.org/10.4049/jimmunol.1101602>.
18. Haylock-Jacobs, S.; Comerford, I.; Bunting, M.; Kara, E.; Townley, S.; Klingler-Hoffmann, M.; Vanhaesebroeck, B.; Puri, K.D.; McColl, S.R. PI3K δ Drives the Pathogenesis of Experimental Autoimmune Encephalomyelitis by Inhibiting Effector T Cell Apoptosis and Promoting Th17 Differentiation. *J. Autoimmun.* **2011**, *36*, 278–287. <https://doi.org/10.1016/j.jaut.2011.02.006>.
19. Ambrosi, A.; Espinosa, A.; Wahren-Herlenius, M. IL-17: A New Actor in IFN-Driven Systemic Autoimmune Diseases. *Eur. J. Immunol.* **2012**, *42*, 2274–2284. <https://doi.org/10.1002/eji.201242653>.
20. Wang, Y.; Zhang, L.; Wei, P.; Zhang, H.; Liu, C. Inhibition of PI3K δ Improves Systemic Lupus in Mice. *Inflammation* **2014**, *37*, 978–983. <https://doi.org/10.1007/s10753-014-9818-0>.
21. Park, S.J.; Lee, K.S.; Kim, S.R.; Min, K.H.; Moon, H.; Lee, M.H.; Chung, C.R.; Han, H.J.; Puri, K.D.; Lee, Y.C. Phosphoinositide 3-Kinase Inhibitor Suppresses Interleukin-17 Expression in a Murine Asthma Model. *Eur. Respir. J.* **2010**, *36*, 1448–1459. <https://doi.org/10.1183/09031936.00106609>.
22. Soond, D.R.; Bjørge, E.; Moltu, K.; Dale, V.Q.; Patton, D.T.; Torgersen, K.M.; Galleway, F.; Twomey, B.; Clark, J.; Gaston, J.S.H.; et al. PI3K P110 δ Regulates T-Cell Cytokine Production during Primary and Secondary Immune Responses in Mice and Humans. *Blood* **2010**, *115*, 2203–2213. <https://doi.org/10.1182/blood-2009-07-232330>.
23. Perry, M.W.D.; Abdulai, R.; Mogemark, M.; Petersen, J.; Thomas, M.J.; Valastro, B.; Westin Eriksson, A. Evolution of PI3K γ and δ Inhibitors for Inflammatory and Autoimmune Diseases. *J. Med. Chem.* **2019**, *62*, 4783–4814. <https://doi.org/10.1021/acs.jmedchem.8b01298>.
24. Sutherlin, D.P.; Baker, S.; Bisconte, A.; Blaney, P.M.; Brown, A.; Chan, B.K.; Chantry, D.; Castanedo, G.; DePledge, P.; Goldsmith, P.; et al. Potent and Selective Inhibitors of PI3K δ : Obtaining Isoform Selectivity from the Affinity Pocket and Tryptophan Shelf. *Bioorganic Med. Chem. Lett.* **2012**, *22*, 4296–4302. <https://doi.org/10.1016/j.bmcl.2012.05.027>.
25. Stypik, M.; Zagozda, M.; Michałek, S.; Dymek, B.; Zdzalik-Bielecka, D.; Dziachan, M.; Orłowska, N.; Gunerka, P.; Turowski, P.; Hucz-Kalitowska, J.; et al. Design, synthesis, and Development of Pyrazolo [1,5-*a*]Pyrimidine Derivatives as a Novel Series of Selective PI3K δ Inhibitors. Part I–Indole Derivatives. *Pharmaceuticals* **2022**, *15*. Add doi when accepted.
26. Sutherlin, D.P.; Sampath, D.; Berry, M.; Castanedo, G.; Chang, Z.; Chuckowree, I.; Dotson, J.; Folkes, A.; Friedman, L.; Goldsmith, R.; et al. Discovery of (Thienopyrimidin-2-Yl)Aminopyrimidines as Potent, Selective, and Orally Available Pan-PI3-Kinase and Dual Pan-PI3-Kinase/MTOR Inhibitors for the Treatment of Cancer. *J. Med. Chem.* **2010**, *53*, 1086–1097. <https://doi.org/10.1021/jm901284w>.

27. Folkes, A.J.; Ahmadi, K.; Alderton, W.K.; Alix, S.; Baker, S.J.; Box, G.; Chuckowree, I.S.; Clarke, P.A.; Depledge, P.; Eccles, S.A.; et al. The Identification of 2-(1*H*-Indazol-4-yl)-6-(4-Methanesulfonyl-Piperazin-1-ylmethyl)-4-Morpholin-4-yl-Thieno [3,2-*d*]Pyrimidine (GDC-0941) as a Potent, Selective, Orally Bioavailable Inhibitor of Class I PI3 Kinase for the Treatment of Cancer. *J. Med. Chem.* **2008**, *51*, 5522–5532. <https://doi.org/10.1021/jm800295d>.
28. Chiang, P.-C.; Sutherland, D.; Pang, J.; Salphati, L. Investigation of Dose-Dependent Factors Limiting Oral Bioavailability: Case Study with the PI3K- δ Inhibitor. *J. Pharm. Sci.* **2016**, *105*, 1802–1809. <https://doi.org/10.1016/j.xphs.2016.04.003>.
29. Guo, J.; Pei, Y.; Lang, H. Pyrimidine Derivative, Cytotoxic Agent, Pharmaceutical Composition and Use Thereof. WO Patent 2016127455, 18 August 2016.
30. Samby, K.; Surase, Y.; Amale, S.; Gorla, S.; Patel, P.; Verma, A. 6-Morpholinyl-2-Pyrazolyl-9h-Purine Derivatives and Their Use as Pi3k Inhibitors. WO Patent 2016157074, 29 March 2016.
31. Dymek, B.; Zagozda, M.; Wieczorek, M.; Dubiel, K.; Stańczak, A.; Zdżalik, D.; Gunerka, P.; Sekular, M.; Dziachan, M. 7-(Morpholin-4-yl)Pyrazole [1,5-*a*]Pyrimidine Derivatives Which are Useful for the Treatment of Immune or Inflammatory Diseases or Cancer. WO Patent 2016157091, 6 October 2016.
32. Brown, D.; Matthews, D. (Alpha-Substituted Aralkylamino and Heteroarylalkylamino) Pyrimidinyl and 1,3,5-Triazinyl Benzimidazoles, Pharmaceutical Compositions Containing Them, and These Compounds for Use in Treating Proliferative Diseases. WO Patent 2012135160, 27 March 2012.
33. Brown, D.; Matthews, D. (Fused Ring Arylamino and Heterocyclylamino) Pyrimidinyl and 1,3,5-Triazinyl Benzimidazoles, Pharmaceutical Compositions Thereof, and Their Use in Treating Proliferative Diseases. WO Patent 2012135166, 4 October 2012.
34. Brown, D.; Matthews, D. (Alpha-Substituted Cycloalkylamino and Heterocyclylamino) Pyrimidinyl and 1,3,5-Triazinyl Benzimidazoles, Pharmaceutical Compositions Thereof, and Their Use in Treating Proliferative Diseases. WO Patent 2012135175, 4 October 2012.
35. Hassan, A.S. Synthesis, Characterization, and Cytotoxicity of Some New 5-Aminopyrazole and Pyrazolo[1,5-*a*]Pyrimidine Derivatives. *Scientia Pharmaceutica* **2015**, *83*, 27–39, doi:10.3797/scipharm.1409-14.
36. Al-Azmi, A. Pyrazolo[1,5-*a*]Pyrimidines: A Close Look into Their Synthesis and Applications. *Current Organic Chemistry* **2019**, *23*, 721–743, doi:10.2174/1385272823666190410145238.
37. <https://chemaxon.com/products/instant-jchem> accessed: May 31 2022.
38. Riley, R.J.; McGinnity, D.F.; Austin, R.P. A unified model for predicting human hepatic, metabolic clearance from in vitro intrinsic clearance data in hepatocytes and microsomes. *Drug Metabolism and Disposition* **2005**, *33*, 1304–1311, doi:10.1124/dmd.105.004259.
39. García-Pérez, D.; López, C.; Claramunt, R.; Alkorta, I.; Elguero, J. 19F-NMR Diastereotopic Signals in Two N-CHF₂ Derivatives of (4*S*,7*R*)-7,8,8-Trimethyl-4,5,6,7-Tetrahydro-4,7-Methano-2*H*-Indazole. *Molecules* **2017**, *22*, 2003, doi:10.3390/molecules22112003.
- 37 Trott, O.; Olson, A.J. AutoDock Vina: Improving the Speed and Accuracy of Docking with a New Scoring Function, Efficient Optimization, and Multithreading. *Journal of Computational Chemistry* **2009**, NA-NA, doi:10.1002/jcc.21334.
40. <https://chemaxon.com/products/instant-jchem> accessed: May 31 2022 Sugano, K.; Okazaki, A.; Sugimoto, S.; Tavornvipas, S.; Omura, A.; Mano, T. Solubility and Dissolution Profile Assessment in Drug Discovery. *Drug Metab. Pharmacokinet.* **2007**, *22*, 225–254. <https://doi.org/10.2133/dmpk.22.225>.
41. Guha, R.; Dexheimer, T.S.; Kestranek, A.N.; Jadhav, A.; Chervenak, A.M.; Ford, M.G.; Simeonov, A.; Roth, G.P.; Thomas, C.J. Exploratory Analysis of Kinetic Solubility Measurements of a Small Molecule Library. *Bioorganic Med. Chem.* **2011**, *19*, 4127–4134. <https://doi.org/10.1016/j.bmc.2011.05.005>.

12.3. Publikacja 3 – P3

Article

Tuning the Biological Activity of PI3K δ Inhibitor by the Introduction of a Fluorine Atom Using the Computational Workflow

Wojciech Pietruś^{1,2,*}, Mariola Stypik^{2,3}, Marcin Zagozda², Martyna Banach², Lidia Gurba-Bryśkiewicz²,
Wioleta Maruszak², Arkadiusz Leniak², Rafał Kurczab^{1,*}, Zbigniew Ochal³, Krzysztof Dubiel²
and Maciej Wieczorek²

Citation: Pietruś, W.; Stypik, M.; Zagozda, M.; Banach, M.; Gurba-Bryśkiewicz, L.; Maruszak, W.; Leniak, A.; Kurczab, R.; Ochal, Z.; Dubiel, K.; Wieczorek, M. Tuning the Biological Activity of PI3K δ Inhibitor by the Introduction of a Fluorine Atom Using the Computational Workflow. *Molecules* **2023**, *12*, x.

<https://doi.org/10.3390/xxxxx>

Academic Editor: Elisa Nuti

Received: date

Revised: date

Accepted: date

Published: date



Copyright: © 2023 by the authors.

Submitted for possible open access publication under the terms and conditions of the Creative Commons Attribution (CC BY) license (<https://creativecommons.org/licenses/by/4.0/>).

¹ Department of Medicinal Chemistry, Maj Institute of Pharmacology, Polish Academy of Sciences,

Smetna 12, 31-343 Krakow, Poland

² Celon Pharma S.A., ul. Marymoncka 15, 05-152 Kazuń Nowy, Poland;

mariola.stypik@celonpharma.com (M.S.); marcin.zagozda@celonpharma.com (M.Z.); martyna.banach@celonpharma.com (M.B.); lidia.gurba@celonpharma.com (L.G.-B.); wioleta.maruszak@celonpharma.com (W.M.); arkadiusz.leniak@celonpharma.com (A.L.); krzysztof.dubiel@celonpharma.com (K.D.); maciej.wieczorek@celonpharma.com (M.W.)

³ Faculty of Chemistry, Warsaw University of Technology, ul. Nowakowskiego 3, 00-664 Warsaw, Poland; zbigniew.ochal@pw.edu.pl

* Correspondence: pietrus@if-pan.krakow.pl (W.P.); kurczab@if-pan.krakow.pl (R.K.); Tel.: +48-126-62-3301 (R.K.)

Abstract: As a member of the class I PI3K family, phosphoinositide 3-kinase δ (PI3K δ) is an important signaling biomolecule that controls immune cell differentiation, proliferation, migration, and survival. It also represents a potential and promising therapeutic approach for the management of numerous inflammatory and autoimmune diseases. We designed and assessed the biological activity of new fluorinated analogues of CPL302415, taking into account the therapeutic potential of our selective PI3K inhibitor and fluorine introduction as one of the most frequently used modifications of a lead compound to further improve its biological activity. In this paper, we compare and evaluate the accuracy of our previously described and validated in silico workflow with that of the standard (rigid) molecular docking approach. The findings demonstrated that a properly fitted catalytic (binding) pocket for our chemical cores at the induced-fit docking (IFD) and molecular dynamics (MD) stages, along with QM-derived atomic charges, can be used for activity prediction to better distinguish between active and inactive molecules. Moreover, the standard approach seems to be insufficient to score the halogenated derivatives due to the fixed atomic charges, which do not consider the response and inductive effects caused by fluorine. The proposed computational workflow provides a computational tool for the rational design of novel halogenated drugs.

Keywords: PI3K δ ; asthma; CPL302415; induced-fit docking; QPLD; MD; fluorine; MM-GBSA; molecular docking

1. Introduction

The inhibition of phosphoinositide 3-kinase (PI3K), especially the first class of this family of lipid kinases consisting of α , β , γ , and δ subunits, is a promising approach for the treatment of many inflammatory and autoimmune diseases, such as systemic lupus erythematosus or multiple sclerosis [1–3]. Because PI3K is involved in many cellular processes, including proliferation, growth, migration, metabolism regulation, and embryogenesis (characterized by high expression of this protein in different human cells), it is considered an excellent therapeutic target [4,5].

Fluorine, which is slightly larger than hydrogen and highly electronegative, constitutes a remarkable role in medicinal chemistry [6–11]. Currently, fluorination is a standard strategy to improve the bioavailability of designed drugs and optimize their biological activity [12]. In the last decade, nearly 30% of the drugs approved by the US Food and Drug Administration (FDA) contained fluorine, and fluorinated pharmaceuticals accounted for over 50% of the most profitable drugs worldwide [6,13].

Molecular modeling methods, such as molecular docking, molecular dynamics (MD), or free-energy perturbation, are widely applied during the rational designing of new compounds to evaluate the formation of ligand–receptor complexes [14]. However, the standard (rigid) docking method has two main limitations: (i) the conformation space is reduced due to the limitations imposed on the system (rigid receptor) and (ii) conventional scoring functions do not consider inductive or resonance effects (which is extremely important for fluorine derivatives). Nevertheless, this method can be successfully used to quickly score poses and find promising hits from a large library of compounds [15,16]. Recently, we proposed a method that can overcome some limitations of the standard molecular docking approach [7,9]. We demonstrated that a workflow comprising a combination of more sophisticated methods, such as induced-fit docking (IFD), quantum polarized ligand docking (QPLD), and binding-free energy calculations based on the Generalized Born Surface Area (GBSA), is more accurate in the prediction of the ligand–receptor complex and its energy than the standard docking procedure, but it is more computationally expensive [17].

In this work, we used the previously described *in silico* workflow [7,9] to design and determine the biological activity of new fluorinated analogs of CPL302415 (Figure 1), a PI3K δ inhibitor. The usefulness of this workflow was validated by correlating the biological activity (IC₅₀) with energy changes calculated in the GBSA model.

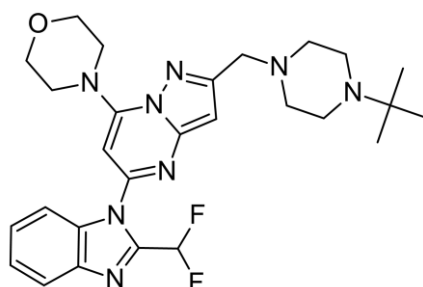


Figure 1. Structure of CPL302415.

2. Results and Discussion

Molecular docking of CPL302415 derivatives was performed on the previously described PI3K δ crystal structure (PDB ID: 2WXL). The binding mode observed for CPL302415 (**2**) was consistent with the previously reported ones [18,19] (Figure 2). The nitrogen of the (difluoromethyl)-1*H*-benzimidazole fragment interacted with the positively charged Lys779, while the morpholine ring at position 7 (which is required for interaction with PI3K δ at its catalytic site) formed a hydrogen bond with the main chain of Val828. The *tert*-butyl piperazine moiety bound to the Trp760 shelf through C-H $\cdots\pi$ /cation $\cdots\pi$ interaction (Figure 2).

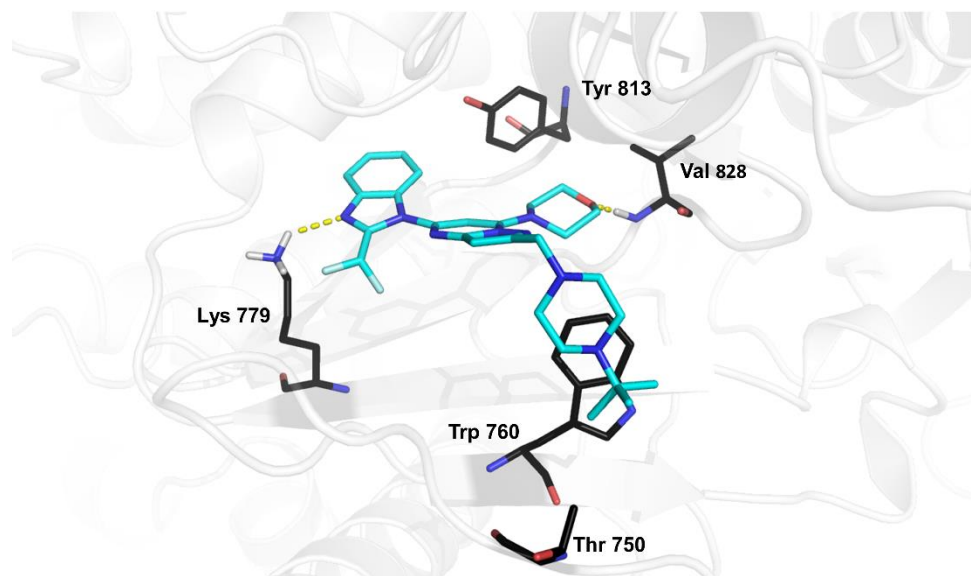


Figure 2. Illustration of the binding mode of CPL302415 (**2**) in the catalytic center of PI3K δ obtained by molecular docking [19].

According to molecular docking, the static nature of biomolecules is the main source of their limitations, as it does not consider the dynamic nature of biological structures [20]. The analysis of the structure–activity relationship (SAR) of our library revealed that the change from the difluoro group (**2**) to the methyl group (**1**) caused a decrease in the activity of the compound, but the introduction of the trifluoromethyl group (**3**) almost inactivated the compound (Table 1). Interestingly, the docking scores of the above-mentioned derivatives indicated that compound **1** should have the highest IC₅₀ value (Table 1) in the series—even if we took into account the average docking score for the top three poses, the tendency was almost identical. We substituted position 3 with chlorine (**4**) or bromine (**5**) and the resulting compounds were the most potent based on docking scores (Table 1), but they had worse IC₅₀ values than compound **2**.

To assess the accuracy of the presented method, correlation coefficients between the IC₅₀ values and the obtained docking scores were calculated (for the first pose and the average of the first three poses, respectively). The tests showed that there was no correlation (0.53; $p > 0.05$, and 0.51; $p > 0.05$).

Table 1. Influence of the fluorine atom(s) on PI3K δ inhibition and the respective docking scores for each derivative.

Compound	R ¹	R ²	IC ₅₀ PI3K δ (nM) ^a	Docking score	
				First Pose	Average of Top Three Poses
1	CH ₃	H	236	-9.3	-8.8
2 (CPL302415)	CHF ₂	H	18	-9.9	-9.8
3	CF ₃	H	907	-9.6	-9.3
4	CHF ₂	Cl	44	-10.4	-10.1
5	CHF ₂	Br	50	-10.5	-10.1

^a IC₅₀ values were determined as the mean from two independent experiments.

Based on the binding mode of CPL302415 (**2**), we decided to substitute *tert*-butyl moiety with a benzyl fragment to increase the number of π - π or hydrophobic interactions with Thr750. Therefore, a series of fluorine derivatives were synthesized using the 7-(morpholin-4-yl)pyrazolo[1,5-*a*]pyrimidin-5-yl]-2-(difluoromethyl)-1*H*-benzimidazole core (**6-9**) as well as with an additional carbonyl group in the 1-[2-(4-benzylpiperazine-1-carbonyl) fragment (substituent in position 2 of the pyrazolo[1,5-*a*]pyrimidine core) (**10-13**) (Table 2). We docked both nonfluorinated (in the aromatic ring) cores with benzyl fragment compounds to the 2WXL crystal structure, and the observed binding modes were similar to those of CPL302415. However, the hydrogen bonds formed by the morpholine fragment in compound **10** with Val828 were characterized by the worst geometric parameters in comparison to compound **6** (Figure 3), which could be associated with the lower activity of compound **10** (Table 2).

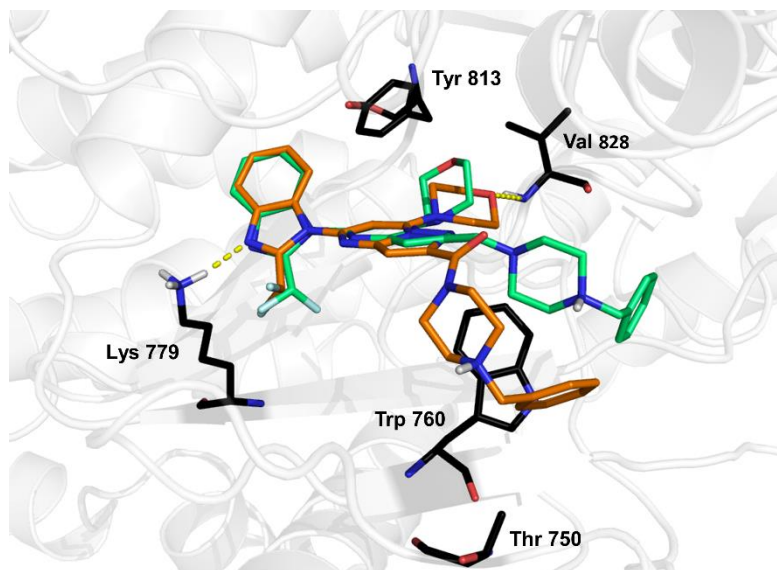
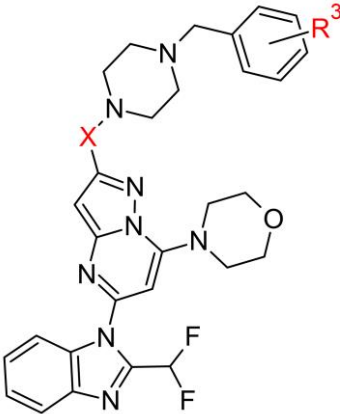


Figure 3. Illustration of the binding modes of compounds **6** (green) and **10** (orange) in the catalytic center of PI3K δ obtained by molecular docking.

Table 2. Influence of the fluorine atom(s) on PI3K δ inhibition and the respective docking scores for each compound.



Compound	X	R ³	IC ₅₀ PI3K δ (nM) ^a	Docking score	
				First Pose	Average of Top Three Poses
6	CH ₂	-	118	-6.8	-6.4
7	CH ₂	<i>o</i> -F	640	-10.8	-10.4
8	CH ₂	<i>m</i> -F	751	-9.0	-8.3
9	CH ₂	<i>p</i> -F	489	-9.2	-8.1
10	CO	-	275	-10.1	-9.1
11	CO	<i>o</i> -F	212	-10.3	-9.3
12	CO	<i>m</i> -F	92	-10.9	-10.8
13	CO	<i>p</i> -F	181	-10.5	-10.1

^aIC₅₀ values were determined as the mean from two independent experiments.

The carbonyl group affected the orientation of the benzylpiperazine fragment, causing a change in the cation $\cdots\pi$ interaction with Trp760 (Figure 3). The analysis of the IC₅₀ values did not allow us to draw any conclusions because in the first series of derivatives (**6–9**), the *meta*-fluoro derivative **8** had the highest IC₅₀ value, while in the second series (**10–13**), the *meta*-fluoro derivative **12** was the best (Table 2), which suggested that carbonyl oxygen had an impact on binding. Interestingly, we found a poor correlation between any docking score (nor the first best and the best three poses) and biological activity (IC₅₀) (correlation coefficients were -0.02 and 0.03, respectively).

Due to the low correlation of the docking scores obtained in the standard molecular docking approach (Tables 1 and 2) with biological activity, a previously described and validated computational workflow [7,9] was used to compensate for the limitations of conventional scoring functions and increase the accuracy of the pose prediction, especially for fluorinated derivatives (Figure 4). Because fluorine is the most electronegative element, its substitution leads to significant changes in the distribution of electron density and as a consequence, resonance and inductive effects. The standard molecular docking approach does not consider these effects, while the QPLD method uses atomic charges of a ligand calculated using the quantum mechanical (QM)/molecular mechanical (MM) approach in the protein environment for docking (Figure 4). To minimize the uncertainty of predicted poses, the binding-free energy was calculated for three poses obtained at the QPLD stage with the smallest root square mean deviation (RMSD) to the core. The energy change ($\Delta\Delta G$) after fluorination was estimated in comparison to the nonfluorinated compound (Figure 4). Additionally, by using the MD of a nonfluorinated compound, our approach enabled us to relax the binding pocket and fit it into the particular core. Due to its small size [6,21], we assumed that the introduction of a fluorine atom would not result in large conformational changes.

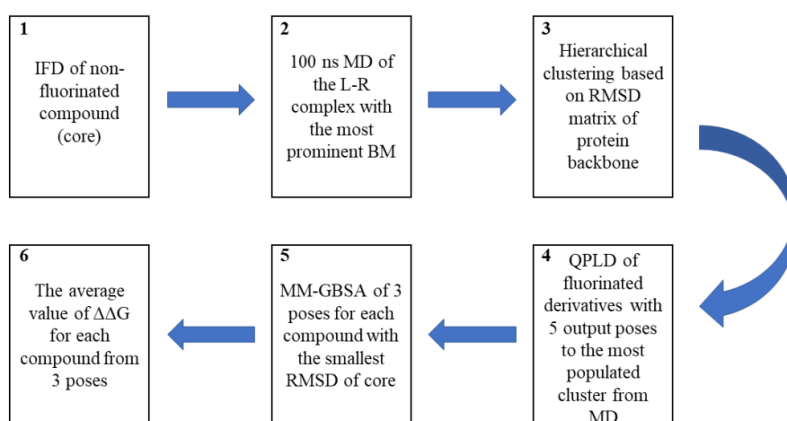


Figure 4. Computational workflow used to predict the most potent fluorine derivative. The workflow began with the IFD of a nonfluorinated compound (core) (1) followed by 100 ns-long MD simulations (2), which were then clustered based on the RMSD matrix of the protein backbone (3). All derivatives were docked to the three most frequently observed conformations of the protein using the QPLD algorithm (4). Using the MM-GBSA approach, the binding energy (ΔG) was calculated for the three conformations of the ligand with the smallest RMSD of the core to nonfluorinated compounds (5). Finally, the difference in the interaction energy between the most active compound and subsequent isomers ($\Delta\Delta G$) was calculated (6).

Analysis of the MD trajectories showed that the previously described binding mode [19] and the formed interactions were highly stable (Figure 5). We found that Lys779 involved in a hydrogen bond with benzimidazole nitrogen and tryptophane, which interacted with the positively charged nitrogen of the piperazine group, had high stability and a permanent position. Additionally, Tyr813 was engaged in a weak hydrogen bond with the CH donor (Figure 5). The substitution of the *tert*-butyl fragment with the benzyl fragment allowed an additional C–H $\cdots\pi$ /hydrophobic interaction with Thr750.

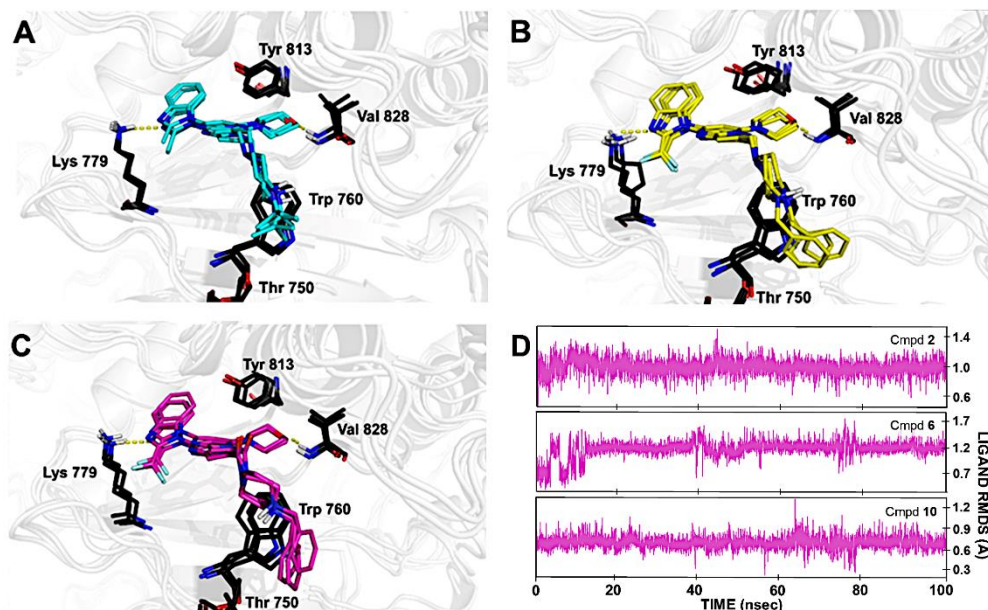


Figure 5. Superposition of the binding modes of core (A) *tert*-butyl piperazine (cyan), (B) benzylpiperazine (yellow), and (C) 4-benzylpiperazine-1-carbonyl (magenta) in the PI3K δ catalytic sites. The selected complexes were the most populated conformations resulting from the clustering of the MD trajectories. The RMSD (\AA) of compounds 2, 6, and 10, respectively, during MD simulations (D) indicates the stability of the ligand with respect to the protein and its binding pocket. Ligand RMSD is a measure of the internal fluctuations of ligand atoms.

The comparison of the first top pose for each compound in the series obtained by applying the standard approach showed that the 7-(morpholin-4-yl)pyrazolo[1,5-*a*]pyrimidin-5-yl]-2-(difluoromethyl)-1*H*-benzimidazole core had less mobility, whereas the *tert*-butyl 1-[2-[(4-*tert*-butylpiperazin-1-yl)] and 1-[2-(4-benzylpiperazine-1-carbonyl)] fragment was directed toward the solvent space, and thus had higher flexibility (Figure 6, I). Since fluorine is a bioisostere of hydrogen [6,8], the substitution of this element should not lead to drastic changes in the binding mode. The comparison of the observed binding modes showed that there was no coherence (Figure 6, I) and that small molecular changes highly affected the position of adjacent fragments of molecules. The results obtained using different methods of atomic charge assignment are clearly different (Figure 6, I and II). Compared to standard docking, in which the *tert*-butyl piperazine or benzylpiperazine fragment resulted in high flexibility and mobility (Figure 6, I), the binding poses obtained by the proposed workflow (where the atomic charges are QM-derived) showed lower RMSD (less than 0.5 Å; Figure 6, II). In the case of the QPLD-docked poses, the introduced fluorine atom did not induce any drastic conformational changes (Figure 6, II). However, due to its high electronegativity, this element may affect the tuning of atomic charges, p*K*_a, and the basicity or acidity (electron density distribution in general) of neighboring functional groups, rather than intermolecular interactions with the biological target [6].

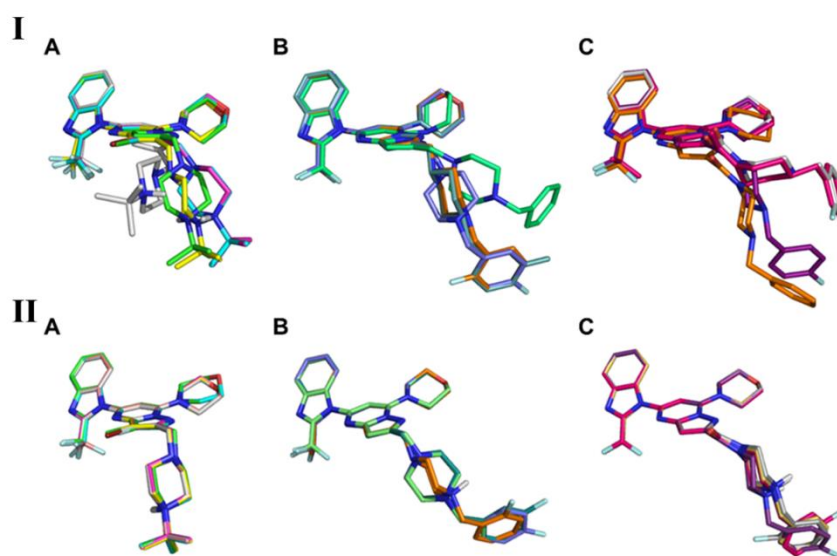


Figure 6. Comparison of the binding mode coherence of core (A) *tert*-butyl piperazine, (B) benzylpiperazine, and (C) 4-benzylpiperazine-1-carbonyl obtained using the standard (rigid) molecular docking approach (I) and the proposed in silico workflow (II).

Using the MM-GBSA approach, the interaction energy of the obtained ligand–receptor complex was calculated as the average of the top three ligand poses ($\overline{\Delta G}$) (Tabs. 3 and 4). The correlation coefficient of the biological activity (IC₅₀) and the MM-GBSA scores of the *tert*-butyl piperazine derivatives was significantly higher with the use of our approach compared to standard docking scores (0.95; $p < 0.05$ and ~ 0.5 , respectively) (Table 3). The results obtained for the *tert*-butyl piperazine derivatives showed that the introduction of a difluoro group to the 2-methyl-1*H*-benzimidazole fragment increased the stabilization energy of the complex ($\Delta\Delta G = -7.6$), whereas a trifluoro group decreased the stability of complexes, which was probably due to steric hindrances and inductive effects (Table 3). Moreover, as shown by Kurczab et al. [22], the MM-GBSA approach can be successfully used for heavier halogens. Therefore, we extended our library with derivatives containing bromine or chlorine at position 3. These derivatives were less active, but the proposed algorithm accurately predicted the energy loss for the difluoromethyl-1*H*-benzimidazole derivative (Table 3).

Table 3. Influence of the fluorine atom(s) on PI3K δ inhibition and the respective ΔG and $\Delta\Delta G$ ^a scores for each compound.

Compound	R ¹	R ²	IC ₅₀ PI3Kδ (nM) ^b	$\overline{\Delta G}$ (kcal/mol)	$\Delta\Delta G$ (kcal/mol)
1	CH ₃	H	236	-75.0	–
2 (CPL302415)	CHF ₂	H	18	-82.6	-7.6
3	CF ₃	H	907	-69.6	5.4
4	CHF ₂	Cl	44	-81.3	1.3 ^c
5	CHF ₂	Br	50	-81.2	1.4 ^c

^aThe interaction energy gain averaged by three ligand–receptor complexes of each derivative selected from the MD simulations. ^bIC₅₀ values were determined as the mean from two independent experiments. ^c $\Delta\Delta G$ values calculated as a difference between a given derivative and its nonhalogenated (difluoromethyl)-1*H*-benzimidazole analog.

For 4-benzylpiperazine and 4-benzylpiperazine-1-carbonyl fluorine derivatives, the correlation coefficient was almost equal to 1 (0.9; $p < 0.05$ and 0.95; $p < 0.05$, respectively), which implies that although there was no correlation with the docking scores, we obtained a perfect correlation here (Table 4).

Table 4. Influence of the fluorine atom(s) on PI3Kδ inhibition and the respective ΔG and $\Delta\Delta G$ ^a scores for each compound.

Compound	X	R ³	IC ₅₀ PI3Kδ (nM) ^b	$\overline{\Delta G}$ (kcal/mol)	$\Delta\Delta G$ (kcal/mol)
6	CH ₂	–	118	-86.7	–
7	CH ₂	<i>o</i> -F	640	-83.4	3.3
8	CH ₂	<i>m</i> -F	751	-81.8	4.9
9	CH ₂	<i>p</i> -F	489	-84.1	2.6
10	CO	–	275	-78.9	–
11	CO	<i>o</i> -F	212	-83.8	-4.9
12	CO	<i>m</i> -F	92	-86.6	-7.7
13	CO	<i>p</i> -F	181	-83.8	-4.9

^aThe interaction energy gain averaged by three ligand–receptor complexes of each derivative selected from the MD simulations. ^bIC₅₀ values were determined as the mean from two independent experiments.

In addition, to demonstrate the superiority of the proposed workflow, the QPLD docking protocol was performed on every stage of kinase flexibility: (i) on rigid crystalized PI3Kδ structure (PDB ID: 2WXL) and (ii) on the induced-fit docked poses chosen for the MD stage. The molecular dynamics were the most time-consuming step; therefore, if, thanks to QM-derived atomic charges (which could help obtain a more accurate ligand–receptor interaction energy), a higher correlation of IC₅₀ values with ΔG values in the previous stages could be achieved, the computational time could be saved compared to the presented workflow. In the same way as in the presented workflow, using the MM-GBSA approach, the interaction energy of the obtained ligand–receptor complex was calculated as the average of the top three ligand poses ($\overline{\Delta G}$) (SI Tables S1–S4). For the rigid conformation of the catalytic pocket, the correlation coefficients of the biological activity (IC₅₀) and the MM-GBSA score of *tert*-butyl piperazine derivatives were slightly lower (-0.34 ; $p > 0.05$) compared to the standard docking scores (~ 0.5) and proposed workflow (0.95) (SI Table S1). The correlation coefficients for 4-benzylpiperazine (-0.43 ; $p > 0.05$) and 4-benzylpiperazine-1-carbonyl fluorine derivatives (-0.78 ; $p > 0.05$) were better than this obtained with the standard (rigid) approach (~ 0.0) but lower than those obtained with our workflow (~ 0.93). Next, the QPLD approach was used on grids obtained in the IFD protocol for compounds **1**, **6**, and **10**. The correlation coefficient for *tert*-butyl piperazine derivatives was similar (-0.35 ; $p > 0.05$) to that obtained with a rigid catalytic pocket (-0.34), whereas the correlation was better for 4-benzylpiperazine (0.60; $p > 0.05$) and 4-benzylpiperazine-1-carbonyl fluorine derivatives (-0.78 ; $p > 0.05$) compared to those obtained with the non-flexible structure of PI3Kδ (-0.43 ; -0.78 , respectively). Nevertheless, the correlation coefficient obtained with the described workflow was higher (~ 0.93), which confirms the importance of all stages in the proposed workflow.

It is worth stressing that the correlation of IC₅₀ values with ΔG values increases with greater flexibility of the catalytic pocket and its fit to the molecular core. These results suggest that properly prepared catalytic pockets for chemical cores in the IFD and MD stages, combined with QM-derived atomic charges, can be effectively used for prediction as well as to improve the discrimination of active compounds from inactive ones.

3. Materials and Methods

3.1. Chemistry

The compounds **1–14** discussed in this work were synthesized following the general procedures presented in our previous papers [19,23]. The synthesis pathway has multiple steps, of which the last one is described here. The final compounds were synthesized via reactions such as reductive amination, amidation, or coupling reactions including the Buchwald–Hartwig reaction, and their yields varied depending on the structure. The Buchwald–Hartwig reaction, amidation reaction, and reductive amination are especially described in this work.

3.2. General Information

The reagents (at least 95% purity) were purchased from ABCR (Dallas, TX, USA), Acros (Geel, Belgium), Alfa Aesar (Haverhill, MA, USA), Combi-Blocks (San Diego, CA, USA), Fluorochem (Hadfield, UK), (Buchs, Switzerland), Merck (Darmstadt, Germany), and Sigma Aldrich (Saint Louis, MI, USA) and were used without additional purification. Solvents were purified according to the standard procedures if required. Air- or moisture-sensitive reactions were carried out under an argon atmosphere. The progress of all reactions was routinely monitored by thin-layer chromatography (TLC). TLC was performed on silica gel-coated plates (Kieselgel F254), which were visualized using a UV light. Flash chromatography was performed on Merck silica gel 60 (230–400 mesh ASTM). ¹H NMR spectra were acquired using JOEL JNMR-ECZS 400 and 600 MHz spectrometers (¹H observed at 400, and 600 MHz, respectively). ¹³C NMR spectra were recorded at 101 and 151 MHz, respectively. Due to the poor solubility of some final compounds, the usual characterization using ¹³C NMR was omitted. Chemical shifts for ¹H and ¹³C NMR spectra were reported in *d* (ppm) using tetramethylsilane as an internal standard or based on the residual undeuterated solvent signal (2.50 ppm for DMSO-*d*₆ and 7.26 ppm for CDCl₃). The abbreviations for multiplets of ¹H signals are as follows: s (singlet), d (doublet), t (triplet), m (multiplet), dd (doublet of doublets), dt (doublet of triplet), and q (quartet). Coupling constants (J) are expressed in Hertz. A JEOL Royal HFX probe head was used for recording the ¹³C NMR spectrum as it allows measurements to be taken with the simultaneous decoupling of both ¹H and ¹⁹F nuclei [24]. Atmospheric pressure ionization and electrospray ionization mass spectra were obtained using an Agilent 6130 LC/MSD spectrometer or Agilent 1290 UHPLC system coupled with an Agilent QTOF 6545 mass spectrometer. All spectra of the final compounds are shown in the Supplementary Materials.

3.3. Synthesis

Compounds **1** and **2** were synthesized according to the procedures described in our previous publications [19,23].

3.3.1. General Procedure for the Buchwald–Hartwig Reaction

To a pressure, microwave vessel, 5-chloro-pyrazolo[1,5-*a*]pyrimidine (1.0 eq), amine (1.5 eq), tris(dibenzylideneacetone)dipalladium (0.05 eq), 9,9-dimethyl-4,5-bis(diphenyl phosphino)xanthene (0.1 eq), cesium carbonate (2.0 eq), and solvent (10 mL/1 g pyrazolo[1,5-*a*]pyrimidine) were added. The reaction vessel was then sealed and heated to 150 °C for 6 h in a microwave oven at 200 W. After heating, the reaction mixture was filtered through Celite® and concentrated, and the resulting crude product was purified by flash chromatography.

1-{2-[(4-*Tert*-butylpiperazin-1-yl)methyl]-7-(morpholin-4-yl)pyrazolo[1,5-*a*]pyrimidin-5-yl}-2-(trifluoromethyl)-1*H*-benzimidazole (**3**).

Compound **3** was synthesized from 4-{2-[(4-*tert*-butylpiperazin-1-yl)methyl]-5-chloropyrazolo[1,5-*a*]pyrimidin-7-yl}morpholine (0.88 g, 2.04 mmol), 2-(trifluoromethyl)-benzimidazole (0.57 g, 3.06 mmol), tris(dibenzylideneacetone)dipalladium (93.3 mg, 0.102 mmol), 9,9-dimethyl-4,5-

bis(diphenylphosphino)xanthene (124.0 mg, 0.204 mmol), cesium carbonate (1.34 g, 4.08 mmol), and toluene (8.0 mL), according to the general procedure for the Buchwald–Hartwig reaction. The resulting crude product was purified by flash chromatography (0–100% AcOEt gradient in heptane, amine-functionalized gel column) to obtain compound **3** as a white solid (38.0 mg, 0.07 mmol) with a 3% yield. ¹H NMR (600 MHz, CDCl₃) δ 7.94–7.93 (m, 1H, Ar-H), 7.55–7.53 (m, 1H, Ar-H), 7.46–7.42 (m, 2H, Ar-H), 6.63 (s, 1H, Ar-H), 6.16 (s, 1H, Ar-H), 3.98–3.97 (m, 4H, morph.), 3.90–3.89 (m, 4H, morph.), 3.82 (s, 2H, CH₂), 2.67 (d, *J* = 2.1 Hz, 8H, piperaz.), and 1.13–1.06 (m, 9H, *t*-Bu.).

¹³C{¹H, ¹⁹F}NMR (151 MHz, CDCl₃) δ 151.2, 150.2, 147.0, 141.0, 139.9, 135.4, 126.3, 124.5, 121.7, 119.7, 118.0, 111.9, 97.2, 88.1, 66.2, 56.3, 53.8, 48.6, 45.7, 45.0, 29.7, 25.9, and 25.8.

HRMS (ESI/MS): *m/z* calculated for C₂₇H₃₃F₃N₈O [M + H]⁺ 543.2802, found 543.2806.

1-{2-[(4-*Tert*-butylpiperazin-1-yl)methyl]-3-chloro-7-(morpholin-4-yl)pyrazolo[1,5-*a*]pyrimidin-5-yl}-2-(difluoromethyl)-1*H*-benzimidazole (**4**).

To the solution of 1-{2-[(4-*tert*-butylpiperazin-1-yl)methyl]-7-(morpholin-4-yl)pyrazolo[1,5-*a*]pyrimidin-5-yl}-2-(difluoromethyl)-1*H*-benzimidazole (230.0 mg, 0.44 mol, 1.1 eq) in dichloromethane (DCM) (4 mL), *N*-chlorosuccinimide (64.4 mg, 0.48 mmol) was added. The reaction mixture was stirred for 1 h at room temperature. Then, sodium metabisulfite (3 mL) and water (5 mL) were added and the aqueous mixture was extracted with DCM (3 × 5 mL). The combined organic extracts were washed with water, dried over Na₂SO₄, filtered, and concentrated. The resulting crude product was purified by flash chromatography (0–100% ethyl acetate gradient in heptane, amine-functionalized gel column) and crystallization (AcOEt) to obtain compound **4** (134.0 mg; 0.24 mmol) as a white solid with a 55% yield.

¹H NMR (600 MHz, CDCl₃) δ 7.92–7.91 (m, 1H, Ar-H), 7.70–7.69 (m, 1H, Ar-H), 7.46–7.40 (m, 2H, Ar-H), 7.31 (t, *J* = 53.6 Hz, 1H, CHF₂), 6.35 (s, 1H, Ar-H), 3.98–3.96 (m, 4H, morph.), 3.94–3.91 (m, 6H, morph.), 2.71–2.65 (m, 8H), and 1.10 (s, 9H, *t*-Bu.).

¹³C{¹H, ¹⁹F}NMR (151 MHz, CDCl₃) δ 151.3, 150.4, 148.1, 145.2, 144.7, 141.9, 134.5, 125.9, 124.3, 121.6, 111.8, 109.4 (CF₂), 87.7, 66.2, 53.3, 48.7, 45.7, and 25.9 (*t*-Bu.).

HRMS (ESI/MS): *m/z* calculated for C₂₇H₃₃ClF₂N₈O [M + H]⁺ 558.2434, found 538.2442.

1-{3-Bromo-2-[(4-*tert*-butylpiperazin-1-yl)methyl]-7-(morpholin-4-yl)pyrazolo[1,5-*a*]pyrimidin-5-yl}-2-(difluoromethyl)-1*H*-benzimidazole (**5**).

To the solution of 1-{2-[(4-*tert*-butylpiperazin-1-yl)methyl]-7-(morpholin-4-yl)pyrazolo[1,5-*a*]pyrimidin-5-yl}-2-(difluoromethyl)-1*H*-benzimidazole (500.0 mg, 0.94 mol) in DCM (7 mL), *N*-bromosuccinimide (204.0 mg, 1.13 mmol, and 1.2 eq) was added. The reaction mixture was stirred for 1 h at room temperature. Then, sodium metabisulfite (5 mL) and water (10 mL) were added and the aqueous mixture was extracted with DCM (3 × 10 mL). The combined organic extracts were washed with water, dried over Na₂SO₄, filtered, and concentrated. The resulting crude product was purified by flash chromatography (0–100% ethyl acetate gradient in heptane, amine-functionalized gel column) and crystallization (AcOEt) to obtain compound **5** (370.0 mg; 0.61 mmol) as a white solid with a 65% yield.

¹H NMR (600 MHz, CDCl₃) δ 7.92–7.91 (m, 1H, Ar-H), 7.71–7.70 (m, 1H, Ar-H), 7.46–7.40 (m, 2H, Ar-H), 7.39 (t, *J* = 53.5 Hz, 1H, CHF₂), 6.37 (s, 1H, Ar-H), 3.98–3.96 (m, 4H, morph.), 3.94–3.92 (m, 4H, morph.), 3.90 (s, 2H, CH₂), 2.81–2.57 (m, 8H), and 1.08 (s, 9H, *t*-Bu.).

¹³C{¹H, ¹⁹F}NMR (151 MHz, CDCl₃) δ 151.9, 151.4, 148.4, 146.6, 144.8, 141.9, 134.5, 125.9, 124.3, 121.6, 111.8, 109.4 (CF₂), 87.7, 66.2, 53.6, 48.7, 45.7, and 25.8 (*t*-Bu.).

HRMS (ESI/MS): *m/z* calculated for C₂₇H₃₃BrF₂N₈O [M + H]⁺ 602.1929, found 602.1936.

3.3.2. General Procedure for the Reductive Amination Reaction

To the solution of the corresponding aldehyde (1.0 eq) in a dry DCM (10 mL/1 g aldehyde), an amine derivative (1.2 eq) was added, and the reaction mixture was stirred for 1 h at room temperature. Then, sodium triacetoxyborohydride (1.5 eq) was added and the mixture was stirred for a further 15 h at room temperature. Next, water was added to the reaction mixture and the phases were separated. The aqueous phase was extracted three times with DCM, while the combined organic phases were dried over anhydrous sodium sulfate, filtered, and concentrated. The resulting residue was purified by flash chromatography.

1-{2-[(4-Benzylpiperazin-1-yl)methyl]-7-(morpholin-4-yl)pyrazolo[1,5-*a*]pyrimidin-5-yl}-2-(difluoromethyl)-1*H*-benzimidazole (**6**).

Compound **6** was prepared from aldehyde 5-[2-(difluoromethyl)-1*H*-benzimidazol-1-yl]-7-(morpholin-4-yl)pyrazolo[1,5-*a*]pyrimidine-2-carbaldehyde (0.15 g, 0.37 mmol), 1-benzylpiperazine (0.80 g, 0.45 mmol) as an amine, DCM (3.0 mL), and sodium triacetoxyborohydride (0.12 g, 0.56 mmol), according to the general procedure for reductive amination reaction. The resulting crude product was purified by flash chromatography (0–10% MeOH gradient in AcOEt) to obtain compound **6** (0.1 g, 0.18 mmol) with a 47% yield.

¹H NMR (600 MHz, DMSO-*d*₆) δ 7.88–7.87 (m, 1H, Ar-H), 7.81 (d, *J* = 7.6 Hz, 1H, Ar-H), 7.58 (t, *J* = 52.5 Hz, 1H, CHF₂), 7.47–7.41 (m, 2H, Ar-H), 7.31–7.26 (m, 4H, Ar-H), 7.24–7.21 (m, 1H, Ar-H), 6.65 (s, 1H, Ar-H), 6.52 (s, 1H, Ar-H), 3.93–3.91 (m, 4H, morph.), 3.83 (t, *J* = 4.6 Hz, 4H, morph.), 3.68 (s, 2H, CH₂), 3.44 (s, 2H, CH₂), 2.50–2.48 (m, 4H, piperaz.), and 2.39–2.37 (m, 4H, piperaz.).

¹³C NMR (151 MHz, DMSO-*d*₆) δ 154.9, 150.8, 149.6, 147.0, 144.6, 141.2, 138.2, 134.0, 128.7, 128.1, 126.8, 125.4, 123.9, 120.6, 112.4, 108.5, 95.4, 87.8, 65.5, 62.0, 55.7, 52.6, 52.6, and 48.1.

HRMS (ESI/MS): *m/z* calculated for C₃₀H₃₂F₂N₈O [M + H]⁺ 558.2667, found 558.2681.

1-[2-((4-(2-Fluorophenyl)methyl)piperazin-1-yl)methyl)-7-(morpholin-4-yl)pyrazolo[1,5-*a*]pyrimidin-5-yl]-2-(propan-2-yl)-1*H*-benzimidazole (**7**).

Compound **7** was prepared from 5-[2-(difluoromethyl)-1*H*-benzimidazol-1-yl]-7-(morpholin-4-yl)pyrazolo[1,5-*a*]pyrimidine-2-carbaldehyde (0.20 g, 0.50 mmol), 1-[(2-fluorophenyl)methyl]piperazine (0.105 mL, 0.12 g, 0.60 mmol) as an amine, DCM (2.0 mL), and sodium triacetoxyborohydride (0.16 g, 0.75 mmol), according to the general procedure for reductive amination reaction. The resulting crude product was purified by flash chromatography (0–100% AcOEt gradient in heptane) to obtain compound **7** (0.74 g, 0.13 mmol) with a 26% yield.

¹H NMR (600 MHz, DMSO-*d*₆) δ 7.88–7.87 (m, 1H, Ar-H), 7.82 (d, *J* = 7.6 Hz, 1H, Ar-H), 7.57 (t, *J* = 52.5 Hz, 1H, CHF₂), 7.46–7.41 (m, 2H, Ar-H), 7.32–7.26 (m, 2H, Ar-H), 7.13–7.10 (m, 2H, Ar-H), 6.65 (s, 1H, Ar-H), 6.56 (s, 1H, Ar-H), 4.37 (dd, *J* = 8.4, 6.5 Hz, 1H), 3.93–3.99 (1H), 3.91–3.90 (m, 4H, morph.), 3.86–3.81 (m, 4H, morph.), 3.45 (s, 2H, CH₂), 3.13 (dd, *J* = 16.2, 8.6 Hz, 1H), 2.99 (dd, *J* = 16.3, 6.4 Hz, 1H), 2.54 (d, *J* = 8.5 Hz, 2H, CH₂), and 2.40–2.32 (m, 4H, piperaz.).

¹³C NMR (151 MHz, DMSO-*d*₆) δ 206.6, 160.7, 155.0, 150.8, 149.4, 147.0, 144.7, 141.2, 134.0, 131.5, 128.9, 125.4, 124.5, 124.0, 123.9, 120.6, 115.0, 112.4, 108.4, 95.2, 87.8, 65.6, 58.2, 54.5, 52.8, 48.1, 43.6, and 30.0.

HRMS (ESI/MS): *m/z* calculated for C₃₀H₃₁F₃N₈O [M + H]⁺ 576.2564, found 576.2573.

1-[2-((4-(3-Fluorophenyl)methyl)piperazin-1-yl)methyl)-7-(morpholin-4-yl)pyrazolo[1,5-*a*]pyrimidin-5-yl]-2-(propan-2-yl)-1*H*-benzimidazole (**8**).

Compound **10** was prepared from 5-[2-(difluoromethyl)-1*H*-benzimidazol-1-yl]-7-(morpholin-4-yl)pyrazolo[1,5-*a*]pyrimidine-2-carbaldehyde (0.25 g, 0.63 mmol), 1-[(3-fluorophenyl)methyl]piperazine (0.15 g, 0.75 mmol) as an amine, DCM (2.5 mL), and sodium triacetoxyborohydride (0.20 g, 0.94 mmol), according to the general procedure for reductive amination reaction. The resulting crude product was purified by flash chromatography (0–10% MeOH gradient in AcOEt) to obtain compound **8** (0.24 g, 0.41 mmol) with a 65% yield.

¹H NMR (600 MHz, DMSO-*d*₆) δ 7.84 (dd, *J* = 40.8, 7.5 Hz, 2H, Ar-H), 7.58 (t, *J* = 52.4 Hz, 1H, CHF₂), 7.47–7.41 (m, 2H, Ar-H), 7.34 (dd, *J* = 14.0, 7.8 Hz, 1H, Ar-H), 7.12–7.03 (m, 3H, Ar-H), 6.65 (s, 1H, Ar-H), 6.52 (d, *J* = 3.5 Hz, 1H, Ar-H), 3.92 (s, 4H, morph.), 3.83 (d, *J* = 4.3 Hz, 4H, morph.), 3.69 (s, 2H, CH₂), 3.47 (s, 4H, piperaz.), and 2.40 (s, 4H, piperaz.).

¹³C NMR (151 MHz, DMSO-*d*₆) δ 163.0, 161.4, 154.9, 150.9, 149.7, 147.0, 141.5, 141.2, 134.0, 130.0, 125.4, 124.6, 123.9, 120.7, 115.0, 113.7, 112.4, 108.5, 95.4, 87.8, 65.5, 61.2, 55.7, 52.6, and 48.2.

HRMS (ESI/MS): *m/z* calculated for C₃₀H₃₁F₃N₈O [M + H]⁺ 576.2573, found 576.2590.

1-[2-((4-(4-Fluorophenyl)methyl)piperazin-1-yl)methyl)-7-(morpholin-4-yl)pyrazolo[1,5-*a*]pyrimidin-5-yl]-2-(propan-2-yl)-1*H*-benzimidazole (**9**).

Compound **9** was prepared from 5-[2-(difluoromethyl)-1*H*-benzimidazol-1-yl]-7-(morpholin-4-yl)pyrazolo[1,5-*a*]pyrimidine-2-carbaldehyde (0.20 g, 0.50 mmol), 1-[(4-fluorophenyl)methyl]piperazine (0.12 g, 0.60 mmol) as an amine, DCM (2.0 mL), and sodium triacetoxyborohydride (0.16 g, 0.75 mmol), according to the general procedure for reductive amination reaction. The resulting crude product was purified by flash chromatography (0–100% AcOEt gradient in heptane) to obtain compound **9** (0.25 g, 0.44 mmol) with a 88% yield.

¹H NMR (400 MHz, CDCl₃) δ 7.93–7.91 (m, 1H, Ar-H), 7.66–7.64 (m, 1H, Ar-H), 7.45–7.39 (m, 2H, Ar-H), 7.30–7.26 (m, 3H, Ar-H), 7.16 (s, 1H, Ar-H), 7.01–6.97 (m, 2H, Ar-H), 6.59 (s, 1H, Ar-H), 6.30 (s, 1H, Ar-H), 3.98 (q, *J* = 3.1 Hz, 4H, morph.), 3.92–3.88 (m, 4H, morph.), 3.80 (s, 2H, CH₂), 3.48 (s, 2H, CH₂), 2.63 (s, 4H, piperaz.), and 2.51 (s, 4H, piperaz.).

¹³C NMR (101 MHz, CDCl₃) δ 163.2, 160.8, 155.6, 151.3, 150.1, 147.5, 144.7, 141.8, 134.6, 130.7, 130.6, 125.7, 124.2, 121.6, 115.1, 114.9, 111.7, 111.7, 109.3, 96.6, 87.3, 66.2, 62.2, 56.4, 53.1, 48.5, 31.6, 22.6, and 14.1.

HRMS (ESI/MS): *m/z* calculated for C₃₀H₃₁F₃N₈O [M + H]⁺ 576.2573, found 576.2588.

3.3.3. General Procedure for the Amidation Reaction

The corresponding amine (1.05 eq), 2-(7-aza-1*H*-benzotriazole-1-yl)-1,1,3,3-tetramethyluronium hexafluorophosphate (HATU) (1.1 eq), and triethylamine (1.5 eq) were added to the solution of substituted 5-chloro-pyrazolo[1,5-*a*]pyrimidine derivative (1.0 eq) in solvent (10 mL/1 g pyrazolo[1,5-*a*]pyrimidine derivative). The reaction mixture was stirred at room temperature for 2 h. Then, water was added to the mixture and the phases were separated. The aqueous phase was extracted three times with a solvent, while combined organic phases were dried over anhydrous sodium sulfate, filtered, and concentrated. The resulting residue was purified by flash chromatography.

1-[2-(4-Benzylpiperazine-1-carbonyl)-7-(morpholin-4-yl)pyrazolo[1,5-*a*]pyrimidin-5-yl]-2-(difluoromethyl)-1*H*-benzimidazole (**10**).

Compound **10** was prepared from 5-[2-(difluoromethyl)-1*H*-benzimidazol-1-yl]-7-(morpholin-4-yl)pyrazolo[1,5-*a*]pyrimidine-2-carboxylic acid (0.45 g, 1.09 mmol), 1-benzylpiperazine (0.20 g, 1.14 mmol), HATU (0.46 g, 1.19 mmol), TEA (0.23 mL, 0.16 g, and 1.63 mmol), and DCM (4.0 mL), according to the general procedure for amidation reaction. The resulting crude product was purified by flash chromatography (0–10% MeOH gradient in AcOEt) to obtain compound **10** (0.32 g, 0.56 mmol) as a light yellow solid with a 51% yield.

¹H NMR (600 MHz, DMSO-*d*₆) δ 7.89 (d, *J* = 7.6 Hz, 1H, Ar-H), 7.82 (d, *J* = 7.8 Hz, 1H, Ar-H), 7.58 (t, *J* = 52.4 Hz, 1H, CHF₂), 7.48–7.42 (m, 2H, Ar-H), 7.35–7.31 (m, 4H, Ar-H), 7.26 (td, *J* = 5.9, 2.6 Hz, 1H, Ar-H), 6.83 (s, 1H, Ar-H), 6.81 (s, 1H, Ar-H), 3.91–3.90 (m, 4H, morph.), 3.83 (t, *J* = 4.5 Hz, 4H, morph.), 3.72 (d, *J* = 41.1 Hz, 4H, piperaz.), 3.53 (s, 2H, CH₂), and 2.44 (dt, *J* = 23.1, 4.6 Hz, 4H, piperaz.).

¹³C NMR (151 MHz, DMSO-*d*₆) δ 161.6, 151.1, 150.3, 149.2, 147.7, 144.6, 141.2, 137.7, 134.0, 128.9, 127.0, 125.5, 124.0, 120.7, 108.5, 65.5, 52.9, 48.4, 30.9, and 26.8.

HRMS (ESI/MS): *m/z* calculated for C₃₀H₃₀F₂N₈O₂ [M + H]⁺ 572.2460, found 572.2477.

2-(Difluoromethyl)-1-(2-{4-[(2-fluorophenyl)methyl]piperazine-1-carbonyl}-7-(morpholin-4-yl)pyrazolo[1,5-*a*]pyrimidin-5-yl)-1*H*-benzimidazole (**11**).

Compound **11** was prepared from 5-[2-(difluoromethyl)-1*H*-benzimidazol-1-yl]-7-(morpholin-4-yl)pyrazolo[1,5-*a*]pyrimidine-2-carboxylic acid (0.20 g, 0.48 mmol), 1-(2-fluorobenzyl)piperazine (0.89 mL, 0.10 g, and 0.51 mmol), HATU (0.20 g, 0.53 mmol), TEA (0.10 mL, 0.073 g, and 0.72 mmol), and DCM (2.0 mL), according to the general procedure for amidation reaction. The resulting crude product was purified by flash chromatography (0–5% MeOH gradient in AcOEt) to obtain compound **11** (0.17 g, 0.29 mmol) as a white solid with a 60% yield.

¹H NMR (400 MHz, DMSO-*d*₆) δ 7.89 (d, *J* = 7.3 Hz, 1H, Ar-H), 7.82 (d, *J* = 7.3 Hz, 1H, Ar-H), 7.61 (t, *J* = 52.6 Hz, 1H, CHF₂), 7.47–7.41 (m, 3H, Ar-H), 7.33 (d, *J* = 7.7 Hz, 1H, Ar-H), 7.20–7.15 (m, 2H, Ar-H), 6.83 (s, 1H, Ar-H), 6.80 (s, 1H, Ar-H), 3.83 (d, *J* = 3.8 Hz, 4H, morph.), 3.72 (d, *J* = 27.4 Hz, 4H, morph.), 3.60 (s, 2H), and 2.49–2.46 (m, 4H).

¹³C NMR (101 MHz, DMSO-*d*₆) δ 161.7, 159.6, 151.2, 150.2, 149.2, 147.8, 144.7, 141.2, 134.0, 131.7, 129.2, 125.5, 124.2, 124.0, 120.7, 115.3, 112.4, 108.5, 96.7, 89.3, 65.6, 54.4, 52.7, 52.1, 48.4, and 41.8.

HRMS (ESI/MS): *m/z* calculated for C₃₀H₂₉F₃N₈O₂ [M + H]⁺ 590.2366, found 590.2381.

2-(Difluoromethyl)-1-(2-{4-[(3-fluorophenyl)methyl]piperazine-1-carbonyl}-7-(morpholin-4-yl)pyrazolo[1,5-*a*]pyrimidin-5-yl)-1*H*-benzimidazole (**12**).

Compound **12** was prepared from 5-[2-(difluoromethyl)-1*H*-benzimidazol-1-yl]-7-(morpholin-4-yl)pyrazolo[1,5-*a*]pyrimidine-2-carboxylic acid (0.24 g, 0.59 mmol), 1-(3-fluorobenzyl)piperazine (0.12 g, 0.62 mmol), HATU (0.25 g, 0.65 mmol), TEA (0.12 mL, 0.09 g, and 0.88 mmol), and DCM (2.0 mL), according to the general procedure for amidation reaction. The resulting crude product was purified by

flash chromatography (0–15% MeOH gradient in AcOEt) to obtain compound **12** (0.13 g, 0.21 mmol) as a white solid with a 36% yield.

¹H NMR (600 MHz, DMSO-*d*₆) δ 7.89 (d, *J* = 7.6 Hz, 1H, Ar-H), 7.82 (d, *J* = 8.1 Hz, 1H, Ar-H), 7.58 (t, *J* = 52.4 Hz, 1H, CHF₂), 7.48–7.42 (m, 2H, Ar-H), 7.37 (dd, *J* = 14.1, 7.9 Hz, 1H, Ar-H), 7.17–7.15 (m, 2H, Ar-H), 7.10–7.07 (m, 1H, Ar-H), 6.84 (s, 1H, Ar-H), 6.81 (s, 1H, Ar-H), 3.91–3.90 (m, 4H, morph.), 3.84–3.82 (m, 4H, morph.), 3.73 (d, *J* = 41.5 Hz, 4H, piperaz.), 3.56 (s, 2H), 2.68 (s, 3H), 2.44 (d, *J* = 4.5 Hz, 4H, piperaz.), and 2.43 (t, *J* = 4.5 Hz, 2H).

¹³C NMR (151 MHz, DMSO-*d*₆) δ 162.2, 161.7, 151.1, 150.3, 149.2, 147.7, 144.6, 141.2, 140.9, 134.0, 130.1, 125.5, 124.7, 124.0, 120.7, 115.2, 113.8, 112.4, 108.5, 96.7, 89.2, 65.5, 48.4, and 38.2.

HRMS (ESI/MS): *m/z* calculated for C₃₀H₂₉F₃N₈O₂ [M + H]⁺ 590.2366, found 590.2385.

2-(Difluoromethyl)-1-(2-{4-[(4-fluorophenyl)methyl]piperazine-1-carbonyl}-7-(morpholin-4-yl)pyrazolo[1,5-*a*]pyrimidin-5-yl)-1*H*-benzimidazole (**13**).

Compound **13** was prepared from 5-[2-(difluoromethyl)-1*H*-benzimidazol-1-yl]-7-(morpholin-4-yl)pyrazolo[1,5-*a*]pyrimidine-2-carboxylic acid (0.15 g, 0.36 mmol), 1-(4-fluorobenzyl)piperazine (0.075 g, 0.38 mmol), HATU (0.15 g, 0.40 mmol), TEA (0.076 mL, 0.05 g, and 0.54 mmol), and DCM (1.5 mL), according to the general procedure for amidation reaction. The resulting crude product was purified by flash chromatography (0–5% MeOH gradient in AcOEt) to obtain compound **13** (0.13 g, 0.22 mmol) as a white solid with a 62% yield.

¹H NMR (600 MHz, DMSO-*d*₆) δ 7.89 (d, *J* = 7.4 Hz, 1H, Ar-H), 7.82 (d, *J* = 7.8 Hz, 1H, Ar-H), 7.58 (t, *J* = 52.6 Hz, 1H, CHF₂), 7.48–7.42 (m, 2H, Ar-H), 7.37–7.35 (m, 2H, Ar-H), 7.15 (t, *J* = 8.7 Hz, 2H, Ar-H), 6.83 (s, 1H, Ar-H), 6.81 (s, 1H, Ar-H), 3.91 (t, *J* = 4.6 Hz, 4H, morph.), 3.83 (t, *J* = 4.6 Hz, 4H, morph.), 3.72 (d, *J* = 42.1 Hz, 4H, piperaz.), 3.51 (s, 2H, CH₂), and 2.43 (d, *J* = 23.5 Hz, 3H).

¹³C NMR (151 MHz, DMSO-*d*₆) δ 161.7, 151.1, 150.3, 149.2, 147.8, 144.7, 141.2, 134.0, 130.7, 130.7, 125.5, 124.0, 120.7, 115.0, 114.8, 112.4, 108.5, 96.7, 89.3, 65.5, 60.8, and 48.4.

HRMS (ESI/MS): *m/z* calculated for C₃₀H₂₉F₃N₈O₂ [M + H]⁺ 590.2366, found 590.2380.

3.4. *In Vitro* PI3Kδ Inhibition Assay

All compounds were tested by a biochemical assay that measured the inhibition of phosphatidylinositol (4,5)-bisphosphate (PIP2) production by PI3K isoform. The potency of the tested compounds was assessed by determining the ability of PI3Kδ enzymes (Merck Millipore) to convert ATP to ADP during an enzymatic reaction in the presence of these compounds at decreasing doses. The experiments were carried out using the ADP-Glo kinase assay kit (Promega), according to the manufacturer's protocol. PIP2 lipid vesicles containing phosphoserine (ThermoFisher Scientific, Waltham, MA, USA) were used as a substrate in the enzymatic reaction. The composition of the reaction mixture and reaction conditions for PI3Kδ were as follows: concentration of PI3Kδ enzyme: 10 ng; reaction temperature and time: 25 °C and 1 h; final concentration of PIP2 substrate: 30 μM; and reaction buffer: 50 mM of HEPES (pH 7.5), 50 mM NaCl, 3 mM MgCl₂, and 0.025 mg/mL of BSA.

After the reaction, the ADP-Glo reagent and the kinase detection reagent were sequentially added. The reaction mixture was incubated for 40 min (25 °C, 600 rpm) after the addition of each reagent. Finally, luminescence intensity was measured and the IC₅₀ value was calculated using GraphPad Prism 7 software (GraphPad, Boston, MA, USA). The results were presented as the mean value of IC₅₀ obtained from at least two independent experiments.

3.5. Computational Workflow Used to Predict the Most Potent Fluorine Derivative

We used a previously described computational workflow involving IFD, MD simulations, and QPLD combined with energy calculations (applying the MM-GBSA method). The crystal structure of PI3Kδ protein (PDB ID: 2WXL) [25] that was successfully used in our previous study to support the SAR analysis [19] was retrieved from Protein Data Bank [26,27]

3.5.1. IFD

The three-dimensional structures of the ligands were prepared using LigPrep v3.6 [28], and appropriate ionization states at pH 7.0 ± 0.5 were assigned using Epik v3.4 [29]. The Protein Preparation Wizard tool [28] was used to assign bond orders and appropriate amino acid ionization states and to

check for steric clashes for the PI3K δ crystal structure. The receptor grid was generated (OPLS3 force field [30]) by centering the grid box with a size of 8 Å on crystalized ligands (ZSTK474). Automated flexible docking [31,32] of nonfluorinated compounds was performed using Glide v6.9 [33–35] at the SP level.

3.5.2. MD

MD simulations (100 ns long) were performed using Schrödinger Desmond software [36,37]. Each ligand–receptor complex selected based on the IFD analysis was joined with the POPC (309.5 K) membrane bilayer. The system was solvated by water molecules described by the TIP4P potential [38] in orthorhombic box with a distance of 10 Å from the complex, using the OPLS3e force field [30] for all atoms. NaCl (0.15 M) was added to mimic the ionic strength inside the cell. The simulations were carried out using the NPAT protocol at a temperature of 309.5 K and a pressure of 1013.25 hPa.

3.5.3. QPLD

The grids for the receptors were generated (OPLS3e force field) by centering the grid box (size 8 Å) on a ligand. Docking of all fluorinated compounds was performed by the QPLD [16] procedure involving the QM-derived ligand atomic charges in the protein environment at the BLYP/cc-pVDZ level [39,40]. Five poses were obtained for each ligand.

3.5.4. Binding-Free Energy Calculations

Using GBSA, the binding-free energy was calculated based on the ligand–receptor complexes generated by the QPLD procedure. The ligand poses were minimized using the local optimization feature in Prime. The distance of the flexible residue from a ligand pose was set to 6 Å. Ligand charges obtained in the QPLD stage were used. The energies of complexes were calculated with the OPLS3e force field and the GBSA continuum solvent model. To assess the influence of a given substituent on binding, $\Delta\Delta G$ was calculated as the difference between the binding-free energy (ΔG) of the nonfluorinated compound and its fluorinated analogs.

4. Conclusions

We evaluated a workflow involving IFD, MD, and QM/MM docking (QPLD) with the MM-GBSA calculation to score halogenated derivatives of CPL302415, a clinical PI3K δ selective inhibitor, and compared the results with those obtained by the Glide scoring function. Additionally, we synthesized a series of novel fluorinated compounds to estimate the accuracy of the pose prediction in the molecular docking procedure.

We found that a properly prepared catalytic (binding) pocket for chemical cores in the IFD and MD stages, combined with QM-derived atomic charges, can be effectively used for prediction, as well as to improve the discrimination of active compounds from inactive ones. Moreover, the standard approach (rigid docking) seems to be less effective at scoring halogenated derivatives due to the fixed atomic charges and the fact that it does not consider the response and inductive effects caused by fluorine. Our results suggest that the proposed computational workflow may be a valuable tool for the rational design of new halogenated drugs.

Supplementary Materials: The following supporting information can be downloaded at: www.mdpi.com/xxx/s1. It contains NMR and MS data for all compounds and additional results obtained from presented workflow.

Author Contributions: W.P.: conceptualization, methodology, validation, formal analysis, investigation, writing—original draft, visualization; R.K.: writing—original draft, M.S.: synthesis, conceptualization, formal analysis, investigation, writing—original draft, M.Z.: writing—original draft, M.B.:—biological evaluation, L.G.-B., W.M. and A.L.—analytical evaluation, K.D. and Z.O.—project administration, M.W.: funding acquisition. All authors have read and agreed to the published version of the manuscript.

Funding: The study was financially supported by the National Science Center, Poland (grant No. 2019/35/N/NZ7/04312).

Institutional Review Board Statement: Not applicable.

Informed Consent Statement: Not applicable.

Data Availability Statement: Data are contained within the article and supplementary material.

Acknowledgments: The authors acknowledge the financial support from the National Science Centre, Poland (grant No. 2019/35/N/NZ7/04312). W.P. acknowledges the support of InterDokMed project No. POWR.03.02.00-00-1013. Molecular modeling calculations were performed using the resources of the Department of Medicinal Chemistry, Maj Institute of Pharmacology, Polish Academy of Sciences. The authors thank Michał Słotwiński (Celon Pharma) for providing intermediate product synthesis. We would like to thank Aleksandra Świdorska (Celon Pharma) for NMR analyses and practical suggestions.

Conflicts of Interest: The authors declare no conflict of interest.

Sample Availability: Not applicable.

References

1. Foster, J.G.; Blunt, M.D.; Carter, E.; Ward, S.G. Inhibition of PI3K Signaling Spurs New Therapeutic Opportunities in Inflammatory/Autoimmune Diseases and Hematological Malignancies. *Pharmacol. Rev.* **2012**, *64*, 1027–1054. <https://doi.org/10.1124/pr.110.004051>.
2. Banham-Hall, E. The Therapeutic Potential for PI3K Inhibitors in Autoimmune Rheumatic Diseases. *Open Rheumatol. J.* **2012**, *6*, 245–258. <https://doi.org/10.2174/1874312901206010245>.
3. Stark, A.-K.; Sriskantharajah, S.; Hessel, E.M.; Okkenhaug, K. PI3K inhibitors in inflammation, autoimmunity and cancer. *Curr. Opin. Pharmacol.* **2015**, *23*, 82–91. <https://doi.org/10.1016/j.coph.2015.05.017>.
4. Puri, K.D.; Gold, M.R. Selective inhibitors of phosphoinositide 3-kinase delta: Modulators of B-cell function with potential for treating autoimmune inflammatory diseases and B-cell malignancies. *Front. Immunol.* **2012**, *3*, 256. <https://doi.org/10.3389/fimmu.2012.00256>.
5. Haselmayer, P.; Camps, M.; Muzerelle, M.; El Bawab, S.; Waltzinger, C.; Bruns, L.; Abla, N.; Polokoff, M.A.; Jond-Necand, C.; Gaudet, M.; et al. Characterization of Novel PI3K δ Inhibitors as Potential Therapeutics for SLE and Lupus Nephritis in Pre-Clinical Studies. *Front. Immunol.* **2014**, *5*, 233. <https://doi.org/10.3389/fimmu.2014.00233>.
6. Pietruś, W.; Kafel, R.; Bojarski, A.J.; Kurczab, R. Hydrogen Bonds with Fluorine in Ligand–Protein Complexes—the PDB Analysis and Energy Calculations. *Molecules* **2022**, *27*, 1005. <https://doi.org/10.3390/molecules27031005>.
7. Grychowska, K.; Olejarz-Maciej, A.; Blicharz, K.; Pietruś, W.; Karcz, T.; Kurczab, R.; Koczurkiewicz, P.; Doroz-Płonka, A.; Latacz, G.; Keeri, A.R.; et al. Overcoming undesirable hERG affinity by incorporating fluorine atoms: A case of MAO-B inhibitors derived from 1 H-pyrrolo-[3,2-c]quinolines. *Eur. J. Med. Chem.* **2022**, *236*, 114329. <https://doi.org/10.1016/j.ejmech.2022.114329>.
8. Pietruś, W.; Kurczab, R.; Stumpfe, D.; Bojarski, A.J.; Bajorath, J. Data-driven analysis of fluorination of ligands of aminergic G protein coupled receptors. *Biomolecules* **2021**, *11*, 1647. <https://doi.org/10.3390/biom11111647>.
9. Pietruś, W.; Kurczab, R.; Warszzycki, D.; Bojarski, A.J.; Bajorath, J. Isomeric Activity Cliffs—A Case Study for Fluorine Substitution of Aminergic G Protein-Coupled Receptor Ligands. *Molecules* **2023**, *28*, 490. <https://doi.org/10.3390/molecules28020490>.
10. O’Hagan, D. Understanding organofluorine chemistry. An introduction to the C–F bond. *Chem. Soc. Rev.* **2008**, *37*, 308–319. <https://doi.org/10.1039/B711844A>.
11. Swallow, S. Fluorine in Medicinal Chemistry. In *Progress in Medicinal Chemistry*; Lawton, G., Witty, D.R., Eds.; Elsevier: Amsterdam, The Netherlands, 2015; Volume 54, pp. 65–133. ISBN 0306-0012.
12. Zhou, Y.; Wang, J.; Gu, Z.; Wang, S.; Zhu, W.; Aceña, J.L.; Soloshonok, V.A.; Izawa, K.; Liu, H. Next Generation of Fluorine-Containing Pharmaceuticals, Compounds Currently in Phase II–III Clinical Trials of Major Pharmaceutical Companies: New Structural Trends and Therapeutic Areas. *Chem. Rev.* **2016**, *116*, 422–518. <https://doi.org/10.1021/acs.chemrev.5b00392>.
13. Batta, A.; Kalra, B.S.; Khirasaria, R. Trends in FDA drug approvals over last 2 decades: An observational study. *J. Fam. Med. Prim. Care* **2020**, *9*, 105. https://doi.org/10.4103/JFMPC.JFMPC_578_19.
14. Rojas, S.; Parravicini, O.; Vettorazzi, M.; Tosso, R.; Garro, A.; Gutiérrez, L.; Andújar, S.; Enriz, R. Combined MD/QTAIM techniques to evaluate ligand-receptor interactions. Scope and limitations. *Eur. J. Med. Chem.* **2020**, *208*, 112792. <https://doi.org/10.1016/j.ejmech.2020.112792>.
15. Pinzi, L.; Rastelli, G. Molecular Docking: Shifting Paradigms in Drug Discovery. *Int. J. Mol. Sci.* **2019**, *20*, 4331. <https://doi.org/10.3390/ijms20184331>.
16. Cho, A.E.; Guallar, V.; Berne, B.J.; Friesner, R. Importance of accurate charges in molecular docking: Quantum mechanical/molecular mechanical (QM/MM) approach. *J. Comput. Chem.* **2005**, *26*, 915–931. <https://doi.org/10.1002/jcc.20222>.
17. Xu, M.; Lill, M.A. Induced fit docking, and the use of QM/MM methods in docking. *Drug Discov. Today Technol.* **2013**, *10*, e411–e418. <https://doi.org/10.1016/j.ddtec.2013.02.003>.

18. Trott, O.; Olson, A.J. AutoDock Vina: Improving the speed and accuracy of docking with a new scoring function, efficient optimization, and multithreading. *J. Comput. Chem.* **2009**, *31*, 455–461. <https://doi.org/10.1002/jcc.21334>.
19. Stypik, M.; Michałek, S.; Orłowska, N.; Zagozda, M.; Dziachan, M.; Banach, M.; Turowski, P.; Gunerka, P.; Zdzalik-Bielecka, D.; Stańczak, A.; et al. Design, Synthesis, and Development of Pyrazolo[1,5-a]pyrimidine Derivatives as a Novel Series of Selective PI3K δ Inhibitors: Part II—Benzimidazole Derivatives. *Pharmaceuticals* **2022**, *15*, 927. <https://doi.org/10.3390/ph15080927>.
20. Berry, M.; Fielding, B.; Gamielien, J. Practical Considerations in Virtual Screening and Molecular Docking. In *Emerging Trends in Computational Biology, Bioinformatics, and Systems Biology*; Elsevier: Amsterdam, The Netherlands, 2015; Volume 2, pp. 487–502. ISBN 9788578110796.
21. Pietruś, W.; Kurczab, R.; Kalinowska-Thuścick, J.; Machalska, E.; Golonka, D.; Barańska, M.; Bojarski, A.J. Influence of Fluorine Substitution on Nonbonding Interactions in Selected Para-Halogeno Anilines. *ChemPhysChem* **2021**, *22*, 2115–2127. <https://doi.org/10.1002/cphc.202100383>.
22. Kurczab, R. The evaluation of QM/MM-driven molecular docking combined with MM/GBSA calculations as a halogen-bond scoring strategy. *Acta Crystallogr. Sect. B Struct. Sci. Cryst. Eng. Mater.* **2017**, *73*, 188–194. <https://doi.org/10.1107/S205252061700138X>.
23. Stypik, M.; Zagozda, M.; Michałek, S.; Dymek, B.; Zdzalik-Bielecka, D.; Dziachan, M.; Orłowska, N.; Gunerka, P.; Turowski, P.; Hucz-Kalitowska, J.; et al. Design, Synthesis, and Development of pyrazolo[1,5-a]pyrimidine Derivatives as a Novel Series of Selective PI3K δ Inhibitors: Part I—Indole Derivatives. *Pharmaceuticals* **2022**, *15*, 949. <https://doi.org/10.3390/ph15080949>.
24. García-Pérez, D.; López, C.; Claramunt, R.; Alkorta, I.; Elguero, J. 19F-NMR Diastereotopic Signals in Two N-CHF₂ Derivatives of (4S,7R)-7,8,8-Trimethyl-4,5,6,7-tetrahydro-4,7-methano-2H-indazole. *Molecules* **2017**, *22*, 2003. <https://doi.org/10.3390/molecules22112003>.
25. Berndt, A.; Miller, S.; Williams, O.; Le, D.D.; Houseman, B.T.; Pacold, J.I.; Gorrec, F.; Hon, W.-C.; Ren, P.; Liu, Y.; et al. The p110 δ structure: Mechanisms for selectivity and potency of new PI(3)K inhibitors. *Nat. Chem. Biol.* **2010**, *6*, 117–124. <https://doi.org/10.1038/nchembio.293>.
26. Berman, H.M. The Protein Data Bank. *Nucleic Acids Res.* **2000**, *28*, 235–242. <https://doi.org/10.1093/nar/28.1.235>.
27. Burley, S.K.; Bhikadiya, C.; Bi, C.; Bittrich, S.; Chen, L.; Crichlow, G.V.; Christie, C.H.; Dalenberg, K.; Di Costanzo, L.; Duarte, J.M.; et al. RCSB Protein Data Bank: Powerful new tools for exploring 3D structures of biological macromolecules for basic and applied research and education in fundamental biology, biomedicine, biotechnology, bioengineering and energy sciences. *Nucleic Acids Res.* **2021**, *49*, D437–D451. <https://doi.org/10.1093/nar/gkaa1038>.
28. Madhavi Sastry, G.; Adzhigirey, M.; Day, T.; Annabhimoju, R.; Sherman, W. Protein and ligand preparation: Parameters, protocols, and influence on virtual screening enrichments. *J. Comput. Aided. Mol. Des.* **2013**, *27*, 221–234. <https://doi.org/10.1007/s10822-013-9644-8>.
29. Shelley, J.C.; Cholleti, A.; Frye, L.L.; Greenwood, J.R.; Timlin, M.R.; Uchimaya, M. Epik: A software program for pKa prediction and protonation state generation for drug-like molecules. *J. Comput. Aided. Mol. Des.* **2007**, *21*, 681–691. <https://doi.org/10.1007/s10822-007-9133-z>.
30. Harder, E.; Damm, W.; Maple, J.; Wu, C.; Reboul, M.; Xiang, J.Y.; Wang, L.; Lupyan, D.; Dahlgren, M.K.; Knight, J.L.; et al. OPLS3: A Force Field Providing Broad Coverage of Drug-like Small Molecules and Proteins. *J. Chem. Theory Comput.* **2016**, *12*, 281–296. <https://doi.org/10.1021/acs.jctc.5b00864>.
31. Sherman, W.; Day, T.; Jacobson, M.P.; Friesner, R.A.; Farid, R. Novel Procedure for Modeling Ligand/Receptor Induced Fit Effects. *J. Med. Chem.* **2006**, *49*, 534–553. <https://doi.org/10.1021/jm050540c>.
32. Sherman, W.; Beard, H.S.; Farid, R. Use of an Induced Fit Receptor Structure in Virtual Screening. *Chem. Biol. Drug Des.* **2006**, *67*, 83–84. <https://doi.org/10.1111/j.1747-0285.2005.00327.x>.
33. Friesner, R.A.; Banks, J.L.; Murphy, R.B.; Halgren, T.A.; Klicic, J.J.; Mainz, D.T.; Repasky, M.P.; Knoll, E.H.; Shelley, M.; Perry, J.K.; et al. Glide: A New Approach for Rapid, Accurate Docking and Scoring. 1. Method and Assessment of Docking Accuracy. *J. Med. Chem.* **2004**, *47*, 1739–1749. <https://doi.org/10.1021/jm0306430>.
34. Friesner, R.A.; Murphy, R.B.; Repasky, M.P.; Frye, L.L.; Greenwood, J.R.; Halgren, T.A.; Sanschagrin, P.C.; Mainz, D.T. Extra Precision Glide: Docking and Scoring Incorporating a Model of Hydrophobic Enclosure for Protein–Ligand Complexes. *J. Med. Chem.* **2006**, *49*, 6177–6196. <https://doi.org/10.1021/jm051256o>.
35. Halgren, T.A.; Murphy, R.B.; Friesner, R.A.; Beard, H.S.; Frye, L.L.; Pollard, W.T.; Banks, J.L. Glide: A New Approach for Rapid, Accurate Docking and Scoring. 2. Enrichment Factors in Database Screening. *J. Med. Chem.* **2004**, *47*, 1750–1759. <https://doi.org/10.1021/jm030644s>.
36. *Desmond Molecular Dynamics System*; D. E. Shaw Research: New York, NY, USA, 2021;
37. *Maestro-Desmond Interoperability Tools*; Schrödinger: New York, NY, USA, 2021.
38. Abascal, J.L.F.; Sanz, E.; García Fernández, R.; Vega, C. A potential model for the study of ices and amorphous water: TIP4P/Ice. *J. Chem. Phys.* **2005**, *122*, 234511. <https://doi.org/10.1063/1.1931662>.
39. Dunning, T.H. Gaussian basis sets for use in correlated molecular calculations. I. The atoms boron through neon and hydrogen. *J. Chem. Phys.* **1989**, *90*, 1007–1023. <https://doi.org/10.1063/1.456153>.

40. Woon, D.E.; Dunning, T.H. Gaussian basis sets for use in correlated molecular calculations. IV. Calculation of static electrical response properties. *J. Chem. Phys.* **1994**, *100*, 2975–2988. <https://doi.org/10.1063/1.466439>.

Disclaimer/Publisher's Note: The statements, opinions and data contained in all publications are solely those of the individual author(s) and contributor(s) and not of MDPI and/or the editor(s). MDPI and/or the editor(s) disclaim responsibility for any injury to people or property resulting from any ideas, methods, instructions or products referred to in the content.

13. Oświadczenia współautorów publikacji

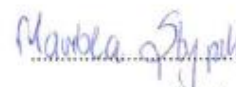
Warszawa, dnia 27.02.2023

Mgr inż. Mariola Stypik

**Politechnika Warszawska
Celon Pharma S.A.**

OŚWIADCZENIA WSPÓLAUTORA

Oświadczam, że w pracy **Stypik, M.**; Zagozda, M.; Michałek, S.; Dymek, B.; Zdżalik-Bielecka, D.; Dziachan, M.; Orłowska, N.; Gunerka, P.; Turowski, P.; Hucz-Kalitowska, J.; Stańczak, A.; Stańczak, P.; Mulewski, K.; Smuga, D.; Stefaniak, F.; Gurba-Bryśkiewicz, L.; Leniak, A.; Ochal, Z.; Mach, M.; Dzwonek, K.; Lamparska-Przybyś, M.; Dubiel, K.; Wieczorek, M.; *Design, Synthesis, and Development of Pyrazolo[1,5-a]pyrimidine Derivatives as a Novel Series of Selective PI3K δ Inhibitors: Part I—Indole Derivatives*; *Pharmaceuticals* **2022**, *15*, 949; mój wkład merytoryczny w przygotowanie, przeprowadzenie i opracowanie badań oraz przedstawienie pracy w formie publikacji to: współpraca przy tworzeniu koncepcji, udział w badaniach literaturowych i patentowych, projektowanie struktur, planowanie syntez i eksperymentów, otrzymanie wszystkich zaplanowanych związków chemicznych, szczegółowa analiza danych, optymalizacja procesu powiększania skali, przygotowanie i edycja manuskryptu.


Podpis

Warszawa, dnia 27.02.2023

Dr inż. Marcin Zagozda

Celon Pharma S.A.

OŚWIADCZENIA WSPÓLAUTORA

Oświadczam, że w pracy Stypik, M.; **Zagozda, M.**; Michalek, S.; Dymek, B.; Zdżalik-Bielecka, D.; Dziachan, M.; Orłowska, N.; Gunerka, P.; Turowski, P.; Hucz-Kalitowska, J.; Stańczak, A.; Stańczak, P.; Mulewski, K.; Smuga, D.; Stefaniak, F.; Gurba-Bryśkiewicz, L.; Leniak, A.; Ochal, Z.; Mach, M.; Dzwonek, K.; Lamparska-Przybysz, M.; Dubiel, K.; Wiczczyński, M.; *Design, Synthesis, and Development of Pyrazolo[1,5-a]pyrimidine Derivatives as a Novel Series of Selective PI3K δ Inhibitors: Part 1—Indole Derivatives; Pharmaceuticals* **2022**, *15*, 949; mój wkład merytoryczny w przygotowanie, przeprowadzenie i opracowanie badań oraz przedstawienie pracy w formie publikacji to: zaprojektowanie odpowiednich struktur, współpraca przy tworzeniu koncepcji i wersji manuskryptu, planu wykonania syntez i eksperymentów, analiza danych.

Jednocześnie wyrażam zgodę na przedłożenie w/w pracy przez mgr inż. Mariolę Stypik jako część rozprawy doktorskiej w formie spójnego tematycznie zbioru artykułów naukowych opublikowanych w czasopiśmie naukowych.


Podpis

Warszawa, dnia 27.02.2023

Mgr inż. Maciej Dziachan

OŚWIADCZENIA WSPÓLAUTORA

Oświadczam, że w pracy Stypik, M.; Zagozda, M.; Michałek, S.; Dymek, B.; Zdzalik-Bielecka, D.; **Dziachan, M.**; Orłowska, N.; Gunerka, P.; Turowski, P.; Hucz-Kalitowska, J.; Stańczak, A.; Stańczak, P.; Mulewski, K.; Smuga, D.; Stefaniak, F.; Gurba-Bryśkiewicz, L.; Leniak, A.; Ochal, Z.; Mach, M.; Dzwonek, K.; Lamparska-Przybysz, M.; Dubiel, K.; Wiczorek, M.; *Design, Synthesis, and Development of Pyrazolo[1,5-a]pyrimidine Derivatives as a Novel Series of Selective PI3K δ Inhibitors: Part I—Indole Derivatives; Pharmaceuticals* **2022**, *15*, 949; mój wkład merytoryczny w przygotowanie, przeprowadzenie i opracowanie badań oraz przedstawienie pracy w formie publikacji to: współpraca przy syntezie części zaplanowanych związków chemicznych, pomoc przy optymalizacji przeskalowania procesu, reakcje w powiększonej skali.

Jednocześnie wyrażam zgodę na przedłożenie w/w pracy przez mgr inż. Mariolę Stypik jako część rozprawy doktorskiej w formie spójnego tematycznie zbioru artykułów naukowych opublikowanych w czasopismach naukowych.



Podpis

Warszawa, dnia 27.02.2023

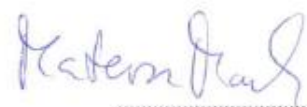
Dr Mateusz Mach

Celon Pharma S.A.

OŚWIADCZENIA WSPÓŁAUTORA

Oświadczam, że w pracy Stypik, M.; Zagozda, M.; Michałek, S.; Dymek, B.; Zdzalik-Bielecka, D.; Dziachan, M.; Orłowska, N.; Gunerka, P.; Turowski, P.; Hucz-Kalitowska, J.; Stańczak, A.; Stańczak, P.; Mulewski, K.; Smuga, D.; Stefaniak, F.; Gurba-Bryśkiewicz, L.; Leniak, A.; Ochal, Z.; **Mach, M.**; Dzwonek, K.; Lamparska-Przybysz, M.; Dubiel, K.; Wieczorek, M.; *Design, Synthesis, and Development of Pyrazolo[1,5-a]pyrimidine Derivatives as a Novel Series of Selective PI3K δ Inhibitors: Part I—Indole Derivatives;* *Pharmaceuticals* **2022**, *15*, 949; mój wkład merytoryczny w przygotowanie, przeprowadzenie i opracowanie badań oraz przedstawienie pracy w formie publikacji to: współudział w edycji i tworzeniu końcowej wersji manuskryptu.

Jednocześnie wyrażam zgodę na przedłożenie w/w pracy przez mgr inż. Mariolę Stypik jako część rozprawy doktorskiej w formie spójnego tematycznie zbioru artykułów naukowych opublikowanych w czasopismach naukowych.



.....
Podpis

Warszawa, dnia 27.02.2023

Dr inż. Damian Smuga

Celon Pharma S.A.

OŚWIADCZENIA WSPÓLAUTORA

Oświadczam, że w pracy Stypik, M.; Zagozda, M.; Michalek, S.; Dymek, B.; Zdżalik-Bielecka, D.; Dziachan, M.; Orłowska, N.; Gunerka, P.; Turowski, P.; Hucz-Kalitowska, J.; Stańczak, A.; Stańczak, P.; Mulewski, K.; **Smuga, D.**; Stefaniak, F.; Gurba-Bryskiewicz, L.; Leniak, A.; Ochal, Z.; Mach, M.; Dzwonek, K.; Lamparska-Przybysz, M.; Dubiel, K.; Wieczorek, M.; *Design, Synthesis, and Development of Pyrazolo[1,5-a]pyrimidine Derivatives as a Novel Series of Selective PI3K δ Inhibitors: Part I—Indole Derivatives; Pharmaceuticals* **2022**, *15*, 949; mój wkład merytoryczny w przygotowanie, przeprowadzenie i opracowanie badań oraz przedstawienie pracy w formie publikacji to: opracowanie metod analitycznych do analizy finalnych związków chemicznych, wykonanie analiz HPLC oraz HRMS.

Jednocześnie wyrażam zgodę na przedłożenie w/w pracy przez mgr inż. Mariolę Stypik jako część rozprawy doktorskiej w formie spójnego tematycznie zbioru artykułów naukowych opublikowanych w czasopismach naukowych.



Podpis

Warszawa, dnia 27.02.2023

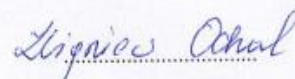
Dr inż. Zbigniew Ochal, prof. PW

Politechnika Warszawska

OŚWIADCZENIA WSPÓLAUTORA

Oświadczam, że w pracy Stypik, M.; Zagozda, M.; Michałek, S.; Dymek, B.; Zdżalik-Bielecka, D.; Dziachan, M.; Orłowska, N.; Gunerka, P.; Turowski, P.; Hucz-Kalitowska, J.; Stańczak, A.; Stańczak, P.; Mulewski, K.; Smuga, D.; Stefaniak, F.; Gurba-Bryśkiewicz, L.; Leniak, A.; **Ochal, Z.**; Mach, M.; Dzwonek, K.; Lamparska-Przybysz, M.; Dubiel, K.; Wieczorek, M.; Wieczorek, M.; *Design, Synthesis, and Development of Pyrazolo[1,5-a]pyrimidine Derivatives as a Novel Series of Selective PI3K δ Inhibitors: Part I—Indole Derivatives.*; *Pharmaceuticals* **2022**, *15*, 949; mój wkład merytoryczny w przygotowanie, przeprowadzenie i opracowanie badań oraz przedstawienie pracy w formie publikacji to: końcowa edycja manuskryptu.

Jednocześnie wyrażam zgodę na przedłożenie w/w pracy przez mgr inż. Mariolę Stypik jako część rozprawy doktorskiej w formie spójnego tematycznie zbioru artykułów naukowych opublikowanych w czasopismach naukowych.



Podpis

Warszawa, dnia 27.02.2023

Mgr inż. Mariola Stypik

**Politechnika Warszawska
Celon Pharma S.A.**

OŚWIADCZENIA WSPÓŁAUTORA

Oświadczam, że w pracy Stypik, M.; Michalek, S.; Orłowska, N.; Zagozda, M.; Dziachan, M.; Banach, M.; Turowski, P.; Gunerka, P.; Zdźalik-Bielecka, D.; Stańczak, A.; Kędzińska, U.; Mulewski, K.; Smuga, D.; Maruszak, W.; Gurba-Bryśkiewicz, L.; Leniak, A.; Pietruś, W.; Ochal, Z.; Mach, M.; Zygmunt, B.; Pieczykolan, J.; Dubiel, K.; Wieczorek, M.; *Design, Synthesis, and Development of Pyrazolo[1,5-a]pyrimidine Derivatives as a Novel Series of Selective PI3K δ Inhibitors: Part II—Benzimidazole Derivatives.*; *Pharmaceuticals* **2022**, *15*, 927; mój wkład merytoryczny w przygotowanie, przeprowadzenie i opracowanie badań oraz przedstawienie pracy w formie publikacji to: współpraca przy tworzeniu koncepcji, udział w badaniach literaturowych i patentowych, projektowanie struktur, planowanie syntez i eksperymentów, otrzymanie wszystkich zaplanowanych związków chemicznych, szczegółowa analiza danych, optymalizacja procesu powiększania skali, przygotowanie i edycja manuskryptu.


Podpis

Warszawa, dnia 27.02.2023

Mgr inż. Maciej Dziachan

OŚWIADCZENIA WSPÓŁAUTORA

Oświadczam, że w pracy Stypik, M.; Michałek, S.; Orłowska, N.; Zagozda, M.; **Dziachan, M.**; Banach, M.; Turowski, P.; Gunerka, P.; Zdzałik-Bielecka, D.; Stańczak, A.; Kędzierska, U.; Mulewski, K.; Smuga, D.; Maruszak, W.; Gurba-Bryśkiewicz, L.; Leniak, A.; Pietruś, W.; Ochal, Z.; Mach, M.; Zygmunt, B.; Pieczykolan, J.; Dubiel, K.; Wieczorek, M.; *Design, Synthesis, and Development of Pyrazolo[1,5- α]pyrimidine Derivatives as a Novel Series of Selective PI3K δ Inhibitors: Part II—Benzimidazole Derivatives; Pharmaceuticals* **2022**, *15*, 927; mój wkład merytoryczny w przygotowanie, przeprowadzenie i opracowanie badań oraz przedstawienie pracy w formie publikacji to: współpraca przy syntezie części zaplanowanych związków chemicznych.

Jednocześnie wyrażam zgodę na przedłożenie w/w pracy przez mgr inż. Mariolę Stypik jako część rozprawy doktorskiej w formie spójnego tematycznie zbioru artykułów naukowych opublikowanych w czasopismach naukowych.



Podpis

Warszawa, dnia 27.02.2023

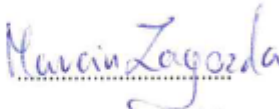
Dr inż. Marcin Zagozda

Celon Pharma S.A.

OŚWIADCZENIA WSPÓŁAUTORA

Oświadczam, że w pracy Stypik, M.; Michałek, S.; Orłowska, N.; **Zagozda, M.**; Dziachan, M.; Banach, M.; Turowski, P.; Gunerka, P.; Zdzałik-Bielecka, D.; Stańczak, A.; Kędzierska, U.; Mulewski, K.; Smuga, D.; Maruszak, W.; Gurba-Bryśkiewicz, L.; Leniak, A.; Pietruś, W.; Ochal, Z.; Mach, M.; Zygmunt, B.; Pieczykolan, J.; Dubiel, K.; Wieczorek, M.; *Design, Synthesis, and Development of Pyrazolo[1,5-a]pyrimidine Derivatives as a Novel Series of Selective PI3K δ Inhibitors: Part II—Benzimidazole Derivatives.*; *Pharmaceuticals* **2022**, *15*, 927; mój wkład merytoryczny w przygotowanie, przeprowadzenie i opracowanie badań oraz przedstawienie pracy w formie publikacji to: zaprojektowanie odpowiednich struktur, współpraca przy tworzeniu koncepcji i wersji manuskryptu, planu wykonania syntez i eksperymentów, analiza danych.

Jednocześnie wyrażam zgodę na przedłożenie w/w pracy przez mgr inż. Mariolę Stypik jako część rozprawy doktorskiej w formie spójnego tematycznie zbioru artykułów naukowych opublikowanych w czasopismach naukowych.


Podpis

Warszawa, dnia 27.02.2023

Dr inż. Damian Smuga

Celon Pharma S.A.

OŚWIADCZENIA WSPÓLAUTORA

Oświadczam, że w pracy Stypik, M.; Michałek, S.; Orłowska, N.; Zagozda, M.; Dziachan, M.; Banach, M.; Turowski, P.; Gunerka, P.; Zdzalik-Bielecka, D.; Stańczak, A.; Kędzierska, U.; Mulewski, K.; **Smuga, D.**; Maruszak, W.; Gurba-Bryśkiewicz, L.; Leniak, A.; Pietruś, W.; Ochal, Z.; Mach, M.; Zygmunt, B.; Pieczykolan, J.; Dubiel, K.; Wieczorek, M.; *Design, Synthesis, and Development of Pyrazolo[1,5-a]pyrimidine Derivatives as a Novel Series of Selective PI3K δ Inhibitors: Part II—Benzimidazole Derivatives; Pharmaceuticals* **2022**, *15*, 927; mój wkład merytoryczny w przygotowanie, przeprowadzenie i opracowanie badań oraz przedstawienie pracy w formie publikacji to: opracowanie metod analitycznych do analizy finalnych związków chemicznych, wykonanie analiz HPLC oraz HRMS.

Jednocześnie wyrażam zgodę na przedłożenie w/w pracy przez mgr inż. Mariolę Stypik jako część rozprawy doktorskiej w formie spójnego tematycznie zbioru artykułów naukowych opublikowanych w czasopismach naukowych.



Podpis

Warszawa, dnia 27.02.2023

Dr Mateusz Mach

Celon Pharma S.A.

OŚWIADCZENIA WSPÓLAUTORA

Oświadczam, że w pracy Stypik, M.; Michałek, S.; Orłowska, N.; Zagozda, M.; Dziachan, M.; Banach, M.; Turowski, P.; Gunerka, P.; Zdzałik-Bielecka, D.; Stańczak, A.; Kędzierska, U.; Mulewski, K.; Smuga, D.; Maruszak, W.; Gurba-Bryśkiewicz, L.; Leniak, A.; Pietruś, W.; Ochal, Z.; **Mach, M.**; Zygmunt, B.; Pieczykołan, J.; Dubiel, K.; Wieczorek, M.; *Design, Synthesis, and Development of Pyrazolo[1,5-a]pyrimidine Derivatives as a Novel Series of Selective PI3K α Inhibitors: Part II—Benzimidazole Derivatives; Pharmaceuticals* **2022**, *15*, 927; mój wkład merytoryczny w przygotowanie, przeprowadzenie i opracowanie badań oraz przedstawienie pracy w formie publikacji to: współudział w edycji i tworzeniu końcowej wersji manuskryptu.

Jednocześnie wyrażam zgodę na przedłożenie w/w pracy przez mgr inż. Mariolę Stypik jako część rozprawy doktorskiej w formie spójnego tematycznie zbioru artykułów naukowych opublikowanych w czasopismach naukowych.



.....
Podpis

Warszawa, dnia 27.02.2023

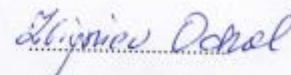
Dr inż. Zbigniew Ochal, prof. PW

Politechnika Warszawska

OŚWIADCZENIA WSPÓLAUTORA

Oświadczam, że w pracy Stypik, M.; Michałek, S.; Orłowska, N.; Zagozda, M.; Dziachan, M.; Banach, M.; Turowski, P.; Gunerka, P.; Zdżalik-Bielecka, D.; Stańczak, A.; Kędzińska, U.; Mulewski, K.; Smuga, D.; Maruszak, W.; Gurba-Bryśkiewicz, L.; Leniak, A.; Pietruś, W.; **Ochal, Z.**; Mach, M.; Zygmunt, B.; Pieczykolan, J.; Dubiel, K.; Wieczorek, M.; *Design, Synthesis, and Development of Pyrazolo[1,5-a]pyrimidine Derivatives as a Novel Series of Selective PI3K δ Inhibitors: Part II—Benzimidazole Derivatives; Pharmaceuticals* **2022**, *15*, 927; mój wkład merytoryczny w przygotowanie, przeprowadzenie i opracowanie badań oraz przedstawienie pracy w formie publikacji to: końcowa edycja manuskryptu.

Jednocześnie wyrażam zgodę na przedłożenie w/w pracy przez mgr inż. Mariolę Stypik jako część rozprawy doktorskiej w formie spójnego tematycznie zbioru artykułów naukowych opublikowanych w czasopismach naukowych.



Podpis

Warszawa, dnia 17.04.2023

Mgr inż. Mariola Stypik

**Politechnika Warszawska
Celon Pharma S.A.**

OŚWIADCZENIE WSPÓLAUTORA

Oświadczam, że w pracy Pietruś W., **Stypik M.**, Banach M., Zagozda M., Gurba-Bryśkiewicz L., Maruszak W., Leniak A., Kurczab R.^{*}, Ochal Z., Dubiel K. and Wieczorek M. *Tuning the biological activity of PI3K δ inhibitor by the introduction of a fluorine atom using the computational workflow* (*Molecules* **2023**, *28*(8), 3531) mój wkład merytoryczny w przygotowanie, przeprowadzenie i opracowanie badań oraz przedstawienie pracy w formie publikacji to: współpraca przy tworzeniu koncepcji, projektowanie struktur, planowanie syntez i eksperymentów, otrzymanie wszystkich zaplanowanych związków chemicznych, analiza danych, przygotowanie części manuskryptu i edycja manuskryptu.


Podpis

Warszawa, dnia 17.04.2023

Dr hab. Wioleta Maruszak

Celon Pharma S.A.

OŚWIADCZENIA WSPÓLAUTORA

Oświadczam, że w pracy Pietruś W., Stypik M., Banach M., Zagozda M., Gurba-Bryśkiewicz L., **Maruszak W.**, Leniak A., Kurczab R., Ochal Z., Dubiel K. and Wieczorek M. *Tuning the biological activity of PI3K δ inhibitor by the introduction of a fluorine atom using the computational workflow (Molecules 2023, 28(8), 3531)* mój wkład merytoryczny w przygotowanie, przeprowadzenie i opracowanie badań oraz przedstawienie pracy w formie publikacji to wykonanie analiz czystości dla wybranych struktur.

Jednocześnie wyrażam zgodę na przedłożenie w/w pracy przez mgr inż. Mariolę Stypik jako część rozprawy doktorskiej w formie spójnego tematycznie zbioru artykułów naukowych opublikowanych w czasopismach naukowych.



Podpis

Warszawa, dnia 17.04.2023

Mgr Lidia Gurba Bryskiewicz

Celon Pharma S.A.

OŚWIADCZENIA WSPÓLAUTORA

Oświadczam, że w pracy Pietruś W., Stypik M., Banach M., Zagozda M., **Gurba-Bryskiewicz L.**, Maruszak W., Leniak A., Kurczab R.^{*}, Ochal Z., Dubiel K. and Wieczorek M. *Tuning the biological activity of PI3K δ inhibitor by the introduction of a fluorine atom using the computational workflow* (*Molecules* **2023**, *28*(8), 3531) mój wkład merytoryczny w przygotowanie, przeprowadzenie i opracowanie badań oraz przedstawienie pracy w formie publikacji to wykonanie analiz czystości dla wybranych struktur.

Jednocześnie wyrażam zgodę na przedłożenie w/w pracy przez mgr inż. Mariolę Stypik jako część rozprawy doktorskiej w formie spójnego tematycznie zbioru artykułów naukowych opublikowanych w czasopismach naukowych.



.....

Podpis

Warszawa, dnia 17.04.2023

Dr Wojciech Pietruś

Celon Pharma S.A.

OŚWIADCZENIE WSPÓLAUTORA

Oświadczam, że w pracy **Pietruś W., Stypik M., Banach M., Zagozda M., Gurba-Bryśkiewicz L., Maruszak W., Leniak A., Kurczab R., Ochal Z., Dubiel K. and Wieczorek M. *Tuning the biological activity of PI3K δ inhibitor by the introduction of a fluorine atom using the computational workflow* (Molecules 2023, 28(8), 3531)** mój wkład merytoryczny w przygotowanie, przeprowadzenie i opracowanie badań oraz przedstawienie pracy w formie publikacji to: tworzenie koncepcji manuskryptu, projektowanie obliczeń, wykonanie wszelkich obliczeń kwantowo-mechanicznych dla wybranych struktur, badania dokowania molekularnego, analiza danych, przygotowanie i edycja manuskryptu.

Jednocześnie wyrażam zgodę na przedłożenie w/w pracy przez mgr inż. Mariolę Stypik jako część rozprawy doktorskiej w formie spójnego tematycznie zbioru artykułów naukowych opublikowanych w czasopismach naukowych.



.....
Podpis

Warszawa, dnia 17.04.2023

Mgr inż. Martyna Banach

Celon Pharma S.A.

OŚWIADCZENIE WSPÓLAUTORA

Oświadczam, że w pracy Pietruś W., Stypik M., **Banach M.**, Zagozda M., Gurba-Bryśkiewicz L., Maruszak W., Leniak A., Kurczab R.^{*}, Ochal Z., Dubiel K. and Wieczorek M. *Tuning the biological activity of PI3Kδ inhibitor by the introduction of a fluorine atom using the computational workflow* (*Molecules* **2023**, *28*(8), 3531) mój wkład merytoryczny w przygotowanie, przeprowadzenie i opracowanie badań oraz przedstawienie pracy w formie publikacji to wykonanie testów kinazowych do przedstawienia wartości parametru IC₅₀ dla wybranych struktur.

Jednocześnie wyrażam zgodę na przedłożenie w/w pracy przez mgr inż. Mariolę Stypik jako część rozprawy doktorskiej w formie spójnego tematycznie zbioru artykułów naukowych opublikowanych w czasopismach naukowych.



Podpis

Warszawa, dnia 17.04.2023

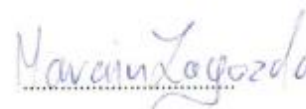
Dr inż. Marcin Zagozda

Celon Pharma S.A.

OŚWIADCZENIE WSPÓLAUTORA

Oświadczam, że w pracy Pietruś W., Stypik M., Banach M., **Zagozda M.**, Gurba-Bryśkiewicz L., Maruszak W., Leniak A., Kurczab R.^{*}, Ochal Z., Dubiel K. and Wieczorek M. *Tuning the biological activity of PI3Kδ inhibitor by the introduction of a fluorine atom using the computational workflow* (*Molecules* **2023**, *28*(8), 3531) mój wkład merytoryczny w przygotowanie, przeprowadzenie i opracowanie badań oraz przedstawienie pracy w formie publikacji to edycja manuskryptu.

Jednocześnie wyrażam zgodę na przedłożenie w/w pracy przez mgr inż. Mariolę Stypik jako część rozprawy doktorskiej w formie spójnego tematycznie zbioru artykułów naukowych opublikowanych w czasopismach naukowych.


Podpis